Organic Synthesis of Endohedral Fullerenes Encapsulating Molecular Hydrogen

Michihisa Murata

2006

Organic Synthesis of Endohedral Fullerenes Encapsulating Molecular Hydrogen

Michihisa Murata

Institute for Chemical Research

Kyoto University

2006

Table of Contents

General Introduction

Since the fullerenes became available in macroscopic quantities in 1990,[1] an enormous number of studies have been carried out in the various fields of science, including chemistry, physics, medicine, pharmacy, biology, and interdisciplinary areas. It has been revealed that fullerene C_{60} exhibits surprising physical properties such as superconductivity upon alkali metal doping[2] and ferromagnetism as a charge transfer complex with tetrakis(dimethylamino)ethylene, as well as biological activity.[3] The high I_h symmetry of C_{60} played a crucial role because larger fullerenes with lower symmetry, i.e., C_{70}, C_{76}, C_{84}, and so on, have so far not yet reported to show such characteristic properties.

There have been reported a wide variety of organic reactions to derivatize C_{60} in order to control the electronic properties of this three-dimensionally π-conjugated system and to endow it new functionalities. The properties of fullerenes should also be controlled by their "inside modification", for example, by incorporating metal atoms inside the empty cavity via formation of "internal" charge transfer complexes.[4] The fullerenes incorporating metal atoms inside the cage, so-called endohedral metallofullerenes, have great possibilities of practical use, for example, in the fields of molecular electronics such as organic filed-effect transistors,[5] and of medical science as a contrast agent for magnetic resonance imaging (MRI).[6] However, development of such applications has so far been hampered by severe limitation of their availability that relied on the hard-to-control physical method of production. For instance, certain metal atoms (La, Y, Sc, Gd, Ca, Sr, Ba, etc.) were incorporated into fullerene cages (C_{72}, C_{76}, C_{78}, C_{80}, C_{82}, C_{84}, etc.) by the use of arc-discharge or laser vaporization of graphite rods containing metal oxides or carbides. This conventional method had almost no selectivity in controlling both cage-size and symmetry of the fullerenes as well. Pure products are only available in μg- to mg-quantities (<< 0.1% yields) after tedious separation processes.[4a,b] Hence, an entirely different approach for the macroscopic production of endohedral fullerenes is apparently required in order to bring about a breakthrough into this situation.[7,8]

It seems quite appealing to produce the endohedral fullerene complexes by using the intact hollow fullerenes as the starting materials. It has been shown that highly reactive

species such as atomic nitrogen or phosphorus, generated by plasma-based ion implantation technique, are able to enter the inside space of C_{60} framework but their formation rate is only 0.01%.[9] More importantly, Saunders et al. reported that noble-gas atoms, such as He, Ne, Ar, Kr, Xe, can be inserted into fullerene cages in ca. 0.1% incorporation yield by treating the fullerene powders under forced conditions (650 °C under 3000 atmosphere of noble gases).[10] It should be noted that ^{3}He is an NMR active nucleus and the chemical shifts for the encapsulated ^{3}He provide valuable information concerning the magnetic field inside the fullerene cages and serve as a powerful tool both for the characterization of fullerenes and their derivatives[11] and for the investigation of the fullerene aromaticity.[12]

The mechanism for the incorporation of these noble-gas atoms was postulated that one or two carbon-carbon bonds of fullerenes were cleaved under extremely high temperature to open a *temporary* hole on the surfaces which allows the noble-gas atoms to enter the fullerene cages.[10e] Therefore, the creation of a large and *permanent* orifice on the fullerene surfaces by organic synthesis should provide a great opportunity to introduce ideally any atom or small molecule inside the cages.[8] In order to realize the chemical synthesis of endohedral fullerenes by this approach, named "molecular surgery",[7] we have to establish a synthetic route to open and close an orifice that will first let some chemical species be encapsulated and then regenerate original form of fullerenes with retention of the incorporated species.

During the past decade, organic chemists have pursued novel reactions to open a large orifice on the surface of C_{60} cage. Despite of a wealth of knowledge of reactivity of the π-bond of C_{60},[13] the task of chemical transformations of the σ-framework itself in a predictable fashion is still a challenging topic. The first ring-opening reaction was discovered by Wudl et al. in 1995.[8] As shown in Scheme 1, they reported that

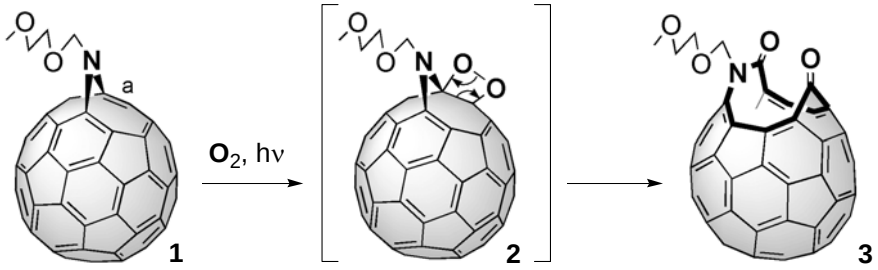

Scheme 1. Formation of the first open-cage fullerene **3**.[8]

[5,6]-azafulleroid **1**[14] reacts with photochemically generated singlet oxygen regioselectively at the strained carbon-carbon double bond, denoted as "a", to afford ketolactam **3** with an 11-membered-ring orifice via dioxetane intermediate **2**. Unfortunately, the orifice was found to be too small for the smallest stable atom, He, to pass through at a temperature as high as 200 °C.[15] Instead, compound **1** was subsequently transformed to a totally new heterofullerene derivative having a $C_{59}N$ skeleton.[16] This revealed that open-cage fullerenes can be potential precursors for the synthesis of novel fullerenes including hetero atom(s) in the σ-frameworks.

In 1996, Rubin et al. reported open-cage fullerene derivative **5** having an eight-membered-ring orifice by developing a sequential intramolecular rearrangements of in situ generated C_{60} derivative **4** fused with 1,3-cyclohexadiene.[17] This process took place under photochemical condition through intramolecular [4+4] cycloaddition and subsequent [2+2+2] cycloreversion, as shown in Scheme 2. Compound **5** was transformed to cobalt(III) complex **6**, whose structure was confirmed by X-ray crystallography, for the first time for an open-cage fullerene derivative. Although the cobalt atom was situated just above an 11-membered-ring orifice, it was found to be impossible to insert it into the fullerene cage by activation in the solid-state with heating at 400 °C or pressurizing up to 40000 atm.[7,18]

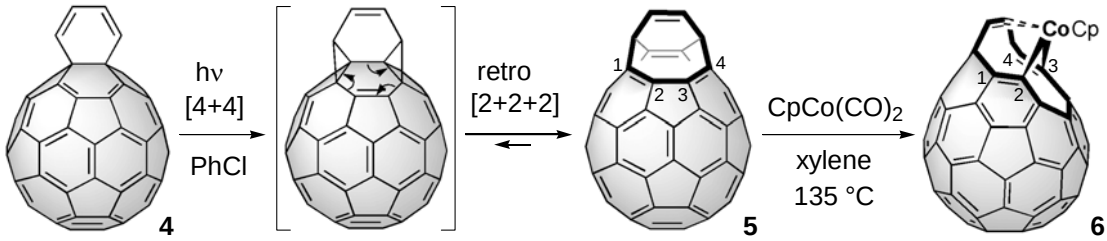

Scheme 2. Synthesis of open-cage fullerene **5** and its cobalt(III) complex **6**.[17a]

After Rubin's discovery of compound **5**, several synthetic routes were developed to produce analogous derivatives **7** – **9**; by way of nickel-promoted ene-diyne cycloaddition on C_{60},[19] [4+2] cycloaddition of palladacyclopentadiene with C_{60},[20] as well as thermal reaction of C_{60} with phthalazine.[21] These eight-membered-ring compounds possess common carbon frameworks having bridgehead carbon-carbon double bonds at the rim of the orifice, denoted as "b" in the structure of **7** shown below. Iwamatsu et al. reported that compound **8** reacts

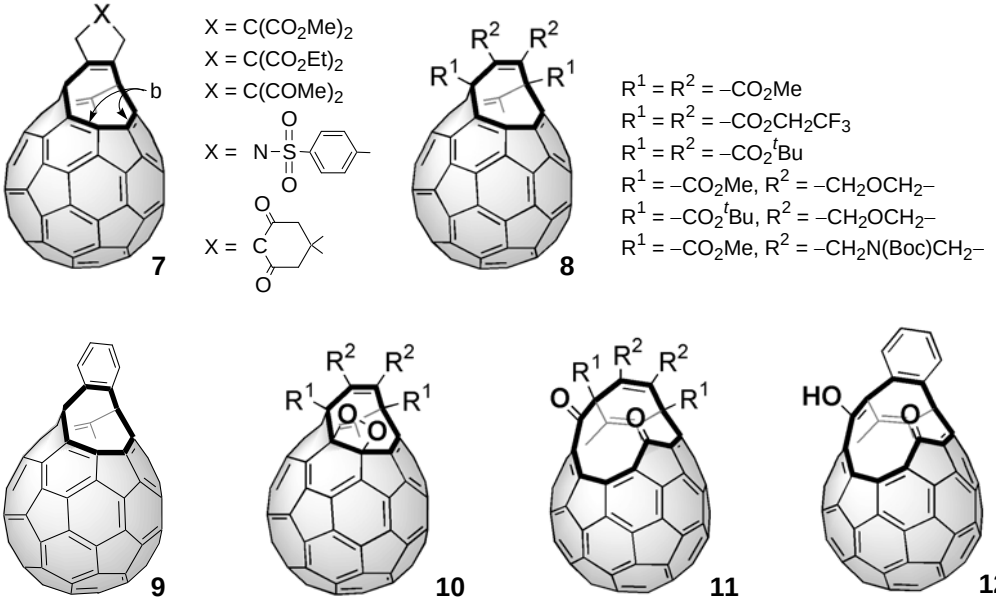

with singlet oxygen regioselectively to afford diketone derivative **11** possessing a 12-membered-ring orifice via dioxetane intermediate **10**[22] in a similar fashion as Wudl's compound **1**[8] (Figure 1). In addition, Komatsu et al. independently found the analogous reaction for **9**, that afforded enol **12** via keto-enol tautomerization.[23]

In 1997, Rubin proposed a new concept that hexa-substituted fullerene **13** should undergo facile rearrangement to afford an open-cage fullerene **14** with a 15-membered-ring orifice through thermally allowed [2+2+2] cycloreversion of the planarized cyclohexane ring (Scheme 3).[7] During the course of this study, Rubin designed 1,4-diphenyl-1,3-butadiene bearing two azido groups **15** possessing three reactive centers and conducted a thermal reaction with C_{60}.[24] However, the reaction did not stop at the stage of **17** and resulted in the

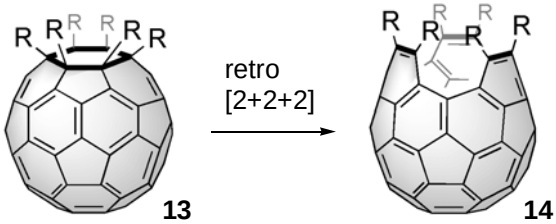

Scheme 3. Conceptual representation of a possible way to open-cage fullerene C_{60} having a 15-membered-ring orifice.[7]

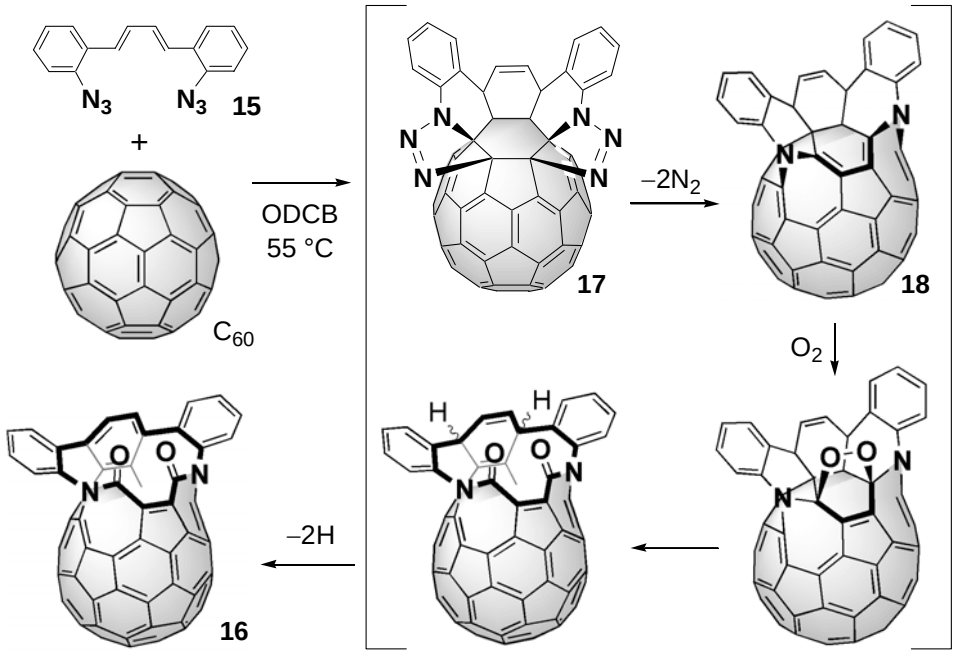

Scheme 4. Possible reaction pathway leading to open-cage fullerene **16**.[24]

formation of an open-cage fullerene **16** having two lactam moieties in 12% yield (Scheme 4). This reaction was intended to proceed via initial addition of **15** (involving both a [4+2] cycloaddition and two 1,3-dipolar additions) to the three carbon-carbon double bonds in a same hexagon of C_{60} to give a target compound **17** with a fully saturated hexagon. However, **17** underwent a facile extrusion of two nitrogen molecules and subsequent nitrogen migration to afford compound **18**. Finally, an electron rich butadiene moiety on the fullerene cage of **18** reacted with singlet oxygen, followed by dehydrogenation to give **16** with a 14-membered-ring orifice.

A significant progress in this research field was triggered by the use of open-cage fullerene **19**, which is di-*tert*-butyl-substituted derivative of **16**. In 2001, Rubin et al. estimated the temperature that was required to insert various neutral atoms or molecules into the C_{60} cage through the orifice of **19** by the theoretical calculations.[25] The insertion of a helium atom or a hydrogen molecule into the C_{60} cage was predicted to take place under significantly milder conditions than that for C_{60} itself such as at the temperature of 124 °C for a helium atom or 397 °C for a hydrogen molecule, albeit the orifice of **19** is rather elliptic in shape. Indeed, by treating a crystalline powder of **19** with ca. 475 atm of helium gas at

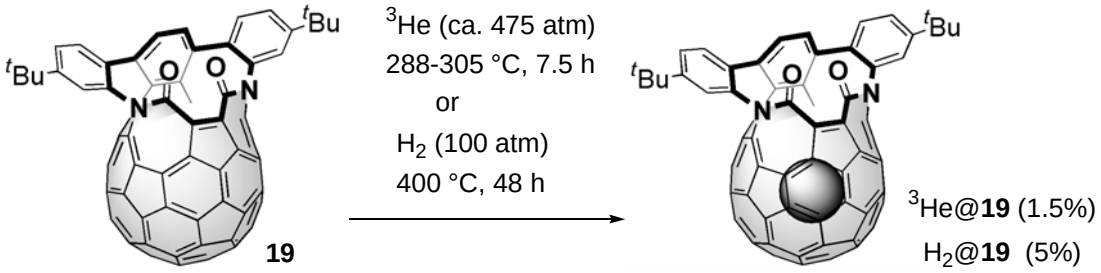

Scheme 5. Insertion of helium and molecular hydrogen into open-cage fullerene **19**.[25]

288-305 °C for 7.5 h, the insertion of a helium atom was achieved in 1.5% for the first time (Scheme 5).[25] A hydrogen molecule was also introduced in ca. 5% under the conditions of 400 °C and 100 atm for 48 h.[25] A highly shielded ^{1}H NMR signal for the encapsulated hydrogen molecule of H_2@**19** (@ stands for encapsulation) was observed at δ –5.43 ppm.[25] These results proved the feasibility of the strategy of molecular surgery approach for organic synthesis of endohedral fullerenes. However, compound **19** was thermally unstable and was partially decomposed during the insertion processes.

Recently, Iwamatsu et al. developed a series of ring-expansion reactions using aromatic hydrazine or diamine derivatives, which resulted in formation of extremely large orifices ranging from 15 to 20-membered ring, although the precise mechanisms for these reactions are not clear.[26-29] For instance, the reaction of open-cage fullerene **11** with an excess amount of 4,5-dimethyl-1,2-phenylenediamine at 60 °C afforded open-cage fullerene **20** with the largest orifice of 20-membered ring, whose structure is close to a bowl shape (Scheme 6).[28] A quite similar reaction was also conducted using Wudl's open-cage C_{60} **3** and 1,2-phenylenediamine in the presence of pyridine, which afforded open-cage fullerene **21** with a 19-membered-ring orifice.[29] In 2004, Iwamatsu's group discovered that a water molecule was spontaneously incorporated inside the molecular framework of **20** up to 75% in a solution of 1,1,2,2-tetrachloroethane-d_2 under ambient conditions, as demonstrated by a sharp ^{1}H NMR signal at δ –11.4 ppm (Scheme 7).[28] However, such a severely ruptured π-system in **20** seems difficult to be restored to the original structure of C_{60}.

On the other hand, we have studied the reactions of C_{60} with diaza or tetraaza aromatic compounds.[21,30] Particularly, the liquid-phase thermal reaction of C_{60} with phthalazine resulted in the formation of **9** having an eight-membered-ring orifice in one-pot,[21] while the

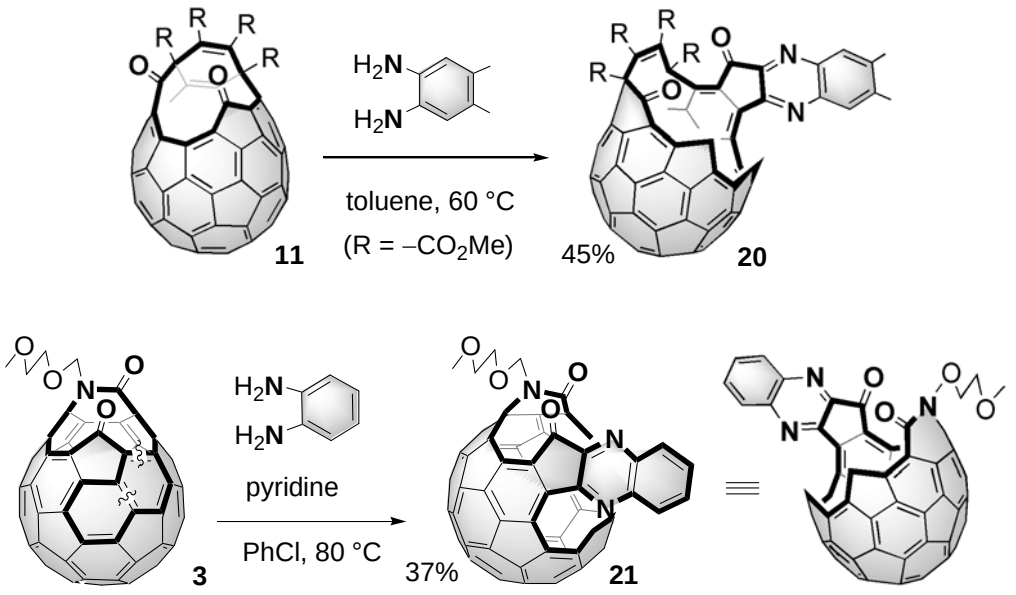

Scheme 6. Ring-expanding reaction of open-cage fullerenes **11** and **3**.[28,29]

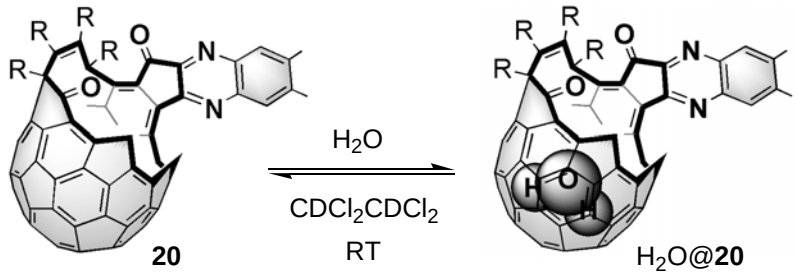

Scheme 7. Encapsulation of molecular water in open-cage fullerene **20**.[28]

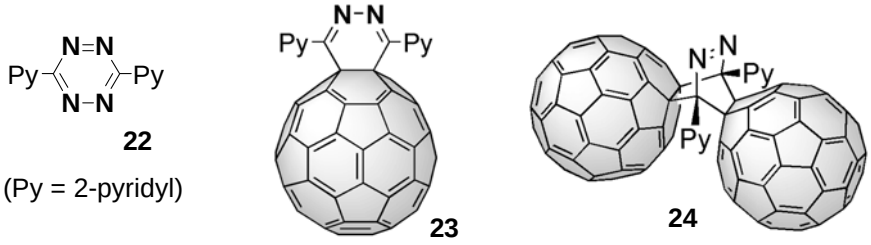

solid state reaction of C_{60} with 3,6-di-(2-pyridyl)-1,2,4,5-tetrazine (**22**) under high-speed vibration milling[31] afforded **23** quantitatively, which could further react with C_{60} to give dimer **24**.[30] These results prompted us to elucidate the reactions of C_{60} with triaza aromatic

compounds, especially in anticipation for the formation of an aza-open-cage fullerenes having a nitrogen atom on the rim of the opening.

The characteristic of this method of opening an orifice resides in the simple and facile reaction. We decided to utilize this method for the molecular surgical synthesis of endohedral fullerenes by further enlargement of the orifice, introduction of some small atom or molecule(s), and complete closure of the orifice. Prior to this study, there has been entirely no report for the attempt on closure or even size-reduction of once formed orifice on the fullerene cage. If this method is successful, this would lead to a new development in the science of endohedral fullerene.

In this thesis, Chapter 1 describes a thermal reaction of C_{60} with 4,6-dimethyl-1,2,3-triazine (**25**), which resulted in an unexpected formation of an open-cage fullerene with an eight-membered-ring orifice **26** bearing no nitrogen atom on the rim of the opening, along with monoadduct **27**. Compound **26** underwent facile orifice-ring enlargement by the reaction with singlet oxygen to afford an open-cage fullerene **28** with a 12-membered-ring orifice.

Chapter 2 describes a thermal reaction of C_{60} with another type of triazine, i.e., 3-(2-pyridyl)-5,6-diphenyl-1,2,4-triazine (**29**), to give a desired aza-open-cage fullerene **30** possessing a nitrogen atom on the rim of an eight-membered-ring orifice. Moreover, after the orifice of **30** was enlarged to a 12-membered ring by the reaction with singlet oxygen (**31**),

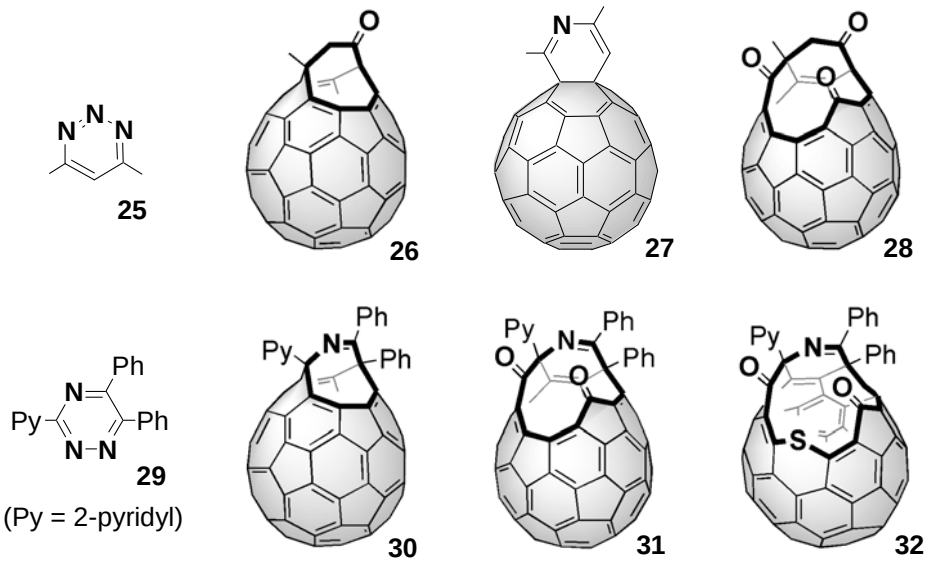

an unprecedented reaction was discovered to effectively enlarge the orifice of **31** by insertion of a sulfur atom to the rim of the orifice, leading to the formation of open-cage fullerene **32** with a 13-membered-ring orifice, which was found to be quite stable against heating.

Chapter 3 describes the first accomplishment of 100% encapsulation of molecular hydrogen inside the fullerene cage of **32** through the orifice. Spectral information of H_2@**32** as well as thermodynamic parameters for the release of molecular hydrogen from H_2@**32** is also presented. In addition, the author describes the results of synchrotron X-ray diffraction experiments on a single crystal of H_2@**32**, which allowed the direct observation of a single hydrogen molecule floating at the center of the hollow cavity in the fullerene cage.

Chapter 4 describes the very first chemical synthesis of an entirely new endohedral fullerene, H_2@C_{60}, in a macroscopic amount via four-step organic reaction to completely close a 13-membered-ring orifice of H_2@**32**. Spectral information and electrochemical properties of H_2@C_{60}, as well as NMR chemical shifts for the encapsulated molecular hydrogen will be discussed.

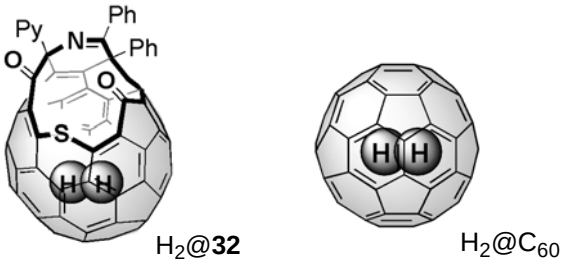

H_2@**32** H_2@C_{60}

As mentioned above, most efforts to open an orifice on the fullerene cages have largely focused on the fullerene C_{60}. In contrast with the development of the synthesis of open-cage fullerene C_{60}, there has been much less attention focused on the synthesis of open-cage fullerene C_{70}.[32] Because the inner cavity of C_{70} is larger than that of C_{60}, it should have a possibility to encapsulate more than one small atom or molecule inside the C_{70} framework.[33]

Hence, Chapter 5 describes the synthesis, structure, and properties of open-cage fullerene C_{70} derivative **33** with a 13-membered-ring orifice. The results of the encapsulation of one and two hydrogen molecules inside the C_{70} cage of **33** through the orifice will be described. Low-temperature NMR studies showing the dynamic behavior of

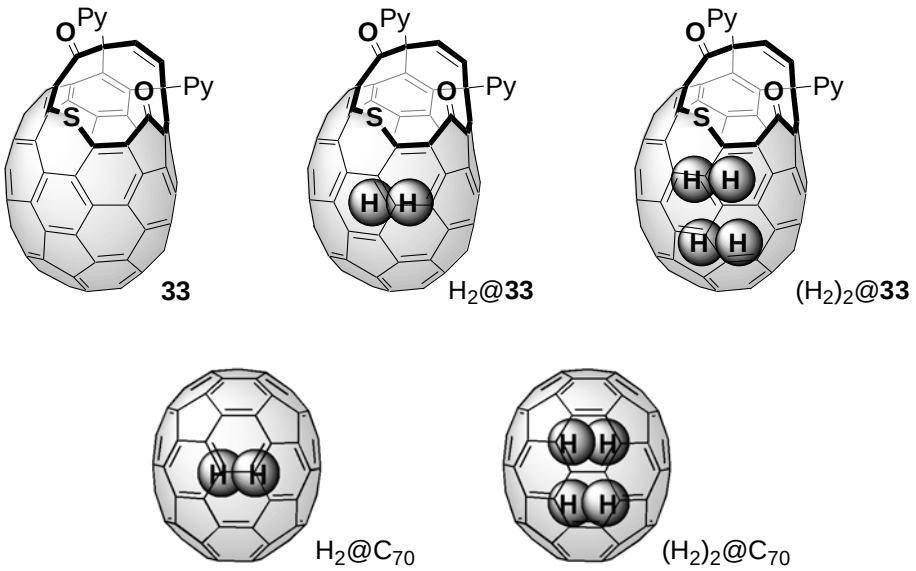

the two hydrogen molecules confined inside the C_{70} framework will be presented. Furthermore, the author describes the complete closure of the orifice of H_2@**33** or $(H_2)_2$@**33**, leading to the first chemical synthesis of endohedral fullerenes $H_2@C_{70}$ and $(H_2)_2@C_{70}$.

Finally, Chapter 6 describes the generation and properties of dianion of open-cage fullerene H_2@$\mathbf{32}^{2-}$, which was prepared in an attempt for introduction of its counter cation (Na^+) inside of the fullerene cage. An unusually downfield shifted NMR signal for the molecular hydrogen of H_2@$\mathbf{32}^{2-}$ will be discussed in connection with local aromaticity of individual pentagons and hexagons of the fullerene cage assessed by the theoretical calculations.

References and Notes

(1) Krätschmer, W.; Lamb, L. D.; Fostiropoulos, K.; Huffman, D. R. *Nature* **1990**, *347*, 354.

(2) (a) Hebard, A. F.; Rosseinsky, M. J.; Haddon, R. C.; Murphy, D. W.; Glarum, S. H.; Palstra, T. T. M.; Ramirez, A. P.; Kortan, A. R. *Nature* **1991**, *350*, 600. (b) Holczer, K.; Klein, O.; Huang, S. M.; Kaner, R. B.; Fu, K. J.; Whetten, R. L.; Diederich, F. *Science* **1991**, *252*, 1154.

(3) Allemand, P. M.; Khemani, K. C.; Koch, A.; Wudl, F.; Holczer, K.; Donovan, S.; Grüner,

G.; Thompson, J. D. *Science* **1991**, *253*, 301.

(4) (a) Shinohara, H. *Rep. Prog. Phys.* **2000**, *63*, 843. (b) Akasaka, T.; Nagase, S. *Endofullerenes*: *A New Family of Carbon Clusters*; Kluwer Academic: Dordrecht, 2002. (c) Liu, S.; Sun, S. *J. Organomet. Chem.* **2000**, *599*, 74. (d) Nagase, S.; Kobayashi, K.; Akasaka, T. *Bull. Chem. Soc. Jpn.* **1996**, *69*, 2131. (e) Bethune, D. S.; Johnson, R. D.; Salem, J. R.; de Vries, M. S.; Yannoni, C. S. *Nature* **1993**, *366*, 123.

(5) Kobayshi, S.-i.; Mori, S.; Iida, S.; Ando, H.; Takenobu, T.; Taguchi, Y.; Fujiwara, A.; Taninaka, H.; Shinohara, H.; Iwasa, Y. *J. Am. Chem. Soc.* **2003**, *125*, 8116.

(6) Kato, H.; Kanazawa, Y.; Okumura, M.; Taninaka, A.; Yokawa, T.; Shinohara, H. *J. Am. Chem. Soc.* **2003**, *125*, 4391.

(7) (a) Rubin, Y. *Chem. Eur. J.* **1997**, *3*, 1009. (b) Rubin, Y. *Chimia* **1998**, *52*, 118. (c) Rubin, Y. *Top. Curr. Chem.* **1999**, *199*, 67.

(8) Hummelen, J. C.; Prato, M.; Wudl, F. *J. Am. Chem. Soc.* **1995**, *117*, 7003.

(9) (a) Murphy, T. A.; Pawlik, T.; Weidinger, A.; Höhne, M.; Alcala, R.; Spaeth, J.-M. *Phys. Rev. Lett.* **1996**, *77*, 1075. (b) Knapp, C.; Weiden, N.; Käss, H.; Dinse, K.-P.; Pietzak, B.; Waiblinger, M.; Weidinger, A. *Mol. Phys.* **1998**, *95*, 999.

(10) (a) Saunders, M.; Jiménez-Vázquez, H. A.; Cross, R. J. *Science* **1993**, *259*, 1428. (b) Saunders, M.; Jiménez-Vázquez, H. A.; Cross, R. J. *J. Am. Chem. Soc.* **1994**, *116*, 2193. (c) Saunders, M.; Jiménez-Vázquez, H. A.; Cross, R. J.; Mroczkowski, S.; Freedberg, D. I.; Anet, F. A. L. *Nature* **1994**, *367*, 256. (d) Saunders, M.; Jiménez-Vázquez, H. A.; Cross, R. J.; Billups, W. E.; Gesenberg, C.; Gonzalez, A.; Luo, W.; Haddon, R. C.; Diederich, F.; Herrmann, A. *J. Am. Chem. Soc.* **1995**, *117*, 9305. (e) Saunders, M.; Cross, R. J.; Jiménez-Vázquez, H. A.; Shimshi, R.; Khong, A. *Science* **1996**, *271*, 1693. (f) Syamala, M. S.; Cross, R. J.; Saunders, M. *J. Am. Chem. Soc.* **2002**, *124*, 6216. (g) Cross, R. J.; Khong, A.; Saunders, M. *J. Org. Chem.* **2003**, *68*, 8281.

(11) For example, see: (a) Saunders, M.; Jiménez-Vázquez, H. A.; Bangerter, B. W.; Cross, R. J.; Mroczkowski, S.; Freedberg, D. I.; Anet, F. A. L. *J. Am. Chem. Soc.* **1994**, *116*, 3621. (b) Smith, A. B.; Strongin, R. M.; Brard, L.; Romanow, W. J.; Saunders, M.; Jiménez-Vázquez, H. A.; Cross, R. J. *J. Am. Chem. Soc.* **1994**, *116*, 10831. (c) Smith, A. B.; Strongin, R. M.; Brard, L.; Furst, G. T.; Atkins, J. H.; Romanow, W. J.; Saunders, M.;

Jiménez-Vázquez, H. A.; Owens, K. G.; Goldschmidt, R. J. *J. Org. Chem.* **1996**, *61*, 1904. (d) Cross, R. J.; Jiménez-Vázquez, H. A.; Lu, Q.; Saunders, M.; Schuster, D. I.; Wilson, S. R.; Zhao, H. *J. Am. Chem. Soc.* **1996**, *118*, 11454. (e) Rüttimann, M.; Haldimann, R. F.; Isaacs, L.; Diederich, F.; Khong, A.; Jiménez-Vázquez, H. A.; Cross, R. J.; Saunders, M. *Chem. Eur. J.* **1997**, *3*, 1071. (f) Birkett, P. R.; Bühl, M.; Khong, A.; Saunders, M.; Taylor, R. *J. Chem. Soc., Perkin Trans. 2* **1999**, 2037. (g) Nossal, J.; Saini, R. K.; Sadana, A. K.; Bettinger, H. F.; Alemany, L. B.; Scuseria, G. E.; Billups, W. E.; Saunders, M.; Khong, A.; Weisemann, R. *J. Am. Chem. Soc.* **2001**, *123*, 8482.

(12) For example, see: (a) Haddon, R. C. *Phys. Rev. B* **1994**, *50*, 16459. (b) Bühl, M. *Chem. Eur. J.* **1998**, *4*, 734. (c) Shabtai, E.; Weitz, A.; Haddon, R. C.; Hoffman, R. E.; Rabinovitz, M.; Khong, A.; Cross, R. J.; Saunders, M.; Cheng, P.-C.; Scott, L. T. *J. Am. Chem. Soc.* **1998**, *120*, 6389. (d) Sternfeld, T.; Hoffman, R. E.; Thilgen, C.; Diederich, F.; Rabinovitz, M. *J. Am. Chem. Soc.* **2000**, *122*, 9038. (e) Buhl, M.; Hirsch, A. *Chem. Rev.* **2001**, *101*, 1153. (f) Sternfeld, T.; Hoffman, R. E.; Saunders, M.; Cross, R. J.; Syamala, M. S.; Rabinovitz, M. *J. Am. Chem. Soc.* **2002**, *124*, 8786. (g) Sternfeld, T.; Saunders, M.; Cross, R. J.; Rabinovitz, M. *Angew. Chem. Int. Ed.* **2003**, *42*, 3136.

(13) (a) Hirsch, A. *The Chemistry of Fullerenes*; Thieme Verlag: Stuttgart, 1994. (b) Diederich, F.; Thilgen, C. *Science* **1996**, *271*, 317. (c) Diederich, F.; Kessinger, R. *Acc. Chem. Res.* **1999**, *32*, 537. (d) Hirsch, A. *Angew. Chem. Int. Ed.* **2001**, *40*, 1195. (e) Hirsch, A. *Fullerenes and Related Structures*; Topics in Current Chemistry 199; Springer: Berlin, 1999. (f) Taylor, R. *Synlett* **2000**, 776. (g) Taylor, R. *Lecture Notes on Fullerene Chemistry*: *A Handbook for Chemists*; Imperial College Press: London, 1999.

(14) (a) Prato, M.; Li, Q.; Wudl, F.; Lucchini, V. *J. Am. Chem. Soc.* **1993**, *115*, 1148. (b) Lamparth, I.; Nuber, B.; Schick, G.; Skiebe, A.; Grösser, T.; Hirsch, A. *Angew. Chem. Int. Ed. Engl.* **1995**, *34*, 2257.

(15) Private communication from H. A. Jiménez-Vázquez, R. J. Cross, and M. Saunders. The author is grateful to Professor R. J. Cross and Professor M. Saunders of Yale University for this information.

(16) (a) Hummelen, J. C.; Knight, B.; Pavlovich, J.; González, R.; Wudl, F. *Science* **1995**, *269*, 1554. (b)Keshavarz-K, M.; González, R.; Hicks, R. G.; Srdanov, G.; Srdanov, V. I.;

Collins, T. G.; Hummelen, J. C.; Bellavia-Lund, C.; Pavlovich, J.; Wudl, F.; Karoly, H. *Nature* **1996**, *383*, 147. (c) Hummelen, J. C.; Bellavia-Lund, C.; Wudl, F. *Top. Curr. Chem.* **1999**, *199*, 93.

(17) (a) Arce, M.-J.; Viado, A. L.; An, Y.-Z.; Khan, S. I.; Rubin, Y. *J. Am. Chem. Soc.* **1996**, *118*, 3775. (b) An, Y.-Z.; Ellis, G. A.; Viado, A. L.; Rubin, Y. *J. Org. Chem.* **1995**, *60*, 6353.

(18) Edwards, C. M.; Butler, I. S.; Qian, W.; Rubin, Y. *J. Mol. Struct.* **1998**, *442*, 169.

(19) Hsiao, T.-Y.; Santhosh, K. C.; Liou, K.-F.; Cheng, C.-H. *J. Am. Chem. Soc.* **1998**, *120*, 12232.

(20) (a) Inoue, H.; Yamaguchi, H.; Suzuki, T.; Akasaka, T.; Murata, S. *Synlett* **2000**, 1178. (b) Iwamatsu, S.-i.; Vijayalakshimi, P. S.; Hamajima, M.; Suresh, C. H.; Koga, N.; Suzuki, T.; Murata, S. *Org. Lett.* **2002**, *4*, 1217.

(21) Murata, Y.; Kato, N.; Komatsu, K. *J. Org. Chem.* **2001**, *66*, 7235.

(22) Inoue, H.; Yamaguchi, H.; Iwamatsu, S.-i.; Uozaki, T.; Suzuki, T.; Akasaka, T.; Nagase, S.; Murata, S. *Tetrahedron Lett.* **2001**, *42*, 895.

(23) Murata, Y.; Komatsu, K. *Chem. Lett.* **2001**, *30*, 896.

(24) Schick, G.; Jarrosson, T.; Rubin, Y. *Angew. Chem. Int. Ed.* **1999**, *38*, 2360.

(25) Rubin, Y.; Jarrosson, T.; Wang, G.-W.; Bartberger, M. D.; Houk, K. N.; Schick, G.; Saunders, M.; Cross, R. J. *Angew. Chem. Int. Ed.* **2001**, *40*, 1543.

(26) Iwamatsu, S.-i.; Ono, F.; Murata, S. *Chem. Commun.* **2003**, 1268.

(27) (a) Iwamatsu, S.-i.; Ono, F.; Murata, S. *Chem. Lett.* **2003**, *32*, 614. (b) Vougioukalakis, G. C.; Prassides, K.; Campanera, J. M.; Heggie, M. I.; Orfanopoulos, M.; *J. Org. Chem.* **2004**, *69*, 4524.

(28) Iwamatsu, S.-i.; Uozaki, T.; Kobayashi, K.; Re, S.; Nagase, S.; Murata, S. *J. Am. Chem. Soc.* **2004**, *126*, 2668.

(29) Iwamatsu, S.-i.; Murata, S. *Tetrahedron Lett.* **2004**, *45*, 6391.

(30) (a) Murata, Y.; Suzuki, M.; Rubin, Y.; Komatsu, K. *Bull. Chem. Soc. Jpn.* **2003**, *76*, 1669. (b) Murata, Y.; Suzuki, M.; Komatsu, K. *Chem. Commun.* **2001**, 2338.

(31) For example, see: (a) Wang, G.-W.; Komatsu, K.; Murata, Y.; Shiro, M. *Nature* **1997**, *387*, 583. (b) Komatsu, K.; Wang, G.-W.; Murata, Y.; Tanaka, T.; Fujiwara, K.; Yamamoto, K.;

Saunders, M. *J. Org. Chem.* **1998**, *63*, 9358. (c) Murata, Y.; Kato, N.; Fujiwara, K.; Komatsu, K. *J. Org. Chem.* **1999**, *64*, 3483. (d) Komatsu, K.; Fujiwara, K.; Murata, Y. *Chem. Commun.* **2000**, 1583.

(32) (a) Birkett, P. R.; Avent, A. G.; Darwish, A. D.; Kroto, H. W.; Taylor, R.; Walton, D. R. M. *J. Chem. Soc., Chem. Commun.* **1995**, 1869. (b) Hasharoni, K.; Bellavia-Lund, C.; Keshavarz-K, M.; Srdanov, G.; Wudl, F. *J. Am. Chem. Soc.* **1997**, *119*, 11128.

(33) (a) Khong, A.; Jiménez-Vázquez, H. A.; Saunders, M.; Cross, R. J.; Laskin, J.; Peres, T.; Lifshitz, C.; Strongin, R.; Smith, A. B. *J. Am. Chem. Soc.* **1998**, *120*, 6380. (b) Laskin, J.; Peres, T.; Lifshitz, C.; Saunders, M.; Cross, R. J.; Khong, A. *Chem. Phys. Lett.* **1998**, *285*, 7. (c) Peres, T.; Cao, B.; Cui, W.; Khong, A.; Cross, R. J.; Saunders, M.; Lifshitz, C. *Int. J. Mass Spectrom.* **2001**, *210*, 241.

Chapter 1

Reaction of Fullerene C_{60} with 4,6-Dimethyl-1,2,3-Triazine: Formation of an Open-Cage Fullerene Derivative

Abstract: A thermal liquid-phase reaction of fullerene C_{60} with 4,6-dimethyl-1,2,3-triazine was investigated at 180 °C in *o*-dichlorobenzene. An aza-cyclohexadiene-fused C_{60} derivative and a new open-cage fullerene derivative with a carbonyl group on the rim of the eight-membered-ring opening were obtained in the yield of 10% and 7%, respectively. The former product is supposed to have been produced by the reaction of C_{60} with in situ generated azete (2,4-dimethylazacyclobutadiene). The latter is considered to have been formed through multistep rearrangements followed by hydrolysis on silica gel. The open-cage fullerene **13** underwent facile ring-enlargement under photochemical conditions by the reaction with singlet oxygen leading to the formation of open-cage fullerene **25** with a 12-membered-ring orifice as a single product. The experimental results are supported by theoretical calculations.

Introduction

As mentioned in General Introduction, systematic studies have been conducted in the author's group on the reactions of fullerene C_{60} with nitrogen-containing (diaza or tetraaza) aromatic compounds.[1] A liquid-phase reaction of C_{60} with phthalazine (**1**) in 1-chloronaphthalene at 255 °C gave an open-cage fullerene derivative **2** with an eight-membered-ring orifice, while a mechanochemical solid-state reaction of the same reactants under high-speed vibration milling (HSVM) conditions followed by heating at 200 °C afforded bisfullerene compound **3** with two C_{60} cages incorporated in a benzobicyclo[2.2.2]octene framework.[1a] On the other hand, the HSVM treatment of C_{60} with 3,6-di-(2-pyridyl)-1,2,4,5-tetrazine (**4**) gave adduct **5** as a single product in more than 90% yield. Compound **5** could undergo further [4+2] cycloaddition with another molecule of C_{60} under the HSVM conditions followed by heating at 150 °C to give bisfullerene compound **6** with two C_{60} cages incorporated in a 2,3-diazabicyclo[2.2.2]oct-2-ene framework.[1b,c]

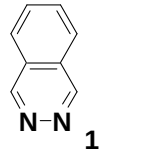

1

2

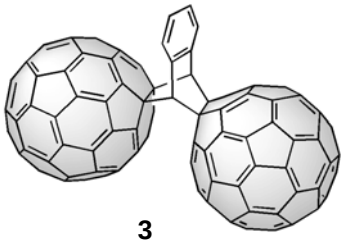

3

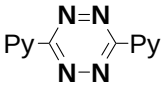

4

(Py = 2-pyridyl)

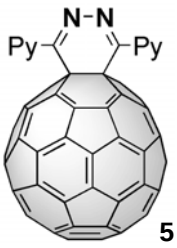

5

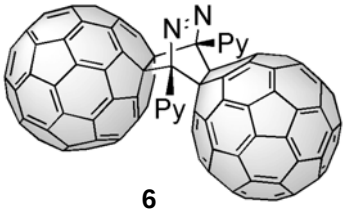

6

4,6-Dimethyl-1,2,3-triazine (**7**) is a triaza-aromatic compound, which is known to be electron-deficient,[2] and therefore its reactivity in [4+2] cycloaddition with an electron-deficient dienophile such as fullerene C_{60}[3] should be low. However, when compound **7** was heated at 180 °C, highly reactive azacyclobutadiene **8** called azete was

reported to be generated by an extrusion of a nitrogen molecule (Scheme 1).[2,4] Thus, it was expected that the thermal reaction of C_{60} with compound **7** would afford azacyclohexadiene-fused C_{60} derivatives such as **9** and **10** by the reaction with in situ generated azete **8**. Then, **9** and **10** might subsequently undergo intramolecular formal [4+4] cycloaddition followed by [2+2+2] cycloreversion under photochemical conditions to give aza-open-cage fullerene derivatives **11** and **12** with an eight-membered-ring orifice.[1a,5-7] By introducing a nitrogen atom into the fullerene cage, electronic properties and the chemical reactivity of the fullerene cage would be altered.[8] In an attempt to synthesize the aza-open-cage fullerenes, we carried out the reaction of C_{60} with 1,2,3-triazine **7**, the results of which are described herein.

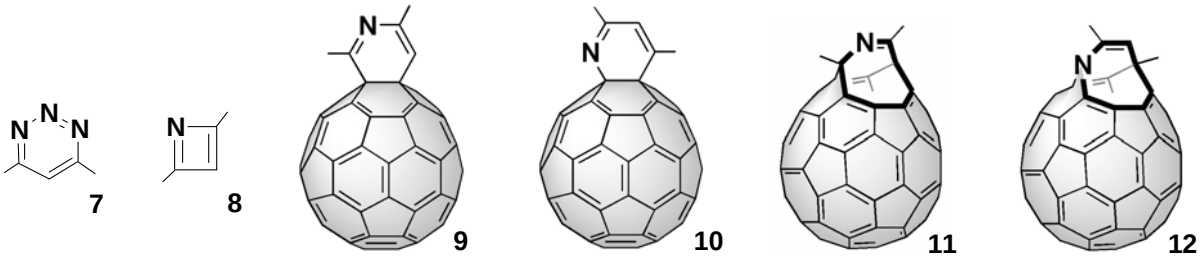

Results and Discussion

The reaction was conducted by heating a solution of fullerene C_{60} with 3 equivalents of 4,6-dimethyl-1,2,3-triazine (**7**)[2d] in *o*-dichlorobenzene (ODCB) at 180 °C for 24 h to afford a dark brown solution with the formation of an insoluble dark brown material (ca. 40% of the total weight of the product). The soluble portion of the reaction mixture was subjected to flash chromatography over silica gel to give two products, **9** (10%) and **13** (7%), as brown powders, together with unreacted C_{60} (30%) (Scheme 1). The structures of the two products were determined as an azacyclohexadiene-fused C_{60} derivative, i.e., **9**, and, unexpectedly, an open-cage fullerene derivative, i.e., **13**, having no nitrogen atom at an eight-membered-ring orifice, as described below.

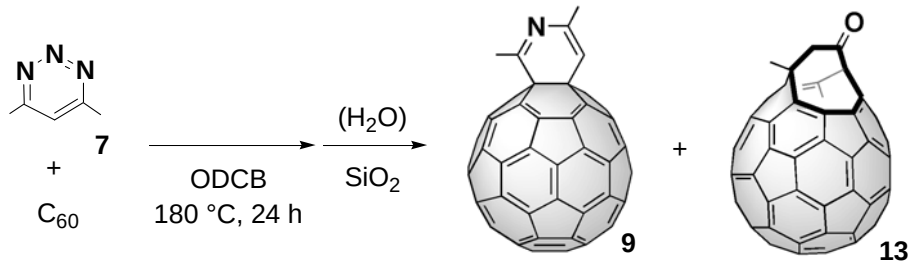

Scheme 1. Thermal reaction of fullerene C_{60} with 4,6-dimethyl-1,2,3-triazine (**7**).

The molecular formula of the first compound was determined as $C_{65}H_7N$ by high-resolution FAB mass spectroscopy, indicating that it was formed by the addition of a C_5H_7N fragment to C_{60}. The ^{1}H NMR exhibited a quartet at δ 6.52 ppm corresponding to an olefinic proton, and doublet and singlet signals of methyl groups at δ 2.64 and 2.52 ppm, respectively. The ^{13}C NMR showed 32 signals in the sp^2-carbon region (including one presumably overlapped signal) and four signals in the sp^3-carbon region at δ 82.38, 60.19, 26.14, and 22.59 ppm. The UV-vis spectrum exhibited a typical absorption pattern of the 1,2-dihydro[60]fullerene derivative characterized by λ_{max} at 433 nm.[9] These data and mechanistic consideration support the structure of this compound to be **9**.

The structural characterization of the second product was not simple and was achieved by comparison of the spectral data with those of open-cage fullerene derivative **14** reported by Rubin and co-workers.[5b] Its molecular formula was determined as $C_{65}H_6O$ by high-resolution FAB mass spectroscopy, indicating that the product has one oxygen atom instead of nitrogen. The IR spectrum showed a strong absorption band at 1723 cm^{-1} indicating the presence of a carbonyl group. The ^{1}H NMR exhibited a doublet at δ 6.50 ppm (J = 1.1 Hz) and a singlet at δ 2.64 ppm, corresponding to a methine proton and methyl protons, respectively. In addition, a doublet at δ 3.29 ppm (J = 20.6 Hz) and a doublet of doublets at δ 2.79 ppm (J = 20.6 Hz and 1.1 Hz) were observed, both corresponding to geminal methylene protons coupled with each other. The ^{13}C NMR showed one signal at δ 200.75 ppm corresponding to a carbonyl carbon, 56 signals in the sp^2-carbon region (with four signals overlapped) and four signals in the sp^3-carbon region at δ 55.24, 46.60, 43.72, and 34.07 ppm. The close resemblance of the chemical shifts of the ^{1}H and ^{13}C NMR as well as the coupling constants of ^{1}H NMR to the reported values for **14** as shown in Figure 1

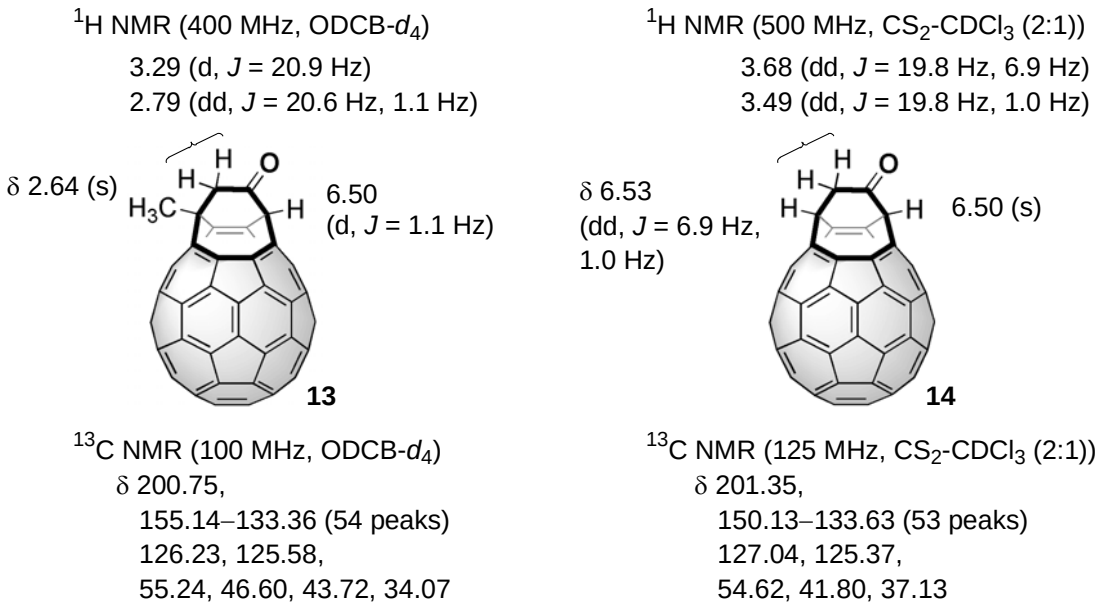

Figure 1. Selected NMR data of **13** and **14**.

strongly supports the structure of this compound as the methyl-substituted derivative of **14**, that is, **13**. The color of the solution of **13** in $CHCl_3$ is purple, and the UV-vis spectrum has a maximum absorption at 533 nm, closely resembling the spectrum of C_{60} and thus indicating that the 60 original fullerene carbons retain their sp^2 hybridization in a π-conjugated system.[5-7]

Plausible mechanisms for the formation of **9** and **13** are shown in Scheme 2. As suggested above, highly reactive azete **8** is generated by thermal extrusion of a nitrogen molecule from **7**[2b,c] and would react with C_{60} in a [4+2] manner to afford intermediate **16**, which gives **9** by ring enlargement. In the case of the formation of **13**, before the generation of azete **8**, diradical **15** is assumed to undergo a 1,3-hydrogen shift to give diradical **17**. The reaction of this diradical with C_{60} is supposed to give imine **18**, which would isomerize to 2-aminodiene **19**. Diene **19** would then undergo intramolecular formal [4+4] cycloaddition to give **20**, followed by the [2+2+2] cycloreversion to produce open-cage enamine **21**, which would be transformed to open-cage imine **22**. Imine **22** is considered to be susceptible to hydrolysis upon contact with trace amount of water in SiO_2 and readily furnishes open-cage ketone **13** after flash chromatography. The relative heats of formation estimated by PM3 calculations are also shown in Scheme 2. The gradual increase in stability observed in

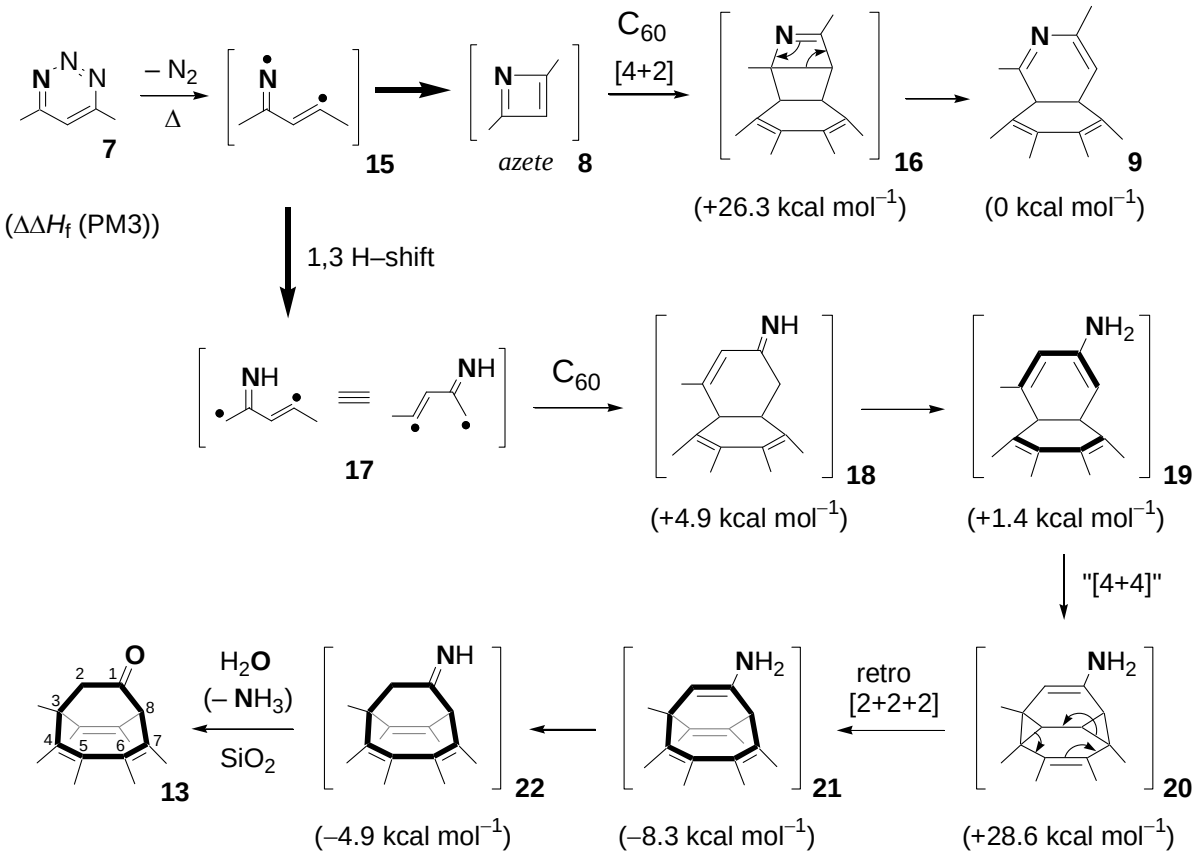

Scheme 2. Possible reaction pathways leading to products **9** and **13**. The relative heat of formation with reference to **9** calculated by PM3 are shown in parentheses.

accord with the progress of the reaction (except for the formation of **20**) is considered to be consistent with the proposed mechanism.

Although it was expected that **9** might rearrange into aza-open-cage fullerene derivative **11** through the formal [4+4] derivative like **20** under photochemical conditions, as has been reported for the carbon analogue,[5a] the irradiation of **9** with a high-pressure mercury lamp with or without heating only gave an insoluble and intractable material. No formation of open-cage fullerene **11** was observed at all.

The open-cage fullerene **13** was sensitive to light and air in a liquid phase and the purple color of the solution in CS_2 turned to brown within 1 h under the irradiation of room light in the presence of oxygen. Thus, a new compound was obtained from **13** as an almost single product after the separation by the use of preparative HPLC equipped with a Cosmosil

5PBB column eluted with ODCB. The structure of this product was determined by the following spectral data and accompanying discussion. The molecular formula was determined as $C_{65}H_6O_3$ by high-resolution FAB mass spectroscopy, indicating that this compound is a product of the addition of two oxygen atoms to **13**. The IR spectrum showed three strong absorption bands at 1741, 1718, and 1697 cm^{-1} indicating the presence of three carbonyl groups. In the ^1H NMR, a large downfield shift of one of the methylene proton's signals was observed (from δ 3.29 ppm for **13** to δ 4.79 ppm for the new product) presumably due to the deshielding by the newly formed carbonyl groups located in close proximity. The ^{13}C NMR showed three signals corresponding to carbonyl carbons at δ 200.42, 198.17 and 193.49 ppm, 52 signals in the sp^2-carbon region (with six signals overlapped), and four signals in the sp^3 carbon region at δ 51.77, 48.61, 47.51, and 37.64 ppm. These data suggest that the product is formed through oxidative cleavage of one of the carbon-carbon double bonds at the orifice of **13** by the reaction with singlet oxygen. It is well recognized that the singlet oxygen is readily generated by the action of the excited fullerene cage by irradiation of visible light.[10]

Prior to this study, there were two reports on the similar oxidative cleavage of the carbon-carbon double bond at the rim of an eight-membered-ring orifice of C_s symmetrical

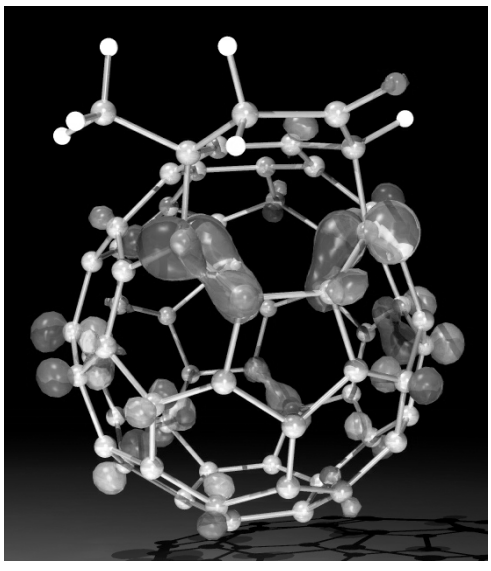

Figure 2. Optimized structure of **13** with HOMO calculated at the B3LYP/6-31G* level.

open-cage fullerene derivatives by the reaction with singlet oxygen.[11] In the case of the C_1 symmetrical molecule **13**, there are two different carbon-carbon double bonds at "C4–C5" and "C6–C7" positions, which were expected to be cleaved. In order to gain insight into the reactivity of **13**, the DFT calculations were carried out at the B3LYP/6-31G* level to indicate that the HOMO of **13** was localized primarily at the two double bonds, i.e., C4–C5 and C6–C7, as expected (Figure 2). However, as the absolute values of the HOMO's coefficients of C4–C5 (–0.32 and –0.27) are calculated to be slightly larger than those of C7–C6 (+0.32 and +0.24), singlet oxygen should preferentially attack the C4–C5 double bond. In order to confirm the structure of the product, DFT calculations for the open-cage fullerene derivatives **25** and its positional isomer **26**, as well as the dioxetane intermediates **23** and **24** at the B3LYP/6-31G* level were conducted (Scheme 3).[12] As the result, the relative energy of thus obtained **25** was calculated to be lower than that of **26** by 4.71 kcal mol^{-1}. Dioxetane intermediate **23** was also shown to be more stable than **24** by 1.04 kcal mol^{-1}.

In order to confirm the structural assignment of **25** based on the ^{13}C NMR spectrum, the GIAO (SCF/6-31G*//B3LYP/6-31G*) calculations were performed for both **25** and **26**. As shown in Figure 3, the calculated spectrum of **25** more closely resembles the experimental

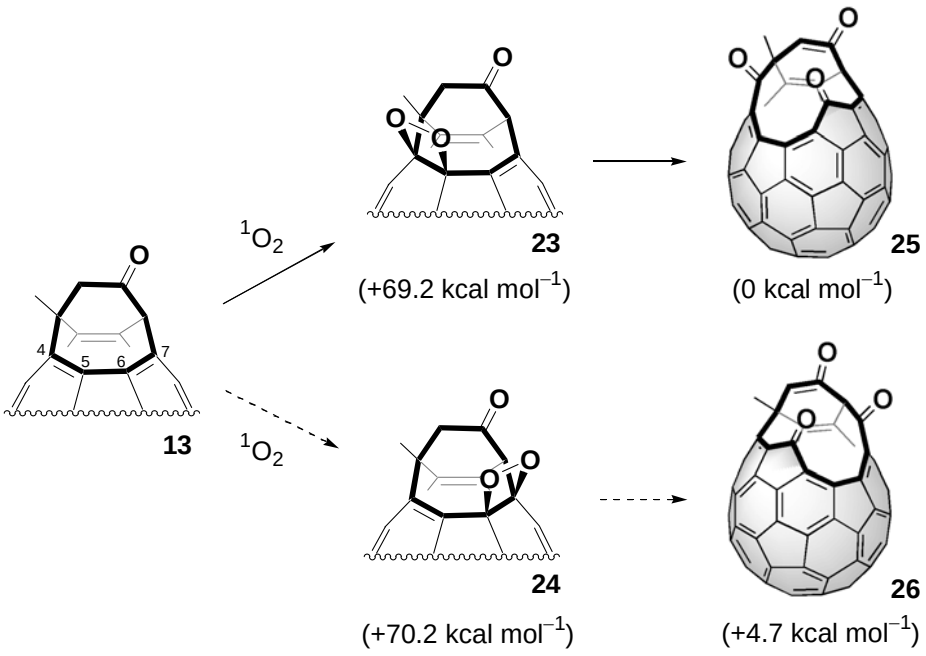

Scheme 3. Reaction of **13** with singlet oxygen. The relative energy with reference to **25** calculated by B3LYP/6-31G* are shown in parentheses.

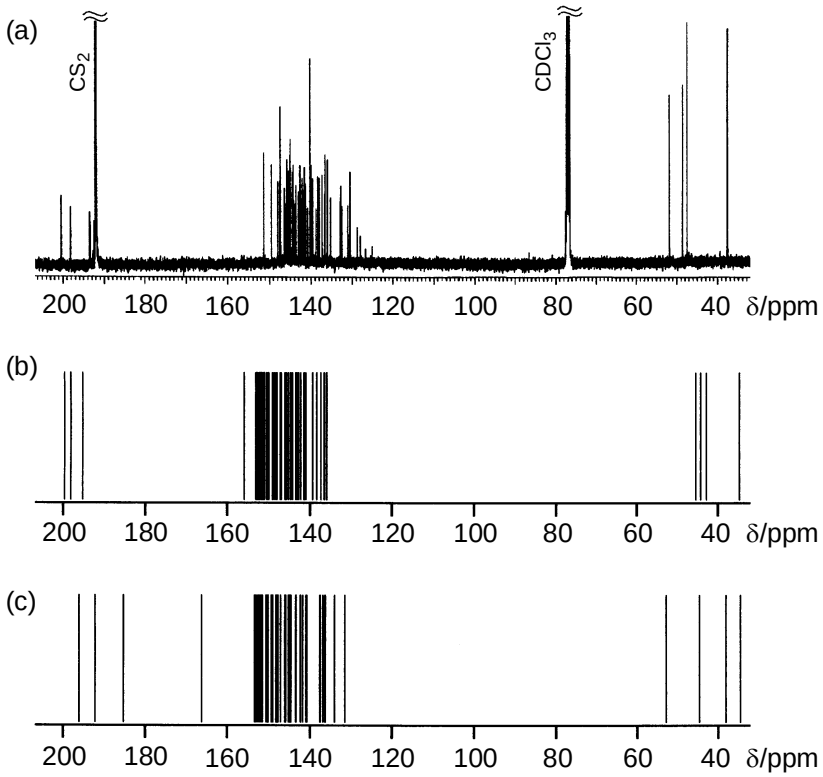

Figure 3. (a) Observed (100 MHz, CS_2-$CDCl_3$ (1:1)) ^{13}C NMR spectrum of **25**. Calculated (GIAO (SCF/6-31G*//B3LYP-6-31G*) ^{13}C NMR spectra of (b) **25** and (c) **26**.

spectrum than does that of **26**. These results of calculations also support the structure of the oxidation product as **25** with a 12-membered-ring orifice on the C_{60} cage.

Conclusion

It was demonstrated that a thermal reaction of fullerene C_{60} with 4,6-dimethyl-1,2,3-triazine causes a competition between the reaction of C_{60} with azete **8** and with rearranged 1,4-diradical intermediate **17**. The former reaction gave azacyclohexadiene-fused derivative **5** via [4+2] cycloaddition, while the latter reaction afforded an unexpected open-cage fullerene derivative **13** by multistep rearrangements and hydrolysis on silica gel. It is rather surprising that such multistep rearrangements could take

place in a one-pot reaction and in a single chromatography column. Theoretical calculations were performed for some of the reaction intermediates and products, supporting the experimentally obtained results quite well. A facile oxidation of derivative **13** was found to take place to give open-cage fullerene derivative **25** with a 12-membered-ring orifice on the fullerene cage.

Experimental Section

General. The ^{1}H and ^{13}C NMR measurements were carried out on a Varian Mercury 300 instrument and JEOL AL-400 instrument and the chemical shifts are reported in ppm with reference to tetramethylsilane. In some cases, the signal of *o*-dichlorobenzene-d_4 (ODCB-d_4) was used as an internal standard (δ 7.20 ppm in ^{1}H NMR, and δ 132.35 ppm in ^{13}C NMR). Preparative HPLC was conducted using a Cosmosil 5PBB column (10 mm × 250 mm) with ODCB as an eluent, detected at 326 nm. Fullerene C_{60} was purchased from Matsubo Co. 4,6-Dimethyl-1,2,3-triazine (**4**) was synthesized by a reported procedure.[2d]

Computational Method. The PM3 calculations were performed using the MOPAC 6.0 semiempirical molecular orbital package on a CRAY T94/4128 computer. All other calculations were performed with the Gaussian 98 series of electronic structure program.[12]

Synthesis of 9 and 13. A solution of C_{60} (133 mg, 0.184 mmol) and 4,6-dimethyl-1,2,3-triazine (**4**) (60 mg, 0.55 mmol) in ODCB (9 mL) was heated at 180 °C for 24 h to give a dark brown solution and some insoluble material. The reaction mixture was subjected to a flash chromatography over silica gel eluted with CS_2 to give unchanged C_{60} (40 mg, 0.056 mmol, 30%) and **9** (14 mg, 0.018 mmol, 10%), and then with toluene to give **13** (10 mg, 0.013 mmol, 7%) as brown powders.

9: IR (KBr) ν 1678 (C=N), 1429, 851, 752, 527 cm^{-1}; UV-vis ($CHCl_3$) λ_{max} (log ε) 258 (5.05), 313 (4.57), 433 (3.50), 698 (2.53) nm; ^{1}H NMR (300 MHz, CS_2–acetone-d_6 (7:1)) δ 6.52 (q, J =1.5 Hz, 1H), 2.64 (d, J = 1.5 Hz, 3H), 2.52 (s, 3H); ^{13}C NMR (75 MHz, CS_2–acetone-d_6 (7:1)) δ 159.35, 153.03, 148.80, 147.86, 147.72, 146.44, 146.35, 146.27, 146.01, 145.97, 145.85, 145.27, 145.25, 145.20, 145.12, 144.65, 144.06, 142.89, 142.52, 142.36, 142.25, 142.03, 141.99, 141.70, 141.47, 140.68, 140.31, 139.46, 138.91, 134.70,

133.02, 119.12, 82.38, 60.19, 26.41, 22.59; HR MS (+FAB) calcd for $C_{65}H_8N$ (MH^+), 802.0657, found 802.0648.

13: IR (KBr) ν 1723 (C=O), 1509, 544, 537 cm^{-1}; UV-vis ($CHCl_3$) λ_{max} (log ε) 261 (5.02), 329 (4.54), 533 (3.02) nm; ^{1}H NMR (400 MHz, ODCB-d_4) δ 6.50 (d, J = 1.1 Hz, 1H), 3.29 (d, J = 20.6 Hz, 1H), 2.79 (dd, J = 20.6 and 1.1 Hz, 1H), 2.64 (s, 3H); ^{13}C NMR (100 MHz, ODCB -d_4) δ 200.75, 155.14, 149.29, 145.53, 145.44, 145.36, 145.23, 145.21, 144.65, 144.56, 144.55, 144.51, 144.32, 144.26, 144.20, 144.13, 144.11, 144.03, 144.00, 143.79, 143.76, 143.70, 143.66, 143.57, 143.52, 143.48, 143.44, 143.32, 143.30, 143.15, 143.13, 142.92, 141.70, 141.08, 140.74, 140.59, 140.49, 140.39, 140.19, 140.10, 139.94, 139.77, 138.90, 138.46, 137.97, 137.92, 137.04, 136.99, 136.86, 136.28, 135.09, 134.40, 134.12, 133.75, 133.36, 126.23, 125.58, 55.24, 46.60, 43.72, 34.07 (the signals at the range of δ 132.4 ~ 126.8 were overlapped with the signals of ODCB-d_4); HR MS (+FAB) calcd for $C_{65}H_6O$ (M^+), 802.0418, found 802.0414.

Synthesis of 25. An air-saturated solution of **13** (10 mg, 0.013 mmol) in CS_2 (30 mL) was stirred at room temperature under the irradiation of room light for 1 h. The color of the solution changed gradually from purple to brown. After removal of the solvent, the residue was purified by HPLC on a 5PBB column eluted with ODCB to afford **25** (7 mg, 0.0078 mmol, 60%) as a brown powder.

25: IR (KBr) ν 1741 (C=O), 1718 (C=O), 1697 (C=O), 553, 528 cm^{-1}; UV-vis ($CHCl_3$) λ_{max} (log ε) 257 (5.04), 325 (4.62), 424 (3.63) nm; ^{1}H NMR (300 MHz, CS_2–$CDCl_3$ (1:1)) δ 5.93 (s, 1H), 4.79 (d, J = 18.5 Hz, 1H), 3.02 (d, J = 18.5 Hz, 1H), 2.23 (s, 3H); ^{13}C NMR (100 MHz, CS_2–$CDCl_3$ (1:1)) δ 200.42, 198.17, 193.49, 151.39, 149.54, 148.06, 147.62, 147.42, 146.41, 146.38, 145.92, 145.88, 145.85, 145.57, 145.49, 145.43, 146.37, 145.29, 145.15, 145.13, 145.10, 145.01, 144.50, 144.27, 144.18, 143.78, 143.64, 142.97, 142.67, 142.20, 142.12, 142.08, 141.59, 141.55, 141.32, 140.84, 140.26, 140.23, 139.95, 139.90, 139.70, 139.55, 138.81, 138.34, 138.00, 137.28, 136.66, 136.60, 135.98, 135.22, 132.85, 132.71, 132.42, 131.02, 130.50, 51.77, 48.61, 47.51, 37.64; HR MS (+FAB) calcd for $C_{65}H_7O_3$ (MH^+), 835.0395, found 835.0403.

References and Notes

(1) (a)Murata, Y.; Kato, N.; Komatsu, K. *J. Org. Chem.* **2001**, *66*, 7235. (b) Murata, Y.; Suzuki, M.; Rubin, Y.; Komatsu, K. *Bull. Chem. Soc. Jpn.* **2003**, *76*, 1669. (c) Murata, Y.; Suzuki, M.; Komatsu, K. *Chem. Commun.* **2001**, 2338.

(2) (a) Neunhoeffer, N. In *Methods of Organic Chemistry: Houben-Weyl*; Schaumann, E., Ed.; Georg Thieme, 1998; Vol. E 9c, p 530 and references therein. (b) Itoh, T.; Okada, M.; Nagata, K.; Yamaguchi, K.; Ohsawa, A. *Chem. Pharm. Bull.* **1990**, *38*, 2108. (c) Itoh, T.; Ohsawa, A.; Okada, M.; Kaihoh, T.; Igeta, H. *Chem. Pharm. Bull.* **1985**, *33*, 3050. (d) Ohsawa, A.; Arai, H.; Ohnishi, H.; Itoh, T.; Kaihoh, T.; Okada, M.; Igeta, H. *J. Org. Chem.* **1985**, *50*, 5520.

(3) (a) Hirsch, A. *The Chemistry of the Fullerenes*; Thieme: New York, 1994. (b) Hirsch, A.; Brettreich, M. *Fullerenes: Chemistry and Reactions*; Wiley-VCH Verlag GmbH & Co. KGaA: Weinheim, 2005.

(4) (a) Regitz, M.; Lenoir, D.; Lippert, T. In *Methoden der Organischen Chemie: Houben-Weyl*; Klamann, D., Ed.; Georg Thieme Verlag: Stuttgart, New York, 1992; Vol. E 16c, p 936. (b) Regitz, M.; Bergstäßer, U. In *Science of Synthesis: Houben-Weyl Methods of Molecular Transformations*; Maas, G., Ed., Georg Thieme Verlag: Stuttgart, New York, 2001; Vol. 9, p 135.

(5) (a) Arce, M.-J.; Viado, A. L.; An, Y.-Z.; Khan, S. I.; Rubin, Y. *J. Am. Chem. Soc.* **1996**, *118*, 3775. (b) Qian, W.; Bartberger, M. D.; Pastor, S. J.; Houk, K. N.; Wilkins, C. L.; Rubin, Y. *J. Am. Chem. Soc.* **2000**, *122*, 8333.

(6) Hsiao, T.-Y.; Santhosh, K. C.; Liou, K.-F.; Cheng, C.-H. *J. Am. Chem. Soc.* **1998**, *120*, 12232.

(7) Inoue, H.; Yamaguchi, H.; Suzuki, T.; Akasaka, T.; Murata, S. *Synlett* **2000**, 1178.

(8) For examples of derivatives of $C_{59}N$, see: (a) Hummelen, J. C.; Knight, B.; Pavlovich, J.; González, R.; Wudl, F. *Science* **1995**, *269*, 1554. (b) Keshavarz-K., M.; González, R.; Hicks, R. G.; Srdanov, G.; Srdanov, V. I.; Collins, T. G.; Hummelen, J. C.; Bellavia-Lund, C.; Pavlovich, J.; Wudl, F.; Holczer, K. *Nature* **1996**, *383*, 147. (c) Bellavia-Lund, C.; González, R.; Hummelen, J. C.; Hicks, R. G.; Sastre, A.; Wudl, F. *J. Am. Chem. Soc.* **1997**, *119*, 2946. (d) Nuber, B.; Hirsch, A. *Chem. Commun.* **1998**, 405. (e) Reuther, U.;

Hirsch, A. *Chem*. *Commun*. **1998**, 1401. (f) Hirsch, A.; Nuber, B. *Acc*. *Chem*. *Res*. **1999**, *32*, 795. (g) Hauke, F.; Hirsch, A. *Tetrahedron* **2001**, *57*, 3697 and references therein.

(9) For example, see: (a) Murata, Y.; Kato, N.; Fujiwara, K.; Komatsu, K. *J*. *Org*. *Chem*. **1999**, *64*, 3483. (b) Murata, Y.; Komatsu, K.; Wan, T. S. M. *Tetrahedron Lett*. **1996**, *37*, 7061. (c) Hirsch, A.; Grösser, T.; Skiebe, A.; Soi, A. *Chem*. *Ber*. **1993**, *126*, 1061.

(10) (a) Arbogast, J. W.; Darmanyan, A. P.; Foote, C. S.; Rubin, Y.; Diederich, F. N.; Alvarez, M. M.; Anz, S. J.; Whetten, R. L. *J*. *Phys*. *Chem*. **1991**, *95*, 11-12. (b) Arbogast, J. W.; Foote, C. S. *J*. *Am*. *Chem*. *Soc*. **1991**, *113*, 8886. (c) Foote, C. S. *Top*. *Curr*. *Chem*. **1994**, *169*, 347.

(11) (a) Inoue, H.; Yamaguchi, H.; Iwamatsu, S.; Uozaki, T.; Suzuki, T.; Akasaka, T.; Nagase, S.; Murata, S. *Tetrahedron Lett*. **2001**, *42*, 895. (b) Murata, Y.; Komatsu, K. *Chem*. *Lett*. **2001**, 896.

(12) Frisch, M. J.; Trucks, G. W.; Schlegel, H. B.; Scuseria, G. E.; Robb, M. A.; Cheeseman, J. R.; Zakrzewski, V. G.; Montgomery, H. A., Jr.; Stratmann, R. E.; Burant, J. C.; Dapprich, S.; Millam, J. M.; Daniels, A. D.; Kudin, K. N.; Strain, M. C.; Farkas, O.; Tomasi, J.; Barone, V.; Cossi, M.; Cammi, R.; Mennucci, B.; Pomelli, C.; Adamo, C.; Clifford, S.; Ochterski, J.; Petersson, G. A.; Ayala, P. Y.; Cui, Q.; Morokuma, K.; Malick, D. K.; Rabuck, A. D.; Raghavachari, K.; Foresman, J. B.; Cioslowski, J.; Ortiz, J. V.; Baboul, A. G.; Stefanov, B. B.; Liu, G.; Liashenko, A.; Piskorz, P.; Komaromi, I.; Gomperts, R.; Martin, R. L.; Fox, D. J.; Keith, T.; Al-Laham, M. A.; Peng, C. Y.; Nanayakkara, A.; Gonzalez, C.; Challacombe, M.; Gill, P. M. W.; Johnson, B.; Chen, W.; Wong, M. W.; Andres, J. L.; Gonzalez, C.; Head-Gordon, M.; Replogle, E. S.; Pople, J. A. *Gaussian 98, Revision A.7*; Gaussian, Inc.: Pittsburgh, PA, 1998.

Chapter 2

Synthesis, Structure, and Properties of Novel Open-Cage Fullerenes Having Heteroatom(s) on the Rim of the Orifice

Abstract: A thermal reaction of fullerene C_{60} with 3-(2-pyridyl)-5,6-diphenyl-1,2,4-triazine (**1**) afforded aza-open-cage fullerene **2** having a nitrogen atom on the rim of an eight-membered-ring orifice. Compound **2** underwent oxidative ring-enlargement by the reaction with singlet oxygen to give aza-dioxo-open-cage fullerenes **6** and its isomer **7**, both of which have a 12-membered-ring orifice, as the primary products. It was then found that the orifice of **6** could be effectively enlarged by a reaction with elemental sulfur in the presence of tetrakis(dimethylamino)ethylene, serving as a π-donating agent for **6**, to give novel aza-dioxo-thia-open-cage fullerene **12** having a 13-membered-ring orifice. The structure of **12** was unambiguously determined by X-ray crystallography. The ring-expanding reactions were rationalized based on the results of molecular orbital calculations. Upon electrochemical measurements, compounds **6** and **7** were found to be more readily reducible than C_{60} by about 0.2 V due to the existence of two carbonyl groups on the rim of the orifice.

Introduction

As mentioned in General Introduction and in Chapter 1, the liquid-phase thermal reaction of fullerene C_{60} with nitrogen-containing aromatic compounds[1] such as phthalazine[1a] and 4,6-dimethyl-1,2,3-triazine[1b] afforded new derivatives of open-cage fullerenes. It should be noted that the open-cage fullerenes with an eight-membered-ring orifice are readily obtained in an one-pot thermal reaction in our works, while synthetic methods developed by other groups consisted of more than one step including photo-irradiation.[2]

In the course of the investigations of thermal reactions of C_{60} with various triazines such as 4-methoxy-1,2,3-benzotriazine, 4-methyl-1,2,3-triazine, and 3-amino-1,2,4-triazine, it was found that the reaction with 5,6-diphenyl-3-(2-pyridyl)-1,2,4-triazine (**1**) could efficiently yield a desired aza-open-cage fullerene with an eight-membered-ring orifice including an unsaturated nitrogen atom on the rim of the opening. Furthermore, by developing novel reactions for stepwise enlargement of the orifice sizes, the author succeeded in obtaining a series of new open-cage fullerene derivatives with 10-, 12-, and 13-membered-ring orifices containing hetero-atom(s) such as nitrogen, oxygen, and sulfur on the rim of the openings. In this chapter, the synthesis, structure, and properties of a series of these newly formed derivatives of open-cage fullerenes are described.

Results and Discussion

Open-cage fullerene derivatives having an eight-membered-ring orifice: A thermal reaction was carried out by heating a solution of C_{60} with one equivalent of 1,2,4-triazine **1** in *o*-dichlorobenzene (ODCB) at 180 °C for 17 h (Scheme 1). The reaction proceeded smoothly to afford almost a single product, exhibiting a purple color in solution, together with unreacted C_{60} in 41% recovery. The structure of the product, which was highly soluble in common organic solvents such as $CHCl_3$, toluene, CS_2, and ODCB due to the presence of phenyl and pyridyl substituents, was determined as an aza-open-cage fullerene derivative **2** having an eight-membered-ring orifice, based on the characterization as described below. The isolated yield of **2** was 50% (85% based on consumed C_{60}).

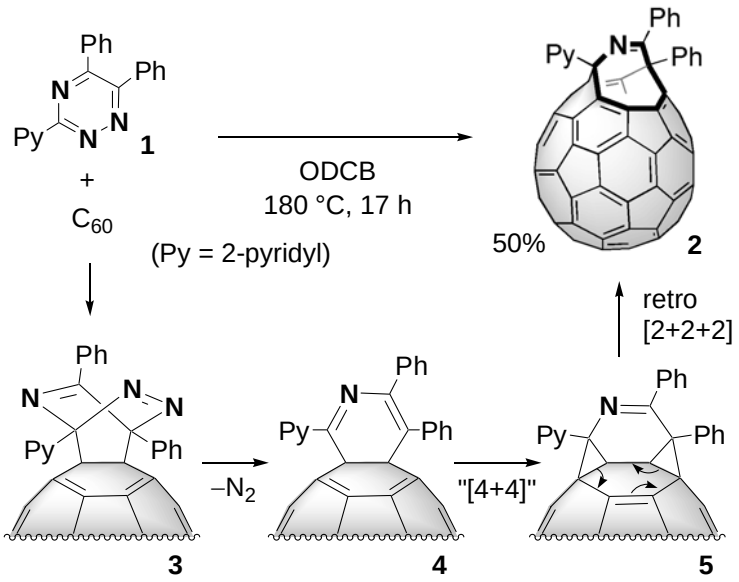

Scheme 1. Formation of open-cage fullerene derivative **2**.

The structure determination of the open-cage fullerene **2** was first attempted based on spectral information. The high-resolution FAB mass spectrum showed the molecular ion peak at *m*/*z* 1003 (MH^+) corresponding to M = $C_{80}H_{14}N_2$, clearly indicating that **2** is formed by addition of 1,2,4-triazine **1** to C_{60} followed by extrusion of N_2. The ^1H NMR spectrum displayed the signals for aromatic protons only, while the ^{13}C NMR spectrum showed 65 signals in the sp^2-carbon region between δ 167.96 and 122.47 ppm (with nine signals overlapped), in addition to two signals at δ 73.02 and 56.35 ppm for the sp^3-carbon atoms, suggesting that **2** has C_1 symmetry. The purple color observed for the $CHCl_3$ solution of **2** and its maximum absorption at 533 nm in the UV-vis spectrum (closely resembling the spectrum of C_{60}) indicates that the 60 original fullerene carbon atoms retain their sp^2 hybridization in a π-conjugated system.[1a,1b,2]

The structure of **2** was unambiguously determined by X-ray crystallography of a single crystal obtained by slow evaporation of a benzene solution of **2**. As shown in Figure 1, the eight-membered-ring orifice composed of C1-C7 and N1 is present on the fullerene cage of **2**. In the eight-membered ring, the C2–C3 (1.406(4) Å), C4–C5 (1.403(4) Å), and C7–N1 (1.270(4) Å) bonds have double bond character, whereas the others have single bond character. The eight-membered ring is in a tub-form with the C1-C2-C3-C4 and

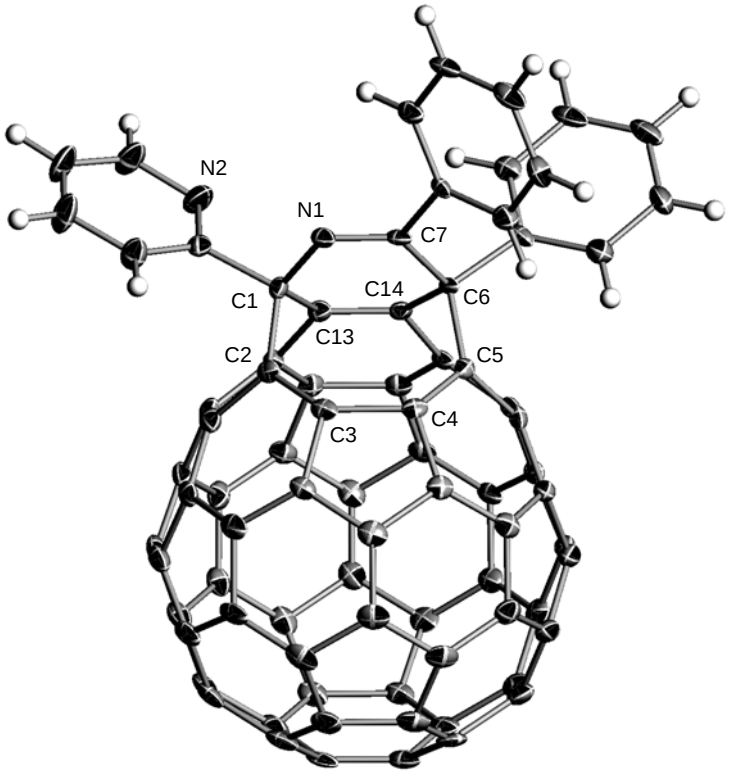

Figure 1. The X-ray structure of open-cage fullerene derivative **2** with displacement ellipsoids drawn at the 50% probability level. Selected distances [Å], bond angles [°], and dihedral angles [°]: C1–C2 1.521(4), C2–C3 1.406(4), C3–C4 1.511(4), C4–C5 1.403(4), C5–C6 1.517(4), C6–C7 1.540(4), C7–N1 1.270(4), N1–C1 1.457(3), C2–C13 2.274(4), C5–C14 2.279(4); C1-C2-C3 124.0(3), C2-C3-C4 129.8(2), C3-C4-C5 128.7(2), C4-C5-C6 124.6(2); C1-C2-C3-C4 –39.0(4) C3-C4-C5-C6 38.8(4), C2-C3-C4-C5 0.4(5).

C3-C4-C5-C6 dihedral angles being –39.0(4)° and 38.8(4)°, respectively, deviating significantly from 0°. The butadiene system, C2-C3-C4-C5, is almost planar with the dihedral angle between the two double bonds being only 0.4(5)°.

A probable reaction mechanism for the formation of **2** is shown in Scheme 1. A [4+2] cycloaddition of 1,2,4-triazine **1** to C_{60} affords **3**, and the following extrusion of N_2 gives 2-aza-1,3-cyclohexadiene-fused C_{60} derivative **4**, which would undergo a formal intramolecular [4+4] cycloaddition to give **5**, and then a [2+2+2] cycloreversion affords **2**.

Enlargement of the orifice in open-cage fullerene 2: As mentioned in Chapter 1, it has been reported both by us and another group that one of the carbon-carbon double bonds in the eight-membered-ring orifice in an open-cage fullerene can undergo oxidative cleavage by the action of photochemically generated singlet oxygen.[1b,3] Since, the carbon-carbon double bonds at "C2–C3" and "C4–C5" positions of **2** are shown to be rather strained by the results of X-ray crystallography, their reactivity should be enhanced.

In order to further gain insight into the reactivity of **2**, DFT calculations were conducted. The geometry of **2** was fully optimized at the B3LYP/6-311G** level of theory[4] to give a structure with the HOMO shape as shown in Figure 2. The HOMO of **2** was found to be localized primarily at the two carbon-carbon double bonds at C2–C3 and C4–C5 positions in the same manner as reported for the carbon analogues,[1b,3] whereas the LUMO was found to be spread over almost all the sp^2-carbon atoms on the fullerene cage. The absolute values of the coefficients of HOMO were 0.33 for C2, 0.22 for C3, 0.21 for C4, and 0.32 for C5. Thus, the electrophilic addition of the singlet oxygen was expected to take place regioselectively on these double bonds.

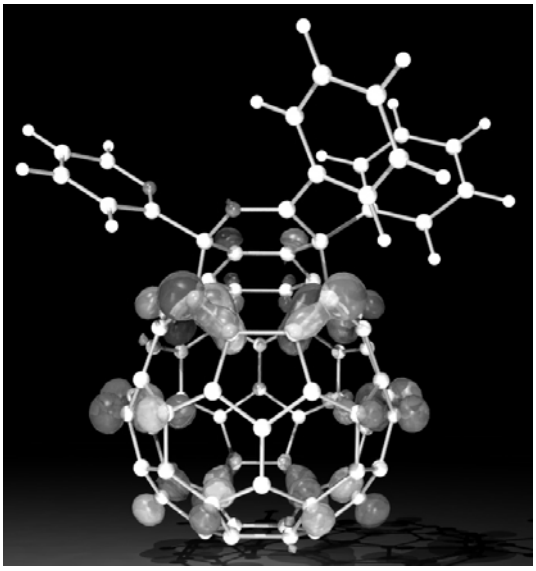

Figure 2. The optimized structure of open-cage fullerene derivative **2** with the contour of the HOMO, calculated at the B3LYP/6-311G** level of theory.

In fact, when an air-saturated solution of **2** in CCl_4 was irradiated with visible light by using a high-pressure mercury lamp for 6 h at room temperature, the color of the solution turned from purple to dark brown. By separating the reaction mixture by the use of HPLC on 5PBB column eluted with ODCB, three oxidation products **6**, **7**, and **8**, all having the molecular formula corresponding to **2** with the addition of O_2 as shown by high-resolution FAB mass spectroscopy, were obtained in 60%, 31%, and 2% yields, respectively. The IR spectra of **6** and **7** exhibited strong carbonyl stretching bands at 1747 and 1748 cm^{-1}, respectively, whereas no carbonyl absorption band was observed for **8**.

Because the full determination of structures of **6**, **7**, and **8** based on spectral information only was quite difficult, each ^{13}C NMR spectrum was simulated by conducting theoretical calculations. In order to confirm the reliability of such simulations, ^{13}C NMR spectrum of **2** was first computed by conducting the gauge-independent atomic orbital (GIAO) calculations[5,6] at various level of theory, and the simulated spectra were compared with the experimental spectrum. The GIAO calculations on **2** were conducted using Hartree-Fock (HF) and density functional theory (B3LYP and B3PW91) methods with both the 6-311G** and TZV basis sets, based on the structure optimized at the B3LYP/6-311G** level of theory.[7] All chemical shifts are given as the values relative to that of tetramethylsilane, also calculated using the same method at the same level of theory as those used for the corresponding GIAO calculations.

As shown in Figure 3a, the experimental ^{13}C NMR spectrum of **2** features two sp^2-carbon signals at δ 167.96 and 164.81 ppm, which are notably downfield shifted, the rest of the sp^2-carbon signals appearing in the range δ 149.10–122.47 ppm (63 signals observed out of 76 expected signals for fullerenyl and aryl carbon atoms), and two sp^3-carbon signals at δ 73.02 and 56.35 ppm. As shown in Figures 3, all six GIAO calculations, conducted with B3PW91/6-311G**, B3LYP/6-311G**, B3PW91/TZV, B3LYP/TZV, HF/6-311G**, and HF/TZV, reproduced the general characteristics of the experimental spectrum fairly well. Particularly, DFT methods were superior to HF methods in accuracy regardless of the basis sets. The contribution of electron correlations seems to play an important role in the properties of compound **2**.[8] A similar trend has also been observed in the calculated ^{13}C NMR chemical shifts on a naphthalene derivative.[9] As shown by the comparison of Figure

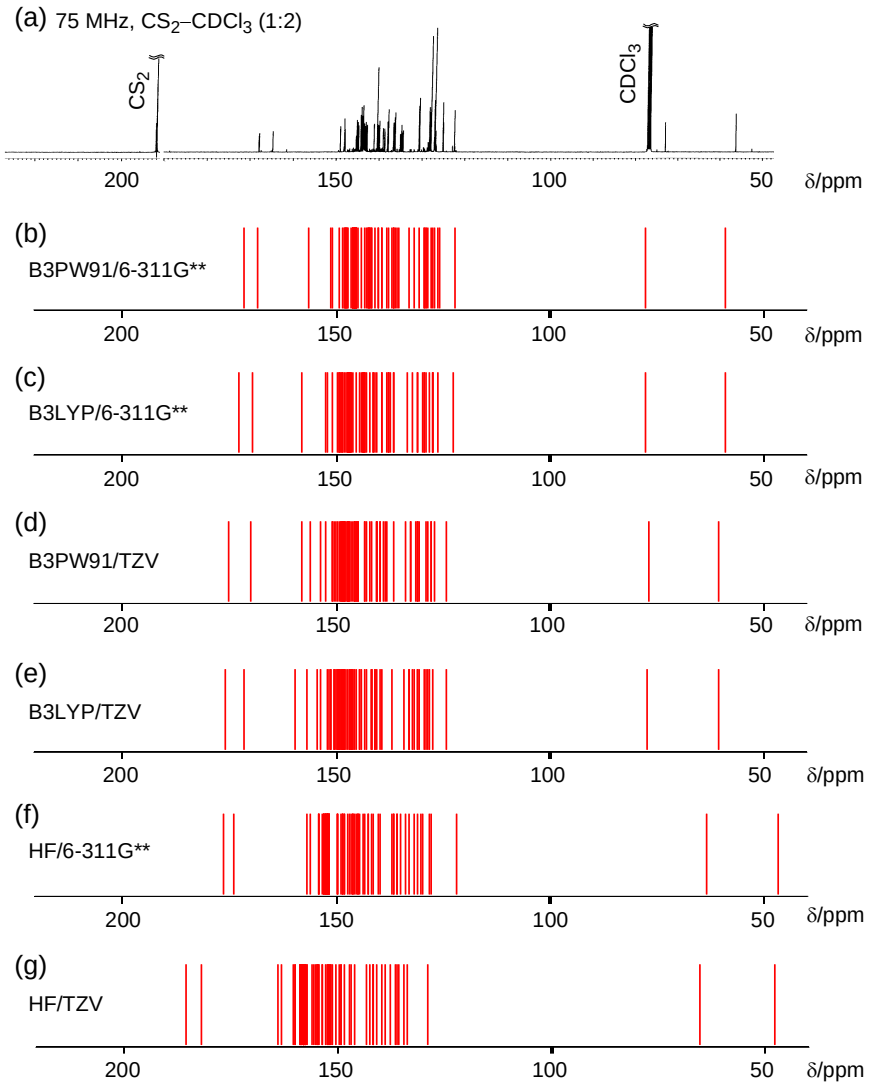

Figure 3. The experimental and calculated ^{13}C NMR spectra of **2**. The GIAO calculations were conducted at different levels of theory and basis sets using the optimized structure at the B3LYP/6-311G** level of theory: (a) experimental spectrum, (b) GIAO-B3PW91/6-311G**, (c) GIAO-B3LYP/6-311G**, (d) GIAO-B3PW91/TZV, (e) GIAO-B3LYP/TZV, (f) GIAO-HF/6-311G**, and (g) GIAO-HF/TZV.

3a with Figure 3b, the GIAO-B3PW91/6-311G** calculation was found to be the best method for reproducing the experimental ^{13}C NMR spectrum for compound **2**.

According to the high-resolution FAB mass and IR spectroscopy described above and the related reports dealing with the photooxidation of carbon analogues of **2**,[1b,3] possible

structures of the two major photo-oxidation products **6** and **7** are supposed to be diketo-compounds, which could be formed by regioselective cleavage of the carbon-carbon double bonds at C2–C3 and C4–C5 positions, respectively. The characterizations of **6** and **7** were achieved by comparing the computed ^{13}C NMR spectra of **6** and **7** at GIAO-B3PW91/6-311G** level of theory with the experimentally observed spectra (Figure 4). Because of the fairly good agreement of the observed spectra with the calculated ones, the structural assignment of **6** and **7** is considered to be correct.

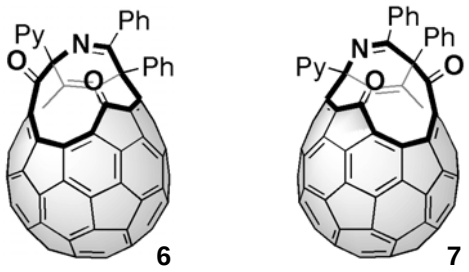

For the minor product **8**, isolated in only 2% yield from the photochemical oxidation of **2**, the experimental ^{13}C NMR spectrum displayed no peak corresponding to a carbonyl carbon as shown in Figure 5a, while the high-resolution FAB mass spectroscopy indicated that two oxygen atoms were incorporated in **2**. In comparison with the ^{13}C NMR spectrum of starting material **2**, a notable downfield shift was observed for one of the sp^3-carbon signals (a signal at δ 73.02 ppm for **2** was shifted to δ 96.47 ppm for **8**), whereas another sp^3-carbon signal remained relatively unchanged (δ 56.35 ppm for **2** and δ 53.26 ppm for **8**). Because the signals at δ 73.02 and 56.35 ppm for **2** are assigned to the C1 and C6 carbon atoms, respectively, based on the GIAO calculations described above, it is implied that the reaction with singlet oxygen has taken place near the C1 carbon atom of **2** without any formation of additional sp^3-carbon atom(s). Thus the most probable structure for this minor product is considered to be **8**, shown below, with a 10-membered-ring orifice on the fullerene cage, resulting from insertion of each of the two oxygen atoms into C1–C2 and C3–C4 single bonds of **2**. This assignment was supported by comparison of the ^{13}C NMR spectra calculated by the GIAO-B3PW91/6-311G** method for **8** and its positional isomer **9** with the experimental ^{13}C NMR spectrum. Clearly, a better agreement was observed for compound **8**, as shown in

Figure 5.

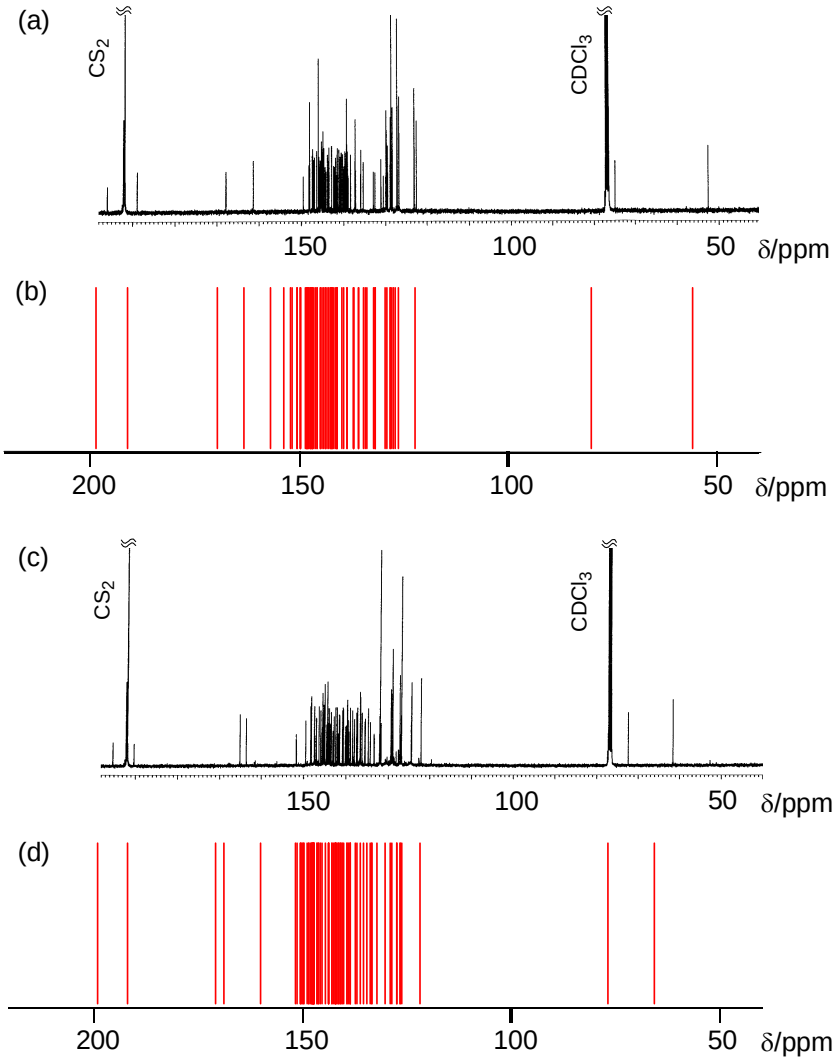

Figure 4. The experimental and calculated ^{13}C NMR spectra of **6** and **7**. The GIAO calculations were conducted at the B3PW91/6-311G** level of theory: (a) observed for **6**, (b) calculated for **6**, (c) observed for **7**, and (d) calculated for **7**.

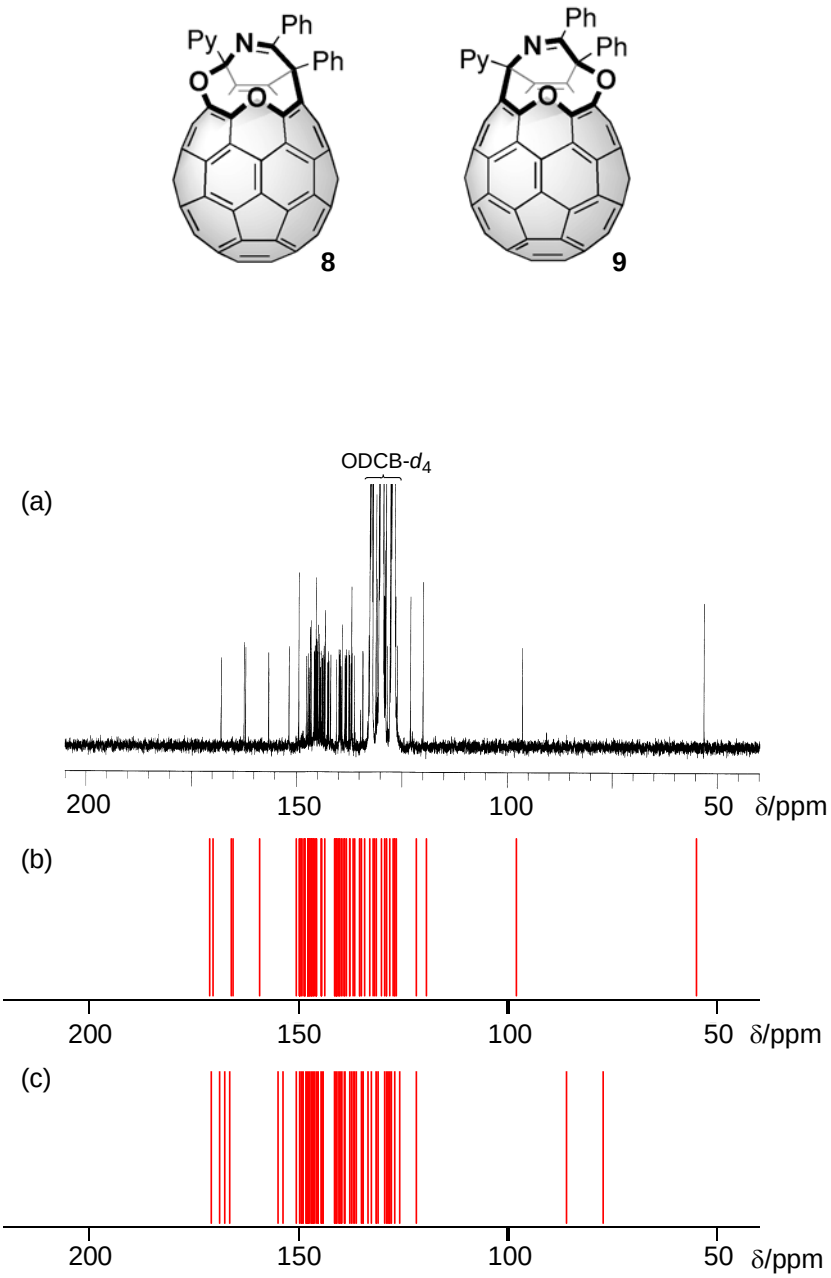

Figure 5. The experimental ^{13}C NMR spectrum of the minor product and calculated ^{13}C NMR spectra of **8** and **9**. The GIAO calculations were conducted at the B3PW91/6-311G** level of theory: (a) observed for the minor product, (b) calculated for **8**, and (c) calculated for **9**.

The formation of three oxidation products **6**, **7**, and **8** by the reaction of **2** with photochemically generated singlet oxygen is explained as follows. As shown in Scheme 2, singlet oxygen adds electrophilically to the strained C2–C3 and C4–C5 double bonds having relatively high coefficients of the HOMO to form intermediate dioxetanes **10** and **11**, respectively. The optimized structures and relative energies of dioxetanes **10** and **11** as well as diethers **8** and **9** were also calculated at the same level of theory (B3LYP/6-311G**). Although the addition of singlet oxygen to the C2–C3 bond would be slightly unfavorable as judged from the relative energy of dioxetanes **10** and **11** calculated at the B3LYP/6-311G** level of theory, it would be kinetically favorable compared with the addition to the C4–C5 bond due to the presence of two bulky phenyl groups in close proximity. Diketone **6** is

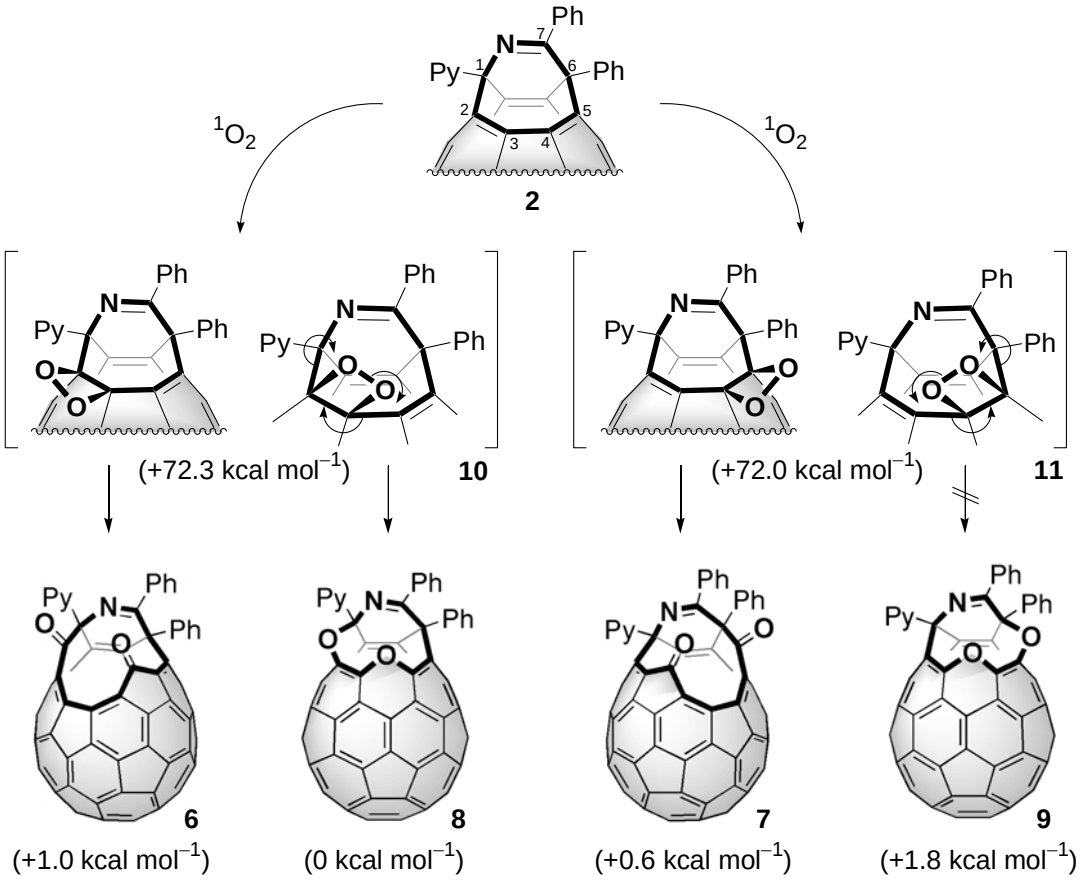

Scheme 2. Formation of open-cage fullerene derivatives **6, 7**, and **8**. The relative energies calculated at the B3LYP/6-311G** level of theory with reference to **8** are shown in parentheses.

formed from dioxetane **10** by the cleavage of the C2–C3 single bond and the O–O bond, whereas diether **9** is produced by means of the insertion of each oxygen atom into the C1–C2 bond and the C3–C4 bond with the concomitant cleavage of the O–O single bond. A similar reaction pathway can be supposed for the formation of diketone **7** from dioxetane **11**, but the formation of diether **9**, which is calculated to be 1.8 kcal mol^{-1} less stable than **11**, was not observed under the present reaction conditions.

An open-cage fullerene derivative having a 13-membered-ring orifice: The 12-membered-ring orifice of **6** was shown to be rather small to introduce even helium atom as judging from the results of theoretical calculations which predicted that the activation energy for the insertion process of helium is rather high, i.e., 39.2 kcal mol^{-1} at the B3LYP/6-31G** level of theory, based on the structure optimized at the B3LYP/3-21G level of theory. In order to further enlarge the 12-membered-ring orifice of **6**, a reaction which causes insertion of a heteroatom at the rim of the orifice appeared quite appealing. It has been shown that a sulfur atom can be inserted into an activated C–C single bond.[10] We therefore attempted a thermal reaction of **6** with elemental sulfur in ODCB and found that the desired reaction actually takes place in the presence of tetrakis(dimethylamino)ethylene (TDAE), which can serve as a π-donor.[11] Heating a mixture of **6**, elemental sulfur (8 equiv), and TDAE (1 equiv) in refluxing ODCB for 30 min efficiently afforded a single product with a high-resolution FAB mass data exhibiting a molecular ion peak at *m*/*z* 1067 corresponding to **6** + S + H, in 77% yield. The similar reactions using elemental selenium or tellurium instead of sulfur were also examined, but they only afford almost insoluble and intractable materials.

In the sulfur insertion reaction, TDAE is supposed to activate **6** either by one-electron transfer or by complexation so that the electrophilic reaction of elemental sulfur to **6** can readily take place. The theoretical calculations for **6** at the B3LYP/6-311G** level of theory demonstrated that the LUMO of **6** is relatively localized at the conjugated butadiene part, C9-C10-C11-C12, on the rim of the orifice (Figure 6); the numbering is shown in Scheme 3 below. The absolute values of the coefficients of the LUMO at C9, C10, C11, and C12 of **6** are 0.29, 0.35, 0.32, and 0.25, respectively. Therefore, it is assumed that the sulfur atom has been inserted into the carbon-carbon single bond at C10-C11 position to give the novel

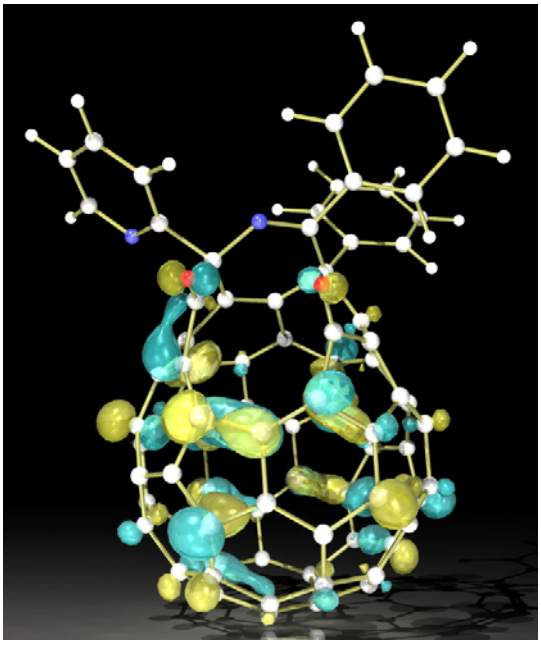

Figure 6. The optimized structure of open-cage fullerene derivative **6** with the contour of the LUMO, calculated at the B3LYP/6-311G** level of theory.

open-cage fullerene derivative **12** having a 13-membered-ring orifice (Scheme 3). The ^{13}C NMR spectrum of this product exhibited two signals for the carbonyl carbon atoms at δ 193.06 and 185.02 ppm, 52 signals (out of possible 76 signals) corresponding to the fullerenyl and aryl sp^2-carbon atoms in the range δ 166.40 to 122.68 ppm, and two signals corresponding to the sp^3-carbons at δ 74.42 and 52.33 ppm. Finally, the validity of the assignment of the structure **12** to this product was unambiguously proved by the X-ray crystallography for the single crystal grown by slow evaporation from a toluene solution of **12** (Figure 7).

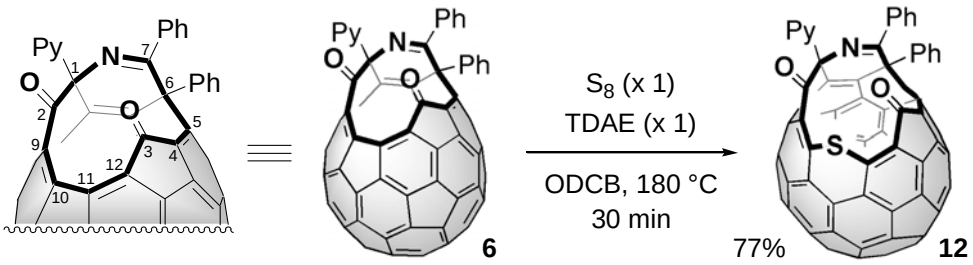

Scheme 3. Synthesis of open-cage fullerene derivative **12**.

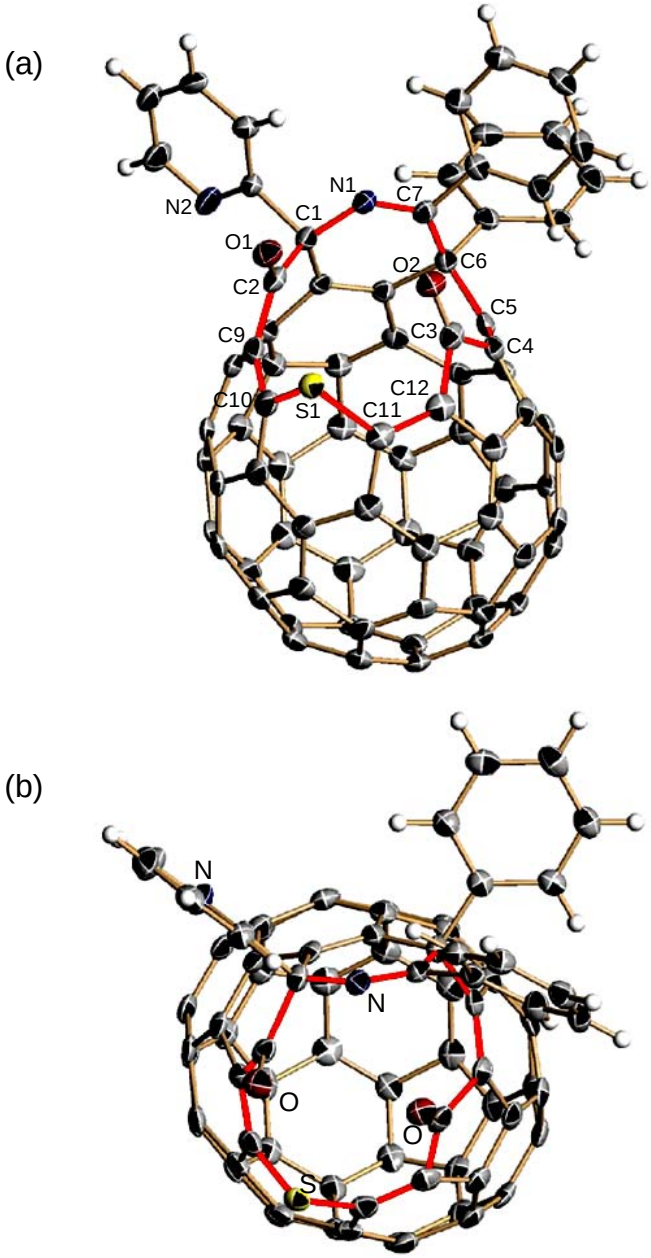

Figure 7. The X-ray structure of open-cage fullerene derivative **12** with the displacement ellipsoids model drawn at the 50% probability level: (a) side view and (b) top view. Selected distances [Å]: N1–C1 1.445(3), C1–C2 1.584(4), C2–O1 1.209(3), C2–C9 1.492(4), C9–C10 1.398(4), C10–S1 1.780(3), S1–C11 1.754(3), C10–C11 2.546(4), C11–C12 1.367(4), C12–C3 1.518(4), C3–O2 1.202(3), C3–C4 1.553(4), C4–C5 1.380(4), C5–C6 1.552(3), C6–C7 1.545(4), C7–N1 1.281(3).

As shown by the X-ray crystal structure given in Figure 7a, compound **12** has a 13-membered-ring orifice on the fullerene cage (shown in red) containing sulfur and nitrogen atoms. The bond lengths of C9–C10, C10–S1, S1–C11, and C11–C12 are 1.398(4), 1.780(3), 1.754(3), and 1.367(4) Å, respectively. Thus a divinyl sulfide moiety was formed in the 13-membered ring as a result of the sulfur-atom insertion into the C10–C11 bond of **6**. Determination of this X-ray structure also confirmed the validity of the structural assignment of the starting material **6**, which was made based on the comparison with the DFT-GIAO calculated ^{13}C NMR spectrum, as described above.

From the top view of the X-ray structure shown in Figure 7b, it can be seen that the 13-membered-ring orifice in **12** has a somewhat more circular shape than the rather elliptic shape observed for the 14-membered-ring orifice (counting the fused benzene-ring carbon atoms) in the bislactam derivative of an open-cage fullerene **13** reported by Rubin and co-workers.[12] This is the largest hole constructed thus far on the surface of C_{60}. Thus, the insertion of a small molecule or atom such as helium, neon, and molecular hydrogen is expected to be possible through the 13-membered-ring orifice in **12**.

13

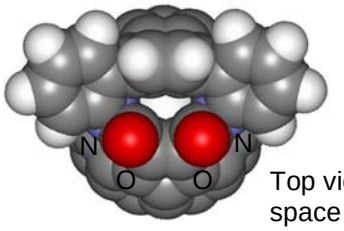

Top view of the space filling model

Properties of open-cage fullerene derivatives: The UV/vis spectra of the obtained open-cage fullerene derivatives, **2, 6, 7, 8**, and **12**, taken in $CHCl_3$ are shown in Figure 8. As mentioned previously, compound **2**, having an eight-membered-ring orifice, displayed a similar absorption pattern to that of C_{60} itself, reflecting the fact that **2** retains the conjugated system composed of 60 sp^2-carbon atoms.[1a,1b,2] Compounds **6** and **7**, which are isomeric, showed quite similar absorptions, that is, strong maximum absorptions in the UV region (257

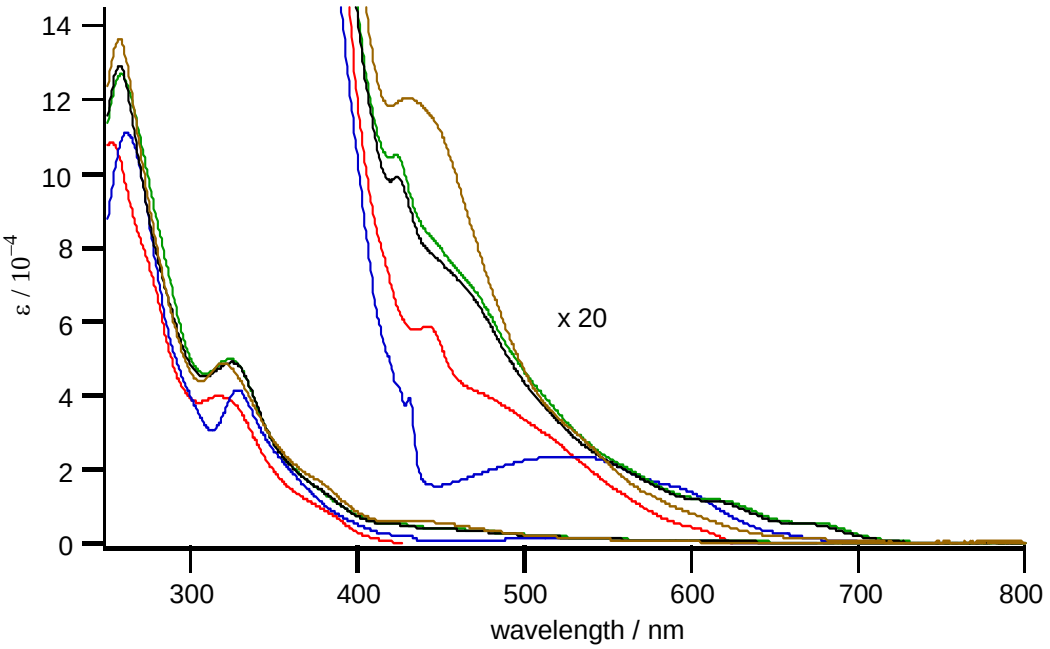

Figure 8. UV/Vis spectra of open-cage fullerene derivatives: blue line (**2**), black (**6**), green (**7**), red (**8**), and brown (**12**) in $CHCl_3$.

and 325 nm for **6**; 259 and 324 nm for **7**), which are commonly observed in C_{60} derivatives, and a small absorption in the visible region (424 nm for **6**; 423 nm for **7**) as well as the long-wavelength visible absorption extending to approximately 700 nm. These absorptions are different from those of an enol-ketone derivative **14**, which has a similar 12-membered-ring orifice. This showed maximum absorptions at 453 and 751 nm.[3a] Compound **8** showed maximum absorptions at 253, 317, and 442 nm. Compound **12**, which has the largest orifice among the compounds examined in this study, showed maximum absorptions at 257 and 319 nm as well as a broad absorption at 430 nm. With the increase in the size of the orifice in the order **6, 7** and **8**, and **12**, the absorption at the visible region lost

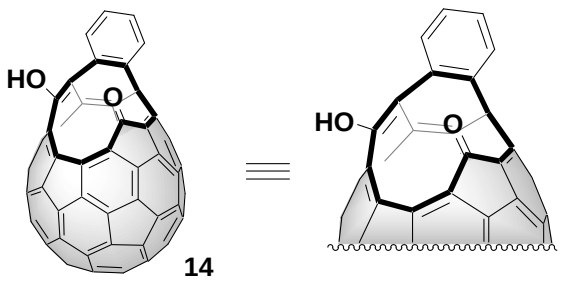

14

their structure. The colors of the solutions of **2, 6, 7, 8**, and **12** in $CHCl_3$ were purple, brown, brown, red-brown, and bright red, respectively.

To examine the electronic properties of the open-cage fullerene derivatives **2, 6, 7, 8**, and **12**, their redox behaviors were studied by cyclic voltammetry (CV) and differential pulse voltammetry (DPV) in ODCB using Bu_4NBF_4 as a supporting electrolyte. Despite the significant change in the π-electronic system resulting from the transformation in the fullerene skeleton made for these derivatives, all compounds showed four quasi-reversible redox waves in the negative scans upon CV. These were quite similar to those observed for C_{60} itself. The corresponding four one-electron reduction peaks were observed upon DPV measurements. As an example, the CV and DPV results for compound **7** are shown in Figure 9, together with those for C_{60}.

The reduction potentials determined by DPV are summarized in Table 1, together with the LUMO energy levels calculated by the B3LYP/6-31G* level of theory. As shown by the values in Table 1, the reduction potentials of compounds **2** and **8** were found to be rather

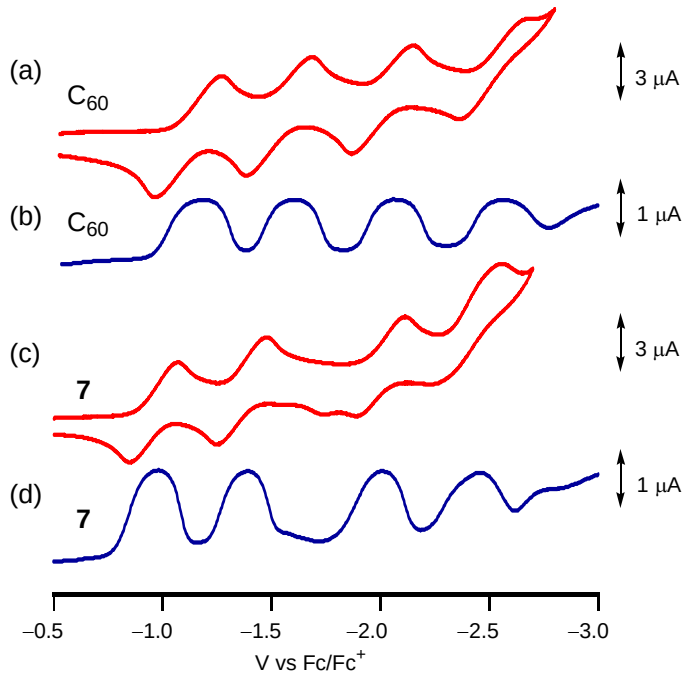

Figure 9. CV and DPV of C_{60} and **7**: 1 mM in ODCB, 0.05 M $TBABF_4$, scan rate 0.02 V s^{-1}; (a) CV of C_{60}, (b) DPV of C_{60}, (c) CV of **7**, and (d) DPV of **7**.

Table 1. Reduction Potentials[a] and Calculated LUMO Levels[b]

compound	E_{red}^{1}[a]	E_{red}^{2}[a]	E_{red}^{3}[a]	E_{red}^{4}[a]	LUMO / eV[b]
C_{60}	–1.17	–1.59	–2.06	–2.56	–3.23
2	–1.21	–1.62	–2.11	–2.62	–3.03
6	–0.97	–1.40	–2.01	–2.43	–3.32
7	–0.98	–1.39	–2.00	–2.44	–3.34
8	–1.18	–1.58	–2.20	–2.70	–3.13
12	–1.15	–1.56	–2.05	–2.52	–3.16
14	–1.07[c]	–1.43[c]	–1.99[c]	–2.29[c]	–3.26[c]

[a] V vs ferrocene/ferrocenium: All reduction potentials were measured by DPV (1 mM sample, 0.05 M Bu_4NBF_4 in ODCB, scan rate 0.02 V s^{-1}). [b] Calculated at the B3LYP/6-31G* level of theory. [c] Values taken from ref. 3a.

similar to those of C_{60}, indicating that the fully conjugated π-electron systems made of 60 sp^2-carbons in **2** and **8** retain the high electron affinities characteristic of C_{60}. Most noteworthy is the observation that compounds **6** and **7** exhibited first reduction waves at potentials as low as –0.97 and –0.98 V versus the ferrocene/ferrocenium couple, respectively, which are approximately 0.2 V lower than that of C_{60} measured under the same conditions. The second to fourth reduction potentials were also lower than those of C_{60}. This enhanced reducibility could be ascribed to the presence of two carbonyl groups directly connected to the partially broken fullerenyl π-system. Actually, the reduction potentials observed for **6** and **7** are lower than those of the monocarbonyl analogue of the similar open-cage fullerene **14** by about 0.1 V.[3a] Therefore, one carbonyl group connected to the fullerenyl π-system is considered to decrease the reduction potential by approximately 0.1 V. This effect is nearly comparable to that of the two cyano groups connected by sp^3-carbon atoms to the C_{58} fullerenyl π-system in $C_{60}(CN)_2$.[14] In contrast, the sulfur-containing derivative **12** displayed its first reduction at –1.15 V, which is more negative than that of **6** and **7** and close to that of C_{60} despite the presence of two carbonyl groups. This is considered to reflect the strong electron-donating effect of a sulfur atom directly bonded to the π-system. As shown in Table 1, the lowered reduction potentials observed for **6** and **7** are in agreement with the low

levels of LUMO predicted for these compounds by theoretical calculations at the B3LYP/6-31G* level of theory.[15]

Conclusion

In summary, an open-cage fullerene derivative having a nitrogen-containing, eight-membered-ring orifice (**2**) was synthesized in high yield (85% based on consumed C_{60} at 59% conversion) by a liquid-phase thermal reaction of C_{60} with 3-(2-pyridyl)-5,6-diphenyl-1,2,4-triazine (**1**) in one pot. The eight-membered-ring orifice was further enlarged to a 12-membered ring containing two carbonyl carbon atoms (**6** and **7**) and a 10-membered ring containing ether linkages (**8**) by photochemical oxidation with singlet oxygen. The structures of these compounds were characterized by spectroscopy and DFT calculations, as well as by the X-ray crystallography for **2**. In particular, the GIAO calculation was found to be a powerful method for structural determination of derivatives such as **6**, **7**, and **8** by comparison of the calculated ^{13}C NMR spectra with the observed ones.

A novel sulfur-atom insertion into the central C–C bond in the butadiene unit of the rim of the 12-membered-ring orifice was developed. It gave a novel fullerene derivative **12** with a 13-membered-ring orifice containing both nitrogen and sulfur atoms on the rim. The X-ray crystallography on this compound indicated that the shape of the orifice is closer to a circle than to an ellipse compared with compound **13**, which has the largest orifice reported thus far.[13] The energy barrier for insertion of a helium atom through the orifice was calculated to be approximately 5.5 kcal mol^{-1} lower for compound **12** than for **13**. This finding is a good indicator that the preparation of endohedral fullerene complexes by means of organic synthesis, which was initiated by Rubin and co-workers, is indeed possible.[13,16]

Experimental Section

General. The ^{1}H and ^{13}C NMR measurements were carried out on a Varian Mercury 300 instrument and a JEOL AL-400 instrument and the chemical shifts are reported in ppm with reference to tetramethylsilane. In some cases, the signal of *o*-dichlorobenzene-d_4

(ODCB-d_4) was used as an internal standard (δ 7.20 ppm in ^{1}H NMR, and δ 132.35 ppm in ^{13}C NMR). UV/vis spectra were recorded on a Shimadzu UV-2100PC spectrometer. IR spectra were recorded with a Shimadzu FTIR-8600 spectrometer. MS spectra were recorded on a JEOL MStation JMS-700. Cyclic voltammetry and differential pulse voltammetry were conducted on a BAS Electrochemical Analyzer CV-100W using a three-electrode cell with a glassy carbon working electrode, a platinum wire counter electrode, and a Ag/0.01 M $AgNO_3$ reference electrode. The potentials were corrected against ferrocene used as an internal standard which was added after each measurement. Fullerene C_{60} was purchased from Matsubo Co. 3-(2-Pyridyl)-5,6-diphenyl-1,2,4-triazine and tetrakis(dimethylamino)ethylene were purchased from Aldrich Co. and used as received. Elemental sulfur was purchased from Nacalai Tesque Co. and used as received.

Computational Method. All calculations were conducted by using the Gaussian 98 series of electronic structure programs.[4] The geometries were fully optimized with the restricted Becke hybrid (B3LYP) method for all compounds. The GIAO calculations were performed at HF/6-311G**, B3LYP/6-311G**, B3PW91/6-31G**, HF/TZV, B3LYP/TZV, and B3PW91/TZV level of theory using the optimized structure at the B3LYP/6-311G** level of theory.

Synthesis of 2. A mixture of fullerene C_{60} (50 mg, 0.069 mmol) and 3-(2-pyridyl)-5,6-diphenyl-1,2,4-triazine (**2**) (21 mg, 0.068 mmol) in ODCB (4 mL) was refluxed at 180 °C for 17 h under argon. The resulting dark purple solution was directly subjected to flash column chromatography over silica gel. Elution with CS_2 gave unreacted C_{60} (20 mg, 41%) while the following elution with CS_2-ethyl acetate (20:1) gave open-cage fullerene derivative **2** (35 mg, 0.035 mmol, 50%) as a brown powder.

2: mp >300 °C (slow decomposition starting at 250 °C); IR (KBr) ν 1749 (C=N) cm^{-1}; UV/vis ($CHCl_3$) λ_{max} (log ε) 262 (5.05), 329 (4.62), 431 (3.29), 533 (3.07) nm; ^{1}H NMR (300 MHz, CS_2–acetone-d_6 (7:1)) δ 8.68 (m, 1H), 8.00-7.90 (m, 2H), 7.76-7.69 (m, 2H), 7.44-7.37 (m, 2H), 7.22-7.10 ppm (m, 7H); ^{13}C NMR (100 MHz, CS_2–$CDCl_3$ (1:2)) δ 167.96, 164.81, 149.10, 148.10, 147.96, 145.40, 145.21, 145.14, 145.12, 145.06, 144.85, 144.37, 144.34, 144.20, 144.15, 144.02, 143.96, 143.94, 143.80, 143.77, 143.71, 143.65, 143.59, 143.54, 143.50, 143.40, 143.35, 143.31, 143.21, 143.19, 143.16, 143.13, 143.02, 142.86, 141.29,

140.53, 140.49, 140.32, 140.23, 140.20, 139.96, 139.18, 138.77, 138.09, 137.92, 136.73, 136.69, 136.57, 136.48, 136.35, 135.18, 135.02, 134.88, 134.60, 134.48, 130.78, 130.65, 128.36, 128.21, 128.00, 127.18, 127.04, 125.17, 125.08, 122.47, 73.02, 56.35; HRMS (+FAB) calcd for $C_{80}H_{15}N_2$ (MH^+), 1003.1235, found 1003.1238.

Synthesis of 6, **7**, **and 8.** A purple solution of compound **2** (66 mg, 0.066 mmol) in CCl_4 (65 mL) in a Pyrex flask was irradiated by a high-pressure mercury lamp (500 W) from a distance of 20 cm for 6 h under air. The resulting brown solution was evaporated and the residual black solid was dissolved in ODCB (3 mL). This was subjected to preparative HPLC using a Cosmosil 5PBB column (10 mm × 250 mm) eluted with ODCB (flow rate, 2 mL min^{-1}) to afford open-cage fullerene derivatives **6** (40 mg, 0.038 mmol, 60%, retention time: 8.7 min), **7** (21 mg, 0.020 mmol, 31%, retention time: 9.2 min), and **8** (1 mg, 0.001 mmol, 2%, retention time: 9.1 min), after nine recycles, all as brown powders.

6: IR (KBr) ν 1747, 1700 (C=O) cm^{-1}; UV/vis ($CHCl_3$) λ_{max} (log ε) 257 (5.11), 325 (4.69), 424 (3.70) nm; ^{1}H NMR (300 MHz, CS_2–acetone-d_6 (7:1)) δ 8.52 (m, 1H), 8.37 (m, 1H), 8.07-7.98 (m, 3H), 7.82 (m, 1H), 7.37-7.03 (m, 8H); ^{13}C NMR (100 MHz, CS_2–$CDCl_3$ (1:2)) δ 196.04, 188.96, 167.84, 161.38, 149.53, 148.22, 148.18, 148.04, 147.43, 147.32, 147.29, 147.15, 146.92, 146.37, 145.99, 145.85, 145.67, 145.53, 145.44, 145.38, 145.32, 145.25, 145.20, 145.19, 144.96, 144.85, 144.67, 144.35, 144.20, 143.79, 143.71, 143.51, 142.87, 142.38, 142.17, 141.95, 141.57, 141.46, 141.11, 140.77, 140.56, 140.24, 140.13, 139.89, 139.73, 139.58, 139.27, 139.13, 138.96, 138.35, 137.30, 137.21, 137.16, 135.97, 135.92, 135.35, 132.90, 132.54, 131.08, 130.48, 129.96, 129.85, 129.78, 129.51, 128.88, 128.69, 128.37, 127.27, 127.17, 126.76, 123.13, 122.60, 74.97, 52.63; HRMS (+FAB) calcd for $C_{80}H_{15}N_2O_2$ (MH^+), 1035.1134, found 1035.1132.

7: IR (KBr) ν 1748 (C=O) cm^{-1}; UV/vis ($CHCl_3$) λ_{max} (log ε) 259 (5.10), 324 (4.70), 423 (3.72) nm; ^{1}H NMR (300 MHz, CS_2–acetone-d_6 (7:1)) δ 8.58 (m, 1H), 8.20-8.17 (m, 2H), 8.02 (m, 1H), 7.93 (m, 1H), 7.37-7.21 (m, 9H); ^{13}C NMR (100 MHz, CS_2–$CDCl_3$ (1:2)): δ 195.31, 190.36, 165.18, 163.66, 151.71, 149.50, 148.38, 148.20, 147.48, 147.40, 147.34, 147.00, 146.37, 145.99, 145.96, 145.61, 145.55, 145.29, 145.22, 145.20, 145.12, 145.10, 144.98, 144.52, 144.39, 144.25, 144.11, 143.89, 143.78, 143.51, 143.05, 142.80, 142.43, 142.06, 141.80, 141.56, 141.49, 140.79, 140.69, 140.62, 140.07, 139.92, 139.63, 139.58,

139.49, 139.27, 138.96, 138.40, 138.00, 137.48, 137.23, 136.58, 136.55, 136.18, 135.51, 135.44, 134.73, 134.23, 133.33, 132.01, 131.91, 131.68, 129.35, 129.32, 128.95, 127.21, 126.87, 124.44, 122.15, 72.42, 61.58; HRMS (+FAB) calcd for $C_{80}H_{15}N_2O_2$ (MH^+) 1035.1134, found 1035.1151.

8: UV/vis ($CHCl_3$) λ_{max} (log ε) 317 (4.64), 442 (3.52) nm; ^{1}H NMR (300 MHz, CS_2–acetone-d_6 (7:1)) δ 8.64 (m, 1H), 8.48 (m, 1H), 8.03-7.89 (m, 4H), 7.66 (m, 1H), 7.39-7.21 (m, 7H); ^{13}C NMR (100 MHz, ODCB-d_4) δ 167.97, 162.52, 162.16, 156.68, 151.84, 149.55, 147.73, 147.37, 147.09, 146.84, 146.82, 146.56, 145.89, 145.75, 145.67, 145.54, 145.45, 145.34, 145.30, 145.18, 145.03, 144.99, 144.67, 144.65, 144.60, 144.41, 144.23, 144.00, 143.81, 143.54, 143.27, 142.68, 142.50, 142.40, 142.00, 140.61, 139.99, 139.91, 139.77, 139.69, 139.54, 139.30, 138.62, 138.52, 138.47, 138.31, 138.18, 137.67, 137.48, 137.15, 137.04, 136.99, 136.91, 136.31, 134.37, 134.30, 132.94, 126.58, 126.15, 123.01, 120.04, 96.47, 53.26 (some signals in the region δ 132.7 ~ 126.9 overlap with the ODCB-d_4 peaks); HRMS (+FAB) calcd for $C_{80}H_{15}N_2O_2$ (MH^+), 1035.1134, found 1035.1121.

Synthesis of 12. To a heated and stirred solution of compound **6** (32 mg, 0.031 mmol) and elemental sulfur (8 mg, 0.031 mmol as S_8) in ODCB (15 mL) was added tetrakis(dimethylamino)ethylene (7.1 μL, 0.031 mmol) at 180 °C under argon. The solution was refluxed at 180 °C for 30 min then the resulting dark red-brown solution was concentrated by evaporation to about 3 mL. This was added to pentane (30 mL) with vigorous stirring to give brown precipitates. The precipitates, collected by centrifuge, were dissolved in ODCB (2 mL). The resulting solution was subjected to flash chromatography on silica gel eluted with toluene-ethyl acetate (30:1) to give open-cage fullerene derivative **12** (25 mg, 0.023 mmol, 77%) as a brown powder.

12: mp >300 °C (slow decomposition starting at 250 °C); IR (KBr) ν 1748 (C=O) cm^{-1}; UV/vis ($CHCl_3$) λ_{max} (log ε) 257 (5.14), 319 (4.69), 430 (3.78) nm; ^{1}H NMR (300 MHz, CS_2–acetone-d_6 (7:1)) δ 8.60 (m, 1H), 8.23 (m, 1H), 8.18-8.15 (m, 2H), 8.02 (m, 1H), 7.53 (m, 1H), 7.36 (m, 1H), 7.30-7.25 (m, 3H), 7.04-6.88 (m, 4H); ^{13}C NMR (75 MHz, ODCB-d_4) δ 193.06, 185.02, 166.40, 164.00, 150.18, 149.19, 149.06, 148.64, 148.57, 148.53, 148.43, 148.23, 148.03, 147.71, 147.59, 147.56, 147.49, 147.40, 147.35, 147.33, 147.20, 146.82, 146.75, 146.56, 145.81, 145.60, 145.28, 144.67, 144.14, 143.73, 142.12, 141.65, 141.32,

141.09, 140.73, 140.30, 140.15, 139.93, 139.13, 138.91, 138.58, 138.54, 138.50, 138.32, 137.97, 137.88, 137.54, 137.39, 137.31, 135.44, 135.19, 135.10, 132.91, 122.68, 74.42, 52.33 (signals in the range δ 132.4-126.9 overlap with the signals of ODCB-d_4); HRMS (+FAB) calcd for $C_{80}H_{15}N_2O_2S$ (MH^+), 1067.0854, found 1067.0814.

X-ray structural analysis of 2 and 12. Single crystals of compounds **2** and **12** suitable for X-ray crystallography were obtained by slow evaporation of the solutions in benzene and in toluene, respectively, over three days at room temperature. Single-crystal diffraction data were collected at 100 K on a Bruker SMART diffractometer equipped with a CCD area detector using Mo-Kα radiation. All structure solutions were obtained by direct methods and refined using full-matrix least-squares with a Bruker SHELXTL (Version 5.1) Software Package. The crystal parameters are summarized in Table 2.

Table 2. Crystallographic Data for Open-Cage Fullerene Derivatives

	2·$(C_6H_6)_3$	**12**·$(C_7H_8)_{0.5}$
empirical formula	$C_{98}H_{32}N_2$	$C_{83.5}H_{18}N_2O_2S$
formula weight	1237.26	1113.06
crystal system	triclinic	triclinic
space group	*P*-1	*P*-1
a [Å]	13.750(2)	10.0158(8)
b [Å]	15.237(2)	13.1987(10)
c [Å]	15.498(2)	17.5019(14)
α [°]	63.891(3)	98.638(2)
β [°]	71.078(4)	91.309(2)
γ [°]	85.258(3)	98.317(2)
V [Å^3]	2751.4(7)	2261.0(3)
Z	2	2
T [K]	100(2)	100(2)
λ [Å]	0.71073	0.71073
μ [mm^{-1}]	0.086	0.142
θ range [°]	1.55-25.50	1.82-25.60

limiting indices	-14≤*h*≤16	-11≤*h*≤12
	-18≤*k*≤18	-15≤k≤16
	-18≤*l*≤18	-21≤*l*≤13
ρ_{calc} [g cm^3]	1.493	1.635
data/restraints/parameters	10201/0/957	8357/34/829
unique reflections	10201	8357
completeness [%]	99.4	98.2
absp correction	SADABS	SADABS
R_{int}	0.0357	0.0188
*R*1 [I>2σ(*I*)][a]	0.0613	0.0559
*wR*2 [I>2σ(*I*)][b]	0.1318	0.1348
*R*1 (all data)[a]	0.1093	0.0792
*wR*2 (all data)[b]	0.1499	0.1439
GOF on F^2	0.931	0.969

[a] $R1 = \Sigma \, | \, |F_c| - |F_o| \, | \, / \, \Sigma \, |F_o|$. [b] $wR2 = \{\Sigma \, [w(F_o^2 - F_c^2)^2] \, / \, \Sigma \, [w(F_o^2)^2]\}^{1/2}$.

References and Notes

(1) (a) Murata, Y.; Kato, N.; Komatsu, K. *J. Org. Chem.* **2001**, *66*, 7235. (b) Murata, Y.; Murata, M.; Komatsu, K. *J. Org. Chem.* **2001**, *66*, 8187. (c) Murata, Y.; Suzuki, M.; Rubin, Y.; Komatsu, K. *Bull. Chem. Soc. Jpn.* **2003**, *76*, 1669. (d) Murata, Y.; Suzuki, M.; Komatsu, K. *Chem. Commun.* **2001**, 2338.

(2) (a) Arce, M.-J.; Viado, A. L.; An, Y.-Z.; Khan, S. I.; Rubin, Y. *J. Am. Chem. Soc.* **1996**, *118*, 3775. (b) Qian, W.; Bartberger, M. D.; Pastor, S. J.; Houk, K. N.; Wilkins, C. L.; Rubin, Y. *J. Am. Chem. Soc.* **2000**, *122*, 8333. (c) Hsiao, T.-Y.; Santhosh, K. C.; Liou, K.-F.; Cheng, C.-H. *J. Am. Chem. Soc.* **1998**, *120*, 12232. (d) Inoue, H.; Yamaguchi, H.; Suzuki, T.; Akasaka, T.; Murata, S. *Synlett* **2000**, 1178. (e) Iwamatsu, S.-i.; Vijayalakshmi, P. S.; Hamajima, M.; Suresh, C. H.; Koga, N.; Suzuki, T.; Murata, S. *Org. Let*t. **2002**, *4*, 1217. (f) Qian, W.; Chuang, S.-C.; Amador, R. B.; Jarrosson, T.; Sander, M.; Pieniazek, S.; Khan, S. I.; Rubin, Y. *J. Am. Chem. Soc.* **2003**, *125*, 2066.

(3) (a) Murata, Y.; Komatsu, K. *Chem. Lett.* **2001**, 896. (b) Inoue, H.; Yamaguchi, H.; Iwamatsu, S.; Uozaki, T.; Suzuki, T.; Akasaka, T.; Nagase, S.; Murata, S. *Tetrahedron Lett*. **2001**, *42*, 895.

(4) Frisch, M. J.; Trucks, G. W.; Schlegel, H. B.; Scuseria, G. E.; Robb, M. A.; Cheeseman, J. R.; Zakrzewski, V. G.; Montgomery, H. A., Jr.; Stratmann, R. E.; Burant, J. C.; Dapprich, S.; Millam, J. M.; Daniels, A. D.; Kudin, K. N.; Strain, M. C.; Farkas, O.; Tomasi, J.; Barone, V.; Cossi, M.; Cammi, R.; Mennucci, B.; Pomelli, C.; Adamo, C.; Clifford, S.; Ochterski, J.; Petersson, G. A.; Ayala, P. Y.; Cui, Q.; Morokuma, K.; Malick, D. K.; Rabuck, A. D.; Raghavachari, K.; Foresman, J. B.; Cioslowski, J.; Ortiz, J. V.; Baboul, A. G.; Stefanov, B. B.; Liu, G.; Liashenko, A.; Piskorz, P.; Komaromi, I.; Gomperts, R.; Martin, R. L.; Fox, D. J.; Keith, T.; Al-Laham, M. A.; Peng, C. Y.; Nanayakkara, A.; Gonzalez, C.; Challacombe, M.; Gill, P. M. W.; Johnson, B.; Chen, W.; Wong, M. W.; Andres, J. L.; Gonzalez, C.; Head-Gordon, M.; Replogle, E. S.; Pople, J. A. *Gaussian 98*, Revision A.7; Gaussian, Inc.: Pittsburgh, PA, 1998.

(5) Wolinski, K.; Hilton, J. F.; Pulay, P. *J. Am. Chem. Soc.* **1990**, *112*, 8251.

(6) For a comprehensive review of the quantum-mechanical determination of NMR chemical shifts, see: Helgaker, T.; Jaszunski, M.; Ruud, K. *Chem. Rev*. **1999**, *99*, 293.

(7) Several GIAO calculations have so far been made on various fullerenes and their derivatives to give satisfactorily reliable results, see ref. (1 b), (3 a) and also see: (a) Sun, G.; Kertesz, M. *New J. Chem.* **2000**, *24*, 741. (b) Bühl, M.; Hirsch, A. *Chem. Rev*. **2001**, *101*, 1153 and references therein. (c) Murata, Y.; Ito, M.; Komatsu, K. *J. Mater. Chem.* **2002**, *12*, 2009. (d) Meier, M. S.; Spielmann, H. P.; Bergosh, R. G.; Haddon, R. C. *J. Am. Chem. Soc*. **2002**, *124*, 8090.

(8) Cybulski, S. M.; Bishop, D. M. *Chem. Phys. Lett*. **1993**, *98*, 8057.

(9) Walker, O.; Mutzenhardt, P.; Tekely, P.; Canet, D. *J. Am. Chem. Soc*. **2002**, *124*, 865.

(10) Toda, F.; Tanaka, K. *Chem. Lett*. **1979**, 1451.

(11) Stephens, P. W.; Cox, D.; Lauher, J. W.; Mihaly, L.; Wiley, J. B.; Allemand, P.-M.; Hirsch, A.; Holczer, K.; Li, Q.; Thompson, J. D.; Wudl, F. *Nature* **1992**, *355*, 331.

(12) Schick, G.; Jarrosson, T.; Rubin, Y. *Angew. Chem. Int. Ed*. **1999**, *38*, 2360.

(13) Rubin, Y.; Jarrosson, T.; Wang, G.-W.; Bartberger, M. D.; Houk, K. N.; Schick, G.;

Saunders, M.; Cross, R. J. *Angew*. *Chem*. *Int*. *Ed*. **2001**, *40*, 1543.

(14) The first reduction potential is lowered by 0.12 V compared with C_{60}: Keshavartz-K, M.; Knight, B.; Srdanov, G.; Wudl, F. *J*. *Am*. *Chem*. *Soc*. **1995**, *117*, 11371.

(15) Suzuki, T.; Maruyama, Y.; Akasaka, T.; Ando, W.; Kobayashi, K.; Nagase, S. *J*. *Am*. *Chem*. *Soc*. **1994**, *116*, 1359.

(16) (a) Rubin, Y. *Chem*. *Eur*. *J*. **1997**, *3*, 1009. (b) Rubin, Y. *Top*. *Curr*. *Chem*. **1999**, *199*, 67. (c) Nierengarten, J.-F. *Angew*. *Chem*. *Int*. *Ed*. **2001**, *40*, 2973.

Chapter 3

100% Encapsulation of a Hydrogen Molecule into an Open-Cage Fullerene Derivative and Gas-Phase Generation of $H_2@C_{60}$

Abstract: By applying high-pressure H_2 gas to a new fullerene derivative, $C_{63}NO_2SPh_2Py$ (**1**), having a 13-membered-ring orifice, 100% incorporation of a hydrogen molecule into the fullerene cage has been achieved for the first time. This result was supported by the theoretical calculations indicating that the energy barrier required for H_2 insertion through an orifice in **1** is considerably low, i.e., 30.1 kcal mol^{-1}. Synchrotron X-ray diffraction analysis of a single crystal of $H_2@$**1** allowed the successful direct observation of a single hydrogen molecule at the center of the hollow cavity of **1**. Upon MALDI-TOF mass spectroscopy, the removal of organic addends from the fullerene derivative $H_2@$**1** and restoration of the pristine C_{60} cage, which retains approximately one-third of incorporated hydrogen molecule, have been observed.

Introduction

The methodology of "molecular surgery" approach to endohedral fullerenes consists of following processes, that is, (1) opening an orifice on the C_{60} framework, (2) enlarging the orifice, (3) putting some atom or small molecule through the orifice, (4) reducing the size of the orifice, and (5) finally reproducing the original C_{60} form by complete closure of the orifice.[1] As mentioned in Chapter 2, the author and co-workers succeeded in the processes (1) and (2) to obtain open-cage fullerene derivative **1** with a 13-membered-ring orifice on the C_{60} cage (Figure 1).[2]

As to the process (3), Rubin et al. succeeded in introducing a helium atom (475 atm, 288-305 °C, 7.5 h) and a hydrogen molecule (100 atm, 400 °C, 48 h) into an open-cage fullerene derivative **2** with a 14-membereb-ring orifice in 1.5% and 5% yields, respectively, for the first time in 2001.[3] However, compound **2** is somewhat unstable at such a high temperature as 400 °C, and actually about 30% of **2** was decomposed during the insertion process of molecular hydrogen. Thus, in order to achieve 100% encapsulation of these gaseous molecules, it was required to synthesize an open-cage fullerene derivative having a larger orifice with sufficient thermal stability. Compound **1** has an orifice, whose size is 5.64 Å along the long axis and 3.75 Å along the short axis, and is thermally stable up to 250 °C. Therefore compound **1** is supposed to be a better host molecule for small atoms and

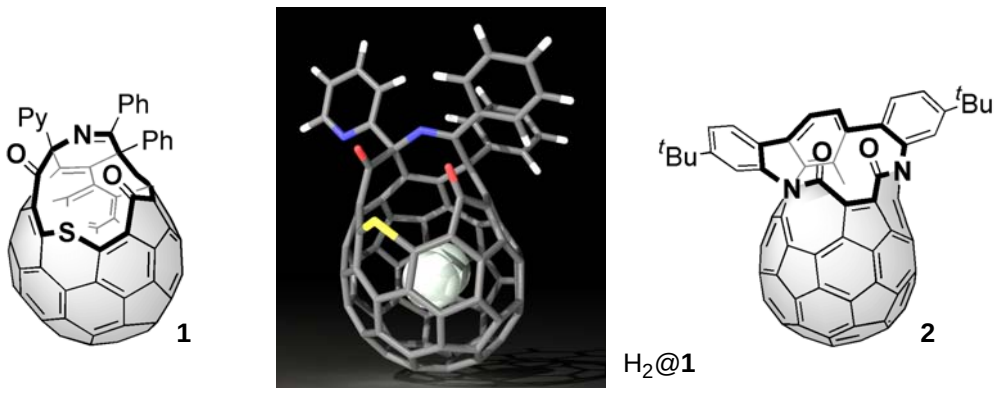

Figure 1. Structures of open-cage fullerene derivatives **1** and **2** and the optimized structure of H_2@**1** calculated at the B3LYP/6-31G** level of theory. The hydrogen molecule is shown as a space-filling model, and the host molecule is shown as a stick model.

molecules than **2**. Here the author shows that the encapsulation of molecular hydrogen into **1** does take place to produce the endohedral complex $H_2@$**1** in 100% yield, and that $H_2@C_{60}$ can be generated upon laser irradiation in the gas phase by self-restoration of the C_{60} cage.

Results and Discussion

In order to gain insight into the feasibility of insertion of some small atom or molecule through the orifice of **1**, theoretical calculations using hybrid density functional theory (B3LYP/6-31G**//B3LYP/3-21G)[4] were conducted. The results are summarized in Table 1 together with the results for compound **2**. The activation energies required for insertion of He, Ne, H_2, and Ar into **1** were calculated to be 19.0, 26.2, 30.1, and 97.8 kcal mol^{-1},

Table 1. Calculated Activation Barriers for Insertion and Escape, and Energies of Encapsulation (in kcal mol^{-1}) for the Guests, He, Ne, H_2, Ar inside **1** and **2** at B3LYP/6-31G**//B3LYP/3-21G level of theory.

Guest	Barrier to insertion		Energy of encapsulation		Barrier to escape	
	1	**2**	**1**	**2**	**1**	**2**
He	+19.0	+24.5[a]	+0.4	+0.2[a]	+18.6	+24.3[a]
Ne	+26.2	+40.6[a]	−1.0	−1.1[a]	+27.2	+41.7[a]
H_2	+30.1	+41.4[a]	+1.4	+1.4[a]	+28.7	+40.0[a]
2nd H_2	+30.2		+9.4		+20.8	
Ar	+97.8	+136.3[a]	+6.2	+6.1[a]	+91.6	+130.2[a]

[a] Values taken from ref. 3b.

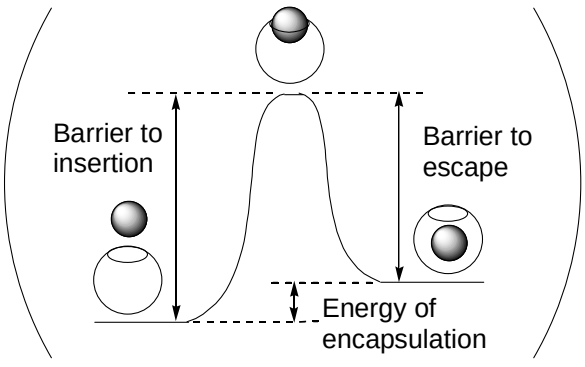

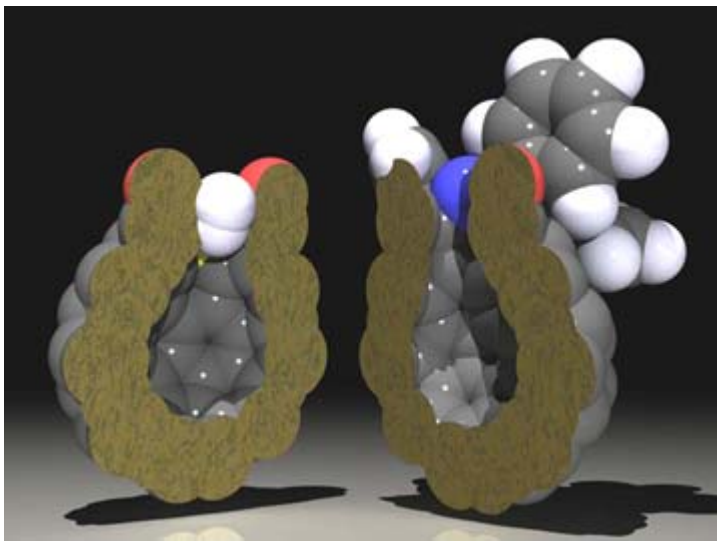

Figure 2. The cut-out view of the transition state for insertion of molecular hydrogen into **1** calculated at the B3LYP/3-21G level of theory.

respectively. These values are considerably lower than the corresponding energies calculated for **2** (24.5, 40.6, 41.4, and 136.3 kcal mol^{-1}),[3b] indicating that encapsulation of atoms or molecule such as He, Ne, and H_2 in **1** is quite promising.

Molecules or molecular systems based on carbon that can freely absorb and release molecular hydrogen are currently attracting great interest as hydrogen storage materials.[5] As mentioned above, the computed activation energy for molecular hydrogen to enter through the orifice is 30.1 kcal mol^{-1} for **1**, which is about 10 kcal mol^{-1} lower than that for **2** (40.1 kcal mol^{-1}).[2b] However, a cut-out view of the transition state shows yet how small this orifice is for molecular hydrogen to pass through (Figure 2).

The actual encapsulation of molecular hydrogen into **1** was attempted by treatment of a powder of **1** with a high-pressure of hydrogen gas (800 atm) at 200 °C in an autoclave (Scheme 1). After 8 h, formation of the endohedral complex H_2@**1** without any decomposition of **1** was confirmed by HPLC and ^{1}H NMR, as described below.

First, the HPLC analysis (Buckyprep/toluene) showed a single peak at exactly the same retention time as that for **1**. Next, the ^{1}H NMR spectrum of the resulting material showed a new sharp signal at such a high field as δ −7.25 ppm in addition to the signals for aromatic protons appearing with exactly the same chemical shifts as those for **1** itself (Figure 3). This

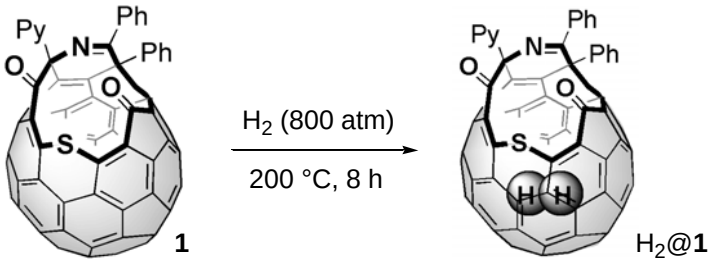

Scheme 1. Insertion of molecular hydrogen in **1**.

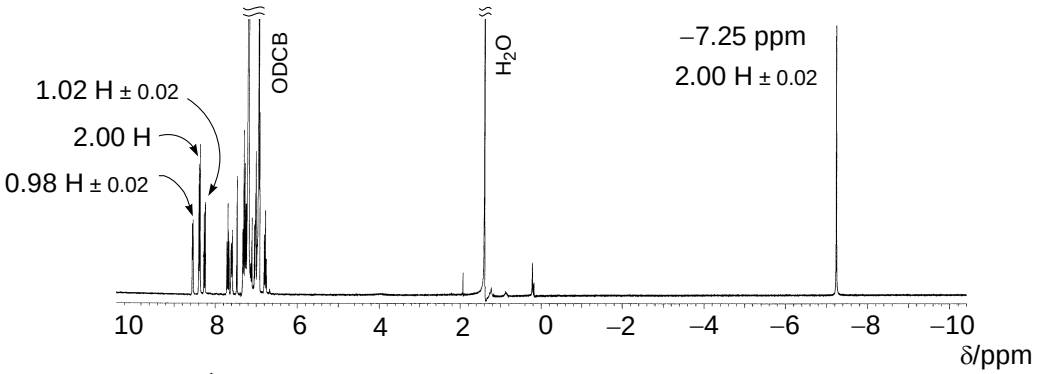

Figure 3. ^{1}H NMR (300 MHz, ODCB-d_4) spectrum of H_2-incoporated **1**.

new signal is assigned to the resonance of the incorporated molecular hydrogen, which is subjected to the strong shielding effect of the fullerene cage.[6] This signal is δ 1.82 ppm more upfield-shifted than the hydrogen signal of H_2@**2** (δ −5.43).[3b] The value of δ −7.25 ppm is between the ^{1}H NMR chemical shifts for hydrogen molecule inside of **1** calculated with the GIAO (gauge-invariant atomic orbital) approach[7] by use of the Hartree-Fock method (GIAO-HF/6-311G**//B3LYP/6-31G**) (δ −9.00) and density functional theory (GIAO-B3PW91/6-311G**//B3LYP/6-31G**) (δ −5.76), confirming the strong shielding effect inside **1**. The integrated relative intensity of the signal was determined to be 2.00 ± 0.02 H by comparison with the intensities of well-resolved aromatic-proton signals at δ 8.55 ppm (1 H), 8.38 (2 H), and 8.26 (1 H), clearly demonstrating that *100% encapsulation* was achieved.

The encapsulation rate was highly dependent on the pressure of hydrogen gas: the yield of H_2@**1** was 90% under 560 atm of H_2 and 51% under 180 atm of H_2, with all other conditions the same.

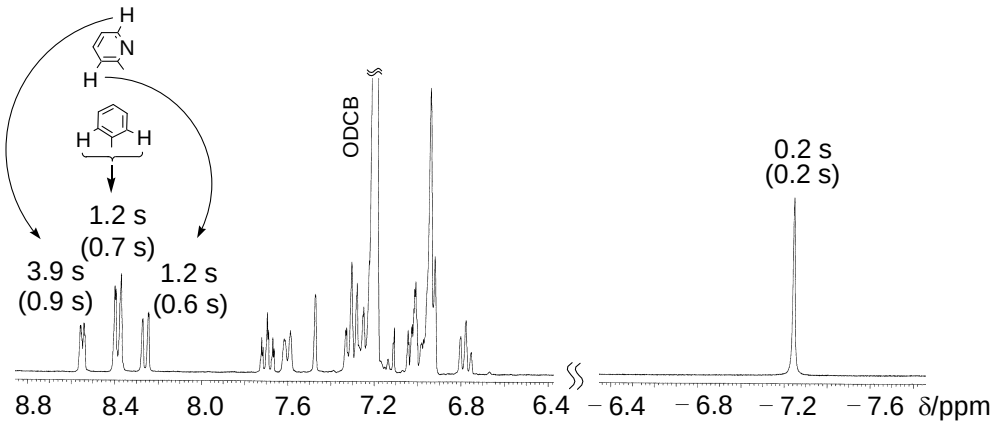

Figure 4. ^{1}H NMR spectrum (300 MHz, *o*-dichlorobenzene-d_4) of H_2@**1**. The values of the spin-lattice relaxation time T_1 obtained for a vacuum-sealed sample for some selected signals; in parentheses are shown the T_1 values obtained for the O_2-saturated sample.

The spin-lattice relaxation time (T_1) of each proton in the ^{1}H NMR was measured, using both a solution of H_2@**1** in *o*-dichlorobenzene-d_4 (ODCB-d_4) sealed under vacuum (<10^{-4} mmHg) and the solution saturated with oxygen (Figure 4). The T_1 values for the signals at δ 8.55 ppm (6-pyridyl), 8.38 (2,6-phenyl), and 8.26 (3-pyridyl) were 3.9 s (0.9 s), 1.2 s (0.7 s), and 1.2 s (0.6 s), respectively, which are in the range of normal values for aromatic protons. In sharp contrast, a very short T_1 value of 0.2 s (0.2 s) was obtained for the encapsulated hydrogen protons. (The values in parentheses are those obtained from the oxygen-saturated solution.) Generally, T_1 values are sensitive to freedom in the motion of the molecule and to an interaction with paramagnetic species such as O_2.[8] The T_1 value for the encapsulated hydrogen molecule was found to suffer no influence of oxygen at all, confirming that it is completely isolated from the outside by the fullerene cage. The remarkably short T_1 value observed for this encapsulated hydrogen molecule might be ascribed to the interaction with the ^{13}C atom(s) in the fullerene cage, or to its hindered rotation caused by the cage, although no line-broadening was observed for the hydrogen signal upon cooling the sample solution to −70 °C.

No escape of the encapsulated molecular hydrogen in H_2@**1** was observed for the sample solution in ODCB-d_4 prepared under vacuum after being kept at room temperature for more than 3 months. However, the molecular hydrogen was gradually released when the

solution was heated above 160 °C, which was monitored as a decrease in the relative integrated intensity of the NMR signal of the encapsulated hydrogen with reference to the aromatic proton signals (Scheme 2). The rate of release monitored at 160, 170, 180, and 190 °C followed first-order kinetics as shown in Figure 5. The resulting rate constants and half-lives for the release at each temperature are summarized in Table 2. The Arrhenius plot

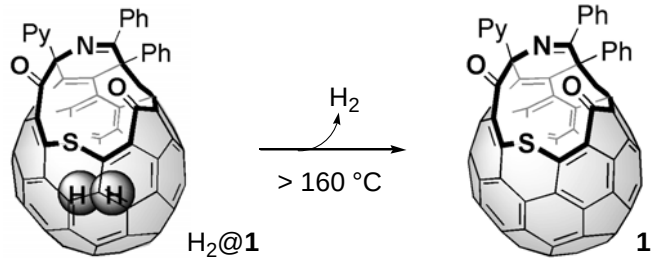

Scheme 2. Release of molecular hydrogen from $H_2@\mathbf{1}$.

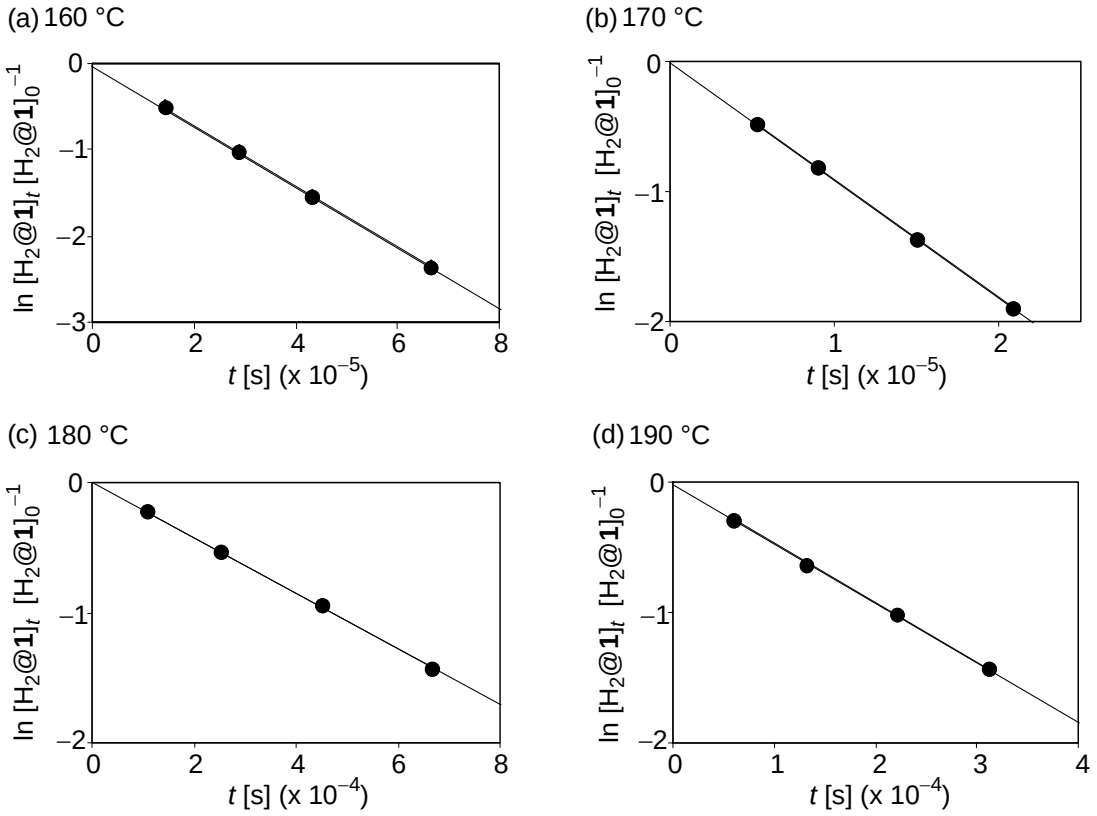

Figure 5. The rate plots for the release of molecular hydrogen from $H_2@\mathbf{1}$ at four temperatures; (a) 160 °C, (b) 170 °C, (c) 180 °C, (d) 190 °C.

gave an excellent linear fit, with the pre-exponential factor (A) and the activation energy (E_a) for the escape of molecular hydrogen from the cage being $10^{11.8\pm0.3}$ and 34.3 ± 0.7 kcal mol^{-1}, respectively (Figure 6). The activation parameters at 25 °C were determined as $\Delta G^{\ddagger}$ = 35.5 ± 0.9 kcal mol^{-1}, $\Delta H^{\ddagger}$ = 33.4 ± 0.4 kcal mol^{-1}, and $\Delta S^{\ddagger}$ = –7 ± 2 cal K^{-1} mol^{-1}. Compared with the $\Delta S^{\ddagger}$ value (–17 cal K^{-1} mol^{-1})[3b] reported for the release of ^{3}He from ^{3}He@**2**, the $\Delta S^{\ddagger}$ value in the present work is less negative, although the hydrogen molecule is expected to have a more highly ordered arrangement in the transition state upon release from **1**. As such, the hydrogen molecule inside of **1** must be already restricted in motion by the interaction with the cage in the ground state.

The compound H_2@**1** is regarded as a unique model that can provide an opportunity to

Table 2. The Rate Constants (k) and Half-Lives ($t_{1/2}$) for the Release of Molecular Hydrogen at Four Temperatures

T [°C]	k [s^{-1}]	$t_{1/2}$ [h]
160 ± 0.5	3.54 x 10^{-6}	54.4
170 ± 0.5	9.05 x 10^{-6}	21.3
180 ± 0.5	2.13 x 10^{-5}	9.0
190 ± 0.5	4.60 x 10^{-5}	4.2

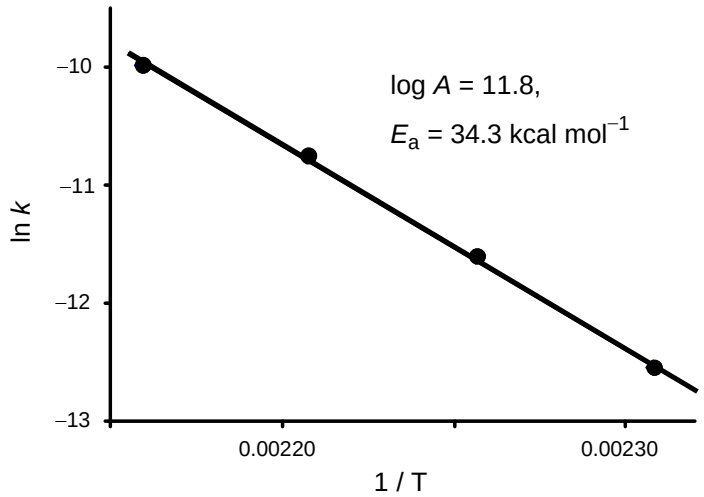

Figure 6. Arrhenius plot for the release of molecular hydrogen from H_2@**1**.

observe a single molecule of hydrogen as a completely isolated species. The extraordinary high-field shift (δ −7.25 ppm) of the ^{1}H NMR signal for the molecular hydrogen surely indicates that molecular hydrogen is encapsulated *somewhere* inside the fullerene cage. X-ray diffraction analysis with synchrotron radiation appeared most suitable for investigating about the location of the molecular hydrogen within the fullerene cage of $H_2@$**1**.

Thus, we conducted an X-ray diffraction study of single crystals of $H_2@$**1**, together with empty **1** as a matching reference, by using synchrotron radiation in the Photon Factory at High-Energy Accelerator Research Organization (KEK), in collaboration with Professor Hiroshi Sawa. The resulting electron-density representations of $H_2@$**1** and empty **1** obtained by maximum entropy method (MEM) analysis[9] are shown in Figure 7 as cut-out views. These representations clearly show an area of electron density floating at the center of the fullerene cage of $H_2@$**1**, whereas no such electron density was observed at all in the case of empty **1**. The number of electrons of this fragment was calculated to be 2.0 ± 0.1, exactly corresponding to that of a hydrogen molecule. These characteristic features are also seen as contour maps in Figure 8. Thus, a single hydrogen molecule encapsulated in the fullerene cage of $H_2@$**1** was directly observed for the first time by the synchrotron X-ray diffraction experiments and MEM analysis.

Finally, we conducted MALDI-TOF mass analysis on $H_2@$**1** using dithranol as a matrix. At a laser power adjusted slightly above the threshold for the ionization of **1**, the molecular ion peak of $H_2@$**1** (*m*/*z* 1068) was clearly observed, along with a peak for empty **1** (*m*/*z* 1066) formed by release of the hydrogen molecule upon laser irradiation (Figure 9a). In addition, a fragment ion peak due to elimination of pyridyl and carbonyl groups (*m*/*z* 960) and a peak due to elimination of pyridyl and phenyl groups (*m*/*z* 911) were observed. When a higher laser power was used (Figure 9b), the peak height for the molecular ion decreased and, instead, the formation of C_{60} (*m*/*z* 720) was clearly observed. This result demonstrates that a highly modified C_{60} derivative such as **1**, having a large orifice, can regenerate the pristine C_{60} cage by self-restoration through the cleavage of organic addends and through closing of the orifice by itself.

More remarkable is the appearance of a peak at *m*/*z* 722, corresponding to $C_{60}H_2$. The intensity of this peak was approximately one-third of that for C_{60}, taking the isotope distribution

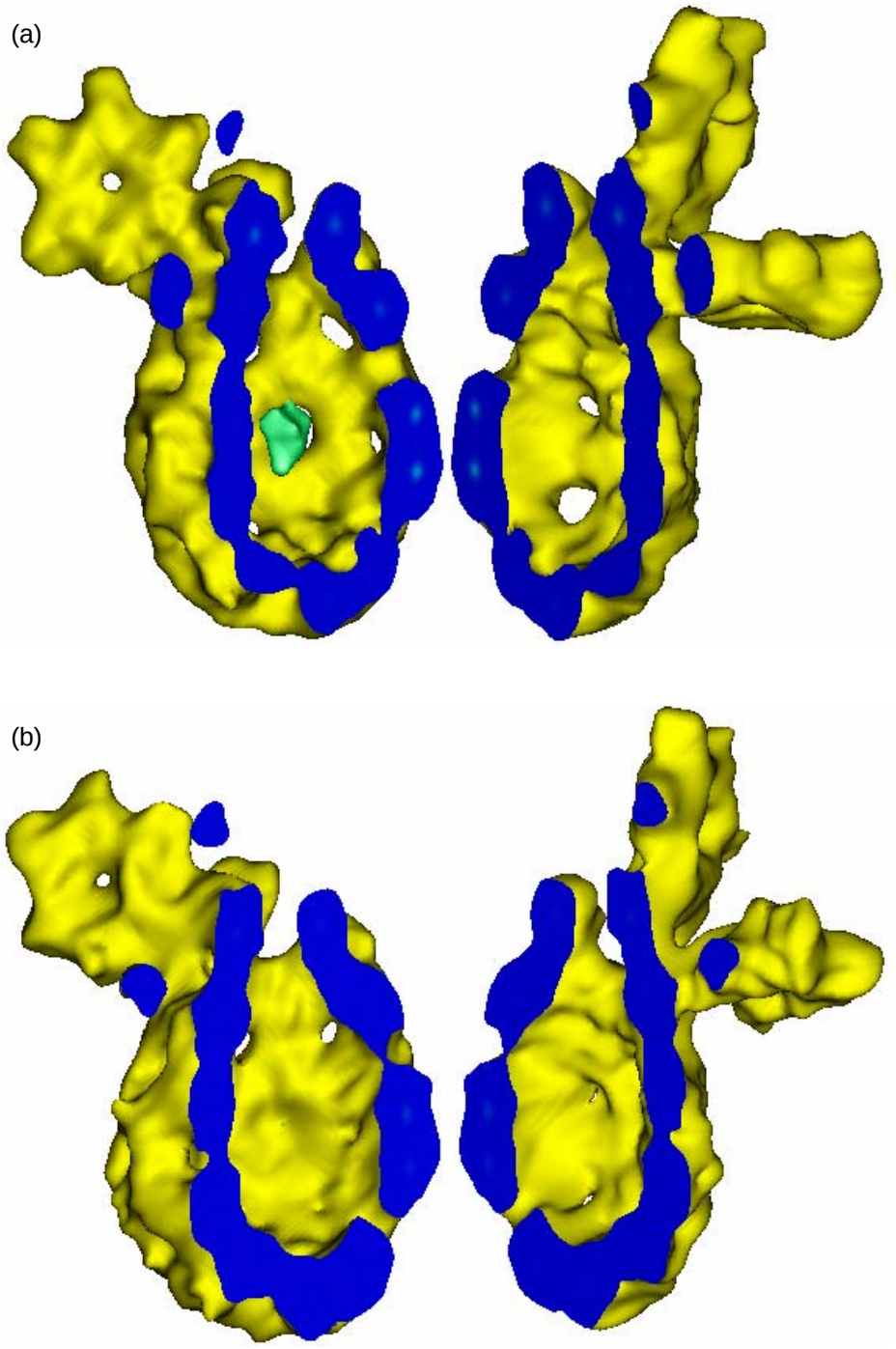

Figure 7. MEM electron densities of (a) H_2@**1** and (b) empty **1** as an equal-density contour surface and as a vertical division. The equicontour level is at 0.4 e $Å^{-3}$. The electron density of the encapsulated molecular hydrogen is colored green in (a).

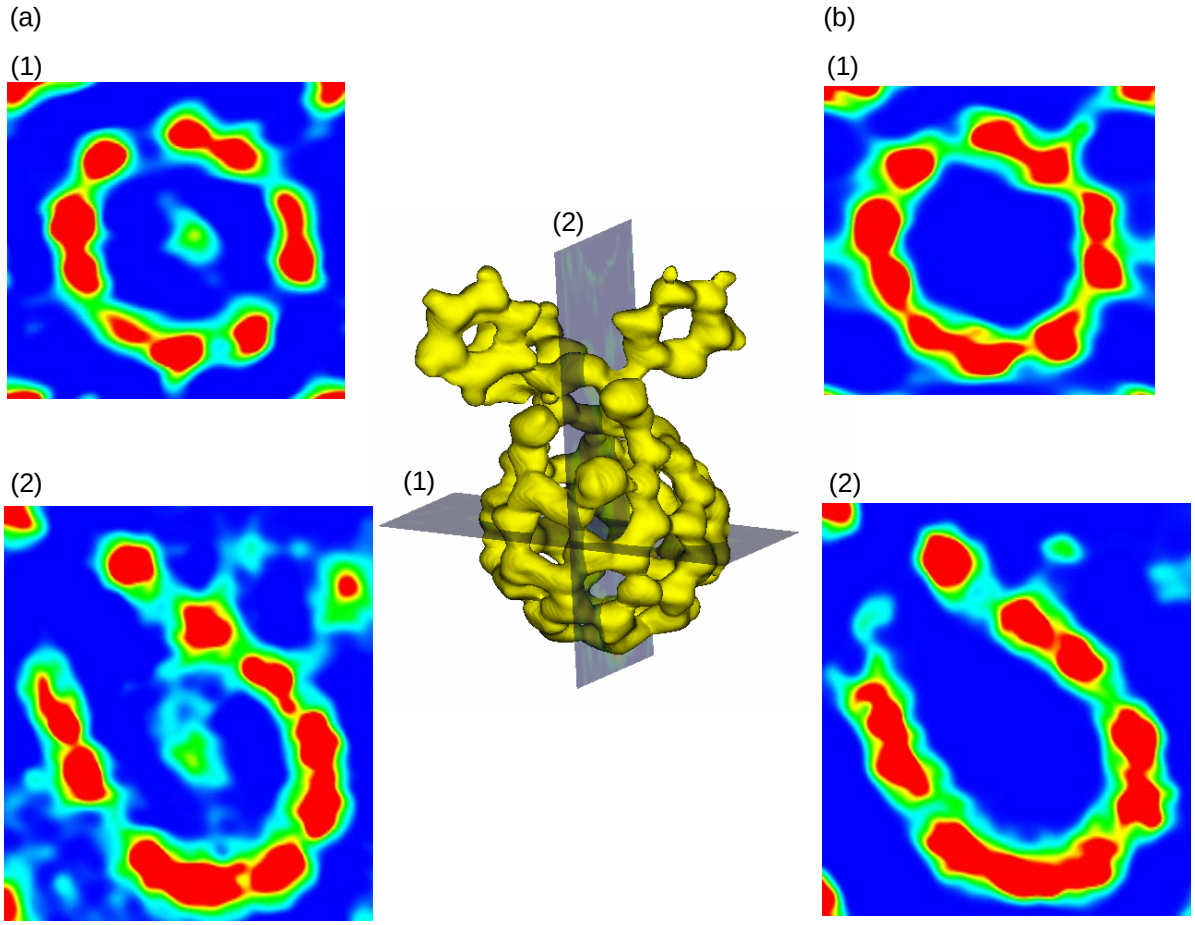

Figure 8. MEM electron-density distributions of (a) $H_2@$**1** and (b) empty **1** for (1) horizontal division and (2) vertical division. The center figure shows the positions of division for (1) and (2). The contour maps are drawn from 0.01 to 0.11 e $Å^{-3}$.

of C_{60} into consideration. Because exohedral hydrogenated fullerene $C_{60}H_2$[10] gave the molecular ion peak not at *m*/*z* 722 but at *m*/*z* 721 and 720 under the same conditions in a separate experiment, this peak at *m*/*z* 722 is assigned to the endohedral complex of C_{60} encapsulating the hydrogen molecule, i.e., $H_2@C_{60}$. Thus, it was shown that, upon laser irradiation, generation of $H_2@C_{60}$ is possible in the gas phase by self-restoration of $H_2@$**1**.

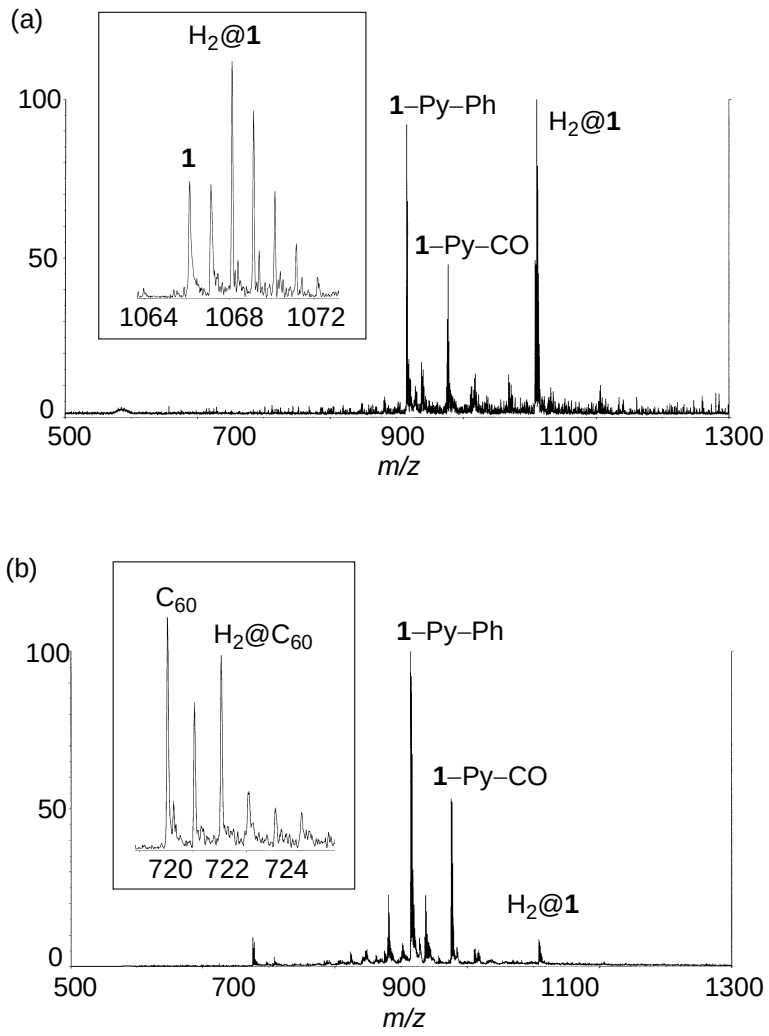

Figure 9. MALDI-TOF mass spectra of H_2@**1** obtained in the negative ionization mode. (a) Spectrum taken with a laser power slightly above the threshold for ion formation. (b) Spectrum taken with a higher laser power. Insets show the expanded spectra.

Conclusion

As described above, we achieved the insertion of molecular hydrogen in the open-cage fullerene derivative **1** in 100% for the first time without any decomposition by applying pressurized hydrogen (800 atm) at 200 °C for 8 h. A ^{1}H NMR signal for the incorporated

hydrogen was observed at such a high field as −7.25 ppm. $H_2@$**1** is quite stable at room temperature, but it releases molecular hydrogen slowly at a temperature above 160 °C and the activation energy was determined as 34.3 kcal mol^{-1}. The encapsulated molecular hydrogen was directly observed to be located at the center of the cage by synchrotron X-ray crystallography and MEM analysis. Upon MALDI-TOF mass measurement of $H_2@$**1**, the formation of C_{60} and $H_2@C_{60}$ was clearly observed in a molar ratio of about 3:1. This result demonstrates that a highly modified C_{60} derivative such as **1** can regenerate the pristine C_{60} cage by self-restoration upon application of high laser power. Considering the history of C_{60}, with its discovery by mass spectrometry,[11] macroscopic isolation,[12] and organic synthesis,[13] this result can be taken as a promising indication for the macroscopic synthesis of $H_2@C_{60}$.

Experimental Section

General. The ^1H and ^{13}C NMR measurements were carried out on a Varian Mercury 300 instrument and the chemical shifts are reported in ppm with reference to the signal of *o*-dichlorobenzene-d_4 (ODCB-d_4) used as an internal standard (δ 7.20 ppm in ^1H NMR). FAB mass spectra were recorded on a JEOL MStation JMS-700. MALDI-TOF mass spectra were measured with an Applied Biosystem Voyager-DE STR spectrometer using dithranol as a matrix. The high-pressure liquid chromatography (HPLC) was performed by the use of a Cosmosil Buckyprep column (4.6 mm × 250 mm) for analytical purpose.

Fullerene C_{60} was purchased from Matsubo Co. Open-cage fullerene **1** was synthesized as described in Chapter 2.

Computational Methods. All calculations were conducted using the Gaussian 98 series of electronic structure programs.[4] The ground-state structure of open-cage fullerene **1**, its inclusion complexes of gases, and the transition-state structures for their encapsulation process were fully optimized at the B3LYP/3-21G level of theory, and the energies were computed based on these geometries using the 6-31G** basis set in the same manner as reported for Rubin's open-cage fullerene **2**.[3b] For each transition structure, a single imaginary vibrational mode was obtained by the frequency calculations: He-**1**, 214*i* cm^{-1}; Ne-**1**, 100*i* cm^{-1}; H_2-**1**, 326*i* cm^{-1}; Ar-**1**, 84*i* cm^{-1}.

Insertion of molecular hydrogen in 1. A powder of open-cage fullerene **1** (775 mg, 0.726 mmol) lightly wrapped in a piece of aluminum foil was heated at 200 °C in an autoclave under a high-pressure H_2 gas (800 atm). A high pressure of 800 atm was generated by introducing H_2 gas of 400 atm, which was generated by compressing H_2 gas of 140 atm from a container by the use of a hydraulic compressor, into a 50-mL autoclave cooled at −78 °C, followed by heating at 200 °C. After 8 h, the powder was recovered by washing the aluminum foil with CS_2. The HPLC analysis (a Buckyprep column eluted with toluene) of the recovered powder showed a single peak at exactly the same retention time as that for **1**. The ^{1}H NMR spectra of the obtained powder were taken with sufficiently long pulse intervals (42 s) to obtain signal intensities as accurately as possible; 300 MHz, in ODCB-d_4 at 25 °C, 9000 Hz frequency range, 7.8 μs irradiation as a 45° pulse. From the ^{1}H NMR spectrum shown in Figure 3 and the FAB mass spectrum, the powder was found to be H_2@**1**: HRMS (+FAB) calcd for $C_{80}H_{17}N_2O_2S$ (MH^+), 1069.1011, found 1069.1040.

Release of hydrogen molecule from H_2@1. A solution of H_2@**1** in ODCB -d_4, which was sealed under vacuum (<10^{-4} mmHg) after three freeze-pump-thaw cycles, was heated at 160, 170, 180, and 190 °C. Each release rate was determined by monitoring a gradual decrease in the relative intensity of the NMR signal of the encapsulated hydrogen molecule with reference to the aromatic proton signals.

Synchrotron X-ray structural analysis of H_2@1 and empty 1. Accurate X-ray diffraction data were obtained by synchrotron radiation with a Weissenberg-type imaging-plate detector at BL-1A in the Photon Factory at High-Energy Accelerator Research Organization (KEK), Japan. The X-ray wavelength was 1.0 Å. The intensity of the Bragg reflections was measured in a half-sphere of reciprocal space in the range 2θ <120°. The sample was cooled at 200 K by a N_2-gas flow-type refrigerator. The Rapid-Auto program by MSC Co. was used for two-dimensional image processing; the Sir2002 program was used for the direct method. The number of observed reflections with I>5s(I) was 9449 for the H_2@**1** crystal and 9302 for the empty **1** crystal. The Shelx97 program was used for refinements. After full refinement, the R factor was 0.09 for the H_2@**1** crystal and 0.08 for the empty one. The MEM (maximum entropy method) analysis was carried out with the Enigma program[9] at a resolution of 128 × 128 × 128 pixels. The *R* factors of the final MEM charge density were

0.028 and 0.024 for H_2@**1** and empty **1**, respectively.

References and Notes

(1) (a) Rubin, Y. *Chem*. *Eur*. *J*. **1997**, *3*, 1009. (b) Rubin, Y. *Top*. *Curr*. *Chem*. **1999**, *199*, 67. (c) Nierengarten, J.-F. *Angew*. *Chem*. *Int*. *Ed*. **2001**, *40*, 2973.

(2) Murata, Y.; Murata, M.; Komatsu, K. *Chem*. *Eur*. *J*. **2003**, *9*, 1600.

(3) (a) Schick, G.; Jarrosson, T.; Rubin, Y. *Angew*. *Chem*. *Int*. *Ed*. **1999**, *38*, 2360. (b) Rubin, Y.; Jarrosson, T.; Wang, G.-W.; Bartberger, M. D.; Houk, K. N.; Schick, G.; Saunders, M.; Cross, R. J. *Angew*. *Chem*. *Int*. *Ed*. **2001**, *40*, 1543.

(4) Frisch, M. J.; Trucks, G. W.; Schlegel, H. B.; Scuseria, G. E.; Robb, M. A.; Cheeseman, J. R.; Zakrzewski, V. G.; Montgomery, H. A., Jr.; Stratmann, R. E.; Burant, J. C.; Dapprich, S.; Millam, J. M.; Daniels, A. D.; Kudin, K. N.; Strain, M. C.; Farkas, O.; Tomasi, J.; Barone, V.; Cossi, M.; Cammi, R.; Mennucci, B.; Pomelli, C.; Adamo, C.; Clifford, S.; Ochterski, J.; Petersson, G. A.; Ayala, P. Y.; Cui, Q.; Morokuma, K.; Malick, D. K.; Rabuck, A. D.; Raghavachari, K.; Foresman, J. B.; Cioslowski, J.; Ortiz, J. V.; Baboul, A. G.; Stefanov, B. B.; Liu, G.; Liashenko, A.; Piskorz, P.; Komaromi, I.; Gomperts, R.; Martin, R. L.; Fox, D. J.; Keith, T.; Al-Laham, M. A.; Peng, C. Y.; Nanayakkara, A.; Gonzalez, C.; Challacombe, M.; Gill, P. M. W.; Johnson, B.; Chen, W.; Wong, M. W.; Andres, J. L.; Gonzalez, C.; Head-Gordon, M.; Replogle, E. S.; Pople, J. A. *Gaussian 98*, Revision A.7; Gaussian, Inc.: Pittsburgh, PA, 1998.

(5) For example, see: Tibbetts, G. G.; Meisner, G. P.; Olk, C. H. *Carbon* **2001**, *39*, 2291.

(6) For example, see: (a) Saunders, M.; Jiménez-Vázquez, H. A.; Cross, R. J.; Mroczkowski, S.; Freedberg, D. I.; Anet, F. A. L. *Nature* **1994**, *367*, 256. (b) Saunders, M.; Jiménez-Vázquez, H. A.; Bangerter, B. W.; Cross, R. J.; Mroczkowski, S.; Freedberg, D. I.; Anet, F. A. L. *J. Am*. *Chem*. *Soc*. **1994**, *116*, 3621. (c) Saunders, M.; Cross, R. J.; Jiménez-Vázquez, H. A.; Shimshi, R.; Khong, A. *Science* **1996**, *271*, 1693.

(7) Helgaker, T.; Jaszuński, M.; Ruud, K. *Chem. Rev.* **1999**, *99*, 293.

(8) Friebolin, H. *Basic One- and Two-Dimensional NMR Spectroscopy*; VCH Publishers: New York, 1991.

(9) H. Tanaka, M. Takata, E. Nishibori, K. Kato, T. Iishi, M. Sakata, *J. Appl. Crystallogr.* **2002**, *35*, 282.

(10) Henderson, C. C.; Cahill, P. A. *Science* **1993**, *259*, 1885.

(11) Kroto, H. W.; Heath, J. R.; O'Brien, S. C.; Curl, R. F.; Smalley, R. E. *Nature* **1985**, *318*, 162.

(12) Krätschmer, W.; Lamb, L. D.; Fostiropoulos, K.; Huffman, D. R. *Nature* **1990**, *347*, 354.

(13) (a) Boorum, M. M.; Vasil'ev, Y. V.; Drewello, T.; Scott, L. T. *Science* **2001**, *294*, 828. (b) Scott, L. T.; Boorum, M. M.; McMahon, B. J.; Hagen, S.; Mack, J.; Blank, J.; Wegner, H.; Meijere, A. *Science* **2002**, *295*, 1500.

Chapter 4

Synthesis and Properties of Endohedral C_{60} Encapsulating Hydrogen Molecule, $H_2@C_{60}$

Abstract: A 13-membered-ring orifice of an open-cage fullerene encapsulating molecular hydrogen in 100% was closed by using four-step organic reactions, which has enabled production of endohedral fullerene, $H_2@C_{60}$, in more than 100-mg quantities. The orifice was first reduced to a 12-membered ring by extrusion of a sulfur atom at the rim of the orifice, and the ring was further reduced into an eight-membered ring by reductive coupling of two carbonyl groups. Final closure of the orifice was completed by a thermal reaction. Purification of $H_2@C_{60}$ was accomplished by recycle HPLC. The gradual downfield shift of ^1H NMR signal for the inner hydrogen observed upon reduction of the orifice size was interpreted based on the gauge-independent atomic orbital (GIAO) and the nucleus-independent chemical shifts (NICS) calculations. The spectral as well as electrochemical examination of the properties of $H_2@C_{60}$ has shown that the electronic interaction between the inner hydrogen and outer C_{60} π-system is quite small but becomes appreciable when the outer π-system acquires more than three extra electrons. Four kinds of exohedral derivatives of $H_2@C_{60}$ were synthesized, and the endohedral NMR chemical shifts of H_2 were found to be quite similar to those for ^3He NMR signals of the corresponding $^3He@C_{60}$ derivatives.

Introduction

As described in General Introduction, the preparation of endohedral fullerenes, the spherical all-carbon molecules incorporating atom(s) or a molecule inside the framework,[1] has so far only relied on hardly controllable physical processes such as co-vaporization of carbon and metal atoms[1b,c] or high-pressure/high-temperature treatment (650 °C/3000 atm) with noble gases,[2] which yield only limited quantities (e.g., a few milligrams) of pure product after laborious isolation procedures. This situation has been a severe obstacle to the development of fundamental as well as application-oriented studies on a series of these molecules of great importance. In order to bring about a breakthrough to this situation and to make their science developed, an entirely new approach for their production is highly desired. In this regard, a molecular surgery approach[3] to endohedral fullerenes is quite appealing, because the efficient production of various endohedral fullerenes in much larger amounts is expected.

As mentioned in Chapter 2 and 3, open-cage fullerene derivative **1** with a 13-membered-ring orifice was synthesized,[4,5] and insertion of molecular hydrogen was achieved to afford H_2@**1** in 100% without any decomposition, by treating a powder of **1** with high-pressure of H_2 gas (800 atm) at 200 °C in an autoclave.[6] This complete encapsulation made it possible to directly observe a single hydrogen molecule at the center of the fullerene cage by the use of the synchrotron X-ray diffraction technique[7] and also with the solid state NMR spectroscopy.[8]

Here, as the final process of the molecular surgery, the author describes complete closure of the orifice of H_2@**1** using organic reactions to afford an entirely new endohedral

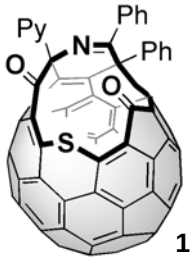

1

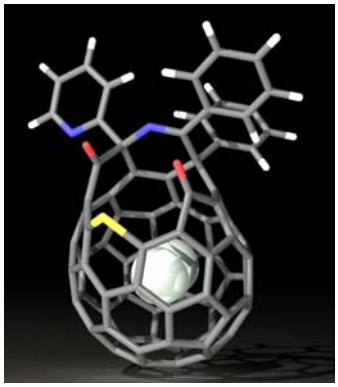

H_2@**1**

fullerene, $H_2@C_{60}$. So far, the ^{3}He NMR chemical shift of fullerenes incorporating ^{3}He in 0.1%[9] has been successfully used as a probe sensitive to the structure of fullerenes.[2a,10] Similarly, the endohedral H_2 chemical shifts should be highly sensitive to the fullerene structure, and this has been examined in detail for a series of open-cage fullerene derivatives incorporating H_2 as well as some of the derivatives of $H_2@C_{60}$ itself.

Results and Discussion

Size-Reduction of the 13-Membered-Ring Orifice of H_2@1: As described in Chapter 3, upon strong laser irradiation in the MALDI-TOF mass measurement of H_2@**1**, a weak peak at *m*/*z* 722 corresponding to $H_2@C_{60}$ was observed, indicating that the orifice of H_2@**1** can be closed by the laser power in the gas phase.[6] However, not only the peak intensity was weak but about 70% of the originally encapsulated hydrogen was shown to escape from C_{60} during the process to close the orifice. This result indicated that it was necessary to reduce the size of the orifice in order to produce $H_2@C_{60}$ without serious loss of the encapsulated hydrogen. Since the hydrogen molecule in H_2@**1** was found to be gradually released with the half-life of 54.4 h at 160 °C or 4.2 h at 190 °C,[6] such a high temperature must be avoided in the process to close the orifice.

At a first glance of the molecular structure of **1**, removal of the sulfur atom appeared as the most facile procedure for the orifice-size reduction. Thus we first conducted an oxidation of the sulfide unit of H_2@**1** by *m*-chloroperbenzoic acid (MCPBA) to make the sulfur atom readily removable.[11] The oxidation reaction proceeded at room temperature smoothly to give the corresponding sulfoxide H_2@**2** quantitatively (Scheme 1 (a)). The product was easily identified: the FAB mass spectrum exhibited a molecular ion peak at *m*/*z* 1084 (M^+) corresponding to H_2@**2** and the IR spectrum showed a prominent sulfinyl stretching band at 1073 cm^{-1}, in addition to NMR data (Experimental Section). Between the two possible stereoisomers H_2@**2**(*exo*) and H_2@**2**(*endo*), the *exo*-isomer is considered to be formed since it can avoid steric repulsion between the sulfinyl group and two carbonyl groups. Indeed, theoretical calculations at the B3LYP/6-31G* level of theory[12] indicated the *exo*-isomer to be more stable than the *endo*-isomer by 8.6 kcal mol^{-1}. The ^{1}H NMR

spectrum of H_2@**2** showed a sharp signal for the encapsulated hydrogen at δ −6.33 ppm in *o*-dichlorobenzene-d_4 (ODCB-d_4) with its integrated peak area of 2.0±0.02 H, which is 0.92 ppm downfield shifted as compared to that of H_2@**1** (δ −7.25 ppm).

As shown in Figure 1, the MALDI-TOF mass spectrum of **2** exhibited three strong peaks, i.e., a molecular ion peak and peaks for **1** and for a derivative having a 12-membered-ring orifice generated by fragmentation of an SO unit as expected.[13] In order to chemically remove the SO unit, first we attempted its thermal extrusion by heating H_2@**2** in refluxing toluene or at 140 °C in ODCB, but there was practically no reaction. In contrast, simple irradiation of a solution of H_2@**2** in benzene with visible light through a Pyrex glass flask by the use of a xenon-lamp at room temperature afforded desired product H_2@**3** in 42% yield (Scheme 1 (b)), with 38% recovery of unreacted H_2@**2**.[14] The structure of H_2@**3** was confirmed by NMR, FAB mass, IR, and UV-vis spectra, which were identical to those of **3**[4] except the following. The ^{1}H NMR spectrum (in ODCB-d_4) clearly exhibited a signal for the encapsulated hydrogen at δ −5.80 ppm with the integrated ratio corresponding to 2.0±0.02 H, which is 0.53 ppm downfield shifted as compared to H_2@**2**.

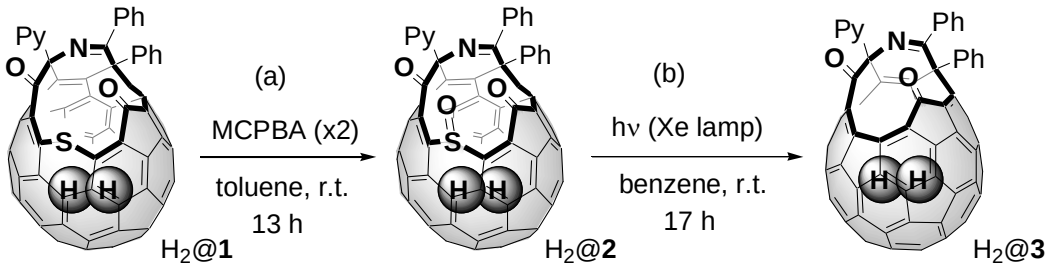

Scheme 1. Size reduction of the orifice of H_2@**1** by removal the sulfur atom.

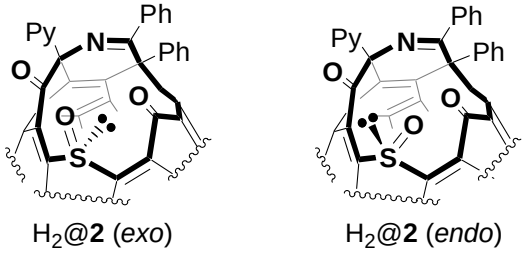

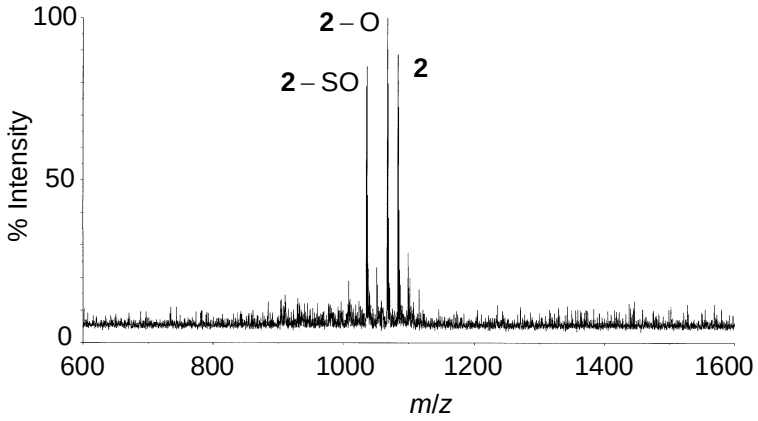

Figure 1. MALDI-TOF mass spectrum of **2** (positive ionization mode, dithranol matrix).

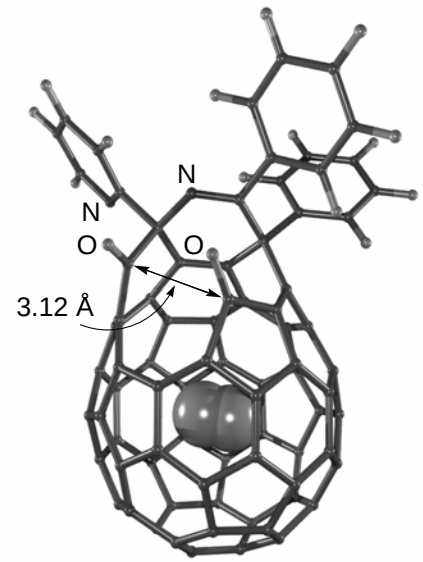

Figure 2. The optimized structure of $H_2@$**3** (B3LYP/6-31G*).

As shown by the optimized structure of $H_2@$**3** at the B3LYP/6-31G* level of theory in Figure 2, removal of the sulfur atom from the 13-membered-ring orifice of $H_2@$**1** brought about a significant size reduction of the orifice. The distance between two carbonyl carbons across the orifice is reduced from 3.89 Å for $H_2@$**1** to 3.12 Å for $H_2@$**3**. Accordingly, the calculated activation energy for an escape of the hydrogen molecule from $H_2@$**3** is estimated as 50.3 kcal mol^{-1}, which is significantly greater than that of 28.7 kcal mol^{-1} for $H_2@$**1**[6] (both

calculated at the B3LYP/6-31G** level with optimized structures at the B3LYP/3-21G level). In fact, we could not observe any escape of the encapsulated hydrogen at all upon heating an ODCB-d_4 solution of H_2@**3** even at 190 °C for 3 days under vacuum, as examined by ^{1}H NMR. This is in a sharp contrast with the case of H_2@**1**, from which the hydrogen molecule was gradually released with the half-life period of 4.2 h under the same conditions.[6] The MALDI-TOF mass spectrum of H_2@**3** showed a dramatic change from that of **1** (Figure 3). Now a peak for $H_2@C_{60}$ was observed as a base peak, indicating its highly enhanced accessibility from H_2@**3**. Unfortunately, however, the spectrum showed that about 20% of the hydrogen molecule escaped from H_2@**3** upon laser irradiation (inset of Figure 3). As a preliminary study, the powder of H_2@**3** was heated at 350 °C under vacuum (ca. 1 mmHg), but this resulted in the formation of $H_2@C_{60}$ in a trace amount. Hence, further reduction of the orifice size was apparently required to produce a macroscopic amount of $H_2@C_{60}$.

For this purpose, the McMurry reaction worked well for reductive coupling of the two carbonyl groups at the orifice of H_2@**3** leading to the formation of open-cage fullerene derivative H_2@**4** with an eight-membered-ring orifice in 88% yield (Scheme 2).[16] The high efficiency of this reaction is quite reasonable since the two carbonyl groups of H_2@**3** are fixed at the parallel orientation in a close proximity, as mentioned above. The structure of H_2@**4** was confirmed by ^{1}H and ^{13}C NMR, FAB mass, IR, and UV-vis spectra, which were identical to those of empty **4**[4] except the ^{1}H NMR (see below). The MALDI-TOF mass spectrum of

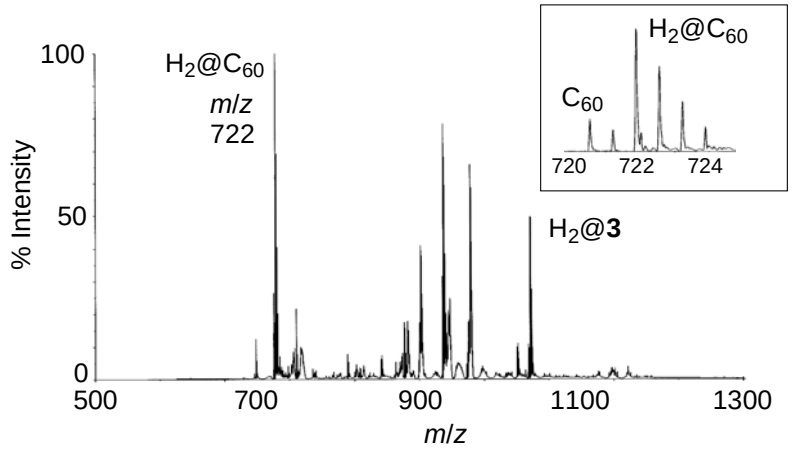

Figure 3. MALDI-TOF mass spectrum of H_2@**3** (positive ionization mode, dithranol matrix). Inset shows the expanded spectrum.

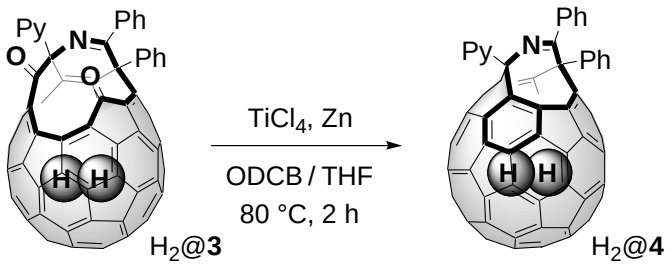

Scheme 2. McMurry reaction of $H_2@$**3**.

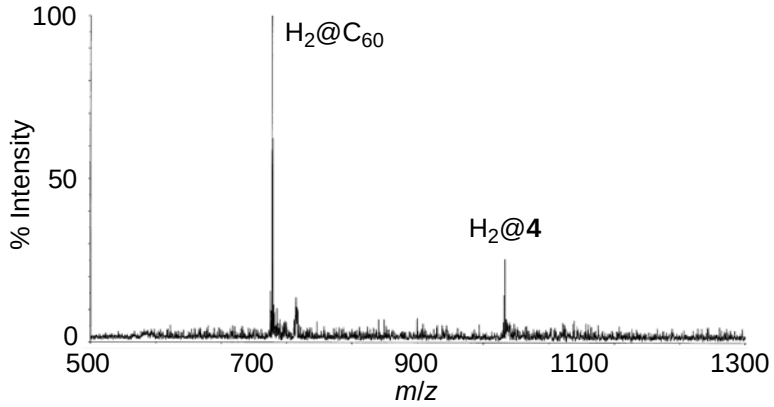

Figure 4. MALDI-TOF mass spectrum of $H_2@$**4** (positive ionization mode, dithranol matrix).

$H_2@$**4** is quite simple exhibiting only two peaks over the range of $m/z > 500$, that is, a base peak corresponding to $H_2@C_{60}$ and a smaller molecular ion peak for $H_2@$**4** (Figure 4). The NMR signal of the encapsulated hydrogen of $H_2@$**4**, with integrated area of 2.0±0.02 H, was observed at δ –2.95 ppm in ODCB-d_4, which was 2.85 ppm downfield shifted as compared to that of $H_2@$**3**.

It is to be noted that the encapsulated hydrogen is completely retained at each step of the process for orifice-size reduction, which was confirmed by comparing the integrated peak area for the encapsulated hydrogen with reference to that for the aromatic protons in each ^{1}H NMR spectrum.

Complete Restoration of the Fullerene Cage; Formation of $H_2@C_{60}$: The final step to completely eliminate extra organic addends and to close the orifice was accomplished by heating a brown powder of $H_2@$**4** (245 mg) in a vacuum-sealed tube placed in an electric furnace at 340 °C for 2 h. The resulting black material was dissolved in CS_2 and was analyzed by HPLC on a Cosmosil Buckyprep column eluted with toluene. As shown in Figure 5, the chromatogram exhibited one prominent peak at the retention time of 8.11 min, which was exactly the same as that for empty C_{60}, while the peak for $H_2@$**4** at the retention time of 4.52 min disappeared. A preparative-scale separation of the C_{60} portion was readily made by flash chromatography over silica gel eluted with CS_2 to give a purple solution containing desired $H_2@C_{60}$ (118 mg, 67%), contaminated by 9% of empty C_{60}, which was proven as described below. Similar results were obtained when $H_2@$**4** was heated at 300 °C for 24 h, or at 400 °C for 2 min.

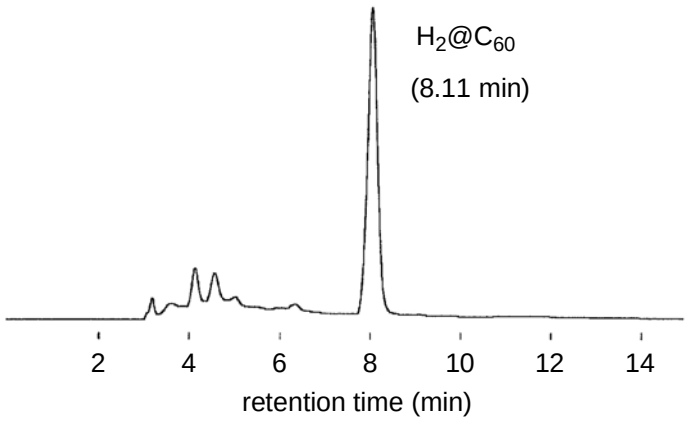

Figure 5. HPLC chart of the crude products obtained by thermal reaction of $H_2@$**4**. Column, Cosmosil Buckyprep (4.6 mm × 250 mm); solvent, toluene; flow rate, 1 mL min^{-1}.

The mechanism for this thermal reaction is considered as shown in Figure 6. An initial [π2s + π2s + π2s] electrocyclization produces intermediate **5** incorporating two cyclopropane rings, which undergoes subsequent radical cleavage to give intermediate **6**. As to the following step, conceptually the most reasonable one is a [π2s + π2s + π2s] cycloreversion reaction to give C_{60} together with 2-cyanopyridine (**7**) and diphenylacetylene (**8**) (Figure 6 (a)). Indeed, **7** and **8** were detected in the crude product as described in the Experimental

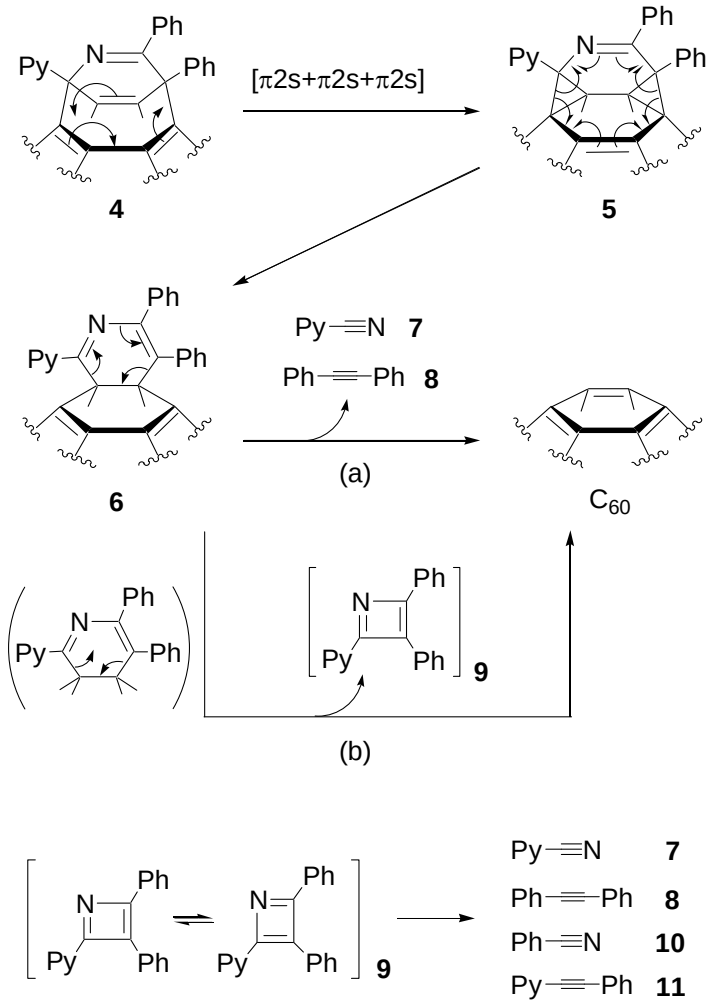

Figure 6. Possible reaction mechanisms for the formation of C_{60} from compound **4**. For the fullerene derivatives only top parts of the molecules are shown.

Section. However, the reaction was not so clean, and, to our surprise, benzonitrile (**10**) and 2-(phenylethynyl)pyridine (**11**) were also formed together with an unknown compound having a molecular formula of Ph_2PyC_3N. This latter fact indicates that occurrence of the reaction pathway shown in Figure 6 (b) cannot be ruled out, although we regrettably do not have a reasonable explanation for the occurrence of this reaction involving an extrusion of highly unstable byproduct such as azacyclobutadiene (called azete) derivative **9**.[17]

It was also unexpected that 9% of encapsulated hydrogen molecule had escaped from the cage during this thermal reaction. Theoretical calculations as well as inspection of the

molecular model suggest that it is impossible for a hydrogen molecule to pass through the eight-membered ring in compound **4**. We tentatively assume that cleavage of some additional single bonds in the fullerene skeleton of H_2@**4** (not shown in Figure 6) also takes place at the temperature higher than 300 °C, which instantaneously opens a window to release the encapsulated hydrogen.[2a]

Purification and Characterization of H_2@C_{60}: Although the desired product of the thermal reaction, H_2@C_{60}, was contaminated by 9% of empty C_{60}, the purification of H_2@C_{60} was achieved by recycling HPLC on a semipreparative Cosmosil Buckyprep column (two directly connected columns; 25-cm length, 10-mm inner diameter; mobile phase, toluene; flow rate, 4 mL min^{-1}) as shown in Figure 7. After 20 recycles, H_2@C_{60} was completely separated, with its total retention time being 399 min while that of C_{60} was 395 min. The adsorption mechanism of the Buckyprep column is mainly based on a π-π interaction with the pyrenyl group attached to the stationary phase by trimethylene alkyl chain. Therefore, a very weak but appreciable van der Waals or electronic interaction would be operating between the inner hydrogen molecule and the π-electron cloud of outer C_{60}, and this is considered to have contributed to this separation. Also in the case of a mixture of C_{60} and E@C_{60} (E = Ar,[18] Kr,[19] and Xe[20]), E@C_{60} is known to be more strongly adsorbed than empty C_{60} to the PYE column,[21] which has also the pyrenyl group attached to the stationary phase. The

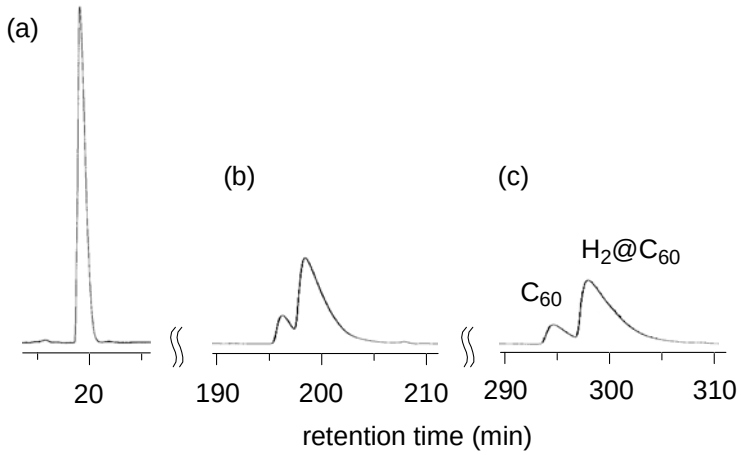

Figure 7. Recycle HPLC chart for the separation of H_2@C_{60} and empty C_{60}. (a) Before recycle, (b) after 10 recycles, and (c) after 15 recycles.

π-electron distribution of C_{60} is considered to be slightly pushed outward by the encapsulated noble-gas atoms in these cases.[18]

The ^{13}C NMR spectrum of the crude C_{60} portion of thermal product readily obtained by passing the CS_2 solution through the silica gel column is shown in Figure 8. Between the two signals at δ 142.844 and 142.766 ppm with an integrated ratio of 10:1, the one at δ 142.766 ppm is identical to that of empty C_{60}, and the other signal is assigned to that of $H_2@C_{60}$. The chemical shift difference is only 0.078 ppm, indicating that an electronic or van der Waals interaction between the inner hydrogen and outer fullerene cage is quite minute. After the HPLC separation, the main product, $H_2@C_{60}$, exhibited a ^{13}C NMR signal only at δ 142.844, and a ^{1}H NMR signal for the inside hydrogen as a sharp singlet at δ −1.44 ppm in ODCB-d_4, which is 1.51 ppm downfield shifted as compared to that of $H_2@$**4**. This is also 5.98 ppm upfield shifted from dissolved free hydrogen. This value is comparable to 6.36 ppm upfield shift of a ^{3}He NMR signal observed for $^{3}He@C_{60}$.[2a,b] This similarity proves that the total shielding effect of the fullerene cage is nearly constant and indifferent to the paramagnetic species inside. The slight difference in the degree of upfield shift between $H_2@C_{60}$ and $^{3}He@C_{60}$ (0.38 ppm) might be attributed to the geometry of each hydrogen atom in the molecule, which should be off-centered as compared with a ^{3}He atom,[22] or, otherwise, to the difference of the paramagnetic property of the encapsulated species. In accord with a very minute effect of encapsulated hydrogen, the IR spectrum was almost the same as that of empty C_{60}, exhibiting four absorption bands at 1429.2, 1182.3, 576.7, and 526.5 cm^{-1} (to be

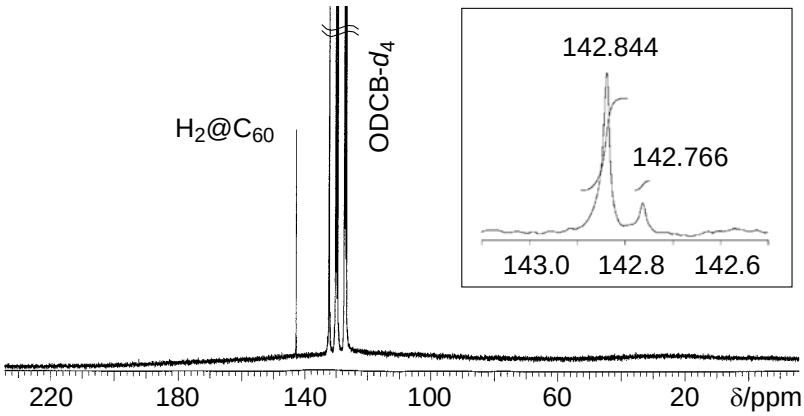

Figure 8. ^{13}C NMR spectrum of $H_2@C_{60}$ (75 MHz, ODCB-d_4). Inset shows the expanded spectrum.

compared with 1429.2, 1182.3, 575.7, and 526.5 cm^{-1} for empty C_{60} measured under exactly the same conditions). The band at 576.7 cm^{-1} of $H_2@C_{60}$, corresponding to an out-of-plane vibration mode, was slightly higher in energy than that of empty C_{60} by 1.0 cm^{-1}, presumably because the deformation of the spherical shape of $H_2@C_{60}$ would increase the repulsive interaction with the inner hydrogen molecule.[23] The UV-vis spectrum was also the same as that of empty C_{60}.[24]

The endohedral fullerene $H_2@C_{60}$ has excellent thermal stability. Upon heating the pure sample of $H_2@C_{60}$ at 500 °C for 10 min, there was no decomposition or release of incorporated hydrogen at all, judging from the ^{13}C NMR and HPLC.

^{1}H NMR Chemical Shift of Hydrogen Inside the Open-Cage Fullerenes: At each step in the chemical transformation to reduce the orifice size, gradual downfield shift was observed for the ^{1}H NMR signal of encapsulated hydrogen: $H_2@$**1**, δ –7.25; $H_2@$**2**, –6.33; $H_2@$**3**, –5.80; $H_2@$**4**, –2.95; $H_2@C_{60}$: –1.45. In order to examine if theoretical calculations can reproduce this tendency, we first conducted the GIAO (gauge-independent atomic orbital) calculations at the B3LYP/6-311G** level of theory for the structures optimized at the B3LYP/6-31G* level, on a series of the open-cage and closed-cage fullerenes containing H_2.[25] All chemical shifts are expressed as the values with reference to tetramethylsilane also calculated using the same level. As shown in Table 1, the GIAO calculations were found to reproduce the trend of gradual downfield shifts, although there was a tendency to underestimate the magnetic shielding effects of the fullerene cage in the extent which gradually increased in the order of $H_2@$**1** (Δδ 1.38) to $H_2@C_{60}$ (Δδ 3.24). Similar tendency

Table 1. Experimental and Calculated NMR Chemical Shifts (in ppm) for Encapsulated Hydrogen of a Series of Open-Cage Fullerene Derivatives and $H_2@C_{60}$

	$H_2@$**1**	$H_2@$**2**	$H_2@$**3**	$H_2@$**4**	$H_2@C_{60}$
Exp.	–7.25	–6.33	–5.80	–2.95	–1.45
Calc.	–5.87	–4.72	–3.85	–0.17	+1.79
Δ	1.38	1.61	1.95	2.78	3.24

of underestimation in the GIAO-DFT calculations for endohedral fullerene has been reported and discussed in detail.[25,26]

The observed gradual downfield shift must be due to the change in magnetic environment of this hydrogen, resulting from the change in diamagnetic and paramagnetic ring currents of hexagons and pentagons, and the consequent total ring currents, of the fullerene cage. In order to prove this, the diamagneticity and paramagneticity of all the π-conjugated five- and six-membered rings in there open-cage fullerenes **1** - **4** and of C_{60} were assessed by the NICS (nucleus-independent chemical shifts) calculations.[25,27,28] The obtained NICS values for each pentagon and hexagon are shown in the Schlegel diagrams of Figure 9. Upon removal of the sulfur atom from the orifice of **1** to give **3**, which caused 1.45 ppm downfield shift, the aromatic character of most of the hexagons (14 out of 18) decreased (decrease in absolute NICS value, 0.5 ~ 2.2 ppm) with exceptions of two rings (increase in absolute NICS value, 0.1 ~ 0.6 ppm) whereas the antiaromatic character of most pentagons (8 out of 9) increased by 1.1 ~ 2.2. A similar trend is also seen in the case of the chemical transformation of **3** to **4**,[29] which caused further downfield shift by 2.85 ppm. In this way, the size reduction of the orifice in each step is shown to lower the aromatic character of the fullerene cage as a whole. A series of these processes should be also accompanied by very slight but gradual increase in strain of the fullerene's σ-frameworks, which should gradually reduce the extent of π-conjugation on the fullerene surface.[10m] These are all taken together as the reason for observed downfield shifts of encapsulated hydrogen's NMR signal upon the reduction of the orifice size.

In the final step, in which the organic addends were completely removed and the original C_{60} structure was restored from $H_2@$**4**, 1.50 ppm downfield shift was observed. The NICS values for C_{60}, calculated in the same way as above, are –2.4 for each hexagon and +11.8 for each pentagon,[28a] clearly indicating that the aromaticity of the hexagon is considerably decreased and the antiaromaticity of pentagons is increased, in spite of the formation of a completely π-conjugated system. Again, the pyramidallization of all sixty carbons and the resulting increase of strain should be related to the lowering of the overall aromaticity. In addition, this last step is accompanied by the formation of two fully π-conjugated antiaromatic pentagons. All these effects are assumed to be added together to

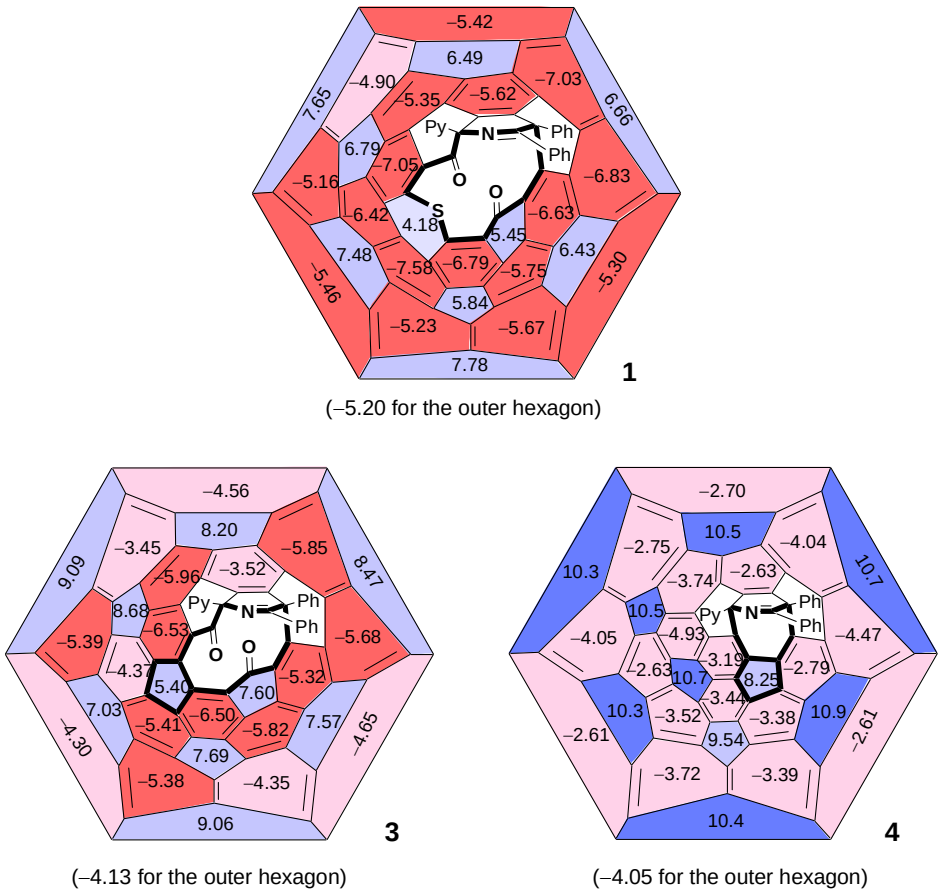

Figure 9. NICS patterns of open-cage fullerene derivatives **1**, **3** and **4**, calculated at the B3LYP/6-31G* level of theory: red regions are for $\delta < -5$ ppm, pink for $\delta = 0 \sim -5$, pale blue for $\delta = +5 \sim +10$, and blue for $\delta > +10$.

cause the downfield shift of the H_2 signal.

Upon oxidation of the sulfur atom of H_2@**1**, 0.92 ppm downfield shift was observed, even though the structure of fullerene skeleton itself was not affected. The NICS values of **2** indicated that the oxidation of S to SO influenced not only the carbocycles in its vicinity but almost all of the cyclic systems of the fullerene cage (Figure 10): the magnetic characters of the most hexagons and pentagons are changed to make the overall aromaticity of **2** lower than **1**. This is presumably due to an electronegative character of the S=O group. As a related example, it has been reported by Taylor and co-workers that ^{3}He NMR signal of ^{3}He@$C_{60}Cl_6$ (δ –12.3 ppm) is 2.8 ppm downfield shifted as compared to that of ^{3}He@$C_{60}Ph_5Cl$ (δ –15.1 ppm) due to the electronegative chloro addends.[10m]

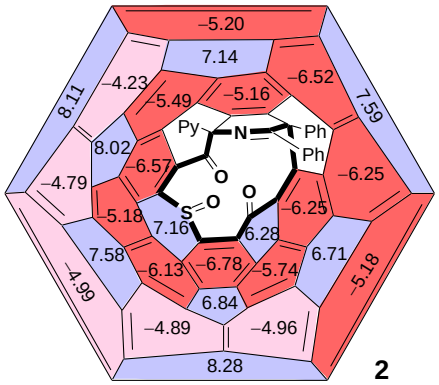

(–4.73 for the outer hexagon)

Figure 10. NICS pattern of open-cage fullerene derivative **2**, calculated at the B3LYP/6-31G* level of theory.

In order to examine the effect of encapsulated hydrogen upon the reactivity of outer fullerene cage, the solid-state mechanochemical dimerization of $H_2@C_{60}$ was conducted under the same conditions as we previously reported.[30] The dumbbell-shaped dimer, $(H_2@C_{60})_2$, was obtained in 30% isolated yield similarly to the reaction of empty C_{60}. Apparently the inside hydrogen does not affect the reactivity of the outer C_{60} cage. The NMR signal for the inside hydrogen was observed as a singlet at δ –4.04 ppm,[31] which is 8.58 ppm upfield shifted from free hydrogen, similar to the case for $^3He@C_{60}$ (8.81 ppm upfield shift from free ^3He).[30b]

In order to further investigate this issue, three additional fullerene derivatives $H_2@$**12**, $H_2@$**13**, and $H_2@$**14** were synthesized by the Bingel reaction,[32] benzyne addition,[33] and Prato reaction.[34] The NMR signal for encapsulated hydrogen was observed in ODCB-d_4 at δ –3.27 ppm for $H_2@$**12** (upfield shifted from dissolved free hydrogen, Δδ, 7.81 ppm), –4.30 ppm for $H_2@$**13** (Δδ, 8.84 ppm), and –4.64 ppm for $H_2@$**14** (Δδ, 9.18 ppm). These upfield shifts are quite similar to those reported for the NMR signal of ^3He encapsulated in the corresponding derivatives for $^3He@C_{60}$ (Δδ, 8.06 ppm, 9.11, and 9.45 ppm, respectively) being constantly less shielded by 0.23 ~ 0.27 ppm.[2a] Thus, the inside molecular hydrogen of C_{60} can be also used as a good probe to investigate the chemical reactions at the exterior of the fullerene cage, just like the ^3He atom inside the fullerene cage.[10] The present result is advantageous in that no particular adjustment of NMR instrument is required.

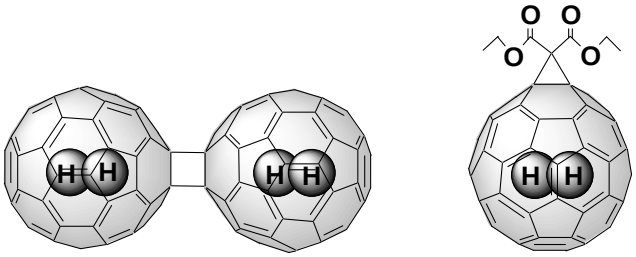

$(H_2@C_{60})_2$

H_2@**12**

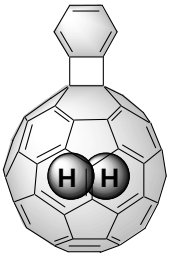

H_2@**13**

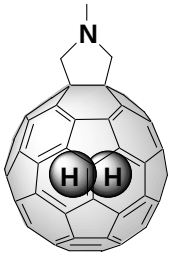

H_2@**14**

Electrochemical Behavior of $H_2@C_{60}$: In order to clarify the electronic properties of $H_2@C_{60}$ in more detail, we conducted cyclic voltammetry (CV) and differential pulse voltammetry (DPV). Upon measurements at room temperature for the range of 0.0 ~ –2.0 V versus the ferrocene/ferrocenium couple in ODCB and for the range of 0.0 ~ +1.0 V in 1,1,2,2-tetrachloroethane, three reversible reduction waves ($E_{1/2}$; –1.13, –1.54, –1.99 V versus the ferrocene/ferrocenium couple) and one irreversible oxidation peak (E_{pa}; +1.62 V) were observed, respectively, virtually at the same potentials as those for empty C_{60}. However, when we applied more negative potential using the conditions reported by Echegoyen in toluene-acetonitrile (5.4 : 1) at –10 °C under vacuum,[35] the reduction of $H_2@C_{60}$ was found to become slightly but gradually more difficult than empty C_{60} as the fullerene cage acquire more number of electron up to six (Figure 11). The reduction potentials estimated from the differential pulse voltammogram were –0.95, –1.37, –1.89, –2.39, –2.95, and ca. –3.5 V for $H_2@C_{60}$ to be compared with –0.95, –1.37, –1.88, –2.35, –2.88, and ca. –3.35 V for empty C_{60}. Thus the difference in reduction potential reaches nearly 0.15 V at the stage of six-electron reduction. Although the extent is so minute, this result is taken as clear evidence that hydrogen, as a slightly electropositive molecule, exerts an appreciable electronic

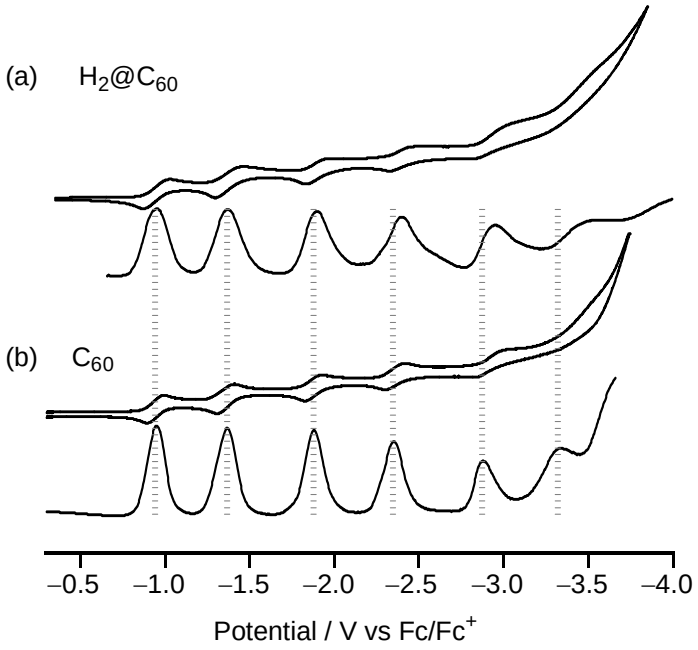

Figure 11. CV and DPV of (a) $H_2@C_{60}$ and (b) C_{60} in toluene-CH_3CN (5.4 : 1) at –10 °C.

repulsion with the outer C_{60} cage when the π-system of the latter is charged with more than four electrons.

Conclusion

In the present study we have demonstrated that an entirely new endohedral fullerene encapsulating molecular hydrogen, $H_2@C_{60}$, can be synthesized in a macroscopic amount by chemically closing the 13-membered-ring orifice of open-cage fullerene **1** incorporating hydrogen. The endohedral chemical shift for the molecular hydrogen in a series of open-cage fullerenes is particularly sensitive to the transformation of the outer cage, and the GIAO and NICS calculations are helpful to rationalize the chemical shift change even for such highly derivatized fullerenes. The endohedral hydrogen's NMR signal of representative derivatives of $H_2@C_{60}$ has indicated that it can serve as a sensitive probe for the exohedral transformation of the fullerene cage. Although the ^{13}C NMR, IR, and UV-vis

spectra of $H_2@C_{60}$ are virtually the same as those of empty C_{60}, the existence of repulsive interaction between inside hydrogen and outer π-electron system of C_{60} in its highly reduced states has been confirmed by electrochemical measurements. The new endohedral fullerene, $H_2@C_{60}$, can be taken as an ideal model to examine specific characteristics of a hydrogen molecule placed in a totally isolated state. A conversion between ortho- and para-hydrogen is certainly one of such issues. On the other hand, the critical temperature for the appearance of superconductivity upon alkali-metal doping should undergo a change. It is evidently possible to apply the present molecular surgery method to synthesize endohedral fullerenes such as $D_2@C_{60}$, $HD@C_{60}$, $He@C_{60}$, as well as a homologous series with C_{70}.

Experimental Section

General. The ^1H and ^{13}C NMR measurements were carried out on a Varian Mercury 300 instrument and the chemical shifts are reported in ppm with reference to tetramethylsilane. In some cases, the signal of *o*-dichlorobenzene-d_4 (ODCB-d_4) was used as internal standard (δ 7.20 ppm in ^1H NMR, and δ 132.35 ppm in ^{13}C NMR). UV-vis spectra were recorded on a Shimadzu UV-3150 spectrometer. IR spectra were taken with a Shimadzu FTIR-8600 spectrometer. MALDI-TOF mass spectra were measured with an Applied Biosystem Voyager-DE STR spectrometer using dithranol as a matrix. FAB mass spectra were recorded on a JEOL MStation JMS-700. APCI mass spectra were measured on a Finnigan-MAT TSQ 7000 spectrometer. GC/MS analyses were conducted on a Shimadzu GCMS-QP5050A spectrometer. The high-pressure liquid chromatography (HPLC) was performed by the use of a Cosmosil Buckyprep column (4.6 mm × 250 mm) for analytical purpose, and the same column (two directly connected columns, 10 mm × 250 mm) for preparative purpose. Fullerene C_{60} was purchased from Matsubo Co. m-Chloroperbenzoic acid was purchased from Aldrich Co. Zinc (sandy) and titanium (IV) chloride was purchased from Wako Co.

Computational Method. All calculations were conducted using the Gaussian 98 series of electronic structure program.[12] The geometries were fully optimized with the restricted Becke hybrid (B3LYP) method for all calculations. The GIAO calculations were performed at B3LYP/6-311G** level of theory using the optimized structures at B3LYP/6-31G* level of

theory. NICS calculations were performed at B3LYP/6-31G* level of theory using the optimized structures at B3LYP/6-31G* level.

Cyclic Voltammetry and Differential Pulse Voltammetry of $H_2@C_{60}$. The measurements were conducted on a BAS electrochemical analyzer ALS600A using a four necked flask equipped with three platinum wires serving as reference, counter, and working electrodes. About 2×10^{-4} M solutions of $H_2@C_{60}$ and C_{60} were used. Tetrabutylammonium hexafluorophosphate ($TBAPF_6$) (0.1 M) was used as supporting electrolyte. A mixture of toluene and acetonitrile (5.4 : 1 by volume) were dried over P_2O_5, degassed by repeated freeze-pump-thaw cycles under 10^{-4} mmHg, and vapor transferred into the electrochemical cell connected to a vacuum line (10^{-4} mmHg). The voltammograms were recorded at −10 °C at the scan rates of 100 mV s^{-1} for CV and 25 mV s^{-1} for DPV. The potentials were corrected against ferrocene used as an internal standard which was added after each measurement.

Oxidation of H_2@1. A mixture of $H_2@$**1** (107 mg, 0.0988 mmol) and *m*-chloroperbenzoic acid (34 mg, 0.20 mmol) in toluene (200 mL) was stirred at room temperature for 13 h under nitrogen. The solvent was evaporated under reduced pressure, and the residual brown solid was washed twice with methanol (50 mL) and dried under vacuum to give $H_2@$**2** (106 mg, 0.0977 mmol, 99%) as a brown solid.

$H_2@$**2**: IR (KBr) ν 1746 (C=O), 1073 (S=O) cm^{-1}; UV-vis ($CHCl_3$) λ_{max} (log ε) 258 (5.14), 320 (4.70) nm; ^{1}H NMR (300 MHz, CS_2-CD_2Cl_2 (5:1)) δ 8.63 (m, 1H), 8.32 (m, 1H), 8.26-8.23 (m, 2H), 8.05 (m, 1H), 7.68 (m, 1H), 7.42-7.34 (m, 4H), 7.17-7.03 (m, 4H), –6.18 (s, 2H); ^{13}C NMR (75 MHz, ODCB-d_4) δ 193.61, 187.54, 167.08, 163.54, 155.72, 154.97, 150.41, 149.06, 148.94, 148.21, 148.00, 147.99, 147.96, 147.79, 147.71, 147.68, 147.40, 147.34, 147.32, 147.14, 147.03, 146.96, 146.89, 146.71, 146.44, 146.29, 146.14, 145.35, 144.27, 143.79, 142.89, 142.54, 142.06, 141.82, 141.79, 141.69, 140.86, 140.81, 140.80, 140.62, 140.46, 140.25, 139.94, 139.79, 139.41, 139.11, 139.05, 138.85, 138.59, 138.58, 138.46, 137.46, 136.01, 135.68, 133.56, 133.08, (132.15, 131.36, 131.29, 131.02, 130.80, 128.87, 128.76), 125.84, 125.09, 122.81, 122.75, 75.10, 52.60 (the signals at the range of δ 132.4 ~ 126.8 were overlapped with the signals of ODCB-d_4); HRMS (+FAB) calcd for $C_{80}H_{16}O_3N_2S$ (M^+), 1084.0882, found 1084.0929.

Photochemical desulfurization of H_2@2. A stirred solution of H_2@**2** (52 mg, 0.048 mmol) in toluene (150 mL) in a Pyrex-glass flask was irradiated with a xenon-lamp (500 W) placed at the distance of 20 cm at room temperature for 17 h under argon. After removal of the solvent under reduced pressure, the residual brown solid was subjected to flash column chromatography over silica gel. Elution with CS_2-ethyl acetate (30:1) gave H_2@**3** (21 mg, 0.020 mmol, 42%) as a brown solid, and following elution with CS_2-ethyl acetate (10:1) gave unreacted H_2@**2** (20 mg, 0.018 mmol, 38%).

H_2@**3**: IR (KBr) ν 1747 (C=O) cm^{-1}; UV-vis ($CHCl_3$) δ_{max} (log ε) 257 (5.09), 324 (4.67) nm; ^{1}H NMR (300 MHz, CS_2-CD_2Cl_2 (5:1)) δ 8.57 (m, 1H), 8.40 (m, 1H), 8.10-7.99 (m, 3H), 7.82 (m, 1H), 7.40-7.35 (m, 4H), 7.27-7.07 (m, 4H), –5.69 (s, 2H); ^{13}C NMR (75 MHz, ODCB-d_4) δ 196.45, 189.88, 168.35, 163.06, 149.82, 148.75, 148.62, 148.42, 147.66, 147.52, 147.17, 146.88, 146.51, 146.08, 145.92, 145.59, 145.56, 145.55, 145.50, 145.43, 145.38, 145.16, 145.08, 144.95, 144.92, 144.59, 144.47, 143.95, 143.89, 143.73, 142.98, 142.60, 142.41, 142.15, 141.82, 141.72, 141.33, 140.93, 140.64, 140.33, 140.11, 139.96, 139.94, 139.70, 139.66, 139.61, 139.15, 138.43, 137.55, 137.43, 137.25, 136.28, 136.14, 135.72, 133.56, 133.17, (131.46, 131.01, 130.77), 123.31, 122.79, 75.67, 53.01 (the signals at the range of δ 132.4 ~ 126.8 were overlapped with the signals of ODCB-d_4); HRMS (+FAB) calcd for $C_{80}H_{17}O_2N_2$ (MH^+), 1037.1290, found 1037.1290.

Reductive coupling of the two carbonyl groups in H_2@3. To a stirred suspension of zinc powder (299 mg, 4.57 mmol) in dry tetrahydrofuran (10 mL) was added titanium tetrachloride (250 μl, 2.28 mmol) drop by drop at 0 °C under argon, and the mixture was refluxed for 2 h. A 1-mL portion of the resulting black slurry was added to a stirred solution of H_2@**3** (49 mg, 0.048 mmol) in ODCB (7 mL) at room temperature under argon. After heating at 80 °C for 2 h, the resulting brownish purple solution was cooled to room temperature. Then the solution was diluted with CS_2 (20 mL), and the resulting solution was washed with saturated aqueous solution of $NaHCO_3$ (50 mL). The organic layer was dried over $MgSO_4$ and evaporated under reduced pressure to give a residual brown solid, which was then subjected to flash column chromatography over silica gel. Elution with CS_2-ethyl acetate (20:1) gave H_2@**4** (42 mg, 0.042 mmol, 88%) as a brown solid.

H_2@**4**: IR (KBr) δ 1748 (C=N) cm^{-1}; UV-vis ($CHCl_3$) λ_{max} (log ε) 262 (5.08), 328

(4.66), 431 (3.33), 532 (3.11) nm; ^{1}H NMR (300 MHz, CS_2-CD_2Cl_2 (5:1)) δ 8.74 (m, 1H), 8.04-7.92 (m, 2H), 7.80 (m, 1H), 7.72 (m, 1H), 7.48-7.39 (m, 2H), 7.29-7.12 (m, 7H), –2.93 (s, 2H); ^{13}C NMR (100 MHz, ODCB-d_4) δ 168.39, 165.87, 149.48, 148.76, 148.41, 145.57, 145.55, 145.48, 145.44, 145.26, 144.69, 144.64, 144.57, 144.53, 144.44, 144.30, 144.28, 144.13, 144.12, 144.10, 144.01, 143.97, 143.92, 143.86, 143.75, 143.69, 143.61, 143.55, 143.52, 143.49, 143.47, 143.45, 143.38, 141.63, 141.12, 141.09, 140.98, 140.84, 140.62, 140.49, 140.26, 139.84, 139.25, 138.95, 138.37, 138.31, 137.26, 137.01, 136.89, 136.78, 136.64, 136.63, 135.68, 135.65, 135.46, 135.23, 134.98, (131.46, 131.02, 128.76, 128.68, 128.66, 127.69, 127.64), 125.55, 125.51, 122.86, 73.70, 56.69 (the signals at the range of δ 132.4 ~ 126.8 were overlapped with the signals of ODCB-d_4); HRMS (+FAB) calcd for $C_{80}H_{17}N_2$ (MH^+), 1005.1392, found 1005.1381.

Synthesis of $H_2@C_{60}$. A powder of $H_2@$**4** (245 mg, 0.244 mmol) lightly wrapped with a piece of aluminum foil was placed in a glass tube (inner diameter 20 mm), which was sealed under vacuum (1 mmHg) and heated with an electric furnace at 340 °C for 2 h. The resulting black solid was completely soluble in CS_2, and the solution was passed through a glass tube packed with silica gel to afford $H_2@C_{60}$ contaminated with 9% of empty C_{60} (total weight 118 mg, 67% (calculated $H_2@C_{60}$ 107 mg, 61%)) as a brown solid. Analytically pure $H_2@C_{60}$ was obtained by separation of this product by the use of HPLC on a preparative Cosmosil Buckyprep column (two directly connected columns, 10 mm × 250 mm, with toluene as a mobile phase; flow rate, 4 mL min^{-1}) after recycling for 20 times (total retention time, 399 min).

$H_2@C_{60}$: mp > 300 °C; IR (KBr) ν 1429, 1182, 577, 527 cm^{-1}; UV-vis (cyclohexane) λ_{max} (log ε) 212 (5.14), 258 (5.17), 330 (4.67), 405 (3.42), 543 (2.84), 600 (2.80), 622 (2.52) nm; ^{1}H NMR (300 MHz, ODCB-d_4) δ –1.44 (s); ^{13}C NMR (75 MHz, ODCB-d_4) δ 142.844; HRMS (+FAB) calcd for $C_{60}H_2$ (M^+), 722.0157, found 722.0163; Anal. calcd for $C_{60}H_2$: C, 99.72; H, 0.28, found: C, 99.04; H, 0.24.

In the similar way, empty **4** (296 mg) wrapped with an aluminum foil was heated in a vacuum-sealed glass tube (1 mmHg) in an electric furnace at 350 °C for 2 h. In the course of the reaction, a yellow-colored oil (10 mg, 3 wt% of the weight of **4**) gradually appeared, together with a slight amount of colorless oil (ca. 1 mg, ca. 0.3 wt% of the weight of **4**). The

yellow oil was a complex mixture containing at least 9 components based on the GC analysis, one of which exhibited a peak on mass analysis at *m*/*z* 282 corresponding to molecular formula Ph_2PyC_3N. The colorless oil consisted of mainly four components based on the GC analysis, and each component exhibited a peak on mass analysis corresponding to 2-cyanopyridine (**7**), diphenylacetylene (**8**), benzonitrile (**10**), and phenyl-(2-pyridyl)acetylene (**11**). The black solid (277 mg, 94 wt% of the weight of **4)** remained inside the aluminum foil.

Solid-state mechanochemical [2+2] dimerization reaction of H_2@C_{60}. H_2@C_{60} (10 mg, 0.014 mmol) and 4-aminopyridine (1.5 mg, 0.016 mmol) were placed in a stainless-steel capsule together with a stainless-steel milling ball. The capsule was sealed under nitrogen, and was vigorously shaken at the speed of 3500 r.p.m. for 30 min by the use of a high-speed vibration mill at room temperature.[30] The reaction mixture was dissolved in ODCB (4 mL), and the solution was subjected to HPLC on a preparative Cosmosil 5PBB column (two directly connected columns, 10 mm × 250 mm, with ODCB as a mobile phase; flow rate, 3 mL min^{-1}) to give unreacted H_2@C_{60} (6.9 mg, 0.0095 mmol, 69%) and [2+2] dimer $(H_2@C_{60})_2$ (3.0 mg, 0.0021 mmol, 30%) as a brown solid.

$(H_2@C_{60})_2$: IR (KBr) ν 1463.9, 1425.3, 1187.1, 796.5, 770.5, 762.8, 746.4, 710.7, 706.9, 612.4, 574.7, 561.2, 550.6, 544.9, 526.5, 480.2, 450.3, 417.6 cm^{-1} (reported values for $(C_{60})_2$[30b]; 1463.9, 1425.3, 1188.1, 796.5, 769.5, 761.8, 746.4, 710.7, 705.9, 612.4, 573.8, 560.3, 550.6, 544.9, 526.5, 479.3, 449.4, 418.5); ^{1}H NMR (300 MHz, ODCB-d_4) δ –4.04 (s). HPLC analysis on a Cosmosil Buckyprep column (25 cm × 4.6 mm inner diameter, with toluene as a mobile phase; flow rate, 1 mL min^{-1}) exhibited a single peak at exactly the same retention time as authentic [2+2] dimer $(C_{60})_2$, 18.7 min.

Synthesis of methanofullerene H_2@12. To a solution of H_2@C_{60} (H_2 content: 2%) (21 mg, 0.029 mmol) and CBr_4 (38 mg, 0.11 mmol) in dry toluene (20 mL) was added diethyl malonate (13 mg, 0.083 mmol) and diazabicyclo[5.4.0]undec-7-ene (DBU) (26 mg, 0.17 mmol), and the mixture was stirred for 1 h at room temperature under argon. After removal of the solvent under reduced pressure, the residual brown solid was subjected to flash column chromatography over silica gel. Elution with CS_2 gave unreacted H_2@C_{60} (2.9 mg, 0.0040 mmol, 14%) and elution with toluene gave H_2@**12** (10 mg, 0.012 mmol, 41%) as a brown

solid.

H_2@**12**: IR (KBr) ν 2978, 1745 (C=O), 1429, 1294, 1267, 1236, 1207, 1184, 1095, 1061 cm^{-1}; ^1H NMR (300 MHz, ODCB-d_4) δ 4.49 (q, J = 6.9 Hz, 2H), 1.37 (t, J = 6.9Hz, 3H), –3.27 (s, 0.02H); HRMS (+FAB) calcd for $C_{67}H_{12}O_4$ (M^+), 880.0736, found 880.0720; (reported data; IR ν 2979, 1745 (C=O), 1428, 1295, 1266, 1234, 1206, 1186, 1095, 1061 cm^{-1}; ^1H NMR (360 MHz, $CDCl_3$) δ 4.57 (q, J = 7.1 Hz, 4H), 1.49 (t, J = 7.1 Hz, 6H)).[36]

Synthesis of benzyne Adduct H_2@13. To a solution of $H_2@C_{60}$ (H_2 content: 7%) (23 mg, 0.032 mmol) and isoamyl nitrite (17 mg, 0.15 mmol) in dry benzene (40 mL) was added anthranilic acid (43 mg, 0.31 mmol), and the mixture was stirred at room temperature under argon. After 2 h, the solution was passed through a glass tube packed with silica gel, and the solvent was removed under reduced pressure. The resulting brown solid was then separated by HPLC on the preparative Cosmosil 5PBB column to give unreacted $H_2@C_{60}$ (7.8 mg, 0.011 mmol, 34%) and H_2@**13** (6.8 mg, 0.0085 mmol, 27%) as a brown solid.

H_2@**13**: IR (KBr) ν 2920, 2849, 1458, 1024 cm^{-1}; ^1H NMR (300 MHz, ODCB-d_4) δ 7.91 (m, 2H), 7.65 (m, 2H), –4.30 (s, 0.07H); HRMS (+FAB) calcd for $C_{66}H_6$ (M^+), 798.0470, found 798.0499; (reported data; IR (KBr) δ 2924, 2854, 1458, 1278, 1024 cm^{-1}; ^1H NMR (500 MHz, CD_2Cl_2) δ 8.02 (m, 4H), 7.78 (m, 4H)).[33]

Synthesis of pyrrolidinofullerene H_2@14. A solution of $H_2@C_{60}$ (H_2 content: 8%) (23 mg, 0.032 mmol), N-methylglycine (2.8 mg, 0.0032 mmol), and paraformaldehyde (5.0 mg, 0.17 mmol) in dry toluene (30 mL) was refluxed for 15 min under argon. After removal of the solvent under reduced pressure, the residual brown solid was subjected to flash column chromatography over silica gel. Elution with toluene gave unreacted $H_2@C_{60}$ (8.7 mg, 0.012 mmol, 38%) and H_2@**14** (8.9 mg, 0.011 mmol, 36%) as a brown solid.

H_2@**14**: IR (KBr) ν 2937, 2835, 2779, 1466, 1443, 1427, 1340, 1184, 1163, 1115 cm^{-1}; ^1H NMR (300 MHz, ODCB-d_4) δ 4.16 (s, 4H), 2.84 (s, 3H), –4.64 (s, 0.08H); HRMS (+FAB) calcd for $C_{63}H_9N$ (M^+), 779.0735, found 779.0743; (reported data; ^1H NMR (200 MHz, CS_2-$CDCl_3$) δ 4.38 (s, 4H), 2.98 (s, 3H)).[34]

References and Notes

(1) (a) *Endofullerenes*: *A New Family of Carbon Clusters*; Akasaka, T., Nagase, S., Eds.: Kluwer Academic Publisher: Dordrecht, 2002. (b) *Fullerenes*: *Chemistry*, *Physics and Technology*; Kadish, K. M., Ruoff, R. S., Eds.: John Wiley & Sons: New York, 2000; pp 357-393. (c) Shinohara, H. *Rep*. *Prog*. *Phys*. **2000**, *63*, 843. (d) Liu, S.; Sun, S. *J*. *Organomet*. *Chem*. **2000**, *599*, 74. (e) Nagase, S.; Kobayashi, K.; Akasaka, T. *Bull*. *Chem*. *Soc*. *Jpn*. **1996**, *69*, 2131. (f) Bethune, D. S.; Johnson, R. D.; Salem, J. R.; de Vries, M. S.; Yannoni, C. S. *Nature* **1993**, *366*, 123.

(2) (a) Saunders, M.; Cross, R. J.; Jiménez-Vázquez, H. A.; Shimshi, R.; Khong, A. *Science* **1996**, *271*, 1693. (b) Saunders, M.; Jiménez-Vázquez, H. A.; Cross, R. J.; Mroczkowski, S.; Freedberg, D. I.; Anet, F. A. L. *Nature* **1994**, *367*, 256. (c) Saunders, M.; Jiménez-Vázquez, H. A.; Cross, R. J. *J*. *Am*. *Chem*. *Soc*. **1994**, *116*, 2193.

(3) (a) Rubin, Y. *Chem*. *Eur*. *J*. **1997**, *3*, 1009. (b) Rubin, Y. *Top*. *Curr*. *Chem*. **1999**, *199*, 67. (c) Nierengarten, J.-F. *Angew*. *Chem*. *Int*. *Ed*. **2001**, *40*, 2973.

(4) Murata, Y.; Murata, M.; Komatsu, K. *Chem*. *Eur*. *J*. **2003**, *9*, 1600.

(5) (a) Yoshimoto, S.; Tsutsumi, E.; Honda, Y.; Murata, Y.; Murata, M.; Komatsu, K.; Ito, O.; Itaya, K. *Angew*. *Chem*. *Ent*. *Ed*. **2004**, *43*, 3044. (b) Yoshimoto, S.; Honda, Y.; Murata, Y.; Murata, M.; Komatsu, K.; Ito, O.; Itaya, K. *J*. *Phys*. *Chem*. *B* **2005**, *109*, 8547. (c) Stanisky, C. M.; Cross, R. J.; Saunders, M.; Murata, M.; Murata, Y.; Komatsu, K. *J*. *Am*. *Chem*. *Soc*. **2005**, *127*, 299.

(6) Murata, Y.; Murata, M.; Komatsu, K. *J*. *Am*. *Chem*. *Soc*. **2003**, *125*, 7152.

(7) Sawa, H.; Wakabayashi, Y.; Murata, Y.; Murata, M.; Komatsu, K. *Angew*. *Chem*. *Int*. *Ed*. **2005**, *44*, 1981.

(8) Carravetta, M.; Murata, Y.; Murata, M.; Heinmaa, I.; Stern, R.; Tontcheva, A.; Samoson, A.; Rubin, Y.; Komatsu, K.; Levitt, M. H. *J*. *Am*. *Chem*. *Soc*. **2004**, *126*, 4092.

(9) The incorporation rate of ^{3}He is increased to 1% by pre-treatment of C_{60} with KCN: Cross, R. J.; Khong, A.; Saunders, M. *J*. *Org*. *Chem*. **2003**, *68*, 8281.

(10) For examples of C_{60} derivatives, see: (a) Saunders, M.; Jiménez-Vázquez, H. A.; Bangerter, B. W.; Cross, R. J. *J*. *Am*. *Chem*. *Soc*. **1994**, *116*, 3621. (b) Saunders, M.; Jiménez-Vázquez, H. A.; Cross, R. J. *Tetrahedraon Lett*. **1994**, *35*, 3869. (c) Smith, A. B.,

III; Strongin, R. M.; Brard, L.; Romanow, W. J.; Saunders, M.; Jiménez-Vázquez, H. A.; Cross, R. J. *J. Am. Chem. Soc.* **1994**, *116*, 10831. (d) Bühl. M.; Thiel, W.; Schneider, U. *J. Am. Chem. Soc.* **1995**, *117*, 4623. (e) Schuster, D. I.; Cao, J.; Kaprinidis, N.; Wu, Y.; Jensen, A. W.; Lu, Q.; Wang, H.; Wilson, S. R. *J. Am. Chem. Soc.* **1996**, *118*, 5639. (f) Cross, R. J.; Jiménez-Vázquez, H. A.; Lu, Q.; Saunders, M.; Schuster, D. I.; Wilson, S. R.; Zhao, H. *J. Am. Chem. Soc.* **1996**, *118*, 11454. (g) Billups, W. E.; Gonzalez, A.; Gesenberg, C.; Luo, W.; Marriott, T.; Alemany, L. B.; Saunders, M.; Jiménez-Vázquez, H. A.; Khong, A. *Tetrahedraon Lett.* **1997**, *38*, 175. (h) Rüttimann, M.; Haldimann, R. F.; Isaacs, L.; Diederich, F.; Khong, A.; Jiménez-Vázquez, H. A.; Cross, R. J.; Saunders, M. *Chem. Eur. J.* **1997**, *3*, 1071. (i) Billups, W. E.; Luo, W.; Gonzalez, A.; Arguello, D.; Alemany, L. B.; Marriott, T.; Saunders, M.; Jiménez-Vázquez, H. A.; Khong, A. *Tetrahedron Lett.* **1997**, *38*, 171. (j) Jensen, A. W.; Khong, A.; Saunders, M.; Wilson, S. R.; Schuster, D. I. *J. Am. Chem. Soc.* **1997**, *119*, 7303. (k) Shabtai, E.; Weitz, A.; Haddon, R. C.; Hoffman, R. E.; Rabinovitz, M.; Khong, A.; Cross, R. J.; Saunders, M.; Cheng, P.-C.; Scott, L. T. *J. Am. Chem. Soc.* **1998**, *120*, 6389. (l) Boltalina, O. V.; Bühl, M.; Khong, A.; Saunders, M.; Street, J. M.; Taylor, R. *J. Chem. Soc., Perkin Trans. 2* **1999**, 1475. (m) Birkett, P. R.; Buhl, M.; Khong, A.; Saunders, M.; Taylor, R. *J. Chem. Soc., Perkin Trans. 2* **1999**, 2037. (n) Wang, G.-W.; Weedon, B. R.; Meier, M. S.; Saunders, M.; Cross, R. J. *Org. Lett.* **2000**, *2*, 2241. (o) Wilson, S. R.; Yurchenko, M. E.; Schuster, D. I.; Khong, A.; Saunders, M. *J. Org. Chem.* **2000**, *65*, 2619. (p) Wang, G.-W.; Saunders, M.; Cross, R. J. *J. Am. Chem. Soc.* **2001**, *123*, 256. (q) Nossal, J.; Saini, R. K.; Sadana, A. K.; Bettinger, H. F.; Alemany, L. B.; Scuseria, G. E.; Billups, W. E.; Saunders, M.; Khong, A.; Weisemann, R. *J. Am. Chem. Soc.* **2001**, *123*, 8482.

(11) For MCPBA oxidation of C_{60}, see: (a) Balch, A. L.; Costa, D. A.; Noll, B. C.; Olmstead, M. M. *J. Am. Chem. Soc.* **1995**, *117*, 8926. (b) Takeuchi, K.; Tajima, Y. *J. Org. Chem.* **2002**, *67*, 1696.

(12) Gaussian 98, Revision A.11, M. J. Frisch, G. W. Trucks, H. B. Schlegel, G. E. Scuseria, M. A. Robb, J. R. Cheeseman, V. G. Zakrzewski, J. A. Montgomery, Jr., R. E. Stratmann, J. C. Burant, S. Dapprich, J. M. Millam, A. D. Daniels, K. N. Kudin, M. C. Strain, O. Farkas, J. Tomasi, V. Barone, M. Cossi, R. Cammi, B. Mennucci, C. Pomelli, C. Adamo,

S. Clifford, J. Ochterski, G. A. Petersson, P. Y. Ayala, Q. Cui, K. Morokuma, P. Salvador, J. J. Dannenberg, D. K. Malick, A. D. Rabuck, K. Raghavachari, J. B. Foresman, J. Cioslowski, J. V. Ortiz, A. G. Baboul, B. B. Stefanov, G. Liu, A. Liashenko, P. Piskorz, I. Komaromi, R. Gomperts, R. L. Martin, D. J. Fox, T. Keith, M. A. Al-Laham, C. Y. Peng, A. Nanayakkara, M. Challacombe, P. M. W. Gill, B. Johnson, W. Chen, M. W. Wong, J. L. Andres, C. Gonzalez, M. Head-Gordon, E. S. Replogle, and J. A. Pople, Gaussian, Inc., Pittsburgh PA, **2001**.

(13) (a) Nelson, C. R.; McCabe, P. H. *Tetrahedron Lett*. **1978**, *19*, 2819. (b) Kobayashi, K.; Mutai, K. *Tetrahedron Lett*. **1981**, *22*, 5201.

(14) Kobayashi, K.; Mutai, K. *Phosphorus and Sulfur* **1985**, *25*, 43 and references therein.

(15) The experimentally determined value is 30.1 kcal mol^{-1}: ref. 6.

(16) McMurry, J. E. *Chem*. *Rev*. **1989**, *89*, 1513.

(17) (a) Regitz, M.; Lenoir, D.; Lippert, T. In *Methoden der Organischen Chemie: Houben-Weyl*; Klamann, D., Ed.; Georg Thieme Verlag: Stuttgart, New York, 1992; Vol. E 16c, p 936. (b) Regitz, M.; Bergsträßer, U. In *Science of Synthesis: Houben-Weyl Methods of Molecular Transformations*; Maas, G., Ed.; Georg Thieme Verlag: Stuttgart, New York, 2001; Vol. 9, p 135.

(18) DiCamillo, B. A.; Hettich, R. L.; Guiochon, G.; Compton, R. N.; Saunders, M.; Jiménez-Vázquez, H. A.; Anthony, K.; Cross, R. J. *J*. *Phys*. *Chem*. **1996**, *100*, 9197.

(19) Yamamoto, K.; Saunders, M.; Khong, A.; Cross, R. J.; Grayson, M.; Gross, M. L.; Benedetto, A. F.; Weisman, R. B. *J*. *Am*. *Chem*. *Soc*. **1999**, *121*, 1591.

(20) Syamala, M. S.; Cross, R. J.; Saunders, M. *J*. *Am*. *Chem*. *Soc*. **2002**, *124*, 6216.

(21) Kimata, K.: Hosoya, K.; Areki, T.; Tanaka, N. *J*. *Org*. *Chem*. **1993**, *58*, 282.

(22) Sternfeld, T.; Hoffman, R. E.; Saunders, M.; Cross, R. J.; Syamala, M. S.; Rabinovitz, M. *J*. *Am*. *Chem*. *Soc*. **2002**, 8786.

(23) Bakowies, D.; Thiel, W. *Chem*. *Phys*. **1991**, *151*, 309.

(24) An attempt to measure the Raman spectrum of $H_2@C_{60}$ was unsuccessful because of strong fluorescence from the outer C_{60} cage. Further trials are now under way.

(25) (a) Bühl, M.; Kaupp, M.; Malkina, O. L.; Malkin, V. G. *J*. *Comput*. *Chem*. **1999**, *20*, 91. (b) Bühl, M.; Hirsch, A. *Chem*. *Rev*. **2001**, *101*, 1153.

(26) Wang, G.-W.; Zhang, X.-H.; Zhan, H.; Guo, Q.-X.; Wu, Y.-D. *J. Org. Chem.* **2003**, *68*, 6732.

(27) Schleyer, P. v. R.; Maerker, C.; Dransfeld, A.; Jiao, H.; Hommes, N. J. R. v. E. *J. Am. Chem. Soc.* **1996**, *118*, 6317.

(28) (a) Bühl, M. *Chem. Eur. J.* **1998**, *4*, 734. (b) Chen, Z.; Cioslowski, J.; Rao, N.; Moncrieff, D.; Bühl, M.; Hirsch, A.; Thiel, W. *Theor. Chem. Acc.* **2001**, *106*, 364.

(29) The aromatic character in all hexagons decreased and the antiaromatic character of all pentagons increased.

(30) (a) Wang, G.-W.; Komatsu, K.; Murata, Y.; Shiro, M. *Nature* **1997**, *387*, 583. (b) Komatsu, K.; Wang, G.-W.; Murata, Y.; Tanaka, T.; Fujiwara, K. *J. Org. Chem.* **1998**, *63*, 9358.

(31) No magnetic interaction was observed between two hydrogen molecules in each fullerene cage.

(32) Camps, X.; Hirsch, A. *J. Chem. Soc., Perkin Trans. 1* **1997**, 1595.

(33) Hoke, S. H., II; Molstad, J.; Dilettato, D.; Jay, M. J.; Carlson, D.; Kahr, B.; Cooks, R. G. *J. Org. Chem.* **1992**, *57*, 5069.

(34) Maggini, M.; Scorrano, G.; Prato, M. *J. Am. Chem. Soc.* **1993**, *115*, 9798.

(35) Xie, Q.; Pérez-Cordero, E.; Echegoyen, L. *J. Am. Chem. Soc.* **1992**, *114*, 3978.

(36) Bingel, C. *Chem. Ber.* **1993**, *126*, 1957.

Chapter 5

Synthesis of Endohedral C_{70} Encapsulating Hydrogen Molecule(s), $H_2@C_{70}$ and $(H_2)_2@C_{70}$

Abstract: Encapsulation of molecular hydrogen into the cavity of fullerene C_{70}, which is larger than that of C_{60}, was conducted. First an open-cage C_{70} derivative having a 13-membered ring orifice (**4**) was synthesized by three-step reactions; thermal reaction of C_{70} with a pyridazine derivative to make an eight-membered-ring orifice, oxidative cleavage of the C=C double bond to enlarge the orifice to a 12-membered ring, and insertion of a sulfur atom to the rim of the orifice to make it a 13-membered ring. The structure of **4** was determined by X-ray crystallography. Upon treatment of **4** with high-pressure H_2 gas, 100% of open-cage C_{70} **4** was filled with hydrogen molecule. Out of this product, 97% contained one molecule of hydrogen, i.e., H_2@**4**, and 3% was found to contain two molecules of hydrogen, i.e., $(H_2)_2$@**4**. The positional exchange of two hydrogen molecules inside **4** was monitored by the dynamic low-temperature NMR measurements. The chemical restoration of C_{70} cage of **4** was carried out to give new endohedral fullerenes, $H_2@C_{70}$ and $(H_2)_2@C_{70}$.

Introduction

As mentioned in Chapter 2 – 4, the molecular surgical approach[1] was proved to be the powerful means to synthesize yet-unknown endohedral fullerene C_{60} encapsulating molecular hydrogen in a macroscopic quantity.[2-4] Considering the thickness of π-electron clouds of fullerene C_{70}, the size of the inner cavity is 4.6 Å along the long axis and 3.6 Å along the short axis, which is larger than that of C_{60} (3.6 Å in inner diameter) (Figure 1). Therefore, by applying the molecular surgery technique to C_{70}, it will become possible to synthesize endohedral C_{70} incorporating more than one small gaseous entity,[5] such as He atom and H_2 molecule. However, most efforts have previously been made only to the synthesis of open-cage C_{60} (but not C_{70}) derivatives[2,6] because of the wealth of knowledge about the chemical reactivity toward the exterior of the C_{60} cage.[7] Thus fur, the reports on the synthesis of open-cage C_{70} derivative have been limited to only three compounds **1**,[8] **2**,[9] and **3**[9] having an 11-membered-ring orifice, as shown below.

The chemical reactivity of C_{70} is generally more complicated due to its lower symmetry than that of C_{60}. There are four different types of C=C double bonds (denoted by α ~ δ in Figure 2), whose reactivities are different basically depending on the surface curvatures of the rugby-ball shaped C_{70}. For example, representative reactions such as [4+2][10a] and [3+2][10b] cycloadditions and hydrogenation[11] mainly take place on the highly strained C=C double

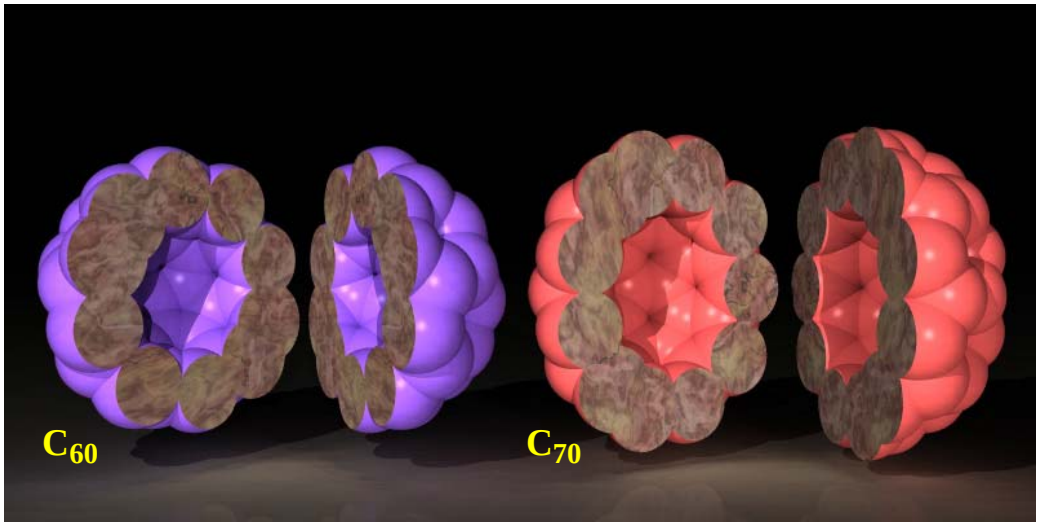

Figure 1. Cutout views of space-filling models for fullerene C_{60} and C_{70}.

bonds such as α- and β-bonds.

In this Chapter is first described the synthesis of open-cage fullerene C_{70} derivative **4** with a 13-membered-ring orifice by applying the similar procedure developed for the synthesis of open-cage C_{60} derivative **5**[2] and then insertion of more than one hydrogen molecule, together with dynamic behavior of the two hydrogen molecules confined to the C_{70} cage. Furthermore, restoration of the fullerene structure of **4** to the original C_{70} form to realize novel endohedral C_{70} incorporating hydrogen molecules, $H_2@C_{70}$ and $(H_2)_2@C_{70}$, will be mentioned.

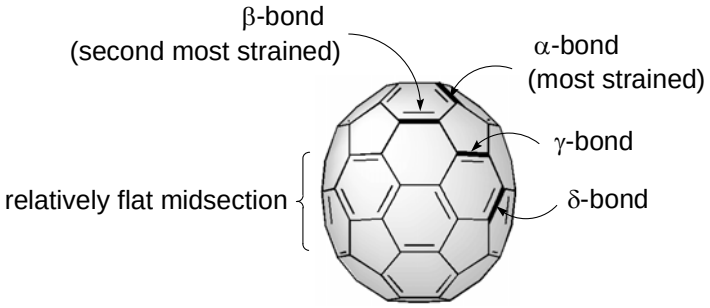

Figure 2. The fullerene C_{70} with the indication of the four types of reactive double bonds (α ~ δ).

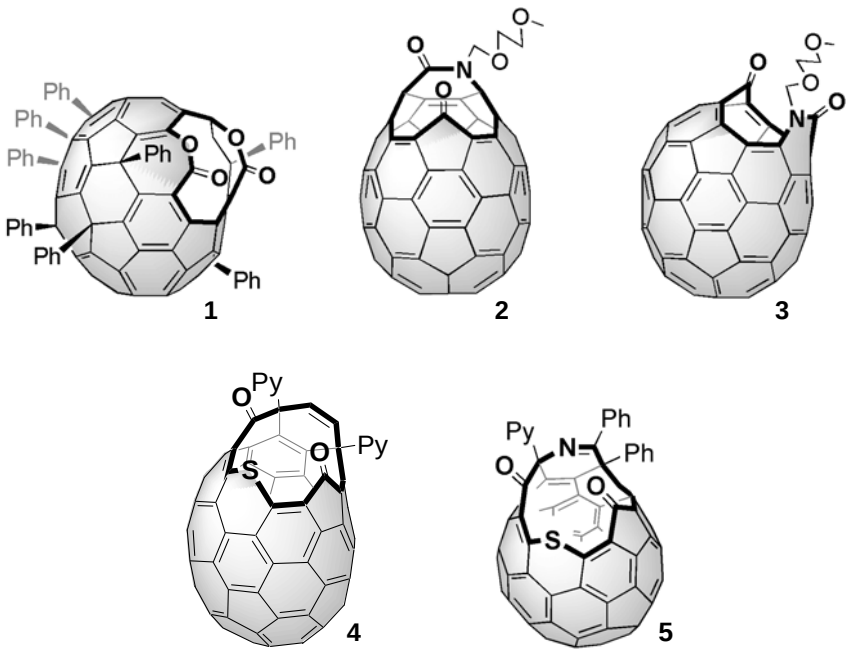

Results and Discussion

Synthesis of open-cage fullerene C_{70} derivatives having an eight-membered-ring orifice: In the same way as the one used for a 13-membered-ring orifice to be opened on the C_{60} surface,[2] the thermal reaction of C_{70} with 3-(2-pyridyl)-5,6-diphenyl-1,2,4-triazine was first carried out, but it resulted in formation of a complex mixture, which was difficult to separate. Then, the thermal reaction with higher symmetrical 3,6-di-(2-pyridyl)-pyridazine (**6**)[12] having higher symmetry (Scheme 1a) was attempted by heating a solution of C_{70} and two equivalents of pyridazine **6** in 1-chloronaphthalene at 255 °C for 24 h. The separation of a resulting material by flash column chromatography over silica gel gave an isomeric mixture of **7** and **8** both having an eight-membered-ring orifice, together with unreacted C_{70} (45%). Further separation using HPLC equipped with a prepacked silica gel column (Yamazen Ultra Pack SI40B; 26 mm × 300 mm) eluted with toluene-ethyl acetate (5:1) afforded open-cage fullerene derivatives **7** (40%) and **8** (5%) both as a brown powder. A probable reaction mechanism for the formation of **7** and **8** is considered to involve the [4+2] cycloaddition, extrusion of N_2, and intramolecular formal [4+4] cycloaddition followed by [2+2+2] cycloreversion (Scheme 1b).[2,13]

The structures of **7** and **8** were characterized based on the spectral information and

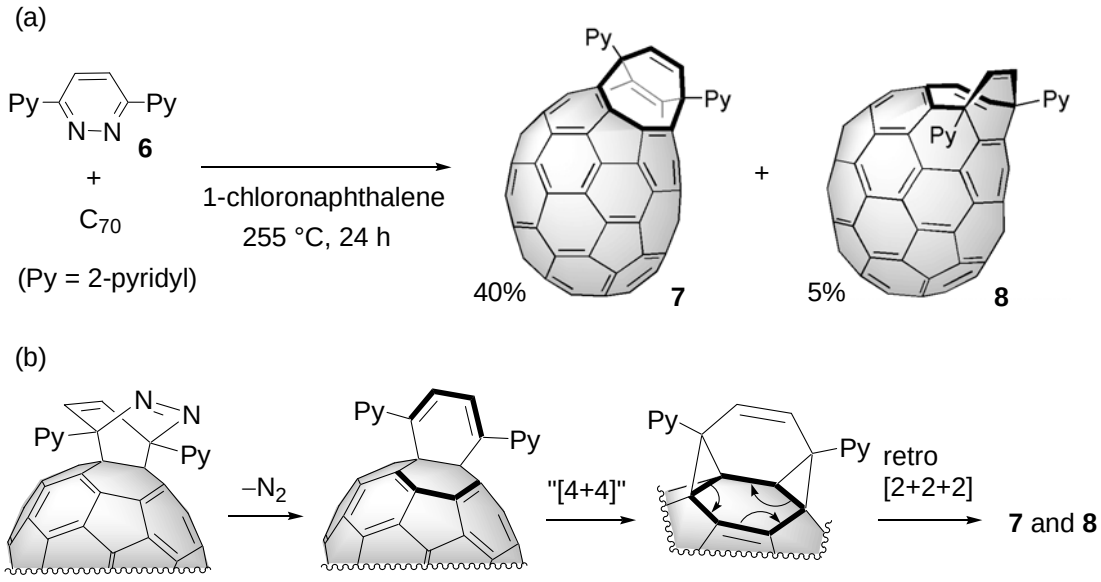

Scheme 1. Thermal reaction of fullerene C_{70} with pyridazine **6**.

computational results[14] as mentioned below. The FAB mass spectra of **7** and **8** showed the same molecular ion peaks at *m*/*z* 1047 ([M+1]) corresponding to M = $C_{84}H_{10}N_2$, which indicated that the products were formed by [4+2] cycloaddition of pyridazine **6** to C_{70} followed by extrusion of N_2. The ^{1}H NMR of **7** exhibited eight signals for pyridyl protons and two doublets for olefinic protons at δ 6.47 ppm (J = 9.5 Hz) and δ 6.27 ppm (J = 9.5 Hz), while the ^{13}C NMR spectrum showed 76 signals in sp^2-carbon region between δ 168.12 and 117.46 ppm, in which six signals are overlapped, in addition to two signals at δ 54.33 and 52.91 ppm for the sp^3-carbon atoms. These data supported the structure of **7** with the C_1 symmetry. On the other hand, the ^{1}H NMR spectrum of **8** exhibited only four signals in aromatic region and one singlet at δ 6.29 ppm, and the ^{13}C NMR exhibited 39 signals for sp^2-carbon atoms between δ 160.57 and 122.47 ppm (two signals are overlapped) and one signal at δ 52.53 ppm for the sp^3-carbon atom, suggesting that **8** has the C_s symmetry. In addition, close resemblance of the electronic spectra of **7** and **8** to that of C_{70} indicated that 70 original fullerene carbons retain their sp^2 hybridization in each π-conjugated system (Figure 3).[2]

Since the reactivity of C_{70} toward [4+2] cycloaddition is known to be higher at the C=C double bonds at α- and β-positions (see Figure 2) due to their higher strains,[10] theoretical

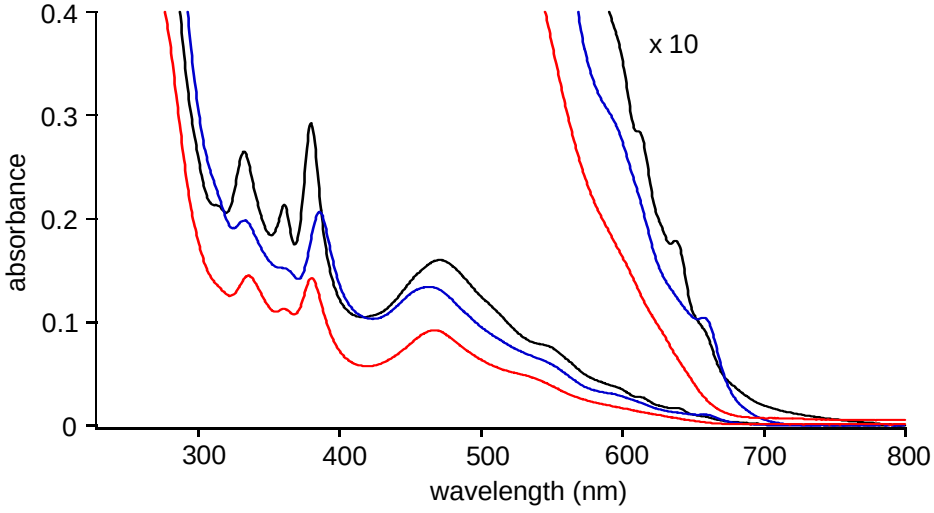

Figure 3. UV-vis spectra of open-cage fullerene derivatives with an eight-membered-ring orifice (**7** and **8**) and C_{70} in $CHCl_3$: black line (C_{70}; 8.25×10^{-5} M), blue (**7**; 6.96×10^{-5} M), red (**8**; 5.25×10^{-5} M).

calculations were carried out for selected intermediates **9** and **10**, having a 1,3-cyclohexadiene ring fused at α- and β-positions, respectively, as well as possible open-cage fullerene derivatives **7**, **8**, and **11** (Figure 4). As expected, the comparison between the relative energies of α-adduct **9** and β-adduct **10**, which formed through the [4+2] cycloaddition between **6** and C_{70} followed by extrusion of N_2 (see Scheme 1b), indicated that **9** is more stable than **10** by 3.2 kcal mol^{-1}. The corresponding γ- and δ-adducts (not shown in Figure 4) were calculated to be less stable than **9** by 21.6 and 7.9 kcal mol^{-1}, respectively. Furthermore, C_1 symmetrical **7** was indicated to be the most stable isomer and, therefore, the structure of the major product was concluded to be **7**. In the case of β-adduct **10**, the intramolecular reactions (see Scheme 1b) can take place in two ways (Figure 4, (a) and (b)) giving rise to the formation of **8** and **11** both with the C_s symmetry. However, because the relative energies showed that the transformation of **10** into **8** is an exothermic process, the obtained minor product was concluded to be **8**.

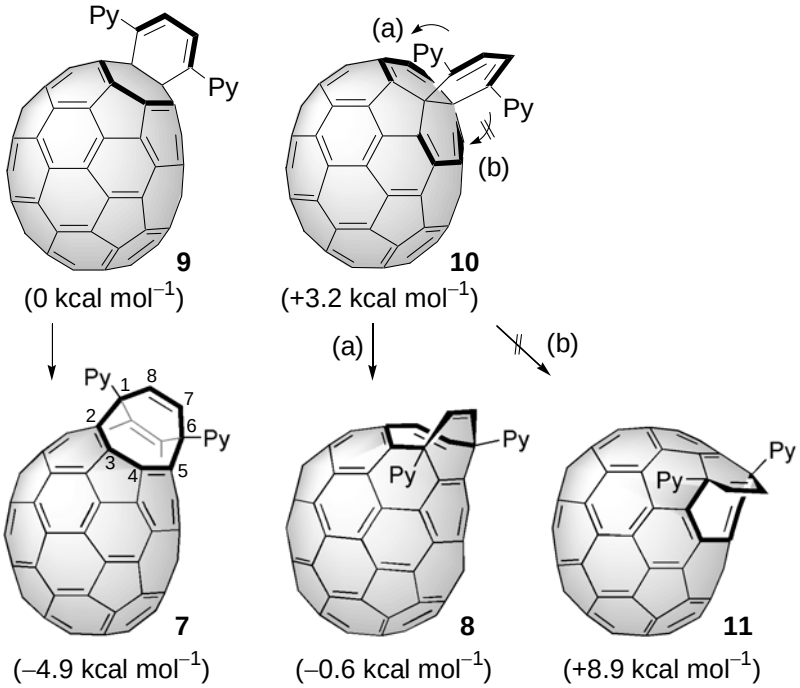

Figure 4. Selected intermediates (**9** and **10**) and open-cage fullerene derivatives (**7**, **8**, and **11**). The relative energies with reference to **9** (B3LYP/6-31G*) are shown in parentheses. Compound **10** is possible to undergo intramolecular reactions in two ways, (a) and (b).

Enlargement of the orifice in open-cage fullerene 7: In order to estimate the reactivity of **7** in the addition of singlet oxygen ($^1O_2$), DFT calculations were carried out. The geometry was optimized at the B3LYP/6-31G* level of theory to give a structure with the shape of HOMO as shown in Figure 5. The HOMO was shown to spread over the whole fullerene cage and to have higher coefficients on the sp^2-carbon atoms at the rim of the orifice, particularly on C2 and C5. Therefore, the [2+2] cycloaddition of $^1O_2$ was expected to take place at the C=C double bonds, C2-C3 or C4-C5, to expand the orifice size of **7**.[2,6d-f]

The reaction of **7** with $^1O_2$ was carried out in an air-saturated solution of CS_2 under irradiation of visible light using a xenon-lamp for 5 h.[2] Then the reaction mixture was separated using HPLC equipped with a prepacked silica gel column (Yamazen Ultra Pack

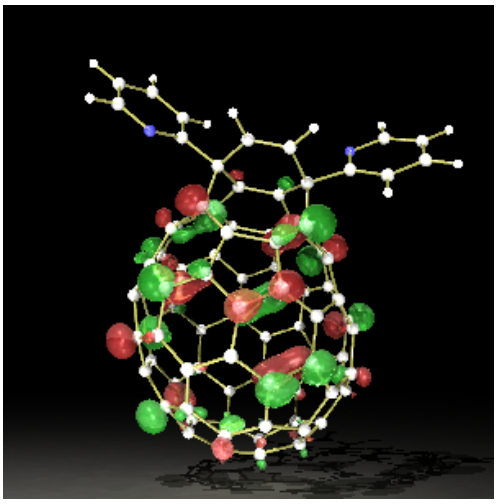

Figure 5. The optimized structure of open-cage fullerene derivative **7** with the contour of the HOMO (B3LYP/6-31G*).

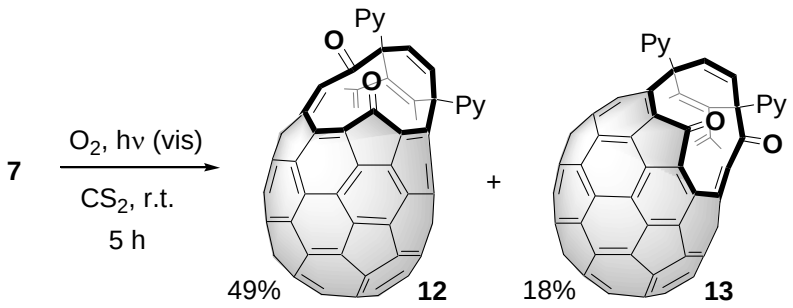

Scheme 2. Enlargement of the orifice size of **7** by photo-oxidation.

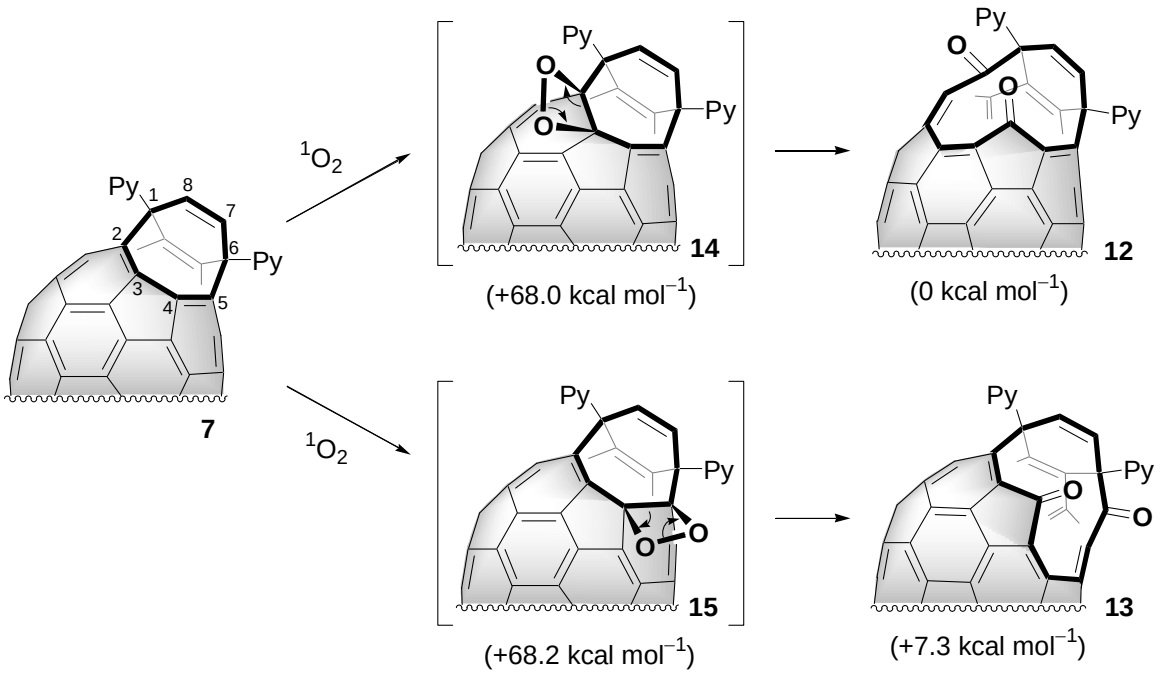

Figure 6. Possible reaction mechanism for the formation of open-cage fullerene derivative **12** and **13**. The relative energies (B3LYP/6-31G*) with reference to **12** are shown in parentheses.

SI40B; 26 mm × 300 mm) to afford two products **12** and **13** having a 12-membered-ring orifice in 49% and 18% yields, respectively (Scheme 2), in addition to unreacted **7** (19%). The structures of **12** and **13** were determined based on spectral information and theoretical calculations as mentioned below.

The FAB mass spectra indicated that both **12** and **13** have the same molecular formula corresponding to **7** with addition of O_2. The IR spectra of **12** and **13** exhibited strong carbonyl stretching bands at 1750 and 1743 cm^{-1} for **12**, and 1737 cm^{-1} for **13**. The formation of two carbonyl groups in **12** and **13** was confirmed by ^{13}C NMR spectra, which exhibited two new signals corresponding to carbonyl carbon atoms at δ 198.32 and 187.46 ppm for **12**, and at δ 194.24 and 188.50 ppm for **13**. These data suggested that either one of the C2-C3 or C4-C5 double bonds was most likely cleaved by photochemically generated $^1O_2$ through the formation of dioxetane intermediates **14** and **15**, respectively, to give the diketo-compounds **12** and **13**, in the same manner as reported for the open-cage C_{60} having an eight-membered-ring orifice,[2,6d-f] as shown in Figure 6. Since theoretical calculations (B3LYP/6-31G*) indicated that compound **12** is more stable than **13** by 7.3 kcal mol^{-1}, even

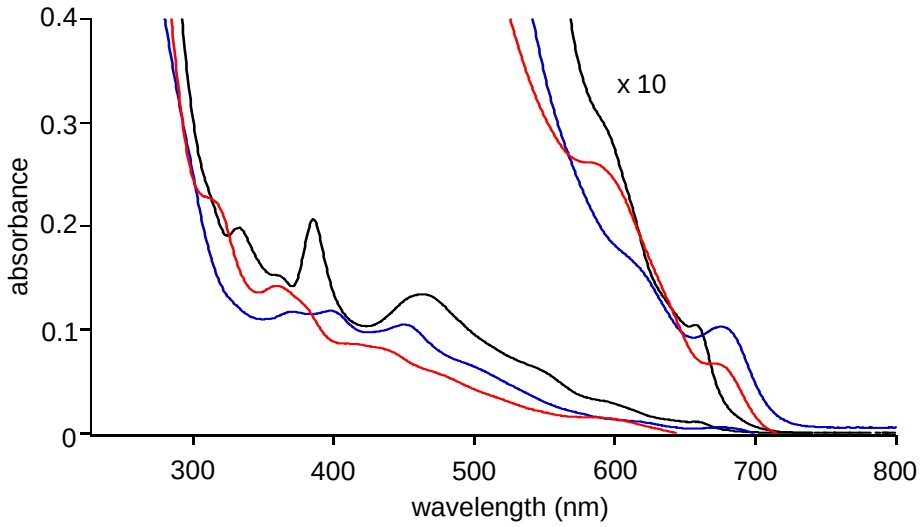

Figure 7. UV-vis spectra of open-cage fullerene derivatives **12** and **13** with a 12-membered-ring orifice and **7** in $CHCl_3$: blue line (**12**; 5.20×10^{-5} M), red (**13**; 5.45×10^{-5} M), black (**7**; 6.96×10^{-5} M).

though there is almost no difference in the relative energies between dioxetane intermediates **14** and **15**, the major and minor products obtained experimentally were determined to be **12** and **13**, respectively. The validity of assignment for the structure of **12** was unambiguously confirmed by the X-ray crystallography, as will be described in detail below.

Compounds **12** and **13**, which are isomeric, exhibited totally different electronic spectra, as shown in Figure 7. This could be ascribed to the fact that **12** formed by the scission of the C=C double bond at α-position of **7** (C2-C3), whereas **13** formed by the cleavage of that at β-position (C4-C5). Actually, it was reported that α-$C_{70}H_2$, having two hydrogen atoms at the α-bond, and its positional isomer β-$C_{70}H_2$ showed quite different UV-vis spectra from each other.[11]

An open-cage fullerene C_{70} derivative having a 13-membered-ring orifice: In order to obtain insight into the reactivity of **12**, which was obtained as the major product upon photo-oxidation of **7**, theoretical calculations were carried out. As shown in Figure 8, the LUMOs of **12** are relatively localized at the conjugated butadiene moiety, C9-C10-C11-C12, on the rim of the orifice (the numbering is shown in Scheme 3), and the LUMO energy level is significantly lowered due to the presence of the two carbonyl groups.[2,6d] This enhanced

electron affinity of **12** was confirmed by the electrochemical measurements by the use of the differential pulse voltammetry (DPV) in *o*-dichlorobenzene (ODCB) using Bu_4NBF_4 as a supporting electrolyte. Compound **12** exhibited the first reduction wave at −1.10 V versus the ferrocene/ferrocenium couple, which is 0.05 V lower than that of C_{70} measured under the same conditions. Judging from these information, the sulfur insertion into the C10-C11 single bond of **12** under the presence of a strong π-electron donor such as tetrakis(dimethylamino)ethylene (TDAE) was quite conceivable, in exactly the same manner as that developed for the synthesis of open-cage C_{60} derivative **5**.[2] Thus, the reaction was conducted by heating a solution of **12**, elemental sulfur, and TDAE in ODCB at 180 °C for 10 h. By subjecting the resulting reaction mixture to flash chromatography over silica gel,

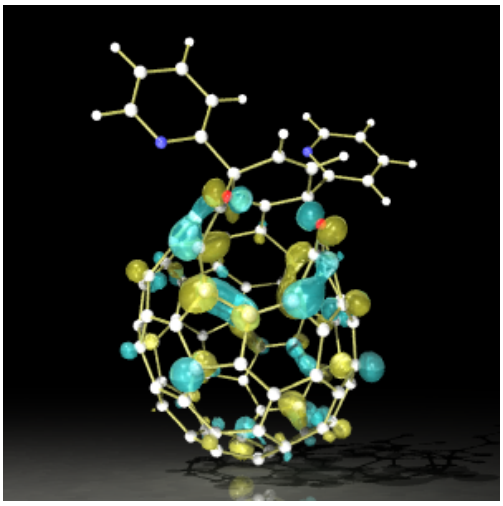

Figure 8. The optimized structure of open-cage fullerene derivative **12** with the contour of the LUMO (B3LYP/6-31G*).

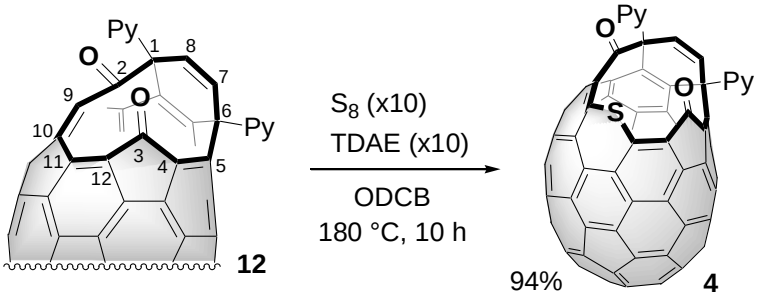

Scheme 3. Enlargement of the orifice size of **12**.

desired open-cage C_{70} derivative **4** with a 13-membered-ring orifice was obtained in 94% yield (Scheme 3).

The structure of **4** was characterized based on the spectral information as described below. The FAB mass spectrum showed molecular ion peak at *m*/*z* 1110 corresponding to **12** + S. The ^{13}C NMR spectrum exhibited two signals for the carbonyl carbon atoms at δ 193.65 and 183.45 ppm, 64 signals (out of 82 expected signals) corresponding to the sp^2-carbon atoms in the range δ 166.18 – 122.02 ppm, and two signals corresponding to the sp^3-carbons at δ 59.48 and 53.37 ppm. These data supported the structure of **4**.

Finally, the structure of **4** was unambiguously determined by the X-ray crystallography for a single crystal grown from a solution of toluene (Figure 9). It was confirmed that compound **4** indeed has a 13-membered-ring orifice (shown in red) containing a sulfur atom on its rim, in the same fashion as the open-cage C_{60} derivative **5**.[2] The orifice size of **4** was found to be very slightly larger than that of **5**, judging from the distance between two carbonyl carbons being 3.83 Å for **4** and 3.75 Å for **5**,[2] respectively. By the X-ray structure of **4**, the previous assignments of the structures for **7** and **12** were proven to be correct.

The electronic spectrum of compound **4** taken in $CHCl_3$ showed maximum absorptions at 438 and 635 nm (Figure 10), which are totally different from that of **12** (λ_{max} 370, 398, 450, 676 nm) reflecting that the π-conjugated system of **12** was partially broken by the insertion of the sulfur atom.[2]

The electrochemical behavior of compound **4** was investigated by cyclic voltammetry (CV) and DPV in ODCB using Bu_4NBF_4 as a supporting electrolyte. As shown in Figure 11, **4** exhibited three reversible reduction waves at −1.18, −1.56, and −1.92 V versus the ferrocene/ferrocenium couple, which are only slightly more negative than those of C_{70} itself (E_{red} = −1.12, −1.52, and −1.95 V) measured under the same conditions. This indicates that **4** still retains the high electron affinity characteristic of C_{70}, albeit the original 70π-conjugated system was heavily broken in **4**.

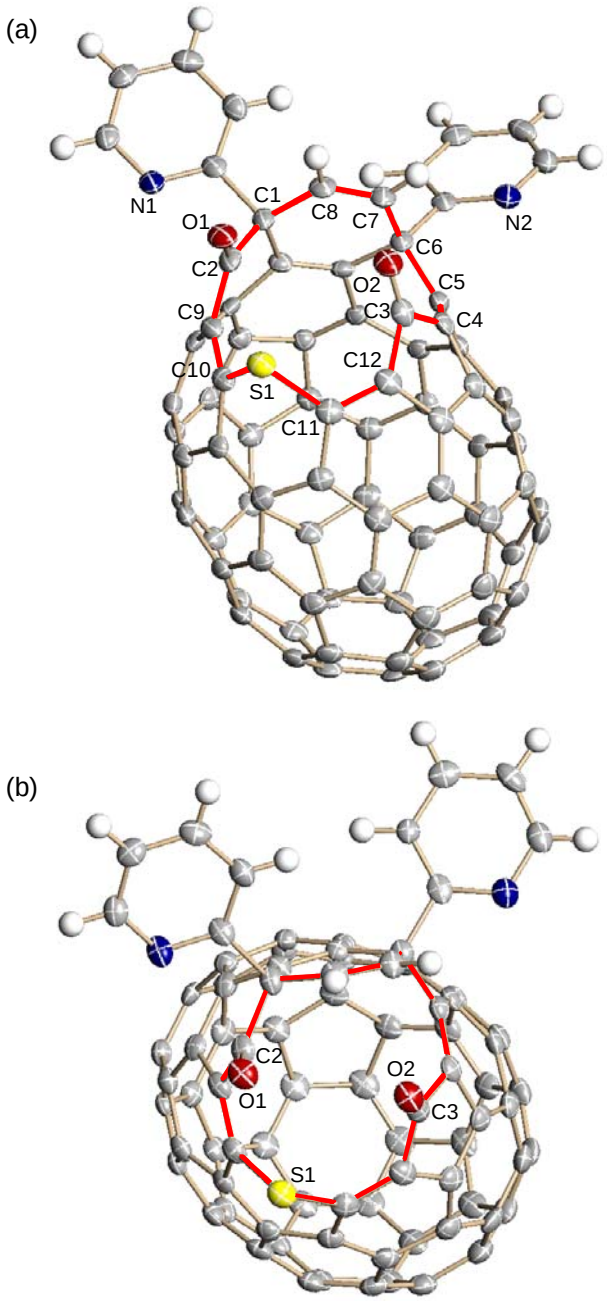

Figure 9. The X-ray structure of open-cage fullerene derivative **4** with displacement ellipsoids drawn at the 50 % probability level. (a) side view and (b) top view. Selected distances [Å]: C1-C2 1.564(5), C2-O1 1.210(4), C2-C9 1.493(4), C9-C10 1.388(4), C10-S1 1.766(3), S1-C11 1.765(3), C11-C12 1.369(4), C12-C3 1.514(5), C3-O2 1.201(4), C3-C4 1.568(4), C4-C5 1.363(4), C5-C6 1.536(4), C6-C7 1.503(4), C7-C8 1.323(4).

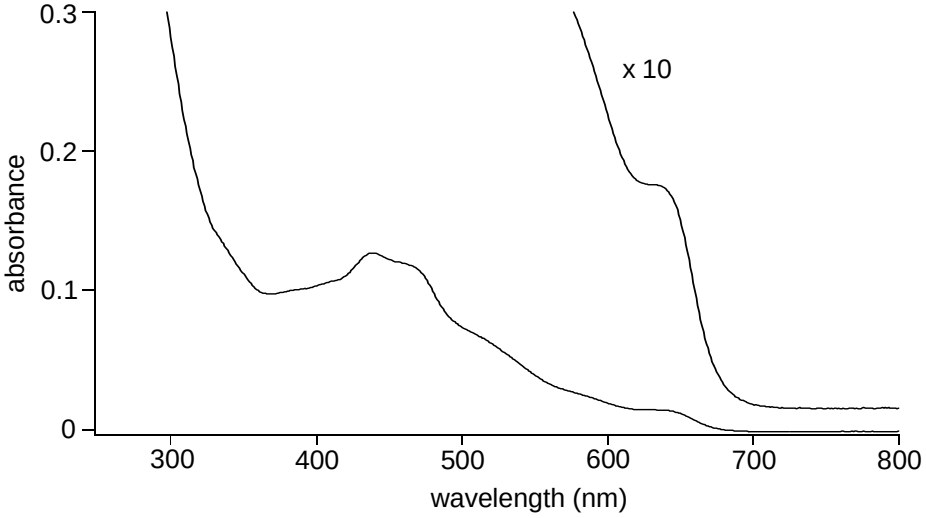

Figure 10. UV-vis spectra of open-cage fullerene derivative **4** (5.38×10^{-5} M) in $CHCl_3$.

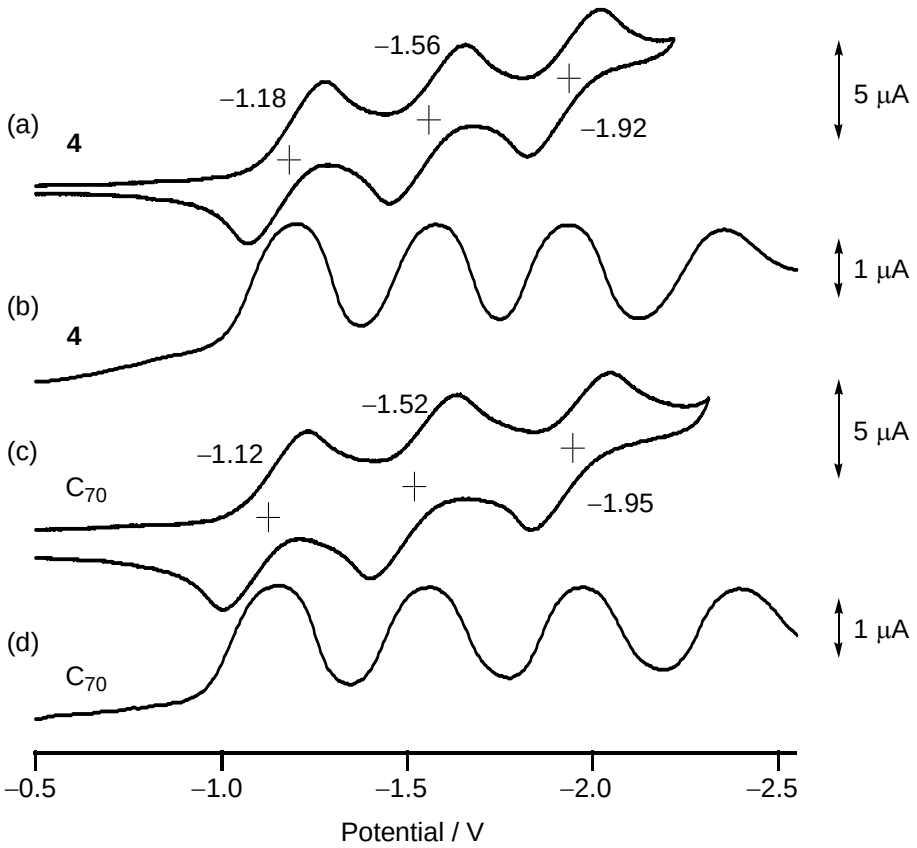

Figure 11. CV and DPV of **4** and C_{70}: 1 mM in ODCB, 0.05 M $TBABF_4$, scan rate 0.02 V s^{-1}; (a) CV of **4**, (b) DPV of **4**, (c) CV of C_{70}, (d) DPV of C_{70}.

Encapsulation of hydrogen molecule(s) in open-cage fullerene C_{70} derivative 4: The orifice size of **4** was found to be very slightly larger than that of **5** based on the X-ray crystallography, indicating that small gaseous entities such as He atom[15] and H_2 molecule[3] would be possible to enter the cage through the 13-membered-ring orifice. The activation energies required for the insertion of He, H_2, Ne, and Ar were caculated by using hybrid density functional theory (B3LYP/6-31G**//B3LYP/3-21G). As to the insertion of H_2, the energy needed to force second H_2 into H_2@**4** to produce $(H_2)_2$@**4** was also computed. As listed in Table 1, activation energies are calculated to be comparable to those of **5**.[3] Most noteworthy is that the destabilization due to steric repulsion caused by the encapsulation of the second hydrogen molecule is only +4.0 kcal/mol, which is considerably smaller than that of C_{60} analogue **5** (+9.4 kcal/mol), implying the possibility of the formation of $(H_2)_2$@**4**.

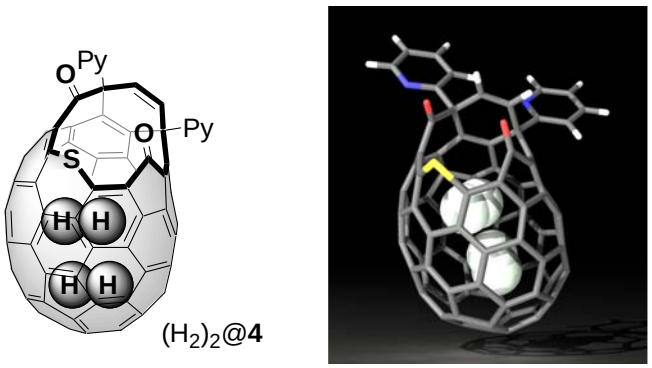

Table 1. Predicted Activation Energies for Insertion, Escape, and Energies of Encapsulation (B3LYP/6-31G*//B3LYP/3-21G, in kcal mol^{-1}) for the molecule of He, Ne, H_2, and Ar inside **4** and **5**.

Guest	Barrier to insertion		Energy of encapsulation		Barrier to escape	
	4	**5**	**4**	**5**	**4**	**5**
He	+20.1	+19.0[a]	+0.3	+0.4[a]	+19.8	+18.6[a]
Ne	+28.6	+26.2[a]	–0.3	–1.0[a]	+28.9	+27.2[a]
H_2	+31.2	+30.1[a]	+1.3	+1.4[a]	+29.9	+28.7[a]
2nd H_2	+31.0	+30.2	+4.0	+9.4	+27.0	+20.8
Ar	+102.3	+97.8[a]	+4.4	+6.2[a]	+97.9	+91.6[a]

[a] Values taken from ref. 3.

The insertion of molecular hydrogen was attempted by treating a power of **4** with high-pressure H_2 gas (800 atm) in an autoclave at 200 °C for 8 h. The HPLC analysis (Cosmosil Buckyprep column eluted with toluene) of the resulting H_2-treated material exhibited a single peak at exactly the same retention time as that for empty **4**, indicating that **4** was totally stable under these conditions. The incorporation of hydrogen molecule was clearly shown by the ^{1}H NMR spectrum, which showed a new sharp signal at unusually high field, δ −16.51 ppm, together with signals for the pyridyl and olefinic protons appearing with completely the same chemical shifts as those for empty **4** itself (Figure 12). The sharp signal (δ −16.51) is considered as the resonance of the hydrogen molecule encapsulated in **4** (H_2@**4**), which was subjected to the quite strong shielding effect characteristic of the highly aromatic π-system of the C_{70} cage.[16] This assignment was supported by theoretical calculations for H_2@**4** using the GIAO (gauge-invariant atomic orbital) approach at B3LYP/6-311G**//B3LYP/6-31G* level, which reproduced the chemical shift of the encapsulated hydrogen molecule quite accurately as δ −16.43 ppm. It should be noted that a small signal was also observed at δ −15.22 ppm. This signal was speculated to be the resonance of two molecules of hydrogen incorporated in **4**, because of a resemblance to a report that a cyclopropanated C_{70} derivative (at α-bond) incorporating two ^{3}He atoms (ca. 0.1% of the 2.6% pure sample) showed a quite tiny ^{3}He NMR signal, which was downfield

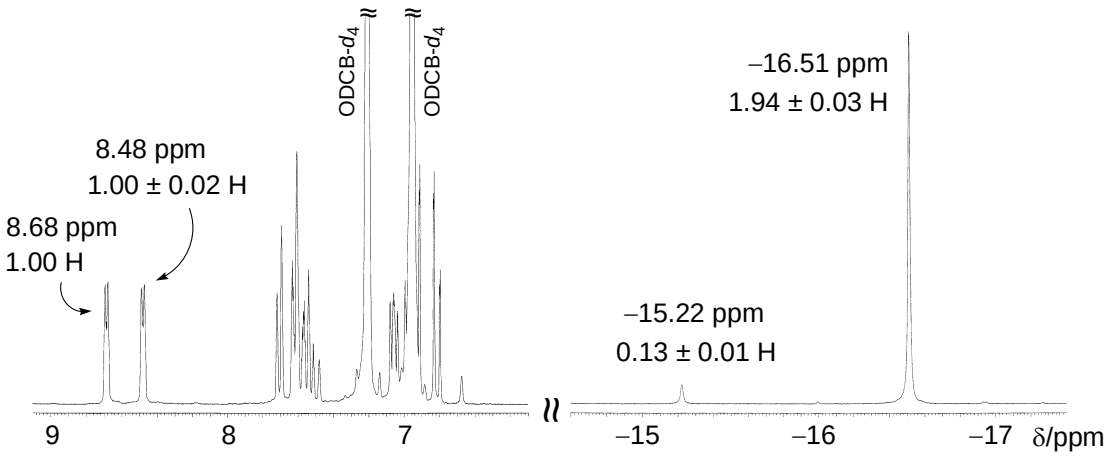

Figure 12. ^{1}H NMR spectrum (300 MHz, ODCB-d_4) of the hydrogen incorporated **4**. The integrated peak areas are shown based on the peak area of the 6-pyridyl proton at δ 8.68 ppm.

shifted as compared to that for the compound incorporating one ^{3}He atom (2.6% pure).[5] The integrated relative intensity of these two signals was determined to be 1.94 H (97% yield) and about 0.13 H (3% yield, calculated as $(H_2)_2$@**4**) by comparison with the intensity of well-resolved pyridyl proton signals at δ 8.68 ppm (1.00 H). The encapsulation rates were highly dependent on the pressure of H_2 gas: the yields decreased to 79% (H_2@**4**) and 2% ($(H_2)_2$@**4**) under 660 atm of H_2, and 54% (H_2@**4**) and 0.3% ($(H_2)_2$@**4**) under 180 atm of H_2, with all other conditions kept the same. Discussion on H_2@**4** will be made first, which will then be followed by that on $(H_2)_2$@**4**.

The endohedral complex H_2@**4** was quite stable at room temperature. However, the hydrogen molecule was released from the cage when the solution in ODCB-d_4 prepared and sealed under vacuum (10^{-4} mmHg) was heated above 160 °C, which was monitored as a gradual decrease in the NMR signal for the incorporated H_2 at δ −16.52 ppm. The escaping rates were monitored at 160, 170, 180, and 190 °C and were found to follow the first-order kinetics as shown in Figure 13. As shown by the data shown in Table 2, the rates for the H_2

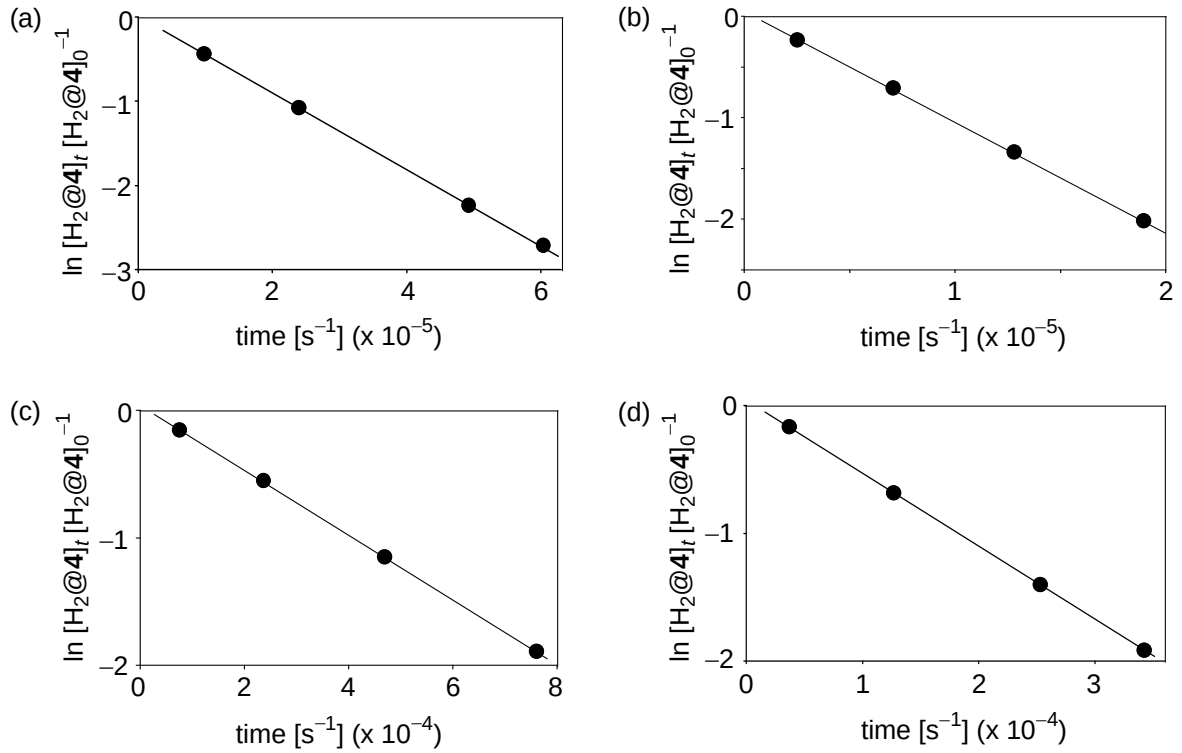

Figure 13. The rate plots for the release of hydrogen molecule from H_2@**4** at four temperatures; (a) 160 °C, (b) 170 °C, (c) 180 °C, (d) 190 °C.

release from $H_2@$**4** were found to be slightly faster than the C_{60} analogue $H_2@$**5**[3] in accord with the results of the X-ray crystallography.[2] The Arrhenius plot gave a good linear fit, with the pre-exponential factor (A) and the activation energy (E_a) being $10^{11.7\pm0.3}$ and 33.8 ± 0.7 kcal mol^{-1}, respectively (Figure 14). This activation energy (E_a) is higher than the predicted value by the DFT calculations (E_a = 29.9 kcal mol^{-1}) as in the case for the $H_2@$**5**.[3] The activation parameters at 25 °C were also determined as $\Delta G^{\ddagger}$ = 35.3 ± 0.9 kcal mol^{-1}, $\Delta H^{\ddagger}$ = 33.2 ± 0.4 kcal mol^{-1}, and $\Delta S^{\ddagger}$ = –7 ± 2 cal K^{-1} mol^{-1}, which are quite similar to those of $H_2@$**5** ($\Delta G^{\ddagger}$ = 35.5 ± 0.9 kcal mol^{-1}, $\Delta H^{\ddagger}$ = 33.4 ± 0.4 kcal mol^{-1}, and $\Delta S^{\ddagger}$ = –7 ± 2 cal K^{-1} mol^{-1}).[3]

Table 2. The Rate Constants (k) and Half–Lives ($t_{1/2}$) for the Release of Molecular Hydrogen from $H_2@$**4** and $H_2@$**5** at Four Temperatures

T [°C]	k [s^{-1}]		$t_{1/2}$ [h]	
	4	**5**[a]	**4**	**5**[a]
160 ± 0.5	4.55 x 10^{-6}	3.54 x 10^{-6}	42.3	54.4
170 ± 0.5	1.09 x 10^{-5}	9.05 x 10^{-6}	17.6	21.3
180 ± 0.5	2.54 x 10^{-5}	2.13 x 10^{-5}	7.6	9.0
190 ± 0.5	5.71 x 10^{-5}	4.60 x 10^{-5}	3.4	4.2

[a] Values taken from ref. 3.

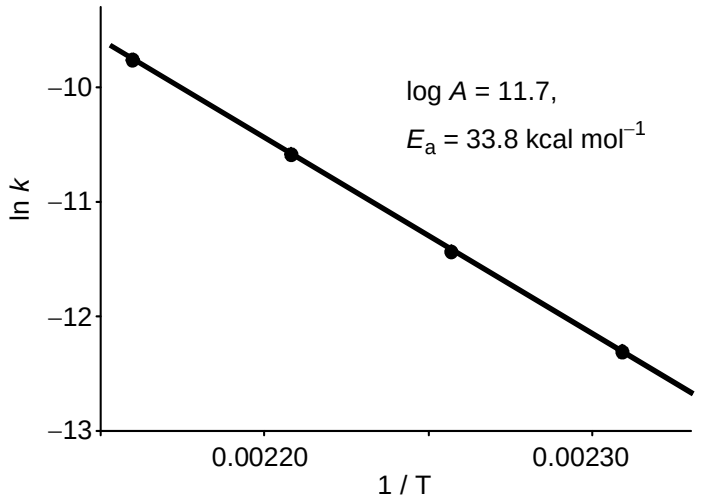

Figure 14. Arrhenius plot for the release of hydrogen molecule from $H_2@$**4**.

The MALDI-TOF mass measurement on H_2@**4** was carried out using dithranol as a matrix. At a laser power adjusted slightly above the threshold for the ionization of **4**, the molecular ion peak of H_2@**4** (*m*/*z* 1112) was clearly observed, along with a peak for empty **4** (*m*/*z* 1110) formed by partial release of a hydrogen molecule upon laser irradiation (Figure 15a). In addition, a fragment ion peak due to elimination of pyridyl group (*m*/*z* 1032) and a

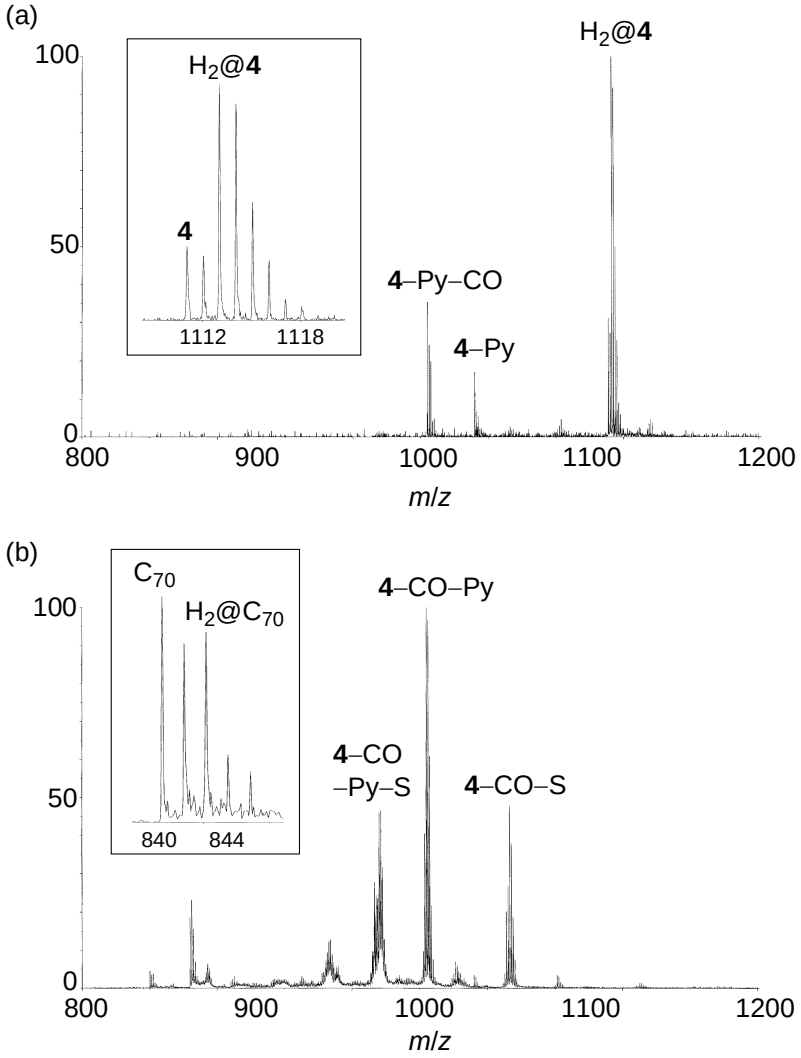

Figure 15. MALDI-TOF mass spectra of H_2@**4**. (a) The produced molecular ion peak is observed at a laser power slightly above the threshold for ion formation. An inset shows an expanded spectrum of the molecular ion peak. (b) With increased laser power, formation of vacant C_{70} and H_2@C_{70} is observed.

peak due to elimination of pyridyl and carbonyl groups (*m*/*z* 1004) were observed. When a higher laser power was used (Figure 15b), the peak for the molecular ion disappeared and, instead, the formation of C_{70} (*m*/*z* 840) and $H_2@C_{70}$ (*m*/*z* 842) was clearly observed. The intensity of the peak for $H_2@C_{70}$ was approximately one-half of that for C_{70}, taking the isotope distribution of C_{70} into consideration. Thus, it was shown that, upon laser irradiation, generation of $H_2@C_{70}$ is possible in the gas phase by self-restoration of $H_2@$**4**, as in the case for $H_2@C_{60}$.[3]

Characterization of open-cage fullerene derivative incorporating two molecules of hydrogen, $(H_2)_2@$4: As mentioned above, upon the ^{1}H NMR measurement of compound **4** treated with high-pressure of H_2 gas, a rather weak signal was observed at δ −15.22 ppm, together with the strong signal for $H_2@$**4** (Figure 12). As depicted in Figure 16, the GIAO calculations (GIAO-B3LYP/6-311G**//B3LYP/6-31G*) of $(H_2)_2@$**4** predicted that the two NMR signals should appear at δ −13.59 ppm for a hydrogen molecule (H_2-a), which is closer to the orifice, and at δ −17.86 ppm for another hydrogen molecule (H_2-b), which is located at the bottom. The difference in the chemical shifts (4.27 ppm) would reflect the large gradient of the magnetic field inside the C_{70} cage of **4** along the long axis induced by the intensive

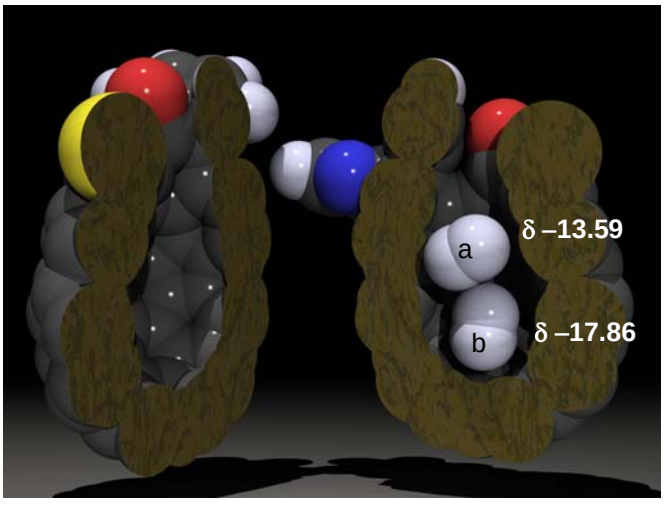

Figure 16. The cut-out view of $(H_2)_2@$**4** with the simulated chemical shifts of the incorporated two hydrogen molecules at the GIAO-B3LYP/6-311G**//B3LYP/6-31G* level of theory.

transformations of the fullerene π-system. The rapid exchange of each position of two hydrogen molecules should give a time-averaged NMR signal at around δ −15.3 ppm, which was indeed close to the experimentally observed value (δ −15.22 ppm). Therefore, by controlling the frequency of the positional exchange by decreasing the temperature, the NMR signal for the two hydrogen molecules inside $(H_2)_2$@**4** was expected to split into two signals.

Prior to the investigation of such behavior of the two hydrogen molecules, enrichment of $(H_2)_2$@**4** (3%) was attempted by the use of recycling HPLC on a Cosmosil Buckyprep column (two directly connected columns; 25-cm length, 10-mm inner diameter; mobile phase, toluene; flow rate, 4 mL min^{-1}). After three recycles, the tailing fraction of the peak was collected; the difference in retention times for two species to be separated was too small to give an even slight shoulder. This process was found to enhance the content of $(H_2)_2$@**4** to 15%. The obtained material was purified again by the same HPLC procedure to give the enriched material containing $(H_2)_2$@**4** in up to 34% in an amount of slightly less than 1 mg.

As shown in Figure 17a, the ^{1}H NMR spectrum of $(H_2)_2$@**4** (containing H_2@**4** in 66%) at 20 °C in a solution of CS_2-CD_2Cl_2 (4:1) prepared under vacuum (10^{-4} mmHg) exhibited the markedly stronger signal for $(H_2)_2$@**4** (δ −15.04 ppm), which was slightly broadened as compared to that for H_2@**4** (δ −16.30 ppm). This difference in line-shape indicates that the motion of the incorporated two hydrogen molecules is already slightly restricted even at 20 °C. As expected, the signal became broader upon cooling the solution to −40 °C, and completely disappeared at −60 °C. Then, the encapsulation of two hydrogen molecules in $(H_2)_2$@**4** was indisputably proved by the appearance of two broad signals at −80 °C, which became much sharper upon cooling to −100 °C. Furthermore, the observed chemical shifts (δ −12.87 and −17.38 ppm) are in good agreement with the predicted values by the DFT calculations (δ −13.59 and −17.86 ppm, see Figure 16). The line-shape analysis revealed that the two hydrogen molecules exchanged their positions with each other at the rate of only 50 times per second at −100 °C, while the rate was increased up to 4.9×10^5 times per second at 20 °C. Arrhenius plot gave an excellent linear fit with the pre-exponential factor (A) and the activation energy (E_a) being $10^{11.7\pm0.3}$ and 8.0 ± 0.4 kcal mol^{-1}, respectively, as shown in Figure 18. The activation parameters were determined as $\Delta G^{\ddagger}$ (25 °C) = 9.4 ± 0.5 kcal mol^{-1}, $\Delta H^{\ddagger}$ = 7.4 ± 0.4 kcal mol^{-1}, and $\Delta S^{\ddagger}$ = −7 ± 2 cal K^{-1} mol^{-1}. It should be noted that the shape

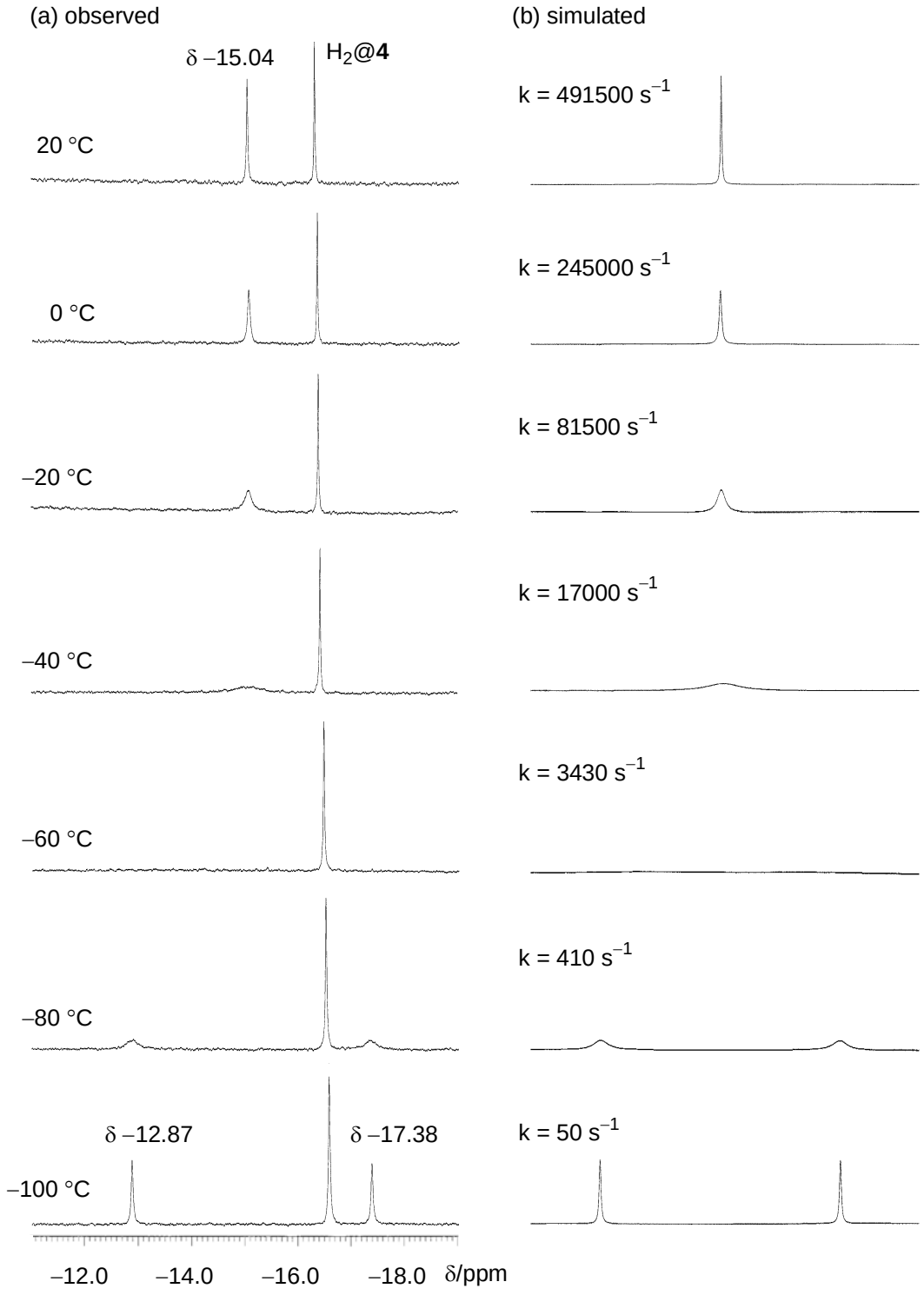

Figure 17. Low-temperature ^{1}H NMR (400 MHz, CS_2-CD_2Cl_2 (4:1)) spectra of the mixture of $(H_2)_2@$**4** and $H_2@$**4** (1:2); (a) observed spectra and (b) simulated spectra shown together with estimated values of rate constants.

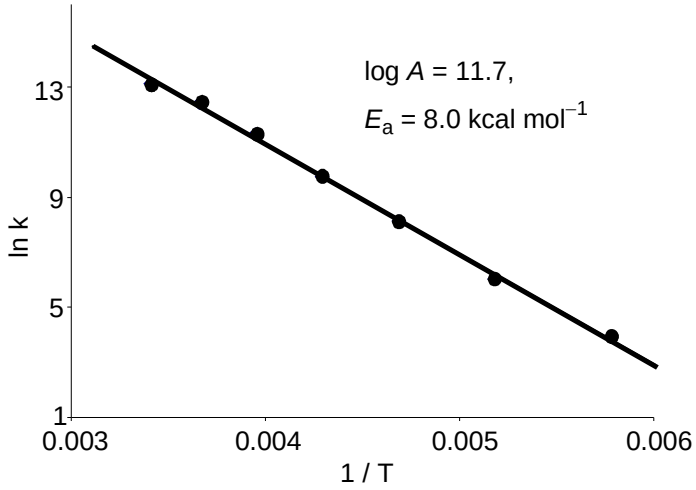

Figure 18. Arrhenius plot for the positional exchange between two hydrogen molecules of $(H_2)_2$@**4**.

of the signal for H_2@**4** remained unchanged throughout these low-temperature NMR measurements, reflecting the free rotation of a single hydrogen molecule in the C_{70} cage.

Restoration of the Fullerene Cage; Formation of H_2@C_{70} and $(H_2)_2$@C_{70}: The size reductions of the 13-membered-ring orifice of H_2@**4** and $(H_2)_2$@**4** were carried out by applying the similar reactions developed for the synthesis of H_2@C_{60},[4] mentioned in Chapter 4. Since the yield of $(H_2)_2$@**4** was quite small (3%) to be isolated in a large amount, a mixture of H_2@**4** and $(H_2)_2$@**4** (97:3) was subjected to the following chemical transformations. As shown in Scheme 4, an oxidation of the sulfide moiety on the rim of the orifice was first conducted by adding 1.6 equivalents of *m*-chloroperbenzoic acid (MCPBA) to a solution of $(H_2)_n$@**4** (n = 1, 2) in CS_2. After being stirred at room temperature for 10 h, the crude mixture was subjected to flash chromatography on silica gel to afford the desired sulfoxide derivative $(H_2)_n$@**16** in 66% yield. The sulfinyl group was then removed by irradiation of visible light with a high-pressure mercury lamp to a solution of $(H_2)_n$@**16** in dried and degassed benzene at room temperature for 5 h, followed by separation using flash chromatography on silica gel to afford $(H_2)_n$@**12** having a 12-membered-ring orifice in 86% yield. The two carbonyl groups in $(H_2)_n$@**12** were reductively coupled by the use of Ti(0) at 80 °C for 40 min to give $(H_2)_n$@**7** having an eight-membered-ring orifice. Finally, complete

closure of the orifice was achieved by heating the powder of $(H_2)_n$@**7** in a glass tube sealed under vacuum at 400 °C for 2 h. The obtained crude product was dissolved in CS_2 and passed through a silica gel column to give $(H_2)_n@C_{70}$ (contaminated with approximately 10% of empty C_{70}) in 56% yield.

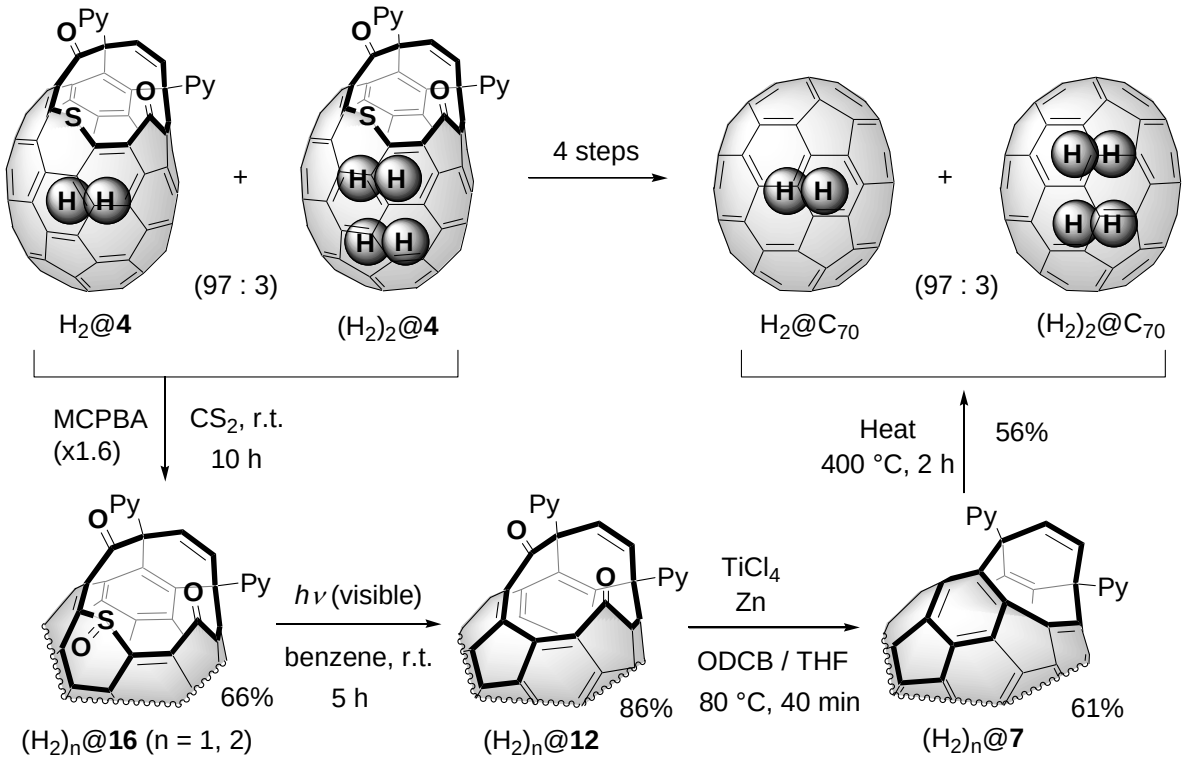

Scheme 4. Synthesis of endohedral fullerenes $H_2@C_{70}$ and $(H_2)_2@C_{70}$.

The ^{1}H NMR spectrum of the crude product of the thermal reaction exhibited a sharp signal for $H_2@C_{70}$ at δ –23.70 ppm and a weak signal for $(H_2)_2@C_{70}$ at δ –23.53 ppm in an integrated ratio of 97 : 6, indicating that hydrogen molecule(s) originally encapsulated in the cage of **4** was not lost at all throughout these transformations. The difference in these ^{1}H NMR chemical shifts was Δδ 0.17 ppm, which is larger than that between $^3He@C_{70}$ (2.6% encapsulation) and $^3He_2@C_{70}$ (0.1% encapsulation) (Δδ 0.02 ppm) in ^{3}He NMR.[5,17] The endohedral chemical shifts reflect an averaged magnetic field at different positions inside C_{70} cage sampled by encapsulated species. Therefore, the observed difference in Δδ values should be ascribed to the larger volume of a hydrogen molecule (19 Å^3)[18] than a ^{3}He atom (11

Å^3),[18] and the geometry of the two hydrogen molecules in $(H_2)_2@C_{70}$, which should be off-centered by the steric reason. In the MALDI-TOF mass spectrum, the molecular ion peak for $H_2@C_{70}$ was clearly observed at *m*/*z* 842, along with a peak for empty C_{70} at *m*/*z* 840, formed by a partial release of molecular hydrogen during the thermal reaction at the final step. The ^{13}C NMR spectrum in ODCB-d_4 exhibited five signals for $H_2@C_{70}$ at δ 150.950, 148.389, 147.709, 145.722, and 131.237 ppm. Each signal was all accompanied by a weak signal corresponding to empty C_{70} (δ 150.904, 148.359, 147.690, 145.669, and 131.171 ppm). The difference in the chemical shifts (Δδ 0.046, 0.030, 0.019, 0.053, and 0.066 ppm, respectively) were smaller than that between $H_2@C_{60}$ and empty C_{60} (Δδ 0.078 ppm)[4]. This indicates that the electronic and/or van der Waals interaction between the C_{70} cage and inside hydrogen in $H_2@C_{70}$ is quite small, even as compared to that of $H_2@C_{60}$, reflecting the larger space inside C_{70}.

Conclusion

By conducting a thermal reaction of fullerene C_{70} with pyridazine derivative **6**, open-cage fullerene derivatives **7** having an eight-membered-ring orifice was obtained as a major product. The orifice of **7** was enlarged by the oxidation with singlet oxygen followed by insertion of a sulfur atom to give open-cage fullerene derivative **4** with a 13-membered-ring orifice, in a way similar to that developed for the synthesis of open-cage C_{60} analogue **5**. The structure of **4** was unambiguously confirmed by X-ray crystallography to show the presence of a slightly larger orifice in **4** than that in **5**. Upon treatment of **4** with high-pressure H_2 gas (800 atm) at 200 °C, two signals were appeared in ^{1}H NMR spectrum at unusually high field region such as δ −16.51 and −15.22 ppm, in an integrated ratio of 97 : 6. It was revealed that the former signal corresponds to $H_2@$**4**, while the later small signal is assigned to encapsulated hydrogen in $(H_2)_2@$**4**. The incorporation of two hydrogen molecules was supported by the GIAO calculations and confirmed by the low-temperature NMR measurements, which showed that a peak at δ −15.22 ppm was clearly split into two signals at −100 °C by the restriction of the positional exchange between two hydrogen molecules. Finally, totally new endohedral fullerene C_{70} encapsulating one or two hydrogen

molecules, $H_2@C_{70}$ and $(H_2)_2@C_{70}$, were synthesized through the four-step organic reactions from $H_2@$**4** and $(H_2)_2@$**4**.

Experimental Section

General. The ^{1}H and ^{13}C NMR measurements were carried out on a Varian Mercury 300 instrument and a JEOL AL-400 instrument and the chemical shifts are reported in ppm with reference to tetramethylsilane. In some cases, the signal of *o*-dichlorobenzene-d_4 (ODCB-d_4) was used as internal standard (δ 7.20 ppm in ^{1}H NMR, δ 132.35 ppm in ^{13}C NMR). UV-vis spectra were recorded on a Shimadzu UV-3150 spectrometer. IR spectra were taken with a Shimadzu FTIR-8600 spectrometer. MALDI-TOF mass spectra were measured with an Applied Biosystem Voyager-DE STR spectrometer using dithranol as a matrix. FAB mass spectra were recorded on a JEOL MStation JMS-700. APCI mass spectra were measured on a Finnigan-MAT TSQ 7000 spectrometer. The high-pressure liquid chromatography (HPLC) was performed by the use of a Cosmosil Buckyprep column (4.6 mm × 250 mm) for analytical purpose, and the same column (two directly connected columns, 10 mm × 250 mm) for preparative purpose. In some cases, HPLC was performed on a prepacked silica gel column (Yamazen Ultra Pack SI40B; 26 mm × 300 mm). Cyclic voltammetry and differential pulse voltammetry were conducted on a BAS Electrochemical Analyzer CV-100W using a three-electrode cell with a glassy carbon working electrode, a platinum wire counter electrode, and a Ag/0.01 M $AgNO_3$ reference electrode. The potentials were corrected against ferrocene used as an internal standard which was added after each measurement. Fullerene C_{70} was purchased from Matsubo Co. Tetrakis(dimethylamino)ethylene were purchased from Aldrich Co. and used as received. Elemental sulfur was purchased from Nacalai Tesque Co. and used as received. *m*-Chloroperbenzoic acid was purchased from Aldrich Co. Zinc (sandy) and titanium (IV) chloride was purchased from Wako Co. 3,6-Di-(2-pyridyl)-pyridazine (**6**) was synthesized following a reported procedure.[12]

Computational Method. All calculations were conducted using the Gaussian 98 series of electronic structure program.[14] The geometries were fully optimized with the restricted

Becke hybrid (B3LYP) method for all calculations. The GIAO calculations were performed at B3LYP/6-311G** level of theory using the optimized structures at B3LYP/6-31G* level of theory.

Synthesis of 7 and 8. A mixture of fullerene C_{70} (50 mg, 0.059 mmol) and 3,6-bis(2-pyridyl)pyridazine (**6**) (28 mg, 0.12 mmol) in 1-chloronaphthalene (2.5 mL) was refluxed at 255 °C for 24 h under an argon. The resulting dark brown solution was directly subjected to flash column chromatography over silica gel. Elution with toluene gave unreacted C_{70} (22 mg, 0.027 mmol, 45%) while the following elution with toluene-ethyl acetate (10:1) gave a mixture of open-cage fullerene derivative **7** and **8**. Further separation of this mixture by HPLC on a prepacked silica gel column (Yamazen Ultra Pack SI40B; 26 mm × 300 mm) eluted with toluene-ethyl acetate (5:1) gave **7** (25 mg, 0.023 mmol, 40%) and **8** (3 mg, 0.003 mmol, 5%) both as brown powders.

7: IR (KBr) ν 1745 (C=N) cm^{-1}; UV/vis ($CHCl_3$) λ_{max} (log ε) 333 (4.46), 386 (4.47), 463 (4.29), 658 (3.18) nm; ^{1}H NMR (300 MHz, $CDCl_3$-CS_2 (1:1)) δ 8.97 (m, 1H), 8.56 (m, 1H), 8.38 (m, 1H), 8.07 (m, 1H), 7.86 (m, 1H), 7.70 (m, 1H), 7.47 (m, 4.8 Hz, 1H), 7.17 (m, 1H), 6.47 (d, *J* = 9.5 Hz, 1H), 6.27 (d, *J* = 9.5 Hz, 1H); ^{13}C NMR (75 MHz, $CDCl_3$-CS_2 (1:1)) δ 168.12, 165.33, 153.50, 150.86, 150.67, 150.46, 150.19, 149.89, 149.22, 149.10, 148.52, 148.49, 148.40, 148.10, 148.03, 148.01, 147.97, 147.94, 147.88, 147.83, 147.51, 147.30, 147.27, 147.24, 147.22, 147.19, 146.91, 146.25, 145.85, 145.79, 145.37, 145.28, 145.07, 144.94, 144.75, 144.33, 144.21, 144.01, 143.98, 143.95, 143.87, 143.21, 143.17, 142.52, 142.11, 141.76, 141.49, 140.98, 140.49, 139.96, 139.21, 138.24, 137.11, 136.53, 136.10, 135.45, 135.07, 133.36, 132.27, 132.25, 132.10, 131.69, 131.10, 130.92, 130.50, 127.66, 126.53, 125.01, 124.73, 124.14, 123.50, 122.24, 122.15, 122.02, 117.46, 54,33, 52.91; HRMS (+FAB) $C_{84}H_{11}N_2$ (M+1), calcd for 1047.0922, found 1047.0898.

8: IR (KBr) ν 1749 (C=N) cm^{-1}; UV/vis ($CHCl_3$) λ_{max} (log ε) 335 (4.44), 361 (4.33), 380 (4.43), 467 (4.25) nm; ^{1}H NMR (300 MHz, CD_2Cl_2-CS_2 (1:1)) δ 8.67 (m, 2H), 7.87 (m, 2H), 7.78 (m, 2H), 7.27 (m, 2H), 6.29 (s, 2H); ^{13}C NMR (75 MHz, $CDCl_3$-CS_2 (1:1)) δ 160.57, 153.36, 150.87, 150.67, 150.44, 149.83, 149.81, 148.70, 148.58, 148.21, 148.19, 148.17, 148.10, 147.94, 147.79, 147.71, 146.86, 145.90, 144.59, 144.46, 143.34, 143.15, 142.96, 142.25, 141.60, 141.07, 140.52, 139.60, 138.43, 137.50, 134.14, 132.14, 130.32, 130.06,

127.57, 125.53, 124.89, 124.27, 122.47, 52.53; HRMS (+FAB) $C_{84}H_{11}N_2$ (M+1), calcd for 1047.0922, found 1047.0933.

Photochemical oxidation of 7. A brown solution of compound **7** (79 mg, 0.076 mmol) in CS_2 (110 mL) in a Pyrex flask was irradiated by a xenon-lamp (500 W) from a distance of 60 cm for 5 h under air. The resulting brown solution was evaporated under reduced pressure and the residual brown solid was dissolved in ODCB (8 mL). This solution was subjected to preparative HPLC on a prepacked silica gel column (Yamazen Ultra Pack SI40B; 26 mm × 300 mm) to afford open-cage fullerene derivatives **12** (40 mg, 0.037 mmol, 49%) and **13** (15 mg, 0.013 mmol, 18%), both as brown powders, together with unreacted **7** (15 mg, 0.015 mmol, 19%).

12: IR (KBr) ν 1750 (C=O), 1743 (C=O) cm^{-1}; UV/vis ($CHCl_3$) λ_{max} (log ε) 370 (4.35), 398 (4.36), 450 (4.30), 676 (3.29) nm; ^{1}H NMR (300 MHz, CD_2Cl_2-CS_2 (1:1)) δ 8.80 (m, 1H), 8.51 (m, 1H), 7.92 (m, 1H), 7.76 (m, 1H), 7.75 (m, 1H), 7.66 (m, 1H), 7.40 (m, 1H), 7.20 (m, 1H), 6.70 (d, *J* = 9.9 Hz, 1H), 6.58 (d, *J* = 9.9 Hz, 1H); ^{13}C NMR (75 MHz, ODCB-d_4) δ 198.32, 187.46, 165.78, 164.06, 154.64, 151.16, 150.84, 150.71, 150.60, 150.44, 150.31, 149.90, 149.31, 149.19, 148.86, 148.68, 148.37, 148.33, 148.13, 148.08, 148.05, 147.95, 147.89, 147.87, 147.75, 147.72, 147.68, 147.48, 146.93, 146.69, 146.58, 145.86, 145.60, 145.37, 145.24, 144.45, 144.21, 144.01, 143.69, 143.31, 143.16, 142.92, 142.77, 142.17, 142.08, 141.59, 140.66, 140.11, 139.80, 138.43, 138.13, 137.99, 137.93, 137.78, 137.08, 136.72, 136.68, 135.13, 134.52, 133.63, 133.32, 126.58, 125.39, 123.15, 122.78, 122.41, 122.02, 60.01, 52.94 (the signals at the range of δ 132.4 ~ 126.8 were overlapped with the signals of ODCB-d_4); HRMS (+FAB) $C_{84}H_{11}N_2O_2$ (M+1), calcd for 1079.0821, found 1079.0842.

13: IR (KBr) ν 1737 (C=O) cm^{-1}; UV/vis ($CHCl_3$) λ_{max} (log ε) 361 (4.42), 673 (3.09) nm; ^{1}H NMR (300 MHz, CD_2Cl_2-CS_2 (1:1)) δ 8.88 (m, 1H), 8.47 (m, 1H), 8.03 (m, 1H), 7.96 (m, 1H), 7.78 (m, 1H), 7.60 (m, 1H), 7.46 (m, 1H), 7.24 (m, 1H), 6.74 (d, *J* = 9.9 Hz, 1H), 6.59 (d, *J*= 9.9 Hz, 1H); ^{13}C NMR (75 MHz, ODCB-d_4) δ 194.24, 188.50, 167.48, 163.23, 153.47, 152.78, 152.36, 152.13, 150.57, 149.75, 149.43, 149.29, 149.22, 149.06, 149.03, 148.28, 147.57, 147.50, 147.23, 147.20, 147.09, 146.75, 146.58, 146.33, 145.99, 145.98, 145.76, 145.74, 145.47, 145.42, 145.37, 145.34, 145.11, 145.02, 144.95, 144.89, 144.87,

144.72, 144.49, 144.41, 144.05, 143.69, 143.46, 142.71, 142.70, 142.05, 141.95, 141.51, 141.30, 140.60, 140.13, 139.48, 139.10, 139.08, 138.26, 137.84, 137.20, 136.94, 136.66, 135.39, 135.35, 134.85, 134.20, 133.82, 133.62, 132.85, 124.56, 123.84, 123.77, 123.37, 122.93, 122.40, 122.34, 122.01, 60.44, 53.70 (the signals at the range of δ 132.4 ~ 126.8 were overlapped with the signals of ODCB-d_4); HRMS (+FAB) $C_{84}H_{11}N_2O_2$ (M+1), calcd for 1079.0821, found 1079.0813.

Synthesis of 4. To a heated and stirred solution of compound **12** (21 mg, 0.019 mmol) and elemental sulfur (49 mg, 0.19 mmol as S_8) in ODCB (10 mL) was added tetrakis(dimethylamino)ethylene (44 μL, 0.19 mmol) at 180 °C under argon. The solution was refluxed at 180 °C for 10 h, and then the resulting dark brown solution was concentrated by evaporation under reduced pressure to about 2 mL. This solution was added to pentane (40 mL) with vigorous stirring to give brown precipitates. The precipitates, collected by centrifuge, were dissolved in CS_2 (20 mL). The resulting solution was subjected to flash chromatography on silica gel eluted with toluene-ethyl acetate (20:1) to give open-cage fullerene derivative **4** (20 mg, 0.018 mmol, 94%) as a brown powder.

4: mp >300 °C (slow decomposition starting at 250 °C); IR (KBr) ν 1747 (C=O) cm^{-1}; UV/vis ($CHCl_3$) λ_{max} (log ε) 438 (4.37), 635 (3.51) nm; ^{1}H NMR (300 MHz, $CDCl_3$-CS_2 (1:1)) δ 8.78 (m, 1H), 8.50 (m, 1H), 7.83 (m, 1H), 7.69 (m, 1H), 7.69 (m, 1H), 7.59 (m, 1H), 7.32 (m, 1H), 7.16 (m, 1H), 6.83 (d, J = 9.9 Hz, 1H), 6.69 (d, J = 9.9 Hz, 1H); ^{13}C NMR (75 MHz, ODCB-d_4) δ 193.65, 183.45, 166.18, 164.61, 152.16, 150.81, 150.55, 150.27, 150.10, 149.93, 149.69, 149.62, 149.27, 149.13, 148.85, 148.73, 148.58, 148.54, 148.31, 148.23, 148.13, 148.10, 148.08, 147.95, 147.67, 147.44, 147.11, 146.94, 146.88, 146.69, 146.64, 145.95, 145.62, 145.20, 144.91, 144.25, 143.60, 143.55, 143.08, 142.76, 142.57, 142.04, 141.15, 141.00, 140.51, 140.19, 138.56, 138.53, 138.35, 138.19, 138.06, 137.42, 137.02, 136.76, 136.45, 136.07, 135.65, 135.54, 134.74, 134.57, 126.10, 122.94, 122.71, 122.35, 122.25, 122.02, 59.48, 53.37 (the signals at the range of δ 132.4 ~ 126.8 were overlapped with the signals of ODCB-d_4); HRMS (+FAB) $C_{84}H_{10}N_2O_2S$ (M), calcd for 1110.0463, found 1110.0474.

X-ray structural analysis of 4. Single crystals of compound **4** suitable for X-ray crystallography were obtained by slow evaporation of the solution in toluene over two weeks at room temperature. Single-crystal diffraction data were collected at 100 K on a Bruker SMART diffractometer equipped with a CCD area detector using Mo-Kα radiation. All structure solutions were obtained by direct methods and refined using full-matrix least-squares with a Bruker SHELXTL (Version 5.1) Software Package. The crystal parameters are as follows: empirical formula $C_{94.5}H_{22}N_2O_2S$, formula weight 1249.20, Monoclinic, P2(1)/c, a = 19.963(3) Å, b = 13.639(2) Å, c = 19.760(3) Å, α = 90°, β = 110.694(3)°, γ = 90°, V = 5032.9(13) Å^3, Z = 4, ρ_{calc} 1.649 g cm^{-3}. The refinement converged to $R1$ = 0.0595, $wR2$ = 0.1158 [$I>2\sigma(I)$], GOF = 1.001.

Insertion of molecular hydrogen in 4. A powder of **4** lightly wrapped in a piece of aluminum foil was heated at 200 °C in an autoclave under a high-pressure H_2 gas (800 atm). A high pressure of 800 atm was generated by introducing H_2 gas of 440 atm, which was generated by compressing H_2 gas of 110 atm from a container by the use of a hydraulic compressor, into a 50-mL autoclave at −78 °C, followed by heating at 200 °C. After 8 h, the powder was recovered by washing the aluminum foil with CS_2. The HPLC analysis (a Buckyprep column eluted with toluene) showed a single peak at exactly the same retention time as that for **4**. The ^{1}H NMR spectra of **4** were taken with sufficiently long pulse intervals (42 s) to obtain signal intensities as accurately as possible; 300 MHz, in ODCB-d_4 at 25 °C, 13000 Hz frequency range, 7.8 μs irradiation as a 45° pulse.

$(H_2)_n@$**4**: IR (KBr) ν 1747 (C=O) cm^{-1}; UV/vis ($CHCl_3$) λ_{max} (log ε) 440 (4.39), 635 (3.48) nm; ^{1}H NMR (300 MHz, ODCB-d_4) δ 8.68 (m, 1H), 8.48 (m, 1H), 7.70 (m, 1H), 7.63-7.48 (m, 3H), 6.81 (d, J = 9.9 Hz, 1H), −15.22 (s, 0.13 H), −16.51 (s, 1.94 H) (the signals at the range of δ 7.20 ~ 6.94 were overlapped with the signals of ODCB); ^{13}C NMR (75 MHz, ODCB-d_4) δ 193.66, 183.48, 166.18, 164.61, 152.22, 150.87, 150.61, 150.34, 150.15, 149.97, 149.73, 149.63, 149.30, 149.13, 148.90, 148.76, 148.62, 148.58, 148.55, 148.36, 148.27, 148.17, 148.06, 148.00, 147.71, 147.48, 147.17, 147.00, 146.93, 146.69, 146.62, 146.00, 145.60, 145.19, 144.95, 144.27, 143.59, 143.53, 143.16, 143.13, 142.78, 142.65, 142.02, 141.26, 141.12, 140.54, 140.20, 138.55, 138.53, 138.47, 138.17, 137.46, 137.03, 136.80, 136.58, 136.10, 135.73, 135.68, 134.87, 134.75, 126.13, 122.96, 122.72,

122.38, 122.27, 122.04, 59.48, 53.35 (the signals at the range of δ 132.4 ~ 126.8 were overlapped with the signals of ODCB-d_4); HRMS (+FAB) $C_{84}H_{13}N_2O_2S$ (MH^+), calcd for 1113.0698, found 1113.0685.

Release of hydrogen molecule from H_2@4. A solution of H_2@**4** in ODCB-d_4, which was sealed under vacuum (10^{-4} mmHg) after degassed by repeating three freeze-pump-thaw cycles, was heated at 160, 170, 180, and 190 °C. Each release rate was determined by monitoring a gradual decrease in the relative intensity of the NMR signal of the encapsulated H_2 with reference to the pyridyl proton signals.

Oxidation of $(H_2)_n$@4 (n = 1, 2). A mixture of $(H_2)_n$@**4** (49 mg, 0.0443 mmol) and *m*-chloroperbenzoic acid (12 mg, 0.069 mmol) in CS_2 (50 mL) was stirred at room temperature for 10 h under argon. The solvent was evaporated under reduced pressure, and the residual brown solid was washed twice with 50 mL of methanol. The solid was dissolved in CS_2 (15 mL), and was subjected to a flash column chromatography eluted with toluene-ethyl acetate (10:1) to give $(H_2)_n$@**16** (33 mg, 0.029 mmol, 66%) as a brown solid.

$(H_2)_n$@**16**: IR (KBr) ν 1746 (C=O), 1076 (S=O) cm^{-1}; ^{1}H NMR (300 MHz, ODCB-d_4) δ 8.72 (m, 1H), 8.46 (m, 1H), 7.67-7.53 (m, 4H), 6.85 (d, J = 9.9 Hz, 1H), 6.79 (d, J = 9.9 Hz, 1H), −15.60 (s, 0.13 H), −16.83 (s, 1.94 H) (the signals at the range of δ 7.20 ~ 6.94 were overlapped with the signals of ODCB); ^{13}C NMR (75 MHz, ODCB-d_4) δ 195.33, 184.93, 165.57, 164.27, 151.76, 150.95, 150.55, 150.42, 150.08, 149.67, 149.52, 149.49, 149.22, 149.16, 148.99, 148.78, 148.60, 148.50, 148.13, 148.07, 147.94, 147.85, 147.81, 147.63, 147.48, 147.31, 146.94, 146.87, 146.72, 146.32, 145.71, 145.67, 145.58, 145.30, 144.43, 144.15, 143.94, 143.02, 142.98, 142.31, 142.18, 141.75, 141.70, 141.38, 140.07, 139.83, 139.80, 139.73, 139.44, 139.21, 139.01, 137.86, 137.20, 137.17, 136.88, 136.36, 135.87, 135.32, 134.94, 134.86, 134.70, 133.82, 126.35, 125.01, 123.45, 122.95, 122.41, 122.35, 122.20, 59.99, 53.16 (the signals at the range of δ 132.4 ~ 126.8 were overlapped with the signals of ODCB-d_4); HRMS (+FAB) $C_{84}H_{13}N_2O_3S$ (MH^+), calcd for 1129.0647, found 1129.0634.

Photochemical desulfurization of $(H_2)_n$@16 (n = 1, 2). A stirred solution of $(H_2)_n$@**16** (80 mg, 0.071 mmol) in degassed benzene (600 mL) in a Pyrex-glass flask was irradiated with a high-pressure mercury lamp placed at the distance of 3 cm at 40 °C for 5 h under argon.

After removal of the solvent under reduced pressure, the residual brown solid was dissolved in CS_2 (10 mL), and was subjected to flash column chromatography over silica gel. Elution with toluene-ethyl acetate (10:1) gave $(H_2)_n$@**12** (66 mg, 0.061 mmol, 86%) as a brown solid.

$(H_2)_n$@**12**: IR (KBr) ν 1751(C=O),1743(C=O) cm^{-1}; UV/vis ($CHCl_3$) λ_{max} (log ε) 369 (4.42), 398 (4.42), 450 (4.37), 676 (3.34) nm; ^{1}H NMR (300 MHz, ODCB-d_4) δ 8.65 (m, 1H), 8.46 (m, 1H), 7.73-7.47 (m, 4H), 6.84 (d, J = 9.9 Hz, 1H), 6.67 (d, J = 9.9 Hz, 1H), –17.06 (s, 0.13 H), –17.95 (s, 1.94 H) (the signals at the range of δ 7.20 ~ 6.94 were overlapped with the signals of ODCB); ^{13}C NMR (75 MHz, ODCB-d_4) δ 198.27, 187.46, 165.78, 164.04, 154.70, 151.25, 150.87, 150.75, 150.65, 150.48, 150.35, 149.95, 149.29, 149.18, 148.16, 148.89, 148.70, 148.39, 148.36, 148.15, 148.10, 148.07, 147.96, 147.92, 147.90, 147.79, 147.75, 147.69, 147.50, 146.96, 146.75, 146.59, 145.89, 145.59, 145.40, 145.24, 144.49, 144.21, 144.05, 143.76, 143.72, 143.33, 143.24, 142.98, 142.82, 142.17, 141.57, 140.73, 140.13, 139.85, 138.48, 138.13, 137.99, 137.92, 137.80, 137.06, 136.81, 136.69, 135.18, 134.65, 133.72, 133.35, 126.60, 123.12, 122.77, 122.38, 121.99, 60.01, 52.93 (the signals at the range of δ 132.4 ~ 126.8 were overlapped with the signals of ODCB-d_4); HRMS (+FAB) $C_{84}H_{13}N_2O_2$ (MH^+), calcd for 1081.0977, found 1081.0990.

Reductive coupling of two carbonyl groups in $(H_2)_n$@12 (n = 1, 2). To a stirred suspension of zinc powder (293 mg, 4.49 mmol) in dry tetrahydrofuran (10 mL) was added titanium tetrachloride (246 μl, 426 mg, 2.25 mmol) drop by drop at 0 °C under argon, and the mixture was refluxed for 1.5 h. A 0.5-mL portion of the resulting black slurry was added to a stirred solution of $(H_2)_n$@**12** (20 mg, 0.019 mmol) in ODCB (4 mL) at room temperature under argon. After heating at 80 °C for 40 min, a resulting black solution was cooled to room temperature. After dilution with CS_2 (20 mL), the solution was washed with saturated aqueous solution of $NaHCO_3$ (50 mL). The organic layer was dried over $MgSO_4$ and evaporated under reduced pressure to give a residual brown solid, which was then subjected to flash column chromatography over silica gel. Elution with toluene-ethyl acetate (10:1) gave $(H_2)_n$@**7** (12 mg, 0.011 mmol, 61%) as a brown solid.

$(H_2)_n$@**7**: IR (KBr) ν 1746 (C=N) cm^{-1}; ^{1}H NMR (300 MHz, ODCB-d_4) δ 8.87 (1H), 8.51 (m, 1H), 8.27 (d, J = 7.8, 1H), 7.87-7.74 (m, 3H), 6.45 (d, J = 9.6 Hz, 1H), 6.25 (d, J = 9.6 Hz, 1H), –20.71 (s, 0.13 H), –21.16 (s, 1.94 H) (the signals at the range of δ 7.20 ~ 6.94

were overlapped with the signals of ODCB); ^{13}C NMR (75 MHz, ODCB-d_4) δ 168.67, 165.93, 153.46, 150.87, 150.71, 150.51, 150.23, 149.91, 149.65, 149.52, 149.28, 149.13, 148.52, 148.47, 148.33, 148.16, 148.07, 148.00, 147.93, 147.77, 147.55, 147.30, 147.22, 146.97, 146.23, 145.91, 145.77, 145.45, 145.28, 145.12, 145.08, 144.95, 144.77, 144.37, 143.99, 143.95, 143.85, 143.34, 143.19, 142.58, 142.11, 141.87, 141.75, 141.18, 140.74, 140.48, 140.13, 139.42, 138.32, 137.82, 137.75, 137.55, 137.03, 136.77, 136.44, 136.23, 135.43, 135.14, 133.39, 126.56, 125.06, 124.65, 124.16, 124.10, 123.48, 122.77, 122.17, 122.06, 121.69, 117.94, 54.75, 53.34 (the signals at the range of δ 132.4 ~ 126.8 were overlapped with the signals of ODCB-d_4); HRMS (+FAB) $C_{84}H_{13}N_2$ (MH^+), calcd for 1049.1079, found 1049.1085.

Synthesis of $(H_2)_n$@C_{70} (n = 1, 2). A powder of H_2@**7** (55 mg, 0.053 mmol) lightly wrapped with a piece of aluminum foil was placed in a glass tube (inner diameter 20 mm) sealed under vacuum (1 mmHg), which was heated in an electric furnace at 400 °C for 2 h. The resulting black solid was washed with CS_2 and evaporated under reduced pressure to give a brown solid, which was then subjected to flash column chromatography over silica gel. Elution with CS_2 gave $(H_2)_n$@C_{70} contaminated with about 10% of empty C_{70} (total weight 25 mg, 56% (calculated $(H_2)_n$@C_{70} 23 mg, 51%)) as a brown solid.

$(H_2)_n$@C_{70}: mp >300 °C; IR (KBr) ν 1460.0, 1431.1, 1415.7, 1134.1, 794.6, 673.1, 642.3, 576.7, 565.1, 534.2, 461.0 cm^{-1} (empty C_{70}: ν 1458.1, 1431.1, 1415.7, 1134.1, 794.6, 673.1, 642.3, 576.7, 565.1, 534.2, 457.1 cm^{-1}); UV/vis ($CHCl_3$) λ_{max} (log ε) 332 (4.45), 361 (4.35), 380 (4.51), 472 (4.23), 639 (3.25) nm (empty C_{70} ($CHCl_3$): λ_{max} (log ε) 332 (4.51), 361 (4.41), 380 (4.55), 470 (4.29), 638 (3.34) nm); ^{1}H NMR (300 MHz, $CDCl_3$-CS_2 (1:1)) δ(H_2) –23.53 (s, 0.13 H), –23.70 (s, 1.94 H); ^{13}C NMR (75 MHz, CS_2-CD_2Cl_2 (4:1)) δ 151.125, 148.552, 147.883, 145.895, 131.415; HRMS (+FAB) $C_{70}H_2$ (M^+), calcd for 842.0157, found 842.0170.

References and Notes

(1) (a) Rubin, Y. *Chem. Eur. J.* **1997**, *3*, 1009. (b) Rubin, Y. *Top. Curr. Chem.* **1999**, *199*, 67. (c) Nierengarten, J.-F. *Angew. Chem. Int. Ed.* **2001**, *40*, 2973.

(2) Murata, Y.; Murata, M.; Komatsu, K. *Chem. Eur. J.* **2003**, *9*, 1600.

(3) Murata, Y.; Murata, M.; Komatsu, K. *J. Am. Chem. Soc.* **2003**, *125*, 7152.

(4) Komatsu, K.; Murata, M.; Murata, Y. *Science* **2005**, *307*, 238.

(5) Khong, A.; Jiménez-Vázquez, H. A.; Saunders, M.; Cross, R. J.; Laskin, J.; Peres, T.; Lifshitz, C.; Strongin, R.; Smith, A. B., III *J. Am. Chem. Soc.* **1998**, *120*, 6380.

(6) For examples of open-cage C_{60} derivatives, see: (a) Hummelen, J. C.; Prato, M.; Wudl, F. *J. Am. Chem. Soc.* **1995**, *117*, 7003. (b) Arce, M.-J.; Viado, A. L.; An, Y.-Z.; Khan, S. I.; Rubin, Y. *J. Am. Chem. Soc.* **1996**, *118*, 3775. (c) Schick, G.; Jarrosson, T.; Rubin, Y. *Angew. Chem. Int. Ed.* **1999**, *38*, 2360. (d) Murata, Y.; Komatsu, K. *Chem. Lett.* **2001**, *30*, 896. (e) Murata, Y.; Murata, M.; Komatsu, K. *J. Org. Chem.* **2001**, *66*, 8187. (f) Inoue, H.; Yamaguchi, H.; Iwamatsu, S.-i.; Uozaki, T.; Suzuki, T.; Akasaka, T.; Nagase, S.; Murata, S. *Tetrahedraon Lett.* **2001**, *42*, 895. (g) Iwamatsu, S.-i.; Ono, F.; Murata, S. *J. Chem. Soc., Chem. Commun.* **2003**, 1268. (h) Iwamatsu, S.-i.; Ono, F.; Murata, S. *Chem. Lett.* **2003**, *32*, 614. (i) Iwamatsu, S.-i.; Uozaki, T.; Kobayashi, K.; Re, S.; Nagase, S. *J. Am. Chem. Soc.* **2004**, *126*, 2668. (j) Iwamatsu, S.-i.; Murata, S. *Tetrahedraon Lett.* **2004**, *45*, 6391. (k) Vougioukalakis, G. C.; Prassides, K.; Campanera, J. M.; Heggie, M. I.; Orfanopoulos, M. *J. Org. Chem.* **2004**, *69*, 4524.

(7) Hirsch, A. *The Chemistry of Fullerenes*; Thieme Verlag: Stuttgart, 1994. (b) Diederich, F.; Kessinger, R. *Acc. Chem. Res.* **1999**, *32*, 537. (c) Taylor, R. *Synlett* **2000**, 776.

(8) Birkett, P. R.; Avent, A. G.; Darwish, A. D.; Kroto, H. W.; Taylor, R.; Walton, D. R. M. *J. Chem. Soc., Chem. Commun.* **1995**, 1869.

(9) Hasharoni, K.; Bellavia-Lund, C.; Keshavarz-K. M.; Srdanov, G.; Wudl, F. *J. Am. Chem. Soc.* **1997**, *119*, 11128.

(10) (a) Herrmann, A.; Diederich, F.; Thilgen, C.; Meer, H.-U.; Müller, W. H. *Helv. Chim. Acta* **1994**, *77*, 1689. (b) Wilson, S. R.; Lu, Q. *J. Org. Chem.* **1995**, *60*, 6496.

(11) Henderson, C. C.; Rohlfing, C. M., Gillen, K. T.; Cahill, P. A. *Science* **1994**, *264*, 397.

(12) Butte, W. A.; Case, F. H. *J. Org. Chem.* **1961**, *26*, 4690.

(13) Murata, Y.; Kato, N.; Komatsu, K. *J. Org. Chem.* **2001**, *66*, 7235.

(14) Gaussian 98, Revision A.11, M. J. Frisch, G. W. Trucks, H. B. Schlegel, G. E. Scuseria, M. A. Robb, J. R. Cheeseman, V. G. Zakrzewski, J. A. Montgomery, Jr., R. E. Stratmann, J. C. Burant, S. Dapprich, J. M. Millam, A. D. Daniels, K. N. Kudin, M. C. Strain, O. Farkas, J. Tomasi, V. Barone, M. Cossi, R. Cammi, B. Mennucci, C. Pomelli, C. Adamo, S. Clifford, J. Ochterski, G. A. Petersson, P. Y. Ayala, Q. Cui, K. Morokuma, P. Salvador, J. J. Dannenberg, D. K. Malick, A. D. Rabuck, K. Raghavachari, J. B. Foresman, J. Cioslowski, J. V. Ortiz, A. G. Baboul, B. B. Stefanov, G. Liu, A. Liashenko, P. Piskorz, I. Komaromi, R. Gomperts, R. L. Martin, D. J. Fox, T. Keith, M. A. Al-Laham, C. Y. Peng, A. Nanayakkara, M. Challacombe, P. M. W. Gill, B. Johnson, W. Chen, M. W. Wong, J. L. Andres, C. Gonzalez, M. Head-Gordon, E. S. Replogle, and J. A. Pople, Gaussian, Inc., Pittsburgh PA, **2001**.

(15) Stanisky, C. R.; Cross, R. J.; Saunders, M.; Murata, M.; Murata, Y.; Komatsu, K. *J. Am. Chem. Soc.* **2005**, *127*, 299.

(16) Rüttimann, M.; Haldimann, R. F.; Isaacs, L.; Diederich, F.; Khong, A.; Jiménez-Vázquez, H. A.; Cross, R. J.; Saunders, M. *Chem. Eur. J.* **1997**, *3*, 1071.

(17) Sternfeld T.; Hoffman, R. E.; Saunders, M.; Cross, R. J.; Syamala, M. S.; Rabinovitz, M. *J. Am. Chem. Soc.* **2002**, *124*, 8786.

(18) Rubin, Y.; Jarrosson, T.; Wang, G.-W.; Bartberger, M. D.; Houk, K. N.; Schick, G.; Saunders, M.; Cross, R. J. *Angew. Chem. Int. Ed.* **2001**, *40*, 1543.

Chapter 6

Generation of Dianionic Open-Cage Fullerene Derivative with a 13-Membered-Ring Orifice

Abstract: Dianion of open-cage fullerene derivative **1** and H_2@**1** having a 13-membered-ring orifice was generated as a stable species in a solution of CD_3CN at 0 °C. The ^{1}H NMR signal of hydrogen molecule encapsulated in dianion H_2@$\mathbf{1}^{2-}$ appeared at δ 8.13 ppm, which is downfield shifted by about 15 ppm as compared with that of neutral H_2@**1** (δ −7.25 ppm). The NICS calculations indicated that the magnetic properties of the pentagons and hexagons of the fullerene cage are completely reversed in dianion $\mathbf{1}^{2-}$ compared to that of the neutral state. In addition, ^{1}H NMR signals of $\mathbf{1}^{2-}$ and of H_2@$\mathbf{1}^{2-}$ were slightly broadened probably due to thermal mixing of the triplet state of $\mathbf{1}^{2-}$ and of H_2@$\mathbf{1}^{2-}$. The dianion $\mathbf{1}^{2-}$ was found to undergo sulfur-elimination reaction to afford open-cage fullerene derivative **2** with a 12-membered-ring orifice under elevated temperature.

Introduction

As mentioned in Chapter 4 and 5, new endohedral C_{60} and C_{70} encapsulating molecular hydrogen, $H_2@C_{60}$, $H_2@C_{70}$, and $(H_2)_2@C_{70}$, were synthesized for the first time by introducing hydrogen molecule(s) into the open-cage fullerene derivatives with a 13-membered-ring orifice under pressurized hydrogen gas, followed by restoration of the fullerene cages. By using this molecular surgery approach, the preparations of endohedral C_{60} and C_{70} incorporating small gaseous entities such as He, HD, and D_2 are expected to be feasible.

So far, various kinds of endohedral metallofullerenes (fullerenes encapsulating metal atom(s)), have been produced by physical techniques such as arc discharge or laser ablation methods, and isolated in a very low yield (<< 0.1%) by laborious methods of HPLC separations,[1] as mentioned in General Introduction. It has been shown that substantial degree of electron transfer takes place from the encapsulated metal atom(s) to the fullerene cages, which can cause considerable perturbation to the properties of the fullerenyl π-systems.[1] It is highly desirable to apply the present efficient molecular surgical method to the production of endohedral metallofullerenes. In order to develop a technique for the insertion of various metal atom(s) into the open-cage fullerenes through the orifice, knowledge on their reduced states is indispensable. However, such researches have been

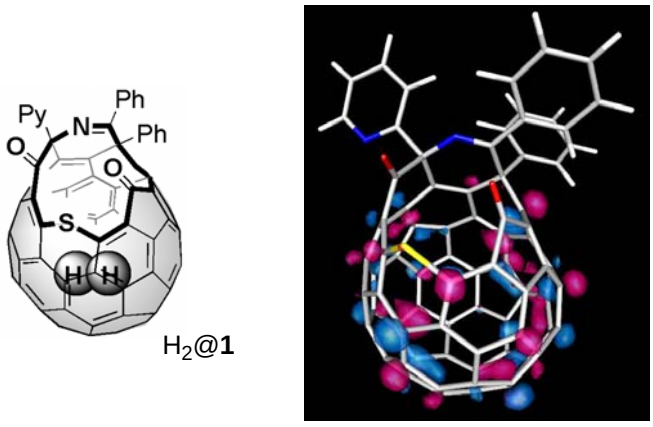

Figure 1. Structure of open-cage fullerene derivatives $H_2@$**1** and the LUMO of **1** calculated at the B3LYP/6-31G* level of theory.

limited to only electrochemical investigations using cyclic voltammetry or differential pulse voltammetry.[2,3] Furthermore, by using the encapsulated hydrogen molecule as an internal NMR probe, the difference in magnetic properties inside the fullerene cages between neutral and reduced states of **1** should be disclosed; that is, the examination of the difference in NMR chemical shifts of encapsulated hydrogen molecules in the same way as ^{3}He has been used in ^{3}He NMR.[4] In addition, as shown in Figure 1, theoretical calculations (B3LYP/6-31G*)[5] indicated that LUMO of **1** is delocalized over the fullerene cage. Hence, dianion of **1** might have possibility to attract and encapsulate metal cations into the fullerene cage by Coulomb interaction. In this chapter will be described the generation, magnetic properties, and thermal stability of the dianion of H_2@**1** and empty **1**.

Results and Discussion

As described in Chapter 2, the reduction potentials of **1** ($E_{1/2}$; –1.15, –1.56, –2.05, –2.52 V versus ferrocene/ferrocenium couple) determined by differential pulse voltammetry are almost comparable to those of C_{60} itself ($E_{1/2}$; –1.17, –1.59, –2.06, –2.56 V versus ferrocene/ferrocenium couple).[3] Therefore, sodium thiomethoxide (CH_3SNa), which is known as a reducing agent for preparation of dianion C_{60}^{2-}, should be able to generate dianion $\mathbf{1}^{2-}$.[6] Actually, as shown in Scheme 1, when **1** or H_2@**1** was treated with about 5 equivalents of CH_3SNa in acetonitrile-d_3 under vacuum (< 10^{-4} mmHg), the brown suspensions smoothly turned to dark green solution within 1 h. The ^{1}H NMR spectrum of each resulting solution is shown in Figure 2.

According to the reports on open-cage fullerene C_{60} derivatives encapsulating hydrogen

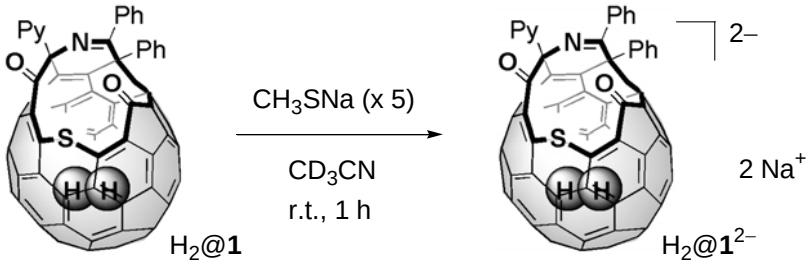

Scheme 1. Generation of dianion of H_2@**1**.

molecule, the NMR signals of the inside hydrogen molecule have always been observed in the range between δ −2 and −12 ppm, reflecting the strong shielding effect of the C_{60} cage.[7,8] However, ^{1}H NMR spectrum of dianion H_2@**1**$^{2-}$ was found to exhibit no signal in such a high field region. Alternatively, there appeared one singlet in the spectrum of H_2@**1**$^{2-}$ at a significantly down field (δ 8.13 ppm), which was not observed in the spectrum of empty dianion **1**$^{2-}$. To confirm that the signal at δ 8.13 ppm is assigned to the incorporated hydrogen molecule in dianion H_2@**1**$^{2-}$, the density functional calculations using the GIAO (gauge-invariant atomic orbital) method were conducted for H_2@**1**$^{2-}$

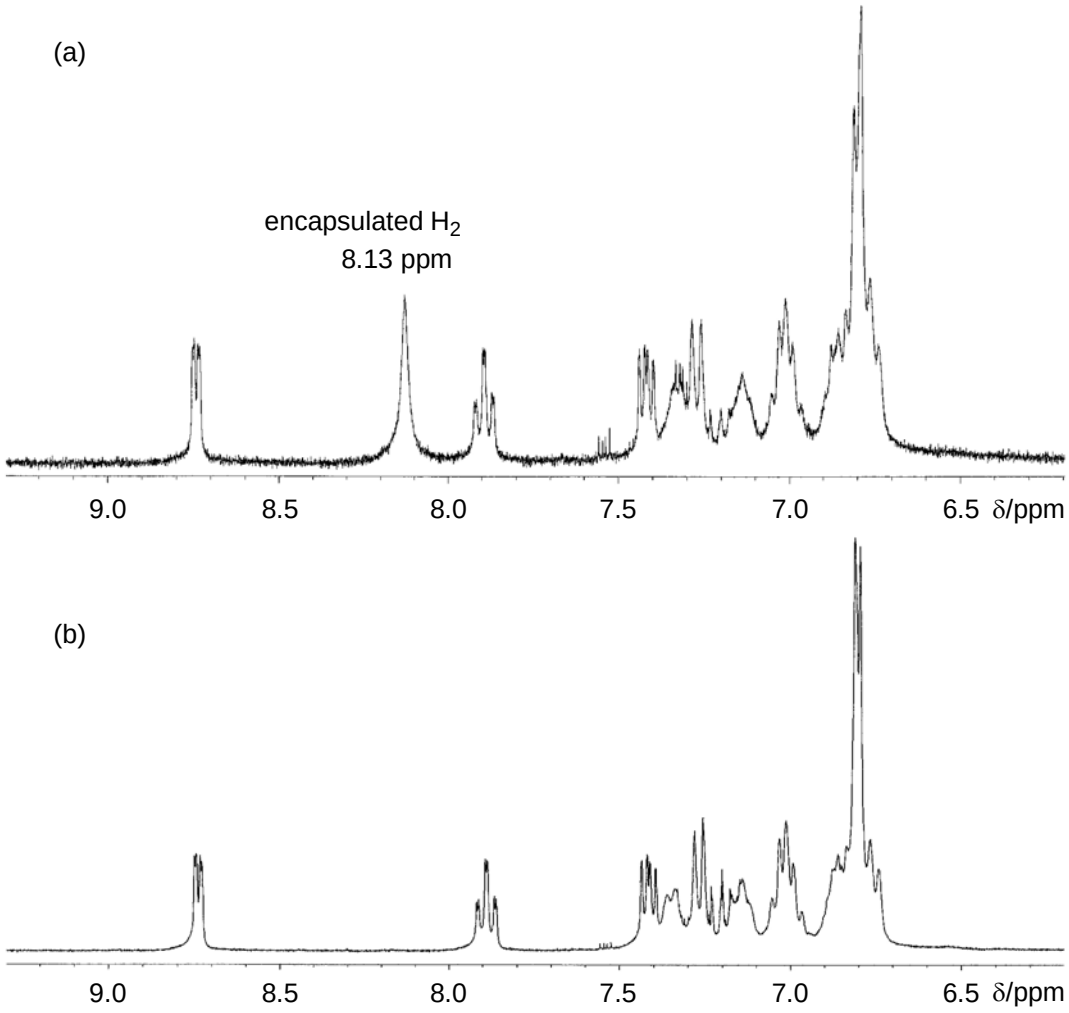

Figure 2. ^{1}H NMR (300 MHz, CD_3CN) spectra of dianion of (a) H_2@**1**$^{2-}$ and (b) empty **1**$^{2-}$. Only downfield regions are shown.

(GIAO-B3LYP/6-31G*//B3LYP/6-31G*). As a result, the chemical shift for the encapsulated hydrogen was predicted to appear at δ 9.43 ppm. This value is in a fair agreement with the experimental value. Thus, we can conclude that the dianion of H_2@**1** was indeed generated and exhibited an NMR signal for inside hydrogen molecule at an unusually down field region, which was shifted by 15 ppm as compared to that of neutral H_2@**1** (δ −7.25 ppm in *o*-dichlorobenzene-d_4).[8] This indicates that the intensity of magnetic field inside the fullerene cage was considerably increased; in other words, the overall aromaticity of the π-conjugated system was markedly decreased upon two electron reduction.

In general, aromaticity of fullerenes is not explicitly defined due to coexistence of the two types of π-electron ring currents, i.e., paramagnetic ring current in pentagons and diamagnetic one in hexagons.[9] These opposite contributions cancel each other in a very delicate fashion to make the prediction of NMR chemical shifts of encapsulated species quite difficult.[4] Moreover, anionic species of fullerenes are known to have entirely different magnetic properties from those of their neutral couterparts.[10] For example, hexaanion C_{60}^{6-} shows only diamagnetic ring currents both in the pentagons and the hexagons.[10,11] Actually, a ^{3}He NMR signal of the ^{3}He atom encapsulated in C_{60}^{6-} was observed at such a high field as δ −48.7 ppm, which is 42.4 ppm upfield shifted as compared to that of ^{3}He in the neutral C_{60}.[12]

In order to gain insight into the observed large downfield shift of the hydrogen signal of H_2@$\mathbf{1}^{2-}$, the local aromaticity and antiaromaticity of each pentagon and hexagon in dianion $\mathbf{1}^{2-}$ and neutral **1** are assessed by the NICS (nucleus-independent chemical shift) calculations.[9,13,14] The resulting NICS values (GIAO-B3LYP/6-31G*//B3LYP/6-31G*) of dianion $\mathbf{1}^{2-}$ and neutral **1** are shown in Figure 3 as the Schlegel diagrams. Upon the two-electron reduction of **1**, it is shown that the magnetic character of each ring was totally altered. Interestingly, the ring currents of most hexagons (16 out of 17) in $\mathbf{1}^{2-}$, which are diamagnetic in the neutral state, become paramagnetic. On the other hand, the ring currents of most pentagons (8 out of 9), which are paramagnetic in the neutral state, turned into diamagnetic. To the best of our knowledge, this is the first case that the magnetic properties of pentagons and hexagons are absolutely inversed as compared to that of neutral fullerene derivatives synthesized thus far.[9a] Since the number of hexagons is larger than that of

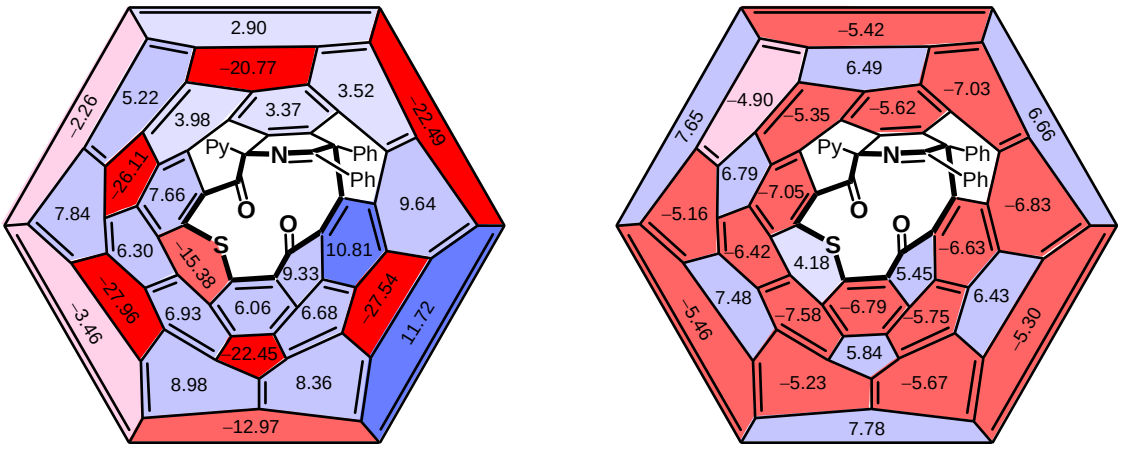

(−3.62 for the outer hexagon) (−5.20 for the outer hexagon)

$\mathbf{1}^{2-}$ (dianion) **1** (neutral)

Figure 3. NICS patterns of $\mathbf{1}^{2-}$ dianion and neutral **1**, calculated at the GIAO-B3LYP/6-31G*//B3LYP/6-31G* level of theory.

pentagons, the overall aromaticity of the fullerene cage would be considerably decreased.

As shown in Figure 2, $H_2@\mathbf{1}^{2-}$ and $\mathbf{1}^{2-}$ in CD_3CN showed that all the ^1H NMR signals are slightly broadened. Furthermore, upon ^{13}C NMR measurement of dianion $H_2@\mathbf{1}^{2-}$, no signal was observed at all at room temperature. These results indicated the existence of certain paramagnetic species in the sample solution. The broadened ^1H NMR signals of $H_2@\mathbf{1}^{2-}$ became slightly sharper when the temperature was lowered to −30 °C, indicating that this broadening is not due to any dynamic phenomenon. Theoretical calculations at the (U)B3LYP/3-21G level of theory indicated that an energy difference between singlet and triplet states of dianion $\mathbf{1}^{2-}$ is quite small (the triplet state was predicted to be more stable by 0.9 kcal mol^{-1} while the singlet state is apparently the ground state according to the experiment). Therefore, the observed NMR spectra was most likely explained by a thermal mixing of the triplet states of dianion $H_2@\mathbf{1}^{2-}$ or $\mathbf{1}^{2-}$, although the possibility of formation of radical trianion $H_2@\mathbf{1}^{\bullet\,3-}$ can not be rigorously ruled out because of an excess amount of CH_3SNa.

Dianion $\mathbf{1}^{2-}$ in a vacuum-sealed solution of CD_3CN is stable at 0 °C, but it was found to decompose slowly at above room temperature. Thus the thermal stability of dianion $\mathbf{1}^{2-}$ was investigated by heating a degassed and dried solution of dianion $\mathbf{1}^{2-}$ in tetrahydrofuran (THF)

at 66 °C for 2 h under nitrogen. The color of the solution changed from dark green to dark brown without forming any insoluble material. After being quenched by excess iodine, the crude reaction mixture was analyzed by HPLC (Buckyprep/toluene). A new peak appeared at exactly the same retention time as open-cage fullerene derivative **2**, while the peak for **1** completely disappeared. Actually, when the crude mixture was separated by flash column chromatography over silica gel, compound **2** was isolated as an almost single product. This reactivity of the facile elimination of a sulfur atom from $\mathbf{1}^{2-}$ makes a sharp contrast to that of **1** in the neutral state, which is quite stable upon heating at 250 °C under ambient atmosphere.[3] Since many sulfur elimination reactions reported so far are considered to take place via episulfide intermediates,[15] the observed reaction of $\mathbf{1}^{2-}$ is also supposed to proceed through episulfide intermediate **3** as shown in Scheme 3.

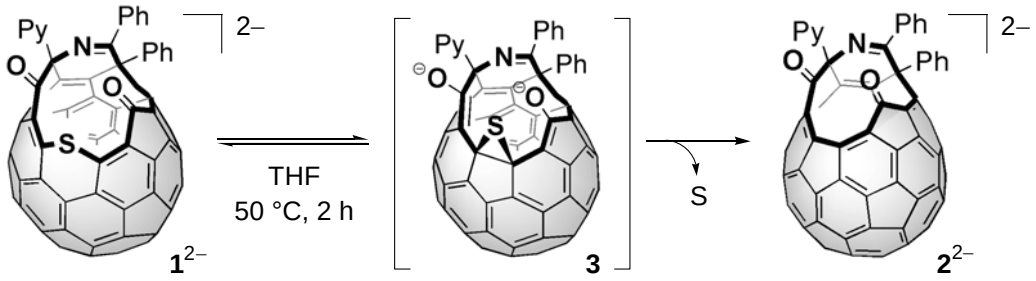

Scheme 3. Plausible reaction mechanism for the elimination of a sulfur atom from $\mathbf{1}^{2-}$ dianion.

No difference was observed at all between the ^{1}H NMR spectra of H_2@$\mathbf{1}^{2-}$ and empty $\mathbf{1}^{2-}$ even upon heating up to 90 °C in CD_3CN, regardless of whether the inside of the fullerene cage was occupied or not.

If the sodium counter cation was encapsulated inside the cage of $\mathbf{1}^{2-}$, the ^{1}H NMR spectrum of $\mathbf{1}^{2-}$ should undergo some change. However, ^{1}H NMR signals for the aromatic protons of H_2@$\mathbf{1}^{2-}$ appeared at exactly the same chemical shifts as those for empty $\mathbf{1}^{2-}$, suggesting that the sodium cation was staying outside of the cage of dianion $\mathbf{1}^{2-}$.

Conclusion

The dianion of open-cage fullerene derivative **1** and H_2@**1** having a 13-membered-ring orifice was generated, which was stable in a solution of CD_3CN at 0 °C. The ^1H NMR signal for the encapsulated hydrogen molecule in dianion H_2@$\mathbf{1}^{2-}$ was observed in unusually downfield region such as δ 8.13 ppm, reflecting the markedly lowered overall aromaticity of the fullerene cage. The NICS calculations of the dianion $\mathbf{1}^{2-}$ indicate that the local aromaticity and antiaromaticity of hexagons and pentagons are totally reversed as compared to neutral **1**. The ^1H NMR spectra of $\mathbf{1}^{2-}$ and H_2@$\mathbf{1}^{2-}$ exhibited slightly broad signals and ^{13}C NMR spectrum showed no signal at all. These observations indicated the possibility of thermal mixing of the triplet states in dianion $\mathbf{1}^{2-}$ and H_2@$\mathbf{1}^{2-}$. The facile sulfur elimination of $\mathbf{1}^{2-}$ took place at elevated temperature to afford open-cage fullerene derivative **2** with a smaller orifice.

Experimental Section

General. The ^1H and ^{13}C NMR measurements were carried out on a Varian Mercury 300 instrument or a JEOL AL-400 instrument and the chemical shifts are reported in ppm with reference to the signal of CD_3CN as an internal standard (δ 1.94 ppm in ^1H NMR). APCI mass spectra were measured on a Finnigan-MAT TSQ 7000 spectrometer. The high-pressure liquid chromatography (HPLC) was performed by the use of a Cosmosil Buckyprep column (4.6 mm × 250 mm) for analytical purpose. Fullerene C_{60} was purchased from Matsubo Co. Sodium thiomethoxide (CH_3SNa) was purchased from Aldrich Co. and stored under argon.

Computational Method. All calculations were conducted using the Gaussian 98 series of electronic structure program.[5] The geometries were fully optimized with the Becke hybrid (B3LYP) method for all calculations. The GIAO calculations were performed at B3LYP/6-31G* level of theory using the optimized structures at B3LYP/6-31G* level of theory.

Generation and NMR measurement of dianion H_2@$\mathbf{1}^{2-}$ and $\mathbf{1}^{2-}$. H_2@**1** (3.8 mg, 0.0036 mmol) and CH_3SNa (1.2 mg, 0.017 mmol) were placed in an NMR tube connected as

a side-arm to a Pyrex tube under argon. The apparatus was connected to a vacuum line and was immediately evacuated. CD_3CN (1.5 mL) was dried over CaH_2, degassed by five freeze-pump-thaw cycles, and vapor-transferred directly into the cooled tube containing H_2@**1** and CH_3SNa. The whole apparatus was sealed under vacuum, and the Pyrex tube was warmed to room temperature. The brown powder of H_2@**1** gradually dissolved within 1 h. The ^{1}H NMR spectrum was taken on the resulting dark green solution at room temperature to give slightly broad signals. The ^{13}C NMR was also taken at room temperature that gave no signal except for signals of CD_3CN and residual toluene. Upon cooling the solution at –30 °C, the ^{1}H NMR spectrum showed slightly sharp signals. The observed NMR chemical shifts for H_2@$\mathbf{1}^{2-}$: ^{1}H NMR (300 MHz, CD_3CN) δ 8.74 (m, 1H), 8.13 (s, 2H), 7.89 (m, 1H), 7.42-6.73 (m, 12H).

Exactly in the same way, **1** (4.2 mg, 0.0039 mmol) and CH_3SNa (1.3 mg, 0.019 mmol) were reacted in degassed and dried CD_3CN (1.5 mL) under vacuum in 1 h. The ^{1}H NMR spectrum was taken on the resulting dark green solution at room temperature to give slightly broad signals. The observed NMR chemical shifts for H_2@$\mathbf{1}^{2-}$: ^{1}H NMR (300 MHz, CD_3CN) δ 8.74 (m, 1H), 7.89 (m, 1H), 7.42-6.73 (m, 12H).

Thermal reaction of dianion $\mathbf{1}^{2-}$. Nitrogen was bubbled into a suspension of **1** (32 mg, 0.030 mmol) in THF (25 mL) rigorously dried over sodium benzophenone ketyl for 1 h. Then CH_3SNa (11 mg, 0.16 mmol) was added to this suspension and the whole mixture was stirred under nitrogen at room temperature for 1 h. The resulting dark green solution was further stirred with heating at 66 °C under nitrogen for 1 h. After the reaction mixture was cooled to room temperature, iodine (103 mg, 0.41 mmol) was added to the dark brown solution as solid. After stirred for 40 min, the reaction mixture was treated with saturated $Na_2S_2O_3$ (aq) (5 mL) and vigorously stirred for 80 min at room temperature. After dilution with toluene (30 mL), the organic layer was washed with water (50 mL × 3). The organic solution was dried over $MgSO_4$ and evaporated under reduced pressure to give brown solids. Flash column chromatography on silica gel gave **2** (9.4 mg, 0.0091 mmol, 30%) as a brown solid. The HPLC and TLC analyses indicated that no other product was present in the crude product.

References and Notes

(1) (a) *Endofullerenes*: *A New Family of Carbon Clusters*; Akasaka, T., Nagase, S., Eds.: Kluwer Academic Publisher: Dordrecht, 2002. (b) *Fullerenes*: *Chemistry, Physics and Technology*; Kadish, K. M., Ruoff, R. S., Eds.: John Wiley & Sons: New York, 2000; pp 357-393. (c) Shinohara, H. *Rep. Prog. Phys.* **2000**, *63*, 843. (d) Liu, S.; Sun, S. *J. Organomet. Chem.* **2000**, *599*, 74. (e) Nagase, S.; Kobayashi, K.; Akasaka, T. *Bull. Chem. Soc. Jpn.* **1996**, *69*, 2131. (f) Bethune, D. S.; Johnson, R. D.; Salem, J. R.; de Vries, M. S.; Yannoni, C. S. *Nature* **1993**, *366*, 123.

(2) Murata, Y.; Komatsu, K. *Chem. Lett.* **2001**, *30*, 896.

(3) Murata, Y.; Murata, M.; Komatsu, K. *Chem. Eur. J.* **2003**, *9*, 1600.

(4) For examples of C_{60} derivatives, see: a) Saunders, M.; Cross, R. J.; Jiménez-Vázquez, H. A.; Shimshi, R.; Khong, A. *Science* **1996**, *271*, 1693. (b) Saunders, M.; Jiménez-Vázquez, H. A.; Bangerter, B. W.; Cross, R. J. *J. Am. Chem. Soc.* **1994**, *116*, 3621. (c) Saunders, M.; Jiménez-Vázquez, H. A.; Cross, R. J. *Tetrahedraon Lett.* **1994**, *35*, 3869. (d) Smith, A. B., III; Strongin, R. M.; Brard, L.; Romanow, W. J.; Saunders, M.; Jiménez-Vázquez, H. A.; Cross, R. J. *J. Am. Chem. Soc.* **1994**, *116*, 10831. (e) Bühl. M.; Thiel, W.; Schneider, U. *J. Am. Chem. Soc.* **1995**, *117*, 4623. (f) Schuster, D. I.; Cao, J.; Kaprinidis, N.; Wu, Y.; Jensen, A. W.; Lu, Q.; Wang, H.; Wilson, S. R. *J. Am. Chem. Soc.* **1996**, *118*, 5639. (g) Cross, R. J.; Jiménez-Vázquez, H. A.; Lu, Q.; Saunders, M.; Schuster, D. I.; Wilson, S. R.; Zhao, H. *J. Am. Chem. Soc.* **1996**, *118*, 11454. (h) Billups, W. E.; Gonzalez, A.; Gesenberg, C.; Luo, W.; Marriott, T.; Alemany, L. B.; Saunders, M.; Jiménez-Vázquez, H. A.; Khong, A. *Tetrahedraon Lett.* **1997**, *38*, 175. (i) Rüttimann, M.; Haldimann, R. F.; Isaacs, L.; Diederich, F.; Khong, A.; Jiménez-Vázquez, H. A.; Cross, R. J.; Saunders, M. *Chem. Eur. J.* **1997**, *3*, 1071. (j) Billups, W. E.; Luo, W.; Gonzalez, A.; Arguello, D.; Alemany, L. B.; Marriott, T.; Saunders, M.; Jiménez-Vázquez, H. A.; Khong, A. *Tetrahedron Lett.* **1997**, *38*, 171. (k) Jensen, A. W.; Khong, A.; Saunders, M.; Wilson, S. R.; Schuster, D. I. *J. Am. Chem. Soc.* **1997**, *119*, 7303. (l) Boltalina, O. V.; Bühl, M.; Khong, A.; Saunders, M.; Street, J. M.; Taylor, R. *J. Chem. Soc., Perkin Trans. 2* **1999**, 1475. (m) Birkett, P. R.; Buhl, M.; Khong, A.; Saunders, M.; Taylor, R. *J. Chem. Soc., Perkin Trans. 2* **1999**, 2037. (n)

Wang, G.-W.; Weedon, B. R.; Meier, M. S.; Saunders, M.; Cross, R. J. *Org. Lett.* **2000**, *2*, 2241. (o) Wilson, S. R.; Yurchenko, M. E.; Schuster, D. I.; Khong, A.; Saunders, M. *J. Org. Chem.* **2000**, *65*, 2619. (p) Wang, G.-W.; Saunders, M.; Cross, R. J. *J. Am. Chem. Soc.* **2001**, *123*, 256. (q) Nossal, J.; Saini, R. K.; Sadana, A. K.; Bettinger, H. F.; Alemany, L. B.; Scuseria, G. E.; Billups, W. E.; Saunders, M.; Khong, A.; Weisemann, R. *J. Am. Chem. Soc.* **2001**, *123*, 8482.

(5) Gaussian 98, Revision A.11, M. J. Frisch, G. W. Trucks, H. B. Schlegel, G. E. Scuseria, M. A. Robb, J. R. Cheeseman, V. G. Zakrzewski, J. A. Montgomery, Jr., R. E. Stratmann, J. C. Burant, S. Dapprich, J. M. Millam, A. D. Daniels, K. N. Kudin, M. C. Strain, O. Farkas, J. Tomasi, V. Barone, M. Cossi, R. Cammi, B. Mennucci, C. Pomelli, C. Adamo, S. Clifford, J. Ochterski, G. A. Petersson, P. Y. Ayala, Q. Cui, K. Morokuma, P. Salvador, J. J. Dannenberg, D. K. Malick, A. D. Rabuck, K. Raghavachari, J. B. Foresman, J. Cioslowski, J. V. Ortiz, A. G. Baboul, B. B. Stefanov, G. Liu, A. Liashenko, P. Piskorz, I. Komaromi, R. Gomperts, R. L. Martin, D. J. Fox, T. Keith, M. A. Al-Laham, C. Y. Peng, A. Nanayakkara, M. Challacombe, P. M. W. Gill, B. Johnson, W. Chen, M. W. Wong, J. L. Andres, C. Gonzalez, M. Head-Gordon, E. S. Replogle, and J. A. Pople, Gaussian, Inc., Pittsburgh PA, **2001**.

(6) (a) Allard, E.; Rivitre, L.; Delaunay, J.; Dubois, D.; Cousseau, J. *Tetrahedron Lett.* **1999**, *40*, 7223. (b) Allard, E.; Delaunay, J.; Cheng, F.; Cousseau, J.; Orduna, J.; Garin, J. *Org. Lett.* **2001**, *3*, 3503. (c) Cheng, F.; Murata, Y.; Komatsu, K. *Org. Lett.* **2002**, *4*, 2541.

(7) (a) Rubin, Y.; Jarrosson, T.; Wang, G.-W.; Bartberger, M. D.; Houk, K. N.; Schick, G.; Saunders, M.; Cross, R. J. *Angew. Chem. Int. Ed.* **2001**, *40*, 1543. (b) Iwamatsu, S.-i.; Murata, S.; Andoh, Y.; Minoura, M.; Kobayashi, K.; Mizorogi, N.; Nagase, S. *J. Org. Chem.* **2005**, *70*, 4820.

(8) (a) Murata, Y.; Murata, M.; Komatsu, K. *J. Am. Chem. Soc.* **2003**, *125*, 7152. (b) Komatsu, K.; Murata, M.; Murata, Y. *Science* **2005**, *307*, 238.

(9) (a) Bühl, M.; Hirsch, A. *Chem. Rev.* **2001**, *101*, 1153. (b) Chen, Z.; King, R. B. *Chem. Rev.* **2005**, *105*, 3613.

(10) Pasquarello, M.; Schluter, M.; Haddon, R. C. *Phys. Rev. A* **1993**, *47*, 1783.

(11) Sternfeld, T.; Wudl, F.; Hummelen, K.; Weitz, A.; Haddon, R. C.; Rabinovitz, M. *Chem.*

Commun. **1999**, 2411.

(12) Shabtai, E.; Weitz, A.; Haddon, R. C.; Hoffman, R. E.; Rabinovitz, M.; Khong, A.; Cross, R. J.; Saunders, M.; Cheng, P.-C.; Scott, L. T. *J*. *Am*. *Chem*. *Soc*. **1998**, *120*, 6389.

(13) Schleyer, P. v. R.; Maerker, C.; Dransfeld, A.; Jiao, H.; Hommes, N. J. R. v. E. *J*. *Am*. *Chem*. *Soc*. **1996**, *118*, 6317.

(14) Bühl, M. *Chem*. *Eur*. *J*. **1998**, *4*, 734. (b) Chen, Z.; Cioslowski, J.; Rao, N.; Moncrieff, D.; Bühl, M.; Hirsch, A.; Thiel, W. *Theor*. *Chem*. *Acc*. **2001**, *106*, 364.

(15) Guziec, F. S., Jr.; Sanfilippo, L. J. *Tetrahedron* **1988**, *44*, 6241 and references therein.

List of Presentations

1. Murata, M.; Murata, Y.; Komatsu, K. “Organic Synthesis of Endohedral C_{60} Encapsulating Molecular Hydrogen, $H_2@C_{60}$” The 2005 International Chemical Congress of Pacific Basin Societies (PACIFICHEM 2005), Honolulu, Hawaii, USA, December 15-20, **2005**.
   (*Student Poster Award*)

2. Murata, M. “Encapsulation of Molecular Hydrogen in Fullerene C_{60} by Organic Synthesis” The 105th ICR Annual Symposium, Kyoto University, December 2, **2005**.
   (*The ICR Award for Young Scientists*)

3. Murata, M.; Murata, Y.; Komatsu, K. “Reactions and Electrochemical Behavior of the Endohedral Fullerene Incorporating Molecular Hydrogen, $H_2@C_{60}$” 35th Symposium on Structural Organic Chemistry, Osaka City University, September 9-10, **2005**.

4. Murata, M.; Murata, Y.; Komatsu, K. “Organic Synthesis of Endohedral C_{60} Encapsulating Molecular Hydrogen, $H_2@C_{60}$” 207th Meeting of the Electrochemical Society, Quebec City, Canada, May 15-20, **2005**.

5. Murata, M.; Murata, Y.; Komatsu, K. “First Organic Synthesis of Fullerene C_{60} Encapsulating Molecular Hydrogen” The 85th Annual Meeting of the Chemical Society of Japan, Kanagawa University, March 26-29, **2005**.
   (*The Best Oral Presentation Award*)

6. Murata, M.; Murata, Y.; Komatsu, K. “Organic Synthesis of Fullerene C_{60} Encapsulating Molecular Hydrogen” The 28th Fullerene-Nanotubes General Symposium, Meijo University, January 7-9, **2005**.

7. Murata, M.; Murata, Y.; Komatsu, K. “An Attempt at the Organic Synthesis of Fullerenes Encapsulating Molecular Hydrogen” The Second Trilateral Workshop on Organic Chemistry, Kyoto University, September 4-6, **2004**.

8. Murata, M.; Murata, Y.; Komatsu, K. “Attempts on the Organic Synthesis of Fullerenes Encapsulating Molecular Hydrogen” 17th Symposium on Fundamental Organic Chemistry, Tohoku University, September 23-25, **2004**.

9. Murata, M.; Murata, Y.; Komatsu, K. “An Attempt for Restoration of the Open-Cage Structure Toward the Organic Synthesis of Endohedral Fullerene $H_2@C_{60}$” The 27th Fullerene-Nanotubes General Symposium, The University of Tokyo, July 28-30, **2004**.

10. Murata, M.; Murata, Y.; Komatsu, K. “Synthesis of Open-Cage Fullerene Derivatives by the Reaction of C_{60} with Triazines” 205th Meeting of the Electrochemical Society, San Antonio, Texas, USA, May 9-13, **2004**.

11. Murata, M.; Murata, Y.; Komatsu, K. “An Attempt to Close an Orifice of an Open-Cage Fullerene Derivative That Encapsulates Molecular Hydrogen in 100%” The 84th Annual Meeting of the Chemical Society of Japan, Kwansei Gakuin University, March 26-29, **2004**.

12. Murata, M.; Murata, Y.; Komatsu, K. “Synthesis of Open-Cage Fullerene Derivatives and 100% Encapsulation of a Hydrogen Molecule” The 3rd International Symposium of the Kyoto COE Project “Elements Science”, Kyoto University, January 9-10, **2004**.

13. Murata, M.; Murata, Y.; Komatsu, K. “Synthesis of Open-Cage Fullerene Derivatives and 100% Encapsulation of a Hydrogen Molecule” The Fourth International Forum on Chemistry of Functional Organic Chemicals (IFOC-4), The University of Tokyo, November 16-17, **2003**.

14. Murata, M.; Murata, Y.; Komatsu, K. “An Attempt to Close an Orifice of the Open-Cage Fullerene Derivative Having a Sulfur Atom on the Rim” 33rd Symposium on Structural Organic Chemistry, Toyama University, October 3-4, **2003**.

15. Murata, M.; Murata, Y.; Komatsu, K. “Encapsulation of Hydrogen Molecule into an Open-Cage Fullerene Derivative” The 83rd Annual Meeting of the Chemical Society of Japan, Waseda University, March 18-21, **2003**.

16. Murata, M.; Murata, Y.; Komatsu, K. “Encapsulation of Hydrogen Molecule in an Open-Cage Fullerene Derivative” The 24th Fullerene-Nanotubes General Symposium, Okazaki, January 8-10, **2003**.

17. Murata, M.; Murata, Y.; Komatsu, K. “Structure and Properties of an Open-Cage Fullerene Derivative Having a Sulfur Atom on the Orifice” 16th Symposium on Fundamental Organic Chemistry, The University of Tokyo, October 3-5, **2002**.
(*The Best Poster Award*)

18. Murata, M.; Murata, Y.; Komatsu, K. “Synthesis, Structure, and Properties of the Open-Cage Fullerene Derivatives” The 23rd Fullerene Nanotubes General Symposium, Matsushima, July 17-19, **2002**.

19. Murata, M.; Murata, Y.; Komatsu, K. “Synthesis and Properties of Aza-Open-Cage Fullerene Derivatives” The 81st Annual Meeting of the Chemical Society of Japan, Waseda University, March 26-29, **2002**.

20. Murata, M.; Murata, Y.; Komatsu, K. “Formation of Open-Cage Fullerenes by the Reaction of C_{60} with Triazines” 31st Symposium on Structural Organic Chemistry, Yamaguchi University, October 27-28, **2001**.

Acknowledgment

The study presented in this thesis has been carried out under the direction of Professor Koichi Komatsu at Institute for Chemical Research of Kyoto University during the period of April 2000 to March 2006.

The author wishes to express his sincerest gratitude to Professor Koichi Komatsu for his kind guidance, valuable discussions, and affectionate encouragement throughout this work. The author would like to show his deep appreciation to Dr. Yasujiro Murata for his helpful suggestions and teaching. The author is also indebted to Associate Professor Toshikazu Kitagawa, Dr. Sadayuki Mori, Dr. Tohru Nishinaga for their helpful advice and kind encouragement. The author is thankful to Mr. Mitsuo Yasumoto for manufacturing and maintenance of the autoclave apparatus.

The author is grateful to Mrs. Kyoko Ohmine and Mrs. Tomoko Terada at Institute for Chemical Research of Kyoto University for their work of NMR spectra and mass spectra, respectively.

The author is deeply grateful to Professor Hiroshi Sawa and Dr. Yusuke Wakabayashi at High-Energy Accelerator Research Organization (KEK) for their valuable collaboration in the synchrotron X-ray analysis.

The author is deeply grateful to the great experimental contribution of Mr. Syuhei Maeda to the results shown in Chapter 5.

The author is grateful to Dr. Akira Matsuura, Dr. Koichi Fujiwara, Dr. Atsushi Wakamiya, Dr. Yangsoo Lee, Dr. Shih-Ching Chuang, Dr. Tomoyuki Saeki, Mr. Mitsuharu Suzuki, Mr. Hirokazu Fujimura, Mr. Daisuke Yamazaki, Mr. Tetsuya Yamazaki for their helpful suggestions and kind friendship.

The author also appreciates all other members of Professor Komatsu’s research group and Professor Tamao’s group.

The author thanks to the Japan Society for the Promotion of Science (JSPS Research Fellowships for Young Scientists) for their financial support.

Finally, the author would like to express his sincerest appreciation to his parents, Dr. Kousaku Murata and Mrs. Youko Murata, and his sister, Mrs. Chisa Tounooka, for their affectionate encouragement and constant assistance.

Michihisa Murata

Institute for Chemical Research

Kyoto University

2006